

**α -Boryl Ether Fragmentation via Boronate Oxidation for Cargo Release: The Total
Synthesis of Simplified Analogues of Bistramide A**

by

Ramsey Dawood Hanna

B.S. Chem., University of Mary Washington, 2012

Submitted to the Graduate Faculty of the
Kenneth P. Dietrich School of Arts and Sciences in partial fulfillment
of the requirements for the degree of
Doctor of Philosophy

University of Pittsburgh

2018

UNIVERSITY OF PITTSBURGH

Dietrich School of Arts and Sciences

This thesis was presented

by

Ramsey Dawood Hanna

It was defended on

May 2nd, 2018

and approved by

Dr. Kazunori Koide, Associate Professor, Department of Chemistry

Dr. Kay Brummond, Professor, Department of Chemistry

Advisor: Dr. Paul Floreancig, Professor, Department of Chemistry

Song Li, Professor, Department of Pharmaceutical Sciences

Copyright © by Ramsey Hanna

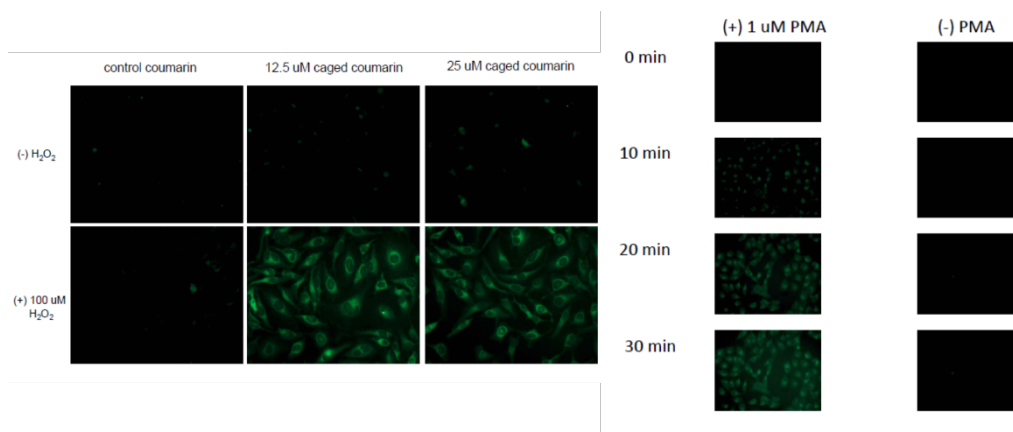
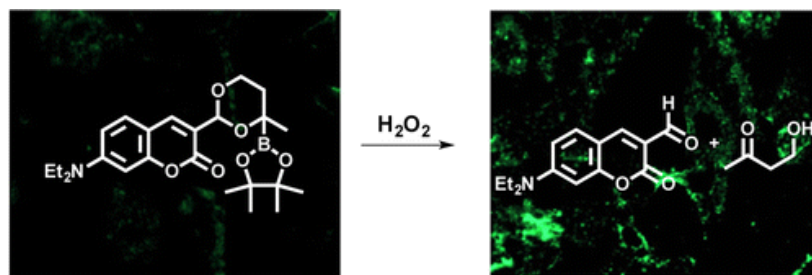
2018

α -Boryl Ether Fragmentation via Boronate Oxidation for Drug Release: The total Synthesis of Simplified Analogues of Bistramide A

Ramsey Dawood Hanna, PhD

University of Pittsburgh, 2018

The first α -boryl ether molecular scaffold for the release of alcohols, aldehydes, and ketones in the presence of H_2O_2 is described. Utilizing novel chemistry that gives access to α -hydroxy boronates as well as methods for their successive etherification and acetalization, alcohols, aldehydes, and ketones can be released *in vivo* in the presence of exogenous and endogenous H_2O_2 .



The synthesis of potent simplified analogues of Bistramide A, the primary cellular receptor for actin and a potent cytotoxin, have been synthesized in 9 steps, an improvement over the previous total synthesis of Bistramide A (14 steps). The key step in the synthesis was accomplished using a one pot hetero diels-alder reaction (HDA), 2,3-Dichloro-5,6-dicyano-1,4-benzoquinone (DDQ) oxidation, and an acid mediated cyclization.

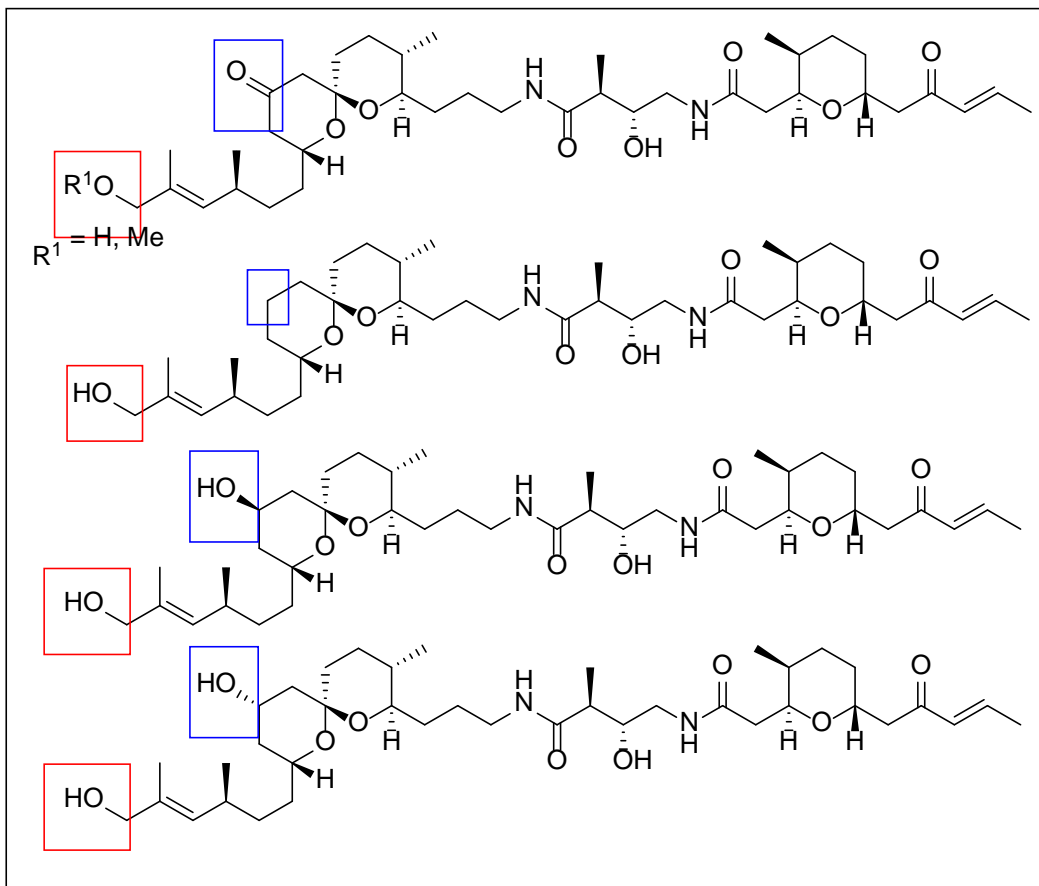
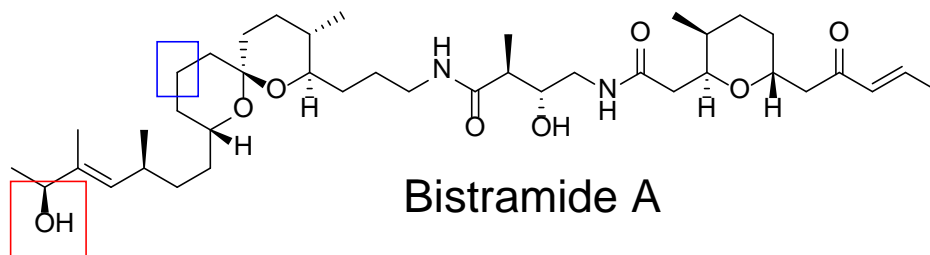


TABLE OF CONTENTS

1.0	THE CHEMISTRY OF BORONATE ESTER AND THEIR APPLICATIONS AS OXIDATIVE TRIGGERS FOR H₂O₂	1
1.1	SELF-IMMOLATIVE-LINKERS: DESIGN FOR ALCOHOLS, AMINES, AND LACTONES	2
1.1.1	Cyclization-based self-immolative linkers	3
1.1.2	Elimination Based Self-immolative linkers	6
1.2	PRODRUG DESIGN FOR ALDEHYDES AND KETONES	9
1.2.1	Oximes as Masking groups for ketones and aldehydes	9
1.2.2	Acetals as masking groups for ketones and aldehydes	11
1.3	THE PROPERTIES OF BORONATE ESTERS	13
1.3.1	The electronic and structural properties of the C-B bond	13
1.3.2	The electronic and structural properties of the B-O bond	14
1.4	THE SYNTHESIS OF BORONATE ESTERS	15
1.4.1	The conversion of organometallic reagents into boronate esters	16
1.4.2	The addition of B-H to double and triple bonds	18
1.4.3	The addition of B-B to unsaturated compounds	20
1.5	BORONATE ESTERS AS SYNTHETIC INTERMEDIATES	27
1.5.1	Transformations that utilize the nucleophilicity of the C-B bond	28
1.6	BORONATE ESTERS AS PRODRUGS AND PROBES FOR H₂O₂	30
1.6.1	Boronate esters as fluorescent probes for H₂O₂	32
1.6.2	Boronate Ester based Prodrugs	34

1.7	BORON CONTAINING DRUGS	38
1.7.1	Boron in Medicinal Chemistry	39
1.7.2	Boron in pharmaceutical agents.....	41
2.0	THE UTILIZATION OF BORONATE ESTERS FOR THE OXIDATIVELY TRIGGERED RELEASE OF ALCOHOLS, KETONES, AND ALDEHYDES	42
2.1	ALCOHOL, ALDEHYDE, AND KETONE LIBERATION AND INTRACELLULAR CARGO RELEASE THROUGH PEROXIDE MEDIATED α-BORYL ETHER FRAGMENTATION	43
2.1.1	Facile access to α-hydroxy boronate esters.....	44
2.1.2	α-hydroxy boronate functionalized acetals and carbonates.....	46
2.1.3	Defining the scope: The synthesis and fragmentation of α-boryl ethers, carbonates, and acetals	49
2.1.4	Defining Limitations: Cyclic acetal discovery.....	53
2.1.5	A novel biorthogonal scaffold for the release of a fluorescent aldehyde..	57
3.0	BISTRAMIDE A	63
3.1	PRIOR SYNTHESSES OF BISTRAMIDE A.....	64
3.1.1	Kozmin's 2004 Synthesis of Bistramide A.....	65
3.1.2	Crimmins 2006 Synthesis of Bistramide A.....	67
3.1.3	Floreancig's 2014 Synthesis of Bistramide A	70
3.2	PREVIOUS ANALOGUES OF BISTRAMIDE A	74
3.2.1	Kozmin's Bistramide Analogues	75
3.2.2	Panek's Bistramide A Stereoisomer Library	77

3.3 NOVEL ANALOGUES OF BISTRAMIDE A, SYNTHETIC OPTIMIZATION, AND BIOLOGICAL ACTIVITY	80
APPENDIX A	88
APPENDIX B	123
APPENDIX C	153
APPENDIX D	192
BIBLIOGRAPHY	213

LIST OF TABLES

Table 2.1 Scope of alcohol release for α -boryl ethers.	50
---	----

LIST OF FIGURES

Figure 1.1 Commonly seen organoboron derivatives	1
Figure 1.2 Quinone Methide byproducts	9
Figure 1.3 1,2 diols used as photolabile protecting groups for aldehydes and ketones	12
Figure 1.4 A progesterone protected by a photolabile ketal	12
Figure 1.5 Intramolecular coordination between a carbonyl group and a boronate ester	14
Figure 1.6 Common hydroboration reagents	19
Figure 1.7 Chiral boronate esters	29
Figure 1.8 Probes for H ₂ O ₂ developed by the Christopher Chang group	33
Figure 1.9 A sample of boronate esters being utilized as bioisosteres for phenols	40
Figure 1.10 Boron-containing drugs approved by the FDA	41
Figure 2.1 Intramolecular bond coordination between the carbonate and the boronate ester	47
Figure 2.2 Monitoring the oxidation of methoxy methyl ether 2.4	48
Figure 2.3 Oxidation of methoxymethyl ether 2.4 at pH 7.2 and 8.0	49
Figure 2.4 Acetal 2.22 and Carbonate 2.23	58
Figure 2.5 Fluorophore fragmentation at low substrate and peroxide concentration and pH stability studies.	59
Figure 2.6 Fluorophore release from acetal 2.21 compared to carbonate 2.23	60
Figure 2.7 Comparison of fluorophore release by different oxidants [2.21] =40 μM [oxidant] = 200 μM.....	60
Figure 2.8 Fluorophore release from 2.21 in HeLa cells treated with exogenous H ₂ O ₂	61

Figure 2.9 Cellular oxidative fluorophore release from acetal 2.21 in the presence of endogenously produced H ₂ O ₂	62
Figure 3.1 Bistramide A, B, C, D, and K.....	63
Figure 3.2 Bistramide A contacts involve with A-Actin recognition	74
Figure 3.3. Rationally designed analogues of Bistramide A, their growth inhibition (GI ₅₀) and their dissociation constants (K _d) with monomeric actin	75
Figure 3.4 Rationally designed Bistramide Analogue for <i>In vivo</i> studies	77
Figure 3.5 Most potent stereoisomers of Bistramide A	79
Figure 3.6 Novel analogues of Bistramide A.....	81
Figure 3.7 GI ₅₀ curves for Bistramide A, 3.73, 3.72,3.74, 3.76, and 3.75 in small cell lung cancer (A549) cells.....	85

LIST OF SCHEMES

Scheme 1.1 Small molecule self-immolative linker design.....	2
Scheme 1.2 Mechanisms for self-immolative linkers.....	3
Scheme 1.3 A cyclization-based self-immolative linker	4
Scheme 1.4 Lactonization rates for tri-methyl lock approach	4
Scheme 1.5 Coumarin derivatives as self-immolative linkers.....	5
Scheme 1.6 A lactonization-based pilocarpine prodrug	5
Scheme 1.7 A lactonization-based propofol prodrug	6
Scheme 1.8 Strategies for elimination-base self-immolative linkers.....	7
Scheme 1.9 Elimination based self-immolative linkers.....	7
Scheme 1.10 Relative release rates for carbonate and ether linkers	8
Scheme 1.11 A 4-amino benzyl alcohol self-immolative linker.....	8
Scheme 1.12 Synthesis of hydroxyimines and their derivatization	10
Scheme 1.13 Synthesis of HI1 and HI2 from nabumetone and ketoprofen.....	10
Scheme 1.14 Mechanism for the hydrolysis of hydroxyimines.....	10
Scheme 1.15 Synthesis and deprotection of acetal and ketal protecting groups	11
Scheme 1.16 Resonance stabilized forms for alkenyl boronate esters	14
Scheme 1.17 Kinetics and the driving force for boronate ester oxidation.....	15
Scheme 1.18 Stability towards hydrolysis for a series of boronate esters	15
Scheme 1.19 A summary of the methods available to synthesize boronate esters.	16
Scheme 1.20 The facile synthesis of borate esters from boric acid.....	17
Scheme 1.21 Mechanism for the conversion of borate esters into boronate esters.	17

Scheme 1.22 Synthesis of 2-pyridyl MIDA boronate ester	18
Scheme 1.23 Hydroboration-oxidation using BH ₃	19
Scheme 1.24 Catalytic cycle for the hydroboration of alkene by HBpin	20
Scheme 1.25 Pt ⁰ catalyzed diboration of alkynes	21
Scheme 1.26 Catalytic cycle for the diboration of alkynes using Pt(PPh ₄)	22
Scheme 1.27. Substrate scope for the catalyzed diboration of unsaturated hydrocarbons	23
Scheme 1.28 A platinum catalyzed diboration of aldimines	23
Scheme 1.29 Cu catalyzed diboration of aldehydes using (ICy)CuOt-Bu	24
Scheme 1.30 Decomposition pathways of borylated aldehydes	24
Scheme 1.31 The synthesis of α -hydroxy potassium trifluoroborate salts.	25
Scheme 1.32 Mechanistic considerations for the diboration of aldehydes by (ICy)Cu-OtBu.....	26
Scheme 1.33 The diboration of sulfinylimine and ketones using (ICy)Cu-OtBu.....	27
Scheme 1.34 Mechanistic consideration for uncatalyzed reactions with boronate esters	28
Scheme 1.35 Uncatalyzed transformations of boronate esters	28
Scheme 1.36 The mechanism for the Petasis reaction.....	29
Scheme 1.37 Mechanism for the oxidation of boronate esters by H ₂ O ₂	31
Scheme 1.38 The first report of a boronate ester based self-immolative linker.	32
Scheme 1.39 Fluorescein Derivative as a probe for H ₂ O ₂	32
Scheme 1.40 Boronate ester oxidation to induce DNA ICLs	35
Scheme 1.41 A boronate ester based cancer prodrug	36
Scheme 1.42 A boronate ester based prodrug that releases cytotoxic cargo and a fluorophore. 36	
Scheme 1.43 BRAP, a boronate ester prodrug for HBA, a potent antioxidant.....	37
Scheme 1.44 A dual stimuli-responsive hybrid anticancer drug	38

Scheme 1.45 Ultimate degradation of organoboron compounds into boric acid.....	39
Scheme 1.46 Boron's coordination preferences with amino acids	39
Scheme 2.1 An oxidatively triggered boronate ester designed to localize in the mitochondria of cells to release an equivalent of quinone methide, and an antioxidant.....	42
Scheme 2.2 A novel scaffold for the release of alcohols that circumvents the release of quinone methide.....	43
Scheme 2.3 Modified protocol for the facile access of α -hydroxy boronate esters	45
Scheme 2.4 Synthesis of carbonate 2.3 and acetal 2.4.....	46
Scheme 2.5 Monitoring the fragmentation of carbonate 2.3 and acetal 2.4	47
Scheme 2.6 Synthesis of carbonate 2.7 from hydroxy boronate 2.8.....	51
Scheme 2.7 Alkoxide generation leads to bora-Brook rearrangement rather than alkylation	51
Scheme 2.8. Etherification to form boronate ester 2.10	52
Scheme 2.9 Reductive etherification to form α -boryl ether 2.12.....	52
Scheme 2.10 Reductive etherification to form α -boryl ether 2.14	53
Scheme 2.11 Attempts to synthesize a 3° aryl-alkyl α -boryl ether	54
Scheme 2.12 Synthesis of acetal 2.16 from α -hydroxy boronate 2.2	54
Scheme 2.13 Attempted etherification with acetophenone.....	55
Scheme 2.14 Unintentional synthesis of a cyclic acetal	55
Scheme 2.15 Synthesis of acetal 2.18 and ketal 2.19 from α -hydroxy boronate ester 2.17	56
Scheme 2.16 Oxidative breakdown of cyclic acetal 2.18 and cyclic ketal 2.19	57
Scheme 2.17 Noyori acetalization of aldehyde 2.20 and α -hydroxy boronate ester 2.8	58
Scheme 3.1 Retrosynthesis of Bistramide A.....	64
Scheme 3.2 Kozmin's Synthesis of the left fragment of Bistramide A.....	65

Scheme 3.3 Kozmin's synthesis of the middle fragment of Bistramide	66
Scheme 3.4 Kozmin's synthesis of the right fragment of Bistramide A	66
Scheme 3.5 Kozmin's final coupling to synthesize Bistramide A	67
Scheme 3.6 Crimmins synthesis of the left fragment of Bistramide A	68
Scheme 3.7 Crimmins Synthesis of the middle fragment of Bistramide A	69
Scheme 3.8 Crimmins Synthesis of <i>Fragment C</i> (3.43)	69
Scheme 3.9. One pot synthesis of the spiroketal portion of Bistramide A	70
Scheme 3.10 Floreancigs Synthesis of Fragment A (3.51).....	71
Scheme 3.11 Floreancig's synthesis of Fragment C.....	72
Scheme 3.12 Coupling of Fragment B and Fragment C to form BR.....	73
Scheme 3.13 Floreancigs completion of Bistramide A	73
Scheme 3.14 Synthesis of 8 stereoisomers of Fragment C of Bistramide A	78
Scheme 3.15 Synthesis of 4 isomers of Fragment B of Bistramide A.....	78
Scheme 3.16 Coupling of Fragment B and Fragment C to synthesize 32 isomers of BR	79
Scheme 3.17 Attempted dimethyl zinc addition into carbonyl 3.71	80
Scheme 3.18 Synthesis of Bistramide analogues 3.74 and 3.75.....	82
Scheme 3.19 Synthesis of 3.72	83
Scheme 3.20 Synthesis of Bistramide analogue 3.73	83
Scheme 3.21 Synthesis of bistramide analogue 3.76.....	84
Scheme 3.22 Synthesis of aldehyde 3.83.....	86
Scheme 3.23 A more convergent route towards the synthesis of a potent Bistramide Analogue	86

ACKNOWLEDGEMENTS

I would like to thank my advisor, Paul Floreancig, for taking so much time and effort to work with me and assist me personally during my time in Pittsburgh. I would most certainly not have completed this degree without his support and encouragement. I would also like to thank my committee members Professor Kay Brummond, Professor Kazunori Koide, and Professor Song Li.

My proposal mentor, Peng Li, played a role in teaching me how to formulate my research idea in a coherent manner (also, he was super patient with me during a very stressful time).

I would like to personally thank Jim Burrows and Lauren Burrows, you were my closest, most supportive friends in Chevron and I most certainly would not have made it through this degree without either of you.

I would like to personally acknowledge Yuta Naro, without his expertise and assistance, the biological data presented in this document would not be here.

Finally, I'd like to thank my partner, Avigayil Diamond, for being incredibly supportive and motivating me to finish this document these past few months.

1.0 THE CHEMISTRY OF BORONATE ESTER AND THEIR APPLICATIONS AS OXIDATIVE TRIGGERS FOR H₂O₂

Boronate esters have emerged as a unique class of compounds that have shown great utility as a tool for synthetic organic chemists and medicinal chemists. The generic structure of boronate esters and their derivatives is presented in Figure 1.1

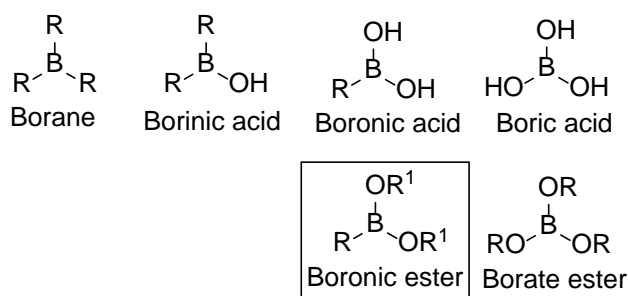
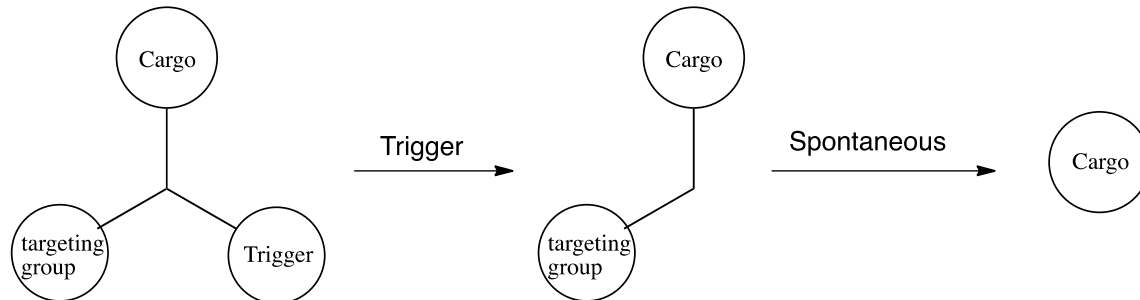


Figure 1.1 Commonly seen organoboron derivatives

Historically, this functional group has seen use throughout organic chemistry as a substrate for the Pd-catalyzed Suzuki coupling reaction.¹ In recent years, boron and subsequently boronate esters have become useful diagnostic tools to probe H₂O₂ in living systems as well as triggers for the release of small molecules in living systems that are undergoing overproduction of reactive oxygen species (ROS).² This chapter will introduce the concept of self-immolative linkers, the chemistry of boron, and research done on the use of boronate esters as biorthogonal probes for H₂O₂. Additionally, pharmaceutical compounds containing boron will be discussed to demonstrate the feasibility of boronate esters as prodrugs.

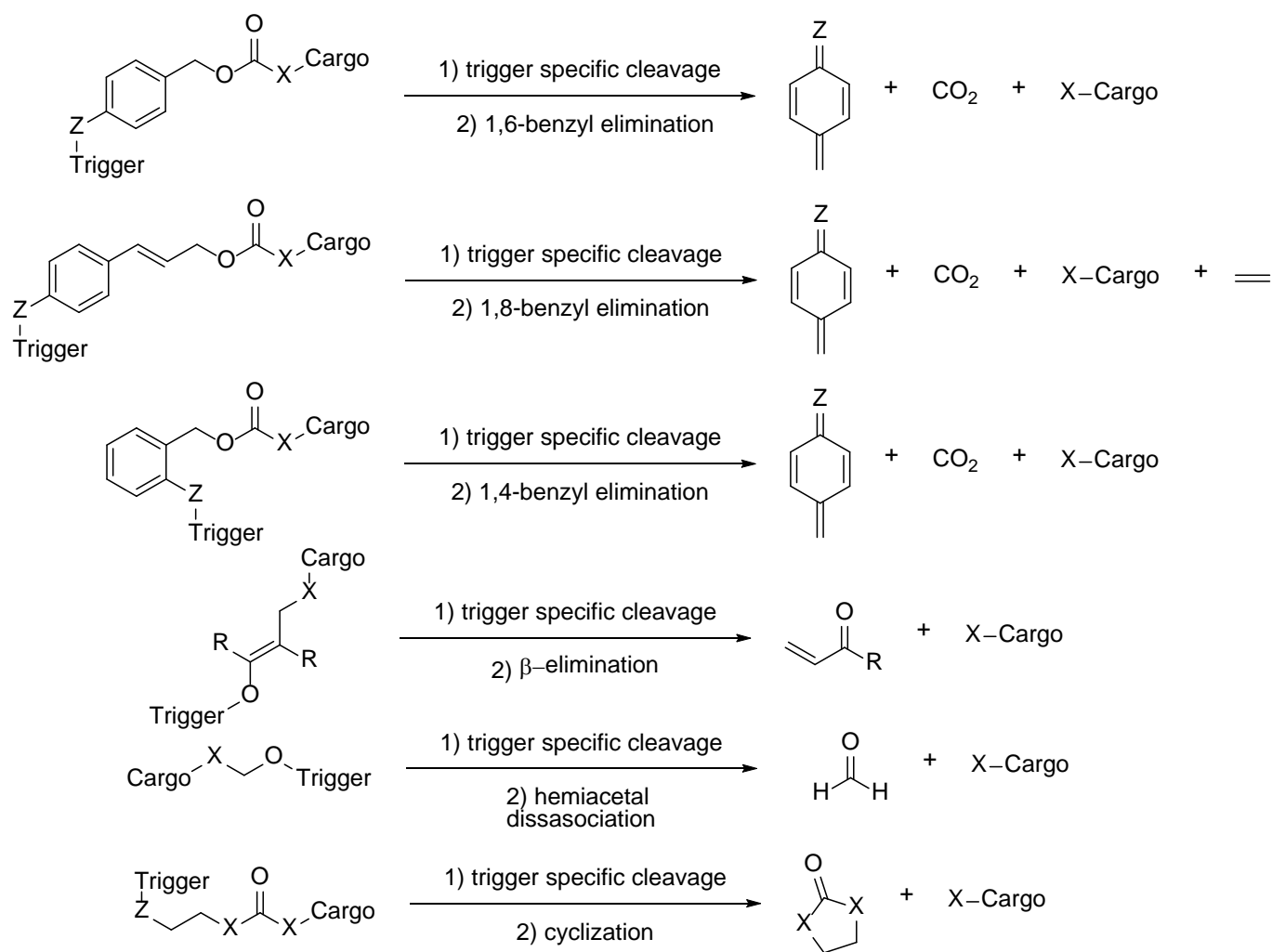
1.1 SELF-IMMOLATIVE-LINKERS: DESIGN FOR ALCOHOLS, AMINES, AND LACTONES

Oftentimes, the release of a small molecule in response to specific stimuli in biological and environmental systems is desired for the development of targeted therapeutic agents and chemoselective small molecule sensors. An attractive solution is to utilize self-immolative linkers that only undergo spontaneous release of the desired cargo in the presence of the appropriate stimulus. Small molecules can be designed that contain: 1) a targeting group that promotes cellular localization, 2) an inactive version of the desired cargo, 3) a cleavable group (trigger) that will react under the desired conditions leading to cargo release (Scheme 1.1).³ Activation of the trigger generates an intermediate that spontaneously decomposes, leading to release of the target molecule.



Scheme 1.1 Small molecule self-immolative linker design

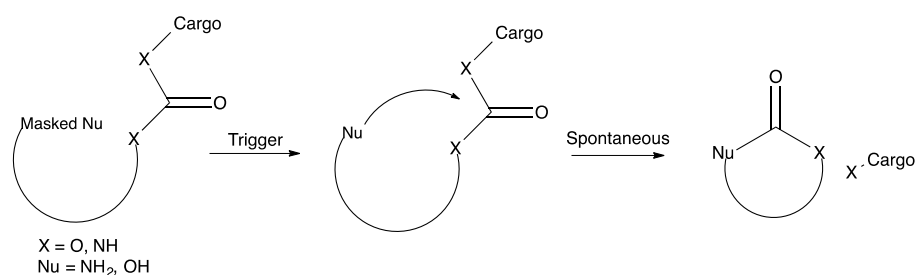
Self-immolative small molecules rely on several different mechanisms, many of which are summarized in Scheme 1.2.



Scheme 1.2 Mechanisms for self-immolative linkers

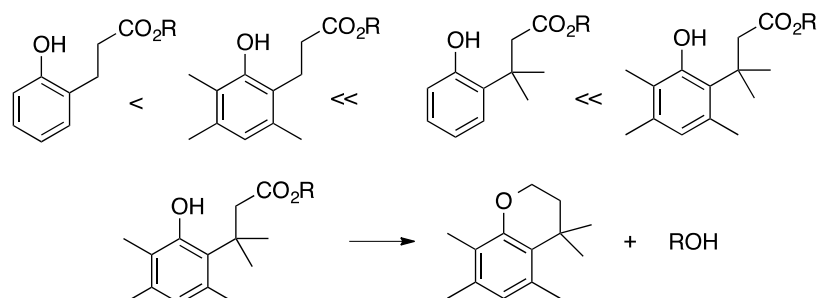
1.1.1 Cyclization-based self-immolative linkers

Several self-immolative linkers rely on a cyclization-based approach in which a nucleophile is masked until it is in the presence of a specific stimulus. Once the nucleophile is unmasked by the stimulus, spontaneous cyclization occurs to release the cargo (Scheme 1.3). Typically, the nucleophile is either a free amine or alcohol and the electrophile is a carbonate, ester, or amide.



Scheme 1.3 A cyclization-based self-immolative linker

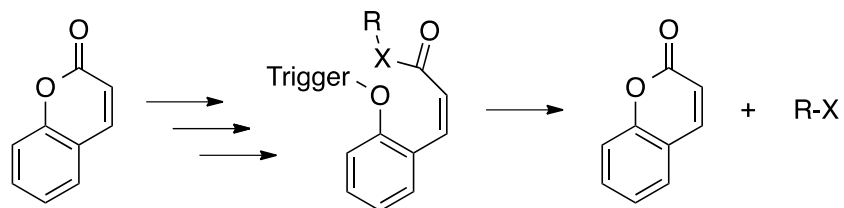
One of the primary methods to release cargo is via intramolecular lactonization. A classic example of a lactonization prodrug system is the tri-methyl lock (TML) approach.⁴ The TML approach utilizes the Thorpe-Ingold effect to enhance the rate of cyclization with the addition of geminal methyl groups (Scheme 1.4).⁵



Scheme 1.4 Lactonization rates for tri-methyl lock approach

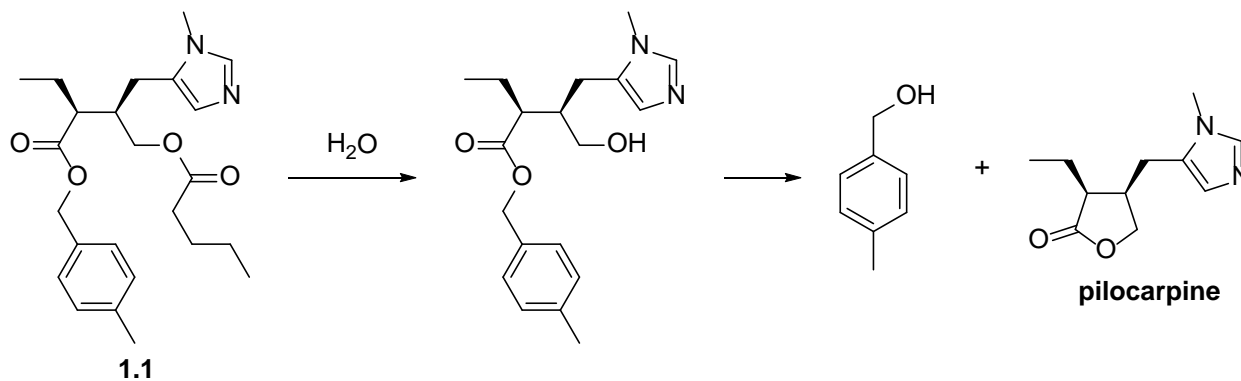
The TML scaffold works by forcing the substrate into a conformation that very closely resembles the transition state of the cyclization reaction, thus increasing the rate. This rate enhancement is so large that even amides can be used as electrophiles after trigger release.⁶ The TML has been used to mask fluorescence,⁶ improve aqueous solubility,⁷ and enhance bioavailability.⁸

A similar cyclization system uses coumarin-containing derivatives.⁹ This design utilizes a quick intramolecular cyclization that occurs between a masked phenol and a carbonyl derivative containing the cargo. This lactonization occurs at rates comparable to the TML system due to the *cis* geometry of the double bond locking the phenol into a transition state required for intramolecular cyclization (Scheme 1.5).¹⁰ Coumarin based self-immolative systems start from readily available, affordable starting materials and the byproducts are known to be non-toxic.⁹



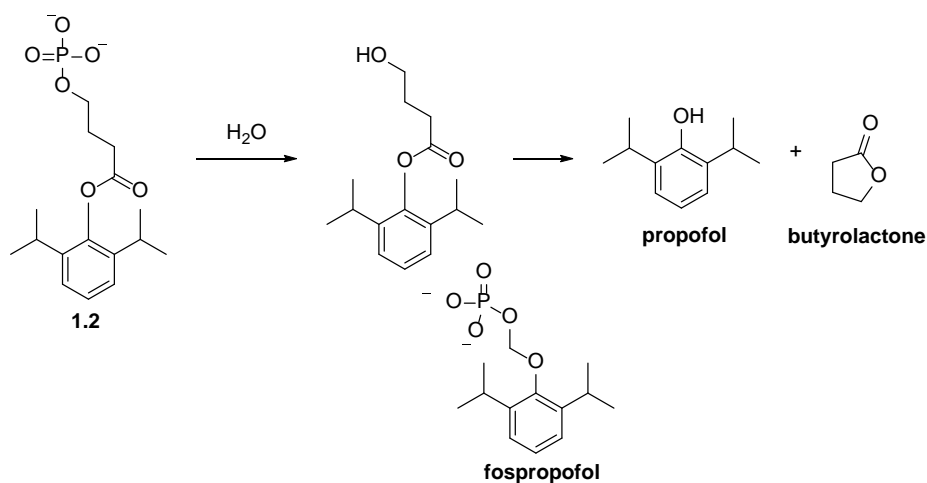
Scheme 1.5 Coumarin derivatives as self-immolative linkers

One of the first examples of a lactonization prodrug was the use of ester **1.1**, an analogue of the drug **pilocarpine**.¹¹ Alkyl ester **1.1** acts as a trigger once *in vivo* leading to an unmasked alcohol, which undergoes spontaneous intramolecular lactonization and quantitative release of pilocarpine (Scheme 1.6). Diester prodrug **1.1** has much higher bioavailability than **pilocarpine**.



Scheme 1.6 A lactonization-based pilocarpine prodrug

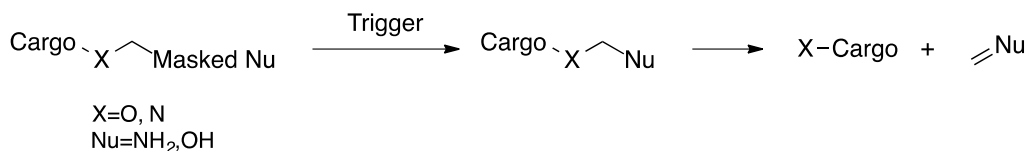
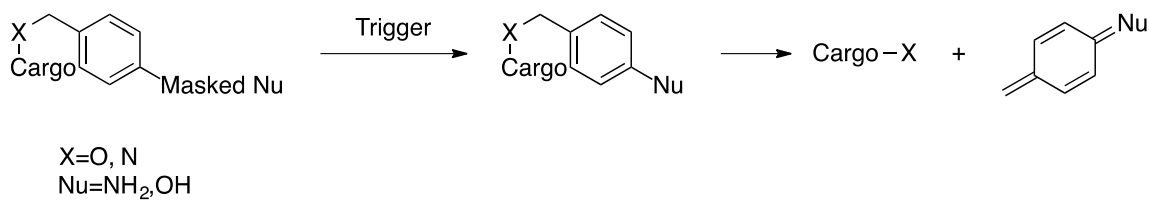
A recent example of a lactonization-based prodrug is the cyclization-based prodrug for **propofol**, phosphate ester **1.2**. **Propofol** is typically administered as an elimination-based prodrug (**fospropofol**) sedative-hypnotic agent for surgical procedures.¹² In this novel system, **1.2** is hydrolyzed *in vivo* to give pendant alcohol **1.3** (Scheme 1.7). The alcohol then undergoes intramolecular cyclization to give **butyrolactone** and **propofol**. Compound **1.2** releases **propofol**, albeit at a slower rate than **fospropofol**.¹³



Scheme 1.7 A lactonization-based propofol prodrug

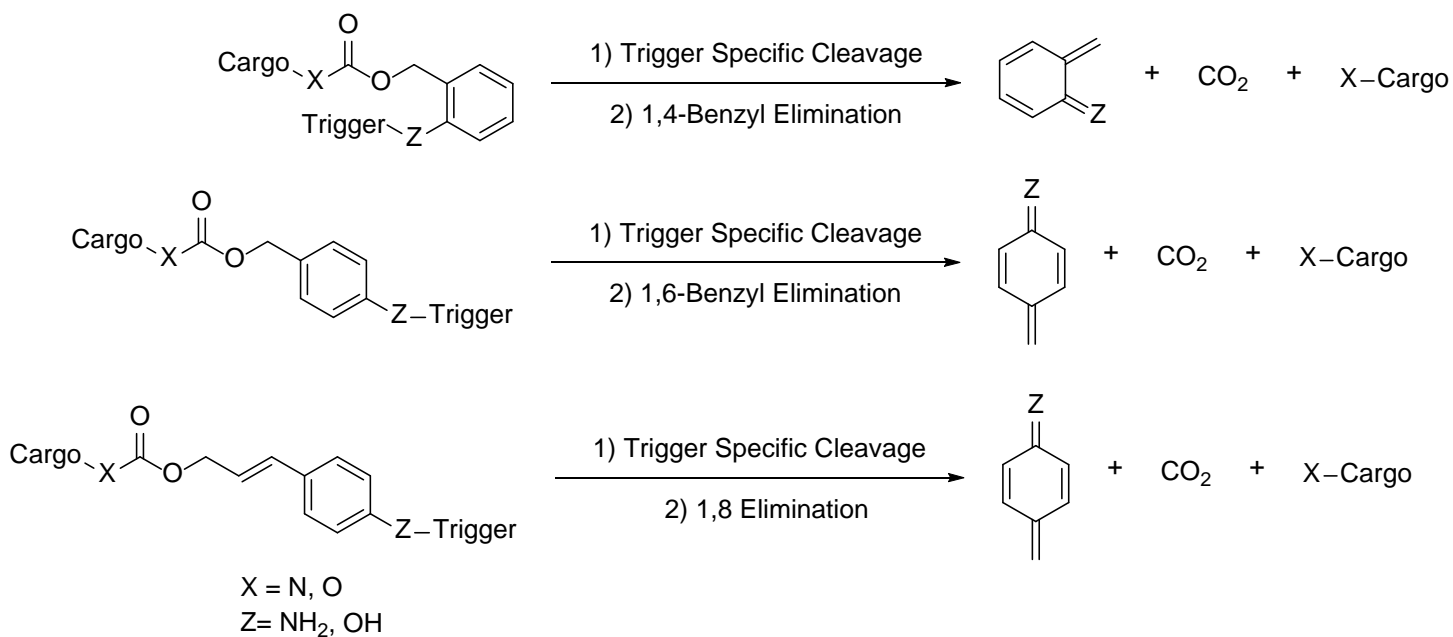
1.1.2 Elimination Based Self-immolative linkers

There are several self-immolative linkers that rely on an elimination-based mechanism to release their cargo (Scheme 1.8). These types of scaffolds rely on a masked nucleophile that will selectively react within the cell leading to the release of the desired drug along with a quinone methide or formaldehyde derivative. Advantages of this strategy are: 1) ease of synthesis compared to cyclization-based prodrugs, 2) cargo release is faster than in cyclization-based systems.^{3, 14}



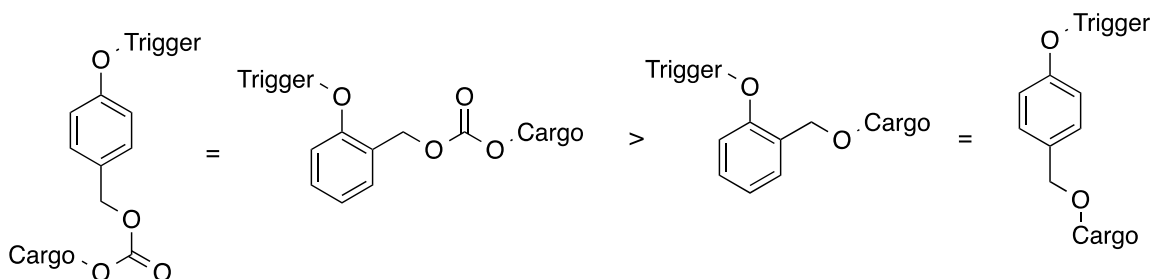
Scheme 1.8 Strategies for elimination-base self-immolative linkers

One scaffold that has been extensively exploited within the literature is an elimination system where the unmasked product is an alcohol or an amine that breaks down to give a quinone or aza-quinone methide (Scheme 1.9). Appendage of the trigger *ortho* to the cargo leads to 1,4-benzyl elimination while appendage of the trigger *para* to the cargo leads to a 1,6 benzyl elimination. Alternatively, an alkene linker can be used, which allows breakdown via 1,8-elimination.¹⁵



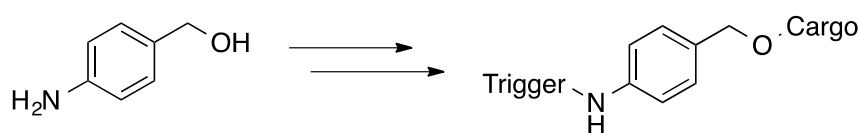
Scheme 1.9 Elimination based self-immolative linkers

A literature comparison of 1,4 and 1,6-benzyl elimination suggests that there is no significant difference in their release rates (Scheme 1.10).¹⁶⁻¹⁷ Rates can be enhanced by appendage of a linker such as a carbonate which is a better leaving group than an alcohol.



Scheme 1.10 Relative release rates for carbonate and ether linkers

A seminal example of an elimination based self-immolative linker is the 4-amino benzyl alcohol scaffold.¹⁴ Starting with 4-amino benzyl alcohol, a simple linker can be synthesized (Scheme 1.11). Attaching the trigger and then appending the desired cargo allows the synthesis of a self-immolative compound in a few simple steps. Exposure to the trigger unmasks the amine which leads to spontaneous 1,6 benzyl elimination and the release of the cargo along with an equivalent of *p*-azaquinone-methide. This linker system is flexible and has been used to: 1) trigger cargo release in a low pH environment by utilization of an acid labile Schiff base, 2) attach antitumor drugs such as taxol and doxorubicin to reduce systemic toxicity *in vivo*, and 3) trigger cargo release via specific enzymatic cleavage of an amide bond.¹⁸



Scheme 1.11 A 4-amino benzyl alcohol self-immolative linker

One disadvantage to quinone-methide and azaquinone-methide elimination systems is the high toxicity of their byproducts (Figure 1.2).¹⁹ These highly reactive compounds are ultimately responsible for the anticancer activity of a number of phenolic anticancer drugs due to their powerful alkylating abilities.¹⁹

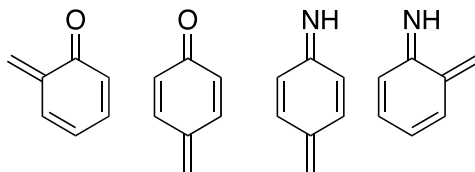


Figure 1.2 Quinone Methide byproducts

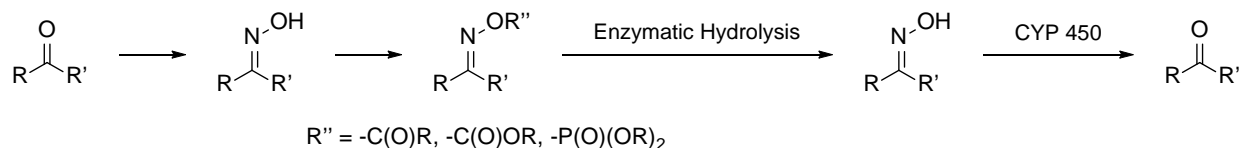
1.2 PRODRUG DESIGN FOR ALDEHYDES AND KETONES

In the previous section, the released cargo is an alcohol, amine, or lactone. Literature precedent for the release of aldehydes and ketones is sparse in comparison and typically relies on the use of oximes or acetals.

1.2.1 Oximes as Masking groups for ketones and aldehydes

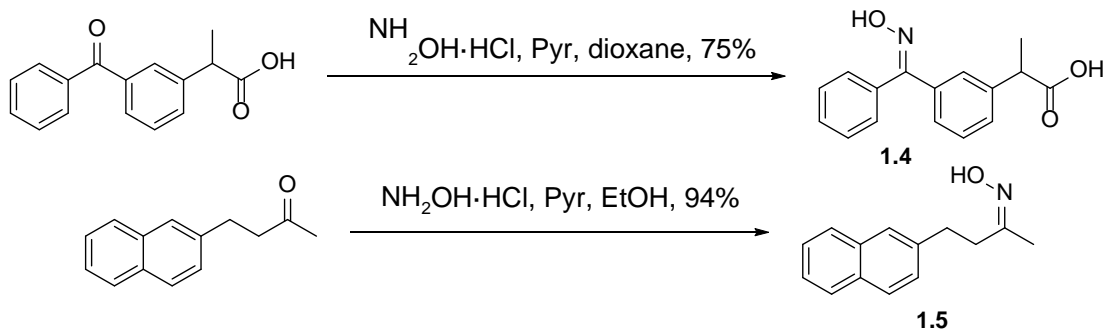
Hydroxyimines are excellent masking groups for ketones and aldehydes in biological systems because they are quickly converted to their carbonyl precursors in the presence of cytochrome P450 (CYP) enzymes. CYP enzymes are promiscuous with their selection of substrates and are found in virtually every tissue of the body; however, they are particularly abundant in the liver and intestinal tract. Hydroxyimines are also easily derivatized as an ester,

phosphate, or carbamate; thus providing “double-masked” molecules because they require a two-step activation process (Scheme 1.12).



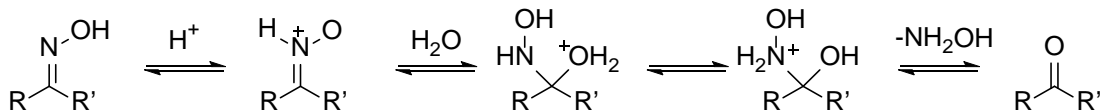
Scheme 1.12 Synthesis of hydroxyimines and their derivatization

One of the first examples of hydroxyimines being used as triggers for the release of ketones and aldehydes was the synthesis and validation of ketoprofen and nabumetone hydroxyimines **1.4** and **1.5**. Synthesis of **1.4** and **1.5** was achieved by treatment with $\text{NH}_2\text{OH}\cdot\text{HCl}$ in the presence of pyridine (Scheme 1.13).



Scheme 1.13 Synthesis of HI1 and HI2 from nabumetone and ketoprofen

1.4 and **1.5** are hydrolyzed to release their parent carbonyl groups (Scheme 1.14). Stability in aqueous conditions increases as pH increases, with a half life of over 16 hours for pH range 5.0-9.0. In human serum (pH 7.4), **1.4** and **1.5** have high stability.

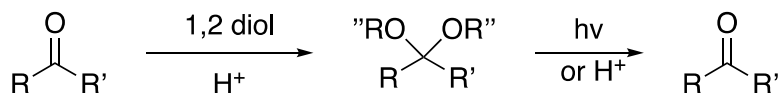


Scheme 1.14 Mechanism for the hydrolysis of hydroxyimines

As predicted **1.4** and **1.5** are oxidized rapidly to their ketone drugs in liver microsome, thus demonstrating the site specificity of hydroxylamine prodrugs. Activation of **1.4** and **1.5** also occurs *in vivo* in rats.

1.2.2 Acetals as masking groups for ketones and aldehydes

Acetals and ketals are excellent functional groups for the masking the functionality of aldehydes and ketones. Classically, these functional groups have been used to protect, 1,2 diols, ketones, and aldehydes in the synthesis of complex natural products. They are easily synthesized from the parent carbonyl compound and a diol with the desired protecting group in the presence of acid (Scheme 1.15).



Scheme 1.15 Synthesis and deprotection of acetal and ketal protecting groups

Acetals and ketals are easily cleaved under acidic conditions to give aldehydes and ketones respectively; however their utility as triggers for cargo release are limited. Hydrolysis of ketals and acetal in biological systems can occur in biological systems at low pH; however, their stability often makes them poor masking groups. Additionally, their utility as pharmaceutical drugs is limited due to the highly acidic conditions found in the stomach.

An elegant solution to this is the use of photolabile aromatic protecting groups.²⁰⁻²² There are several diols that have been developed as protecting groups for aldehydes and ketones that can be removed in the presence of light under simulated physiological conditions to release their parent carbonyl compounds (Figure 1.3).

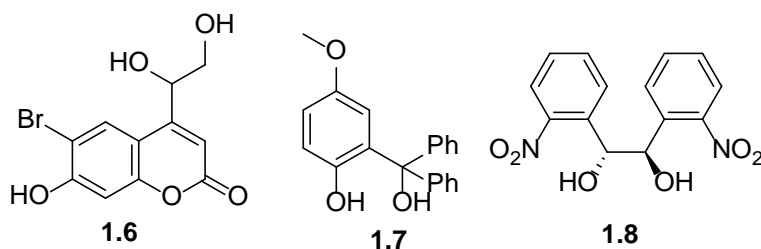


Figure 1.3. 1,2 diols used as photolabile protecting groups for aldehydes and ketones

Coumarin diol **1.6** was used to release benzaldehyde, piperonal, acetophenone, and cyclohexanone under physiological conditions in the presence of 1- or 2-photon excitation.²³ Additionally, diol **1.7** and **1.8** have seen use as photolabile protecting groups in synthesis. Using diol **1.6**, photolabile ketal progesterone derivative **1.9** was synthesized in a single step (Figure 1.4). **1.9** was used to measure changes in the swimming behavior of single human sperm, demonstrating the usefulness of these derivatives under physiologically relevant conditions.²⁴

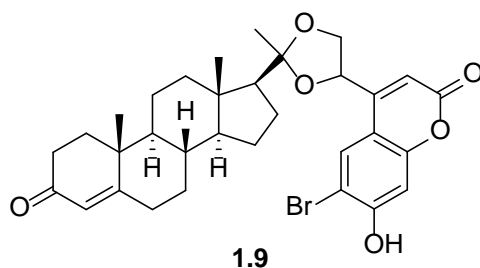


Figure 1.4. A progesterone protected by a photolabile ketal

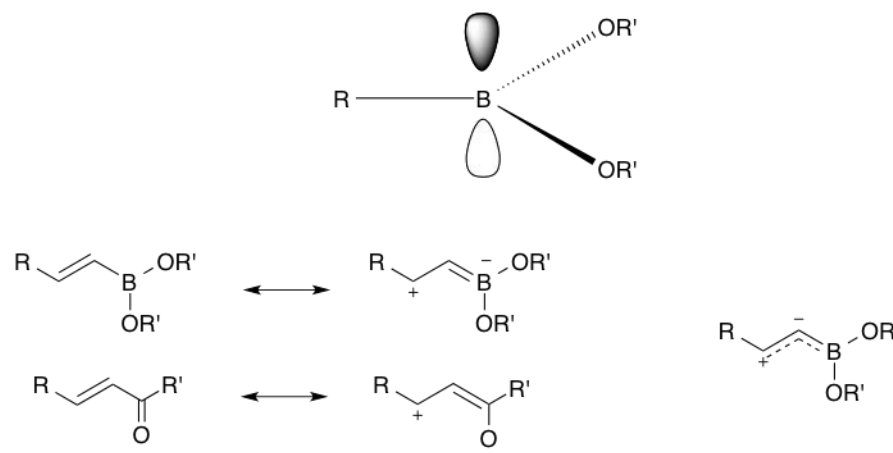
1.3 THE PROPERTIES OF BORONATE ESTERS

Boronate esters are trivalent compounds containing two alkoxy or aryloxy substituents and a single carbon substituent. The three substituents are oriented in a trigonal planar fashion with boron's empty p-orbital orthogonal to its three substituents. This vacant p-orbital is largely responsible for giving boronate esters their Lewis acidic character and unique reactivity. The properties of a boronate ester are largely dependent on the nature of the carbon substituent and the nature of the alkoxy/aryloxy substituents.

1.3.1 The electronic and structural properties of the C-B bond

Boronate esters are typically classified by the hybridization of their single carbon substituent. Due to boron's empty p-orbital, substituents that can donate in electron density can complete boron's octet, decreasing its Lewis acidic character.

C-B bond lengths in alkenyl and aryl boronate esters are shorter than C-B bonds of alkyl boronate esters, this suggests that there is π bonding between alkenyl and aryl substituents with their adjacent boron atoms.²⁵ Further evidence for π bonding in boronate esters is deshielded ^{13}C NMR shifts β to boronate esters that have an alkene as their single substituent compared to analogous alkenes.²⁶ This demonstrates that alkenyl boronate esters can be thought of as analogous to α,β -unsaturated carbonyl compounds, where contribution of the enolate form is important to explain reactivity (Scheme 1.16). These results explain why alkenyl and aryl boronate esters have increased stability compared to alkyl boronate esters.



Scheme 1.16 Resonance stabilized forms for alkenyl boronate esters

Boron's Lewis acidic character can also lend itself to intramolecular coordination. There are a number of examples of compounds containing dative bonds between boron and a heteroatom (O, N).²⁷ One example where the single carbon substituent plays a role in the formation of an intramolecular bond can be seen in Figure 1.5 where there is strong evidence for chelation between the boronate ester and the oxygen on the amide.²⁸

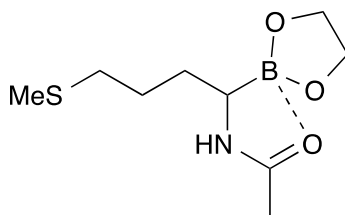
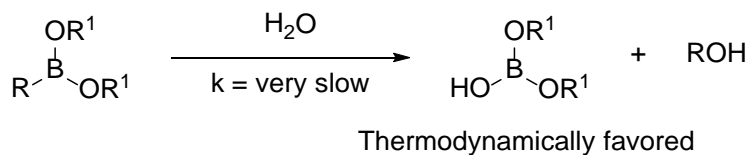


Figure 1.5 Intramolecular coordination between a carbonyl group and a boronate ester

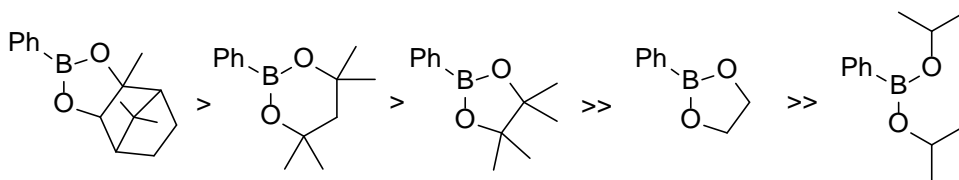
1.3.2 The electronic and structural properties of the B-O bond

The B-O bond is, as expected, stronger than the B-C bond in boronate esters due to the very large electronegativity difference between B and O ($\Delta = 1.4$). The formation of a new B-O bond is the primary thermodynamic driving force for boronate ester oxidation (Scheme 1.17).²⁵



Scheme 1.17 Kinetics and the driving force for boronate ester oxidation

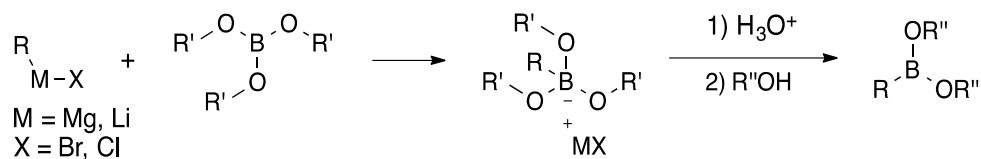
Since alkenyl and aryl boronate esters are less electrophilic than their alkyl counterparts, they also have increased stability to oxidation. Kinetically, hydration of boronate esters by H₂O is a slow process; thus, most boronate esters are stable and can be handled in ambient air. The relative thermodynamic stability of a given boronate ester is largely dependent on the size and electronics of its oxygen substituents. The stability of a wide range of aryl boronate esters has been studied.²⁹ The study showed that cyclic boronate esters are more stable than their non-cyclic analogues, and six-membered cyclic boronate esters are more stable than their five-membered analogues (Scheme 1.18).



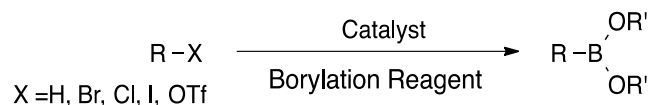
Scheme 1.18 Stability towards hydrolysis for a series of boronate esters

1.4 THE SYNTHESIS OF BORONATE ESTERS

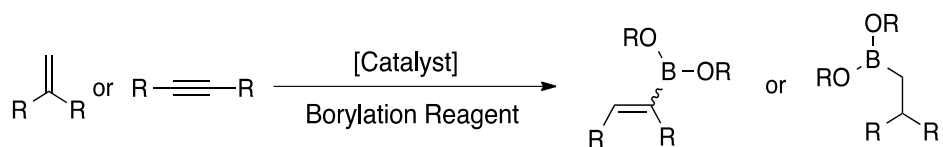
There are number of methods available for the synthesis of boronate esters, most begin with inexpensive boron derivatives or any number of other borylation reagents. A summary of the methods available for boronate ester synthesis is presented in Scheme 1.19.



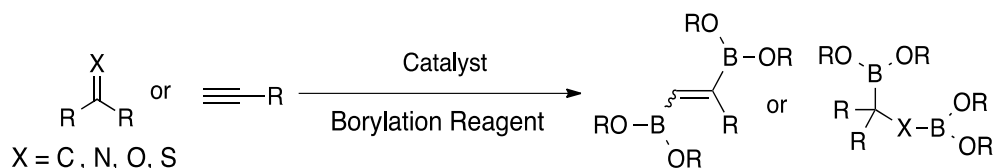
Conversion of grignard and alkyllithium reagents to boronic esters



Transition metal-catalyzed cross coupling of aromatic C-H bonds, organohalides, or triflates with a borylation reagent



addition of B-H bonds to unsaturated hydrocarbons

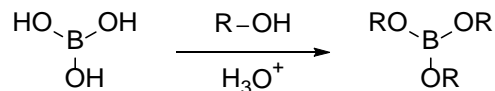


addition of B-B bonds to unsaturated C-C and C-X bonds

Scheme 1.19 A summary of the methods available to synthesize boronate esters.

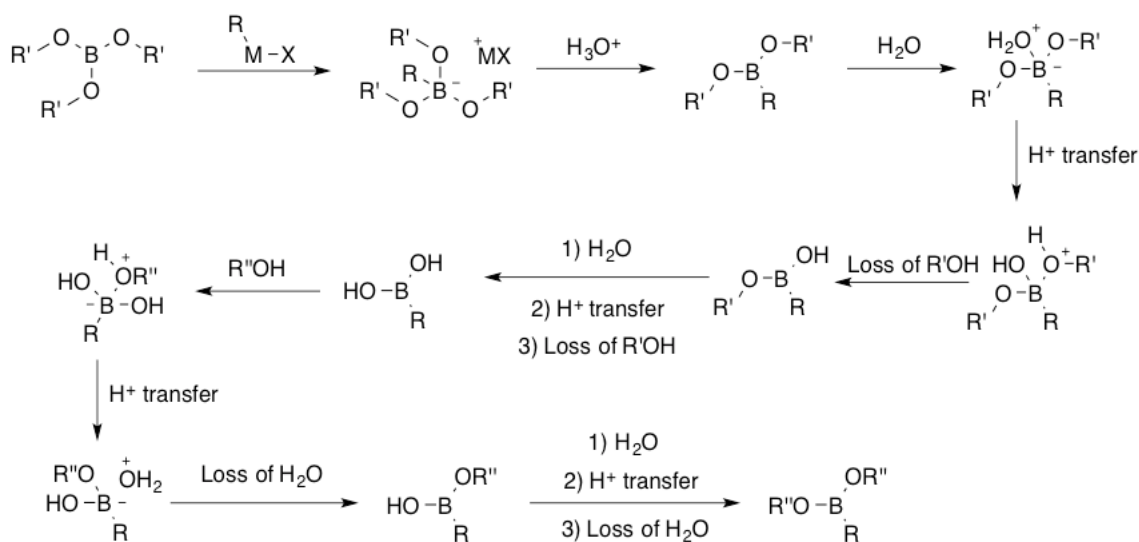
1.4.1 The conversion of organometallic reagents into boronate esters

The ability to convert a Grignard or organolithium reagent into the corresponding boronate ester from the borate ester is a common and well-known reaction.³⁰⁻³¹ The starting borate ester is derived from inexpensive boric acid,³² and a large number of nucleophilic organometallic reagents are available (Scheme 1.20).



Scheme 1.20 The facile synthesis of borate esters from boric acid

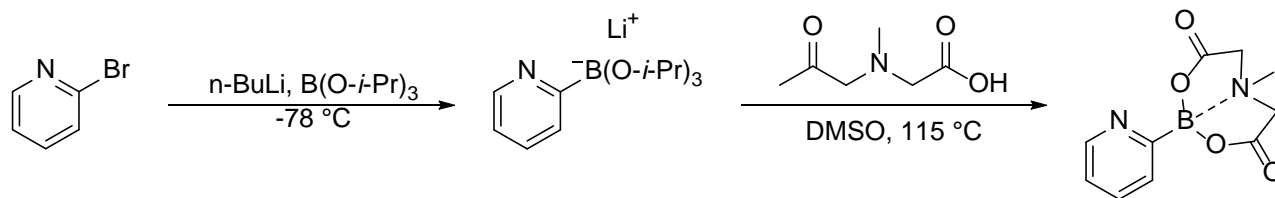
This mechanism follows the reactivity pattern seen in several reactions of boronate esters (Scheme 1.21). The borate ester reacts with the organometallic reagent to form a tetrahedral borate salt, which loses a ligand to acid to restore the trigonal boronate ester, this first step forms the desired C-B bond. The addition of H₂O in the presence of acid leads to formation of the boronate acid, which can undergo transesterification in the presence of a alkoxy/aryloxy ligand to form the desired boronate ester. The boronate acid or initially formed boronate ester can usually be isolated but one pot synthesis of boronate esters is far more common.^{25, 33}



Scheme 1.21 Mechanism for the conversion of borate esters into boronate esters.

A recent example from the literature is the synthesis 2-pyridyl boronate acid surrogates by utilizing N-methyliminodiacetic acid (MIDA) as a ligand and an acid (Scheme 1.22).³⁴ The addition of *n*-butyllithium to 2-bromopyridine followed by triisopropyl borate gives a tetrahedral adduct. The addition of MIDA leads to the boronate acid, and then transesterification with MIDA

forms the boronate ester all in a single step. This elegant example shows the utility of this method to synthesize the otherwise unstable 2-pyridyl boronate acid surrogates.

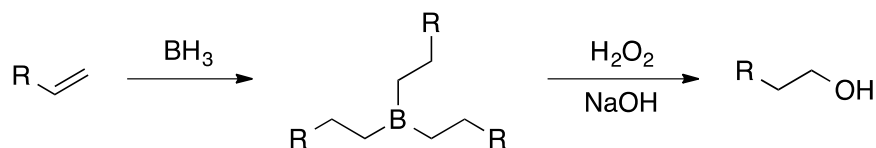


Scheme 1.22 Synthesis of 2-pyridyl MIDA boronate ester

The use of nucleophilic organometallic reagents to synthesize boronate esters allows for selection of the newly formed C-B bond and the desired ligand. One major disadvantage is incompatibility of the highly nucleophilic organometallic reagent with electrophilic functional groups. One way to circumvent this issue is to utilize transition metals in conjunction with borylation reagents.

1.4.2 The addition of B-H to double and triple bonds.

The addition of a B-H bond to a C-C double bond is ubiquitous in organic chemistry and remains an integral part of course curriculum in undergraduate organic chemistry. In fact, the development of the majority of organoboron chemistry can be traced back to 1959 when Herbert C. Brown discovered that the hydroboration-oxidation of terminal alkenes gave primary alcohols in an anti-Markovnikov fashion (Scheme 1.23).³⁵⁻³⁶ Since then, the scope of B-H addition to unsaturated hydrocarbons has expanded to include internal alkenes,³⁷ alkynes,³⁸ allenes,³⁹ 1,4 dienes,⁴⁰ and α,β -unsaturated ketones.⁴¹ Since then, the scope of B-H addition to unsaturated hydrocarbons has expanded to include internal alkenes,³⁷ alkynes,³⁸ allenes,³⁹ 1,4 dienes,⁴⁰ and α,β -unsaturated ketones.⁴¹



Scheme 1.23 Hydroboration-oxidation using BH_3

Hydroboration-oxidation begins with multiple additions of a B-H to an alkene to give an alkylborane intermediate, which can be oxidized to the less-substituted alcohol in the presence of H_2O_2 and NaOH. Some commonly seen hydroboration reagents are shown in Figure 1.6.

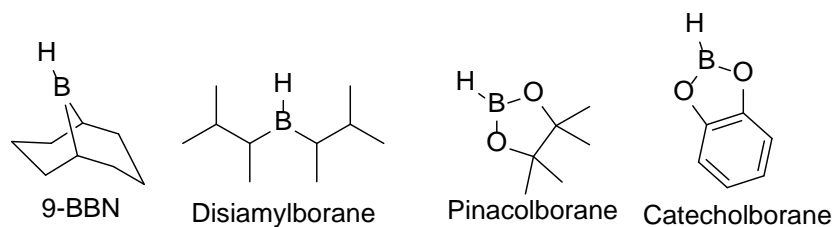
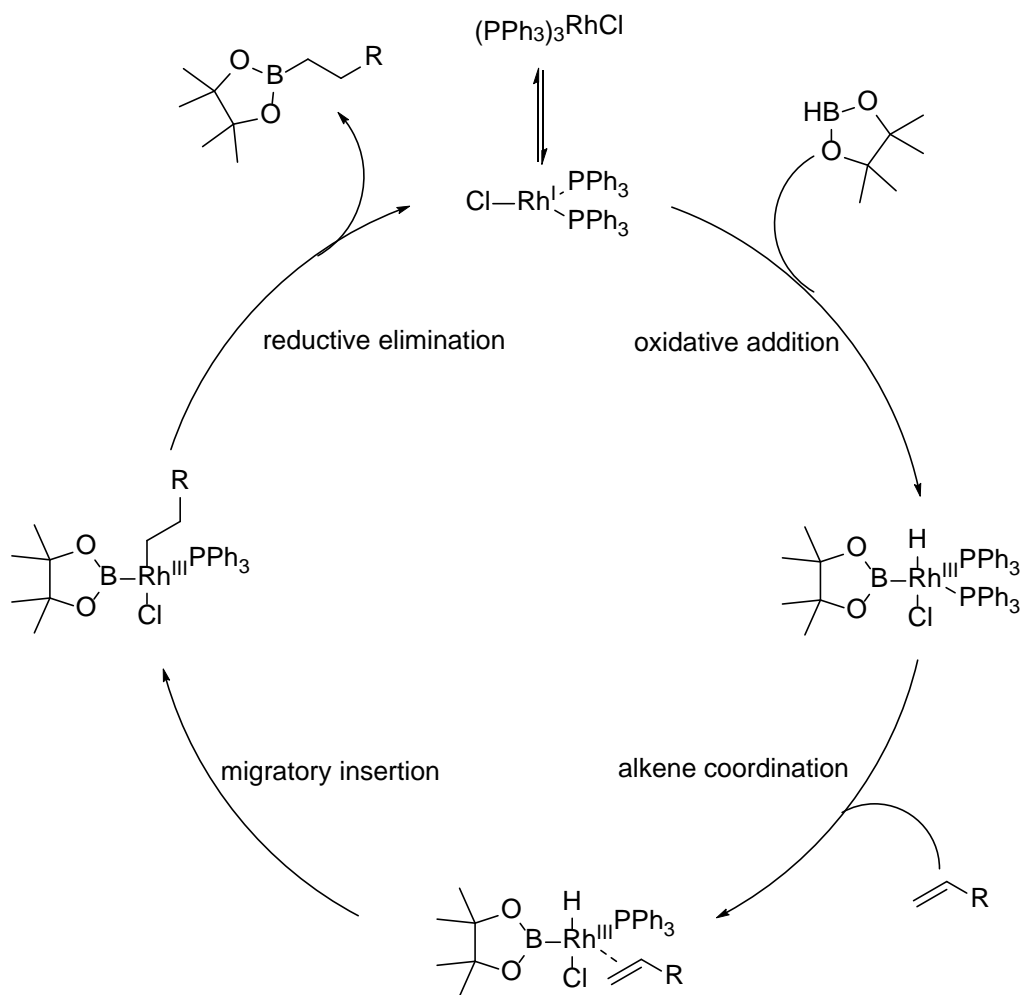


Figure 1.6 Common hydroboration reagents

B-H addition of pinacolborane and catecholborane to form a boronate ester is not as facile as organoborane addition due to the electron-donating abilities of the adjacent oxygens.⁴² To avoid these issues, catalytic methods that utilize $\text{Rh}(\text{PPh}_3)\text{Cl}$ as a catalyst for less reactive borylation reagents such as pinacolborane and catecholborane.

The catalytic cycle (Scheme 1.24) begins with ligand dissociation to give the active Rh(I) catalyst. Oxidative addition of pinacolborane gives a $14 e^-$ Rh(III) boryl species. Alkene coordination followed by migratory insertion into the Rh-H bond attaches the terminal olefin; finally, oxidative addition regenerates the catalyst and gives the borylated product.



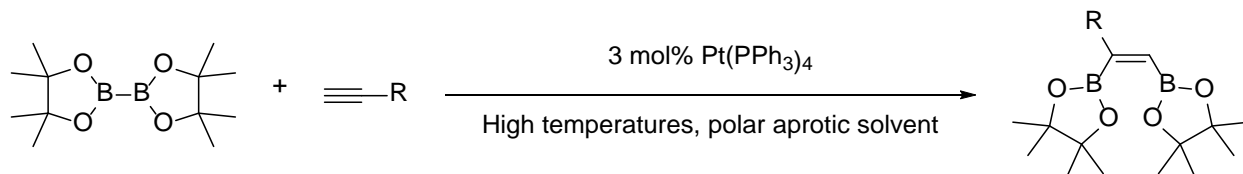
Scheme 1.24 Catalytic cycle for the hydroboration of alkene by HBpin

1.4.3 The addition of B-B to unsaturated compounds

The final method for the synthesis of boronate esters (and the most important in regards to the content of this document) is the addition of B-B to C-C and C-heteroatom multiple bonds.

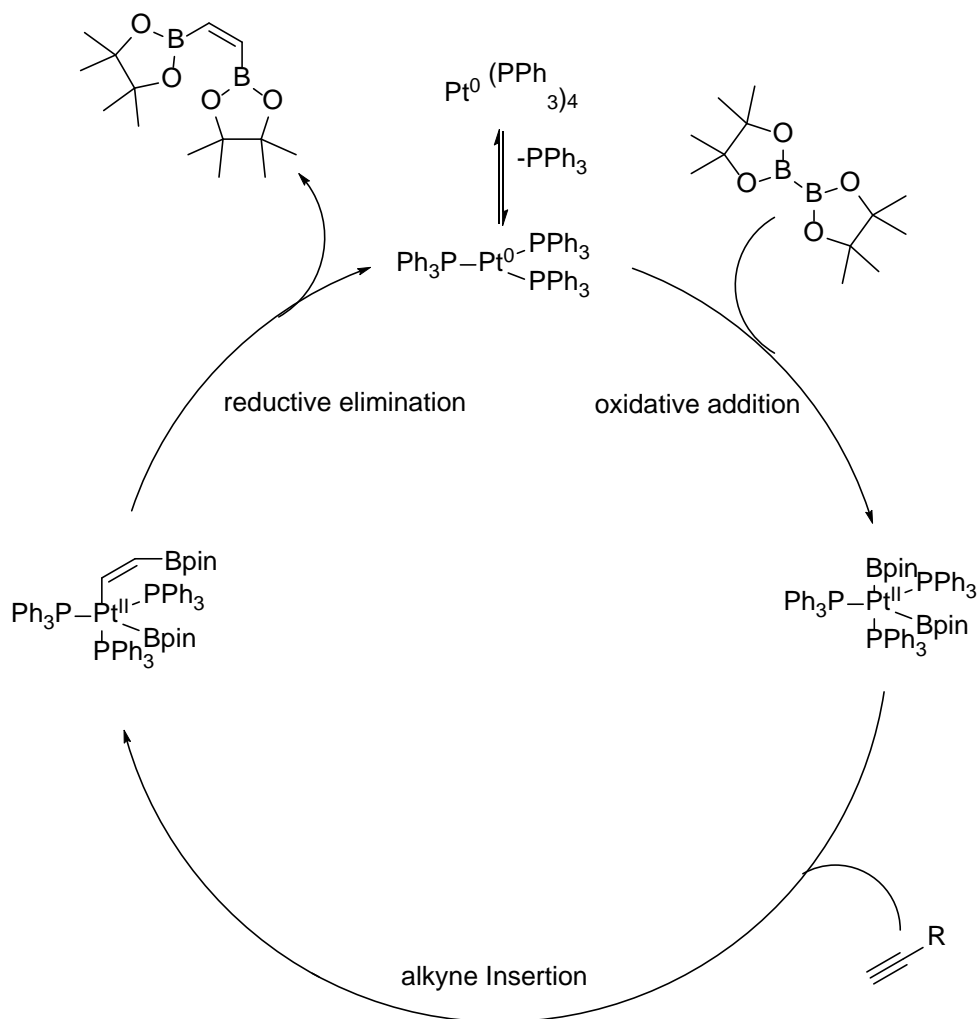
Bis(boronate esters) have attracted a lot of attention as useful synthetic intermediates due to their ability to form multiple C-C bonds in a single step and through functionalization of the C-B bond.

There are a number of synthetic routes to access bis(boronate esters); however, many require the use of specific substrates or harsh reaction conditions.⁴³ The first direct catalytic diboration was developed by Suzuki and Miyaura in 1994, when they discovered that a catalytic amount of $\text{Pt}(\text{PPh}_3)_4$ resulted in the diboration of alkynes by B_2pin_2 (Scheme 1.25).⁴⁴



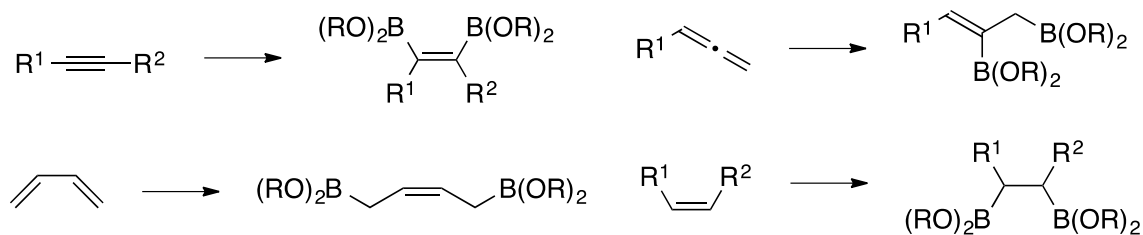
Scheme 1.25 Pt^0 catalyzed diboration of alkynes

The catalytic cycle (Scheme 1.26) begins with ligand dissociation to give the tricoordinated $16 e^- \text{ Pt}(0)$ complex. Oxidative addition of the B-B bond results in the formation of Pt-diboryl species, which undergoes alkyne insertion into the Pt-B bond. Finally, reductive elimination releases the product and regenerates the active catalyst.



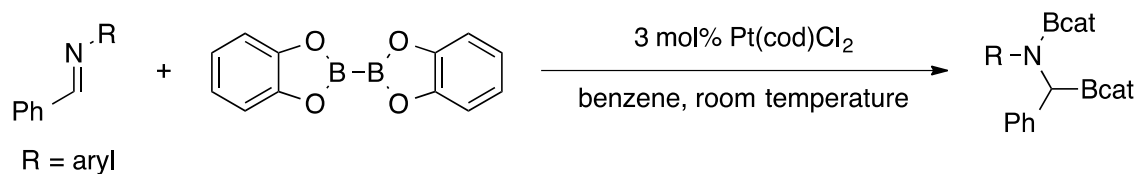
Scheme 1.26 Catalytic cycle for the diboration of alkynes using Pt(PPh₄)

Alkenes,⁴⁵ allenes,⁴⁶ and 1,3 dienes⁴⁷ are all employable as substrates using Pt (0) to give a variety of bis(boronate esters) (Scheme 1.27).⁴⁸ There are also examples of Rh,⁴⁹ Ni,⁵⁰ Pd,⁵¹ Cu⁵², and transition metal free diborations⁵³ of unsaturated compounds.



Scheme 1.27. Substrate scope for the catalyzed diboration of unsaturated hydrocarbons

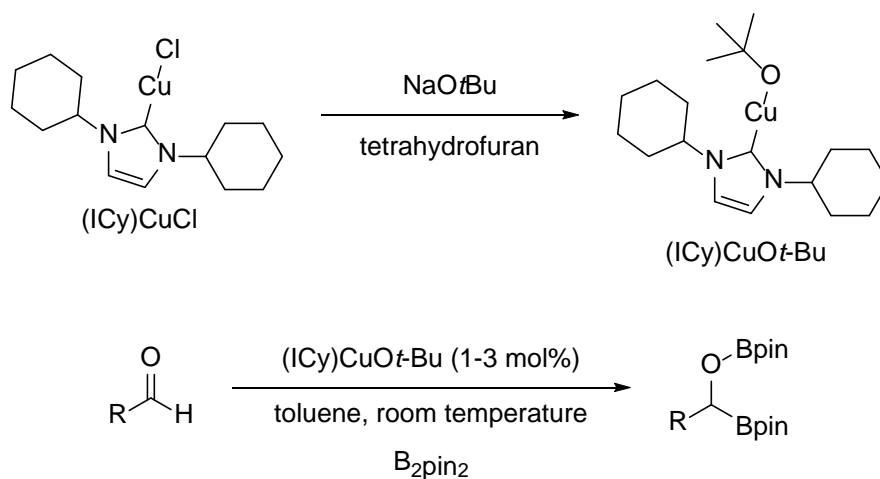
C-heteroatom double bonds are also employable as substrates for B-B additions, this allows for the synthesis of boronate esters that have a heteroatom adjacent to the boronate ester. Aside from their utility as valuable synthetic intermediates, boronate esters that contain an adjacent heteroatom are key intermediates to access the self-immolative linker described in this document. There are several examples of α -heteroatom boronate esters in the literature prior to a catalyzed diboration of a C-heteroatom multiple bond; however, their synthesis requires multiple steps and has limited scope. The first diboration of a C-heteroatom double bond from readily available starting materials utilized a Pt^0 catalyst and B_2cat_2 as a borylation reagent and aldimines as substrates (Scheme 1.28). Unfortunately, due to the labile nature of the B-cat group, selective B-N cleavage was never accomplished.



Scheme 1.28 A platinum catalyzed diboration of aldimines

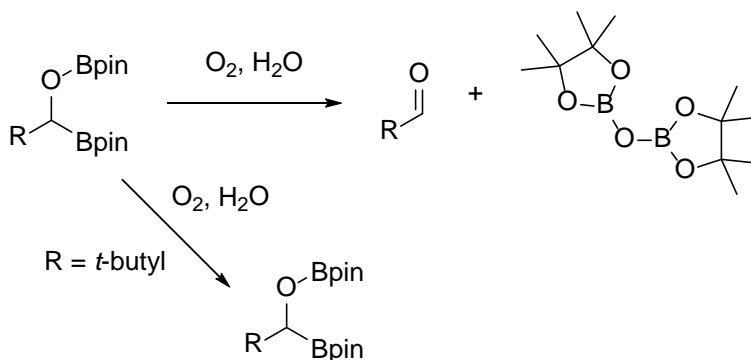
Many years later, an N-heterocycle carbene (NHC) copper catalytic system was developed that used B_2pin_2 as a borylation reagent and aldehydes as substrates (Scheme 1.29).⁵⁴ Synthesis

and handling of the catalyst and resulting products require the use of highly inert conditions and long reaction times.



Scheme 1.29 Cu catalyzed diboration of aldehydes using (ICy)CuOt-Bu

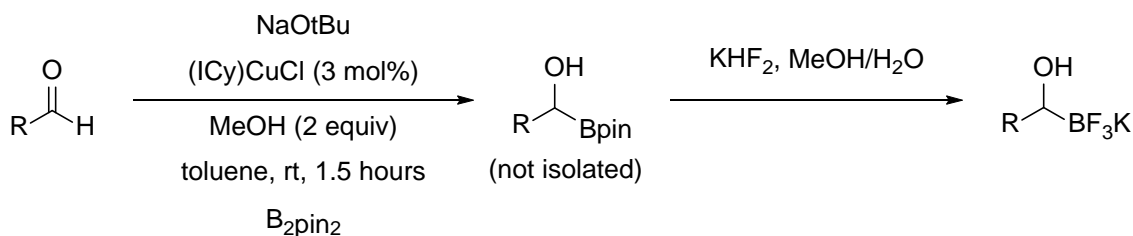
Synthesis of the diboronate ester products without the use of a glove box leads to decomposition into starting aldehyde and pinB-O-Bpin (Scheme 1.30). Only a single α -hydroxy boronate (resulting from selective B-O cleavage) was isolated (derived from pivaldehyde) in moderate yield.



Scheme 1.30 Decomposition pathways of borylated aldehydes

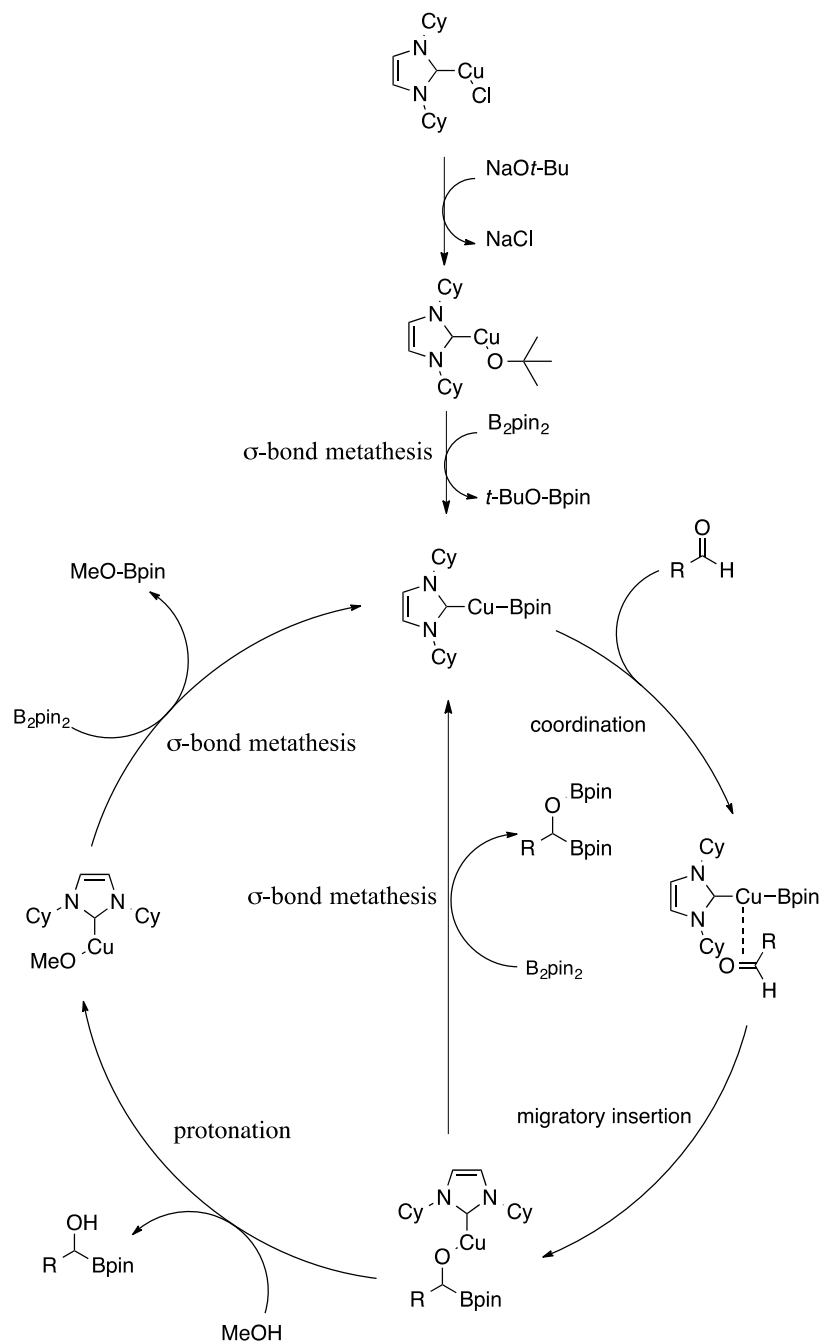
Since the discovery that ICy(Cu)O-tBu could efficiently catalyze the diboration of aldehydes, many improvements have been made to simplify the conditions and increase the scope.

Although only a single α -hydroxy boronate ester derived from an aldehyde has been isolated, α -hydroxy potassium trifluoroborate salts have been synthesized from aldehydes using the (ICy)Cu-*Ot*Bu catalyst system (Scheme 1.31).⁵⁵ The addition of methanol enhances the rate of the reaction, allowing full conversion in 1.5 hours.



Scheme 1.31 The synthesis of α -hydroxy potassium trifluoroborate salts.

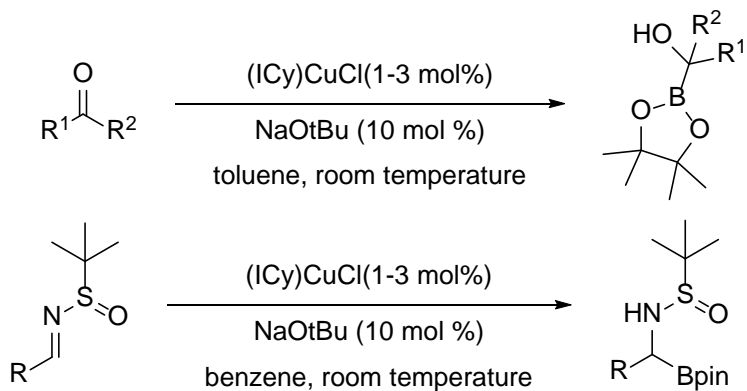
The mechanism for the diboration has been well documented (Scheme 1.32).⁵⁶ The first step is formation of a Cu-boryl species by σ -bond metathesis with Na*Ot*-Bu and B₂pin₂. The highly nucleophilic Cu-B bond adds into the aldehyde by migratory insertion. Density functional theory (DFT) calculations have shown that this is the rate determining step.⁵⁶ The Cu-O bond will then undergo σ -bond metathesis with B₂pin₂ to give the diborated aldehyde and regenerate the catalyst. In the presence of MeOH, it has been proposed that the Cu-O-B complex is protonated, giving the hydroxy boronate ester and a Cu-OMe complex. Cu-OMe can then undergo σ -bond metathesis with B₂pin₂ to regenerate the active catalyst.



Scheme 1.32 Mechanistic considerations for the diboration of aldehydes by $(\text{ICy})\text{Cu-OtBu}$

The scope of the $(\text{ICy})\text{CuOt-Bu}$ catalytic system has been expanded to include aldimines⁵⁷ and ketones (Scheme 1.33).⁵⁸ These are particularly useful substrates because the resulting tertiary

hydroxy and secondary amino-boronate esters can be purified, stored, and used in subsequent transformations.



Scheme 1.33 The diboration of sulfinylimine and ketones using (ICy)Cu-OtBu

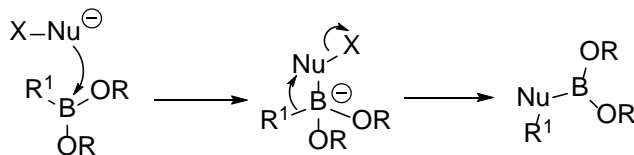
Armed with the knowledge of the synthesis of boronate esters, this discussion will turn towards the value of boronate esters as valuable intermediates to access novel organic compounds.

1.5 BORONATE ESTERS AS SYNTHETIC INTERMEDIATES

Uncatalyzed reactions of boronate esters often utilize the nucleophilicity of the C-B bond in its tetracoordinated form.

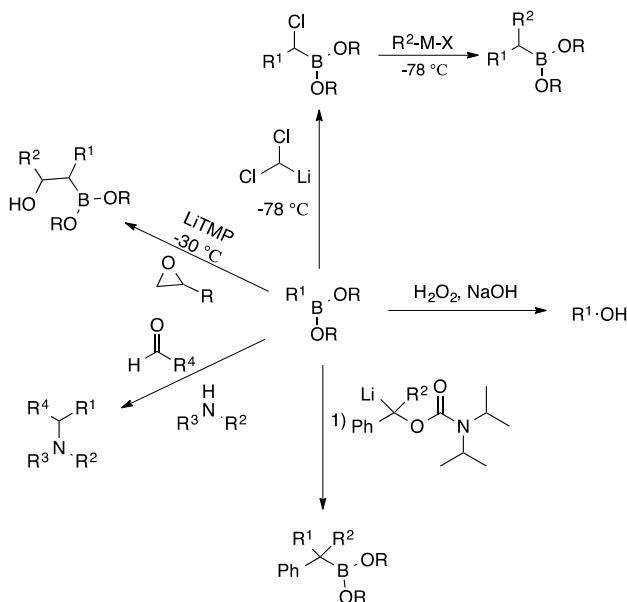
1.5.1 Transformations that utilize the nucleophilicity of the C-B bond.

The primary mode of reactivity that is seen in uncatalyzed reactions of boronate esters involves reaction of a nucleophile adjacent to a leaving group (Scheme 1.34).



Scheme 1.34 Mechanistic consideration for uncatalyzed reactions with boronate esters

The first step is the addition of the nucleophile to boron to form a tetrahedral adduct. The resulting C-B bond is highly nucleophilic and undergoes intramolecular attack on the pendant-leaving group. This mechanism has been consistently seen in almost all non-catalyzed reactions of boronate esters. The array of reactions that have been developed using this strategy is shown in Scheme 1.35.



Scheme 1.35 Uncatalyzed transformations of boronate esters

The first examples of nucleophiles with leaving groups reacting with boronate ester (aside from H_2O_2 oxidation) were homologation reactions using $\text{Cl}_2\text{C}(\text{H})\text{Li}$ to form α -halo boronate esters and subsequent substitutions with organometallic reagents.⁵⁹ These reactions allow for full stereochemical retention. Enantioselectivity can be achieved using chiral boronate esters such as those shown in Figure 1.7.³³

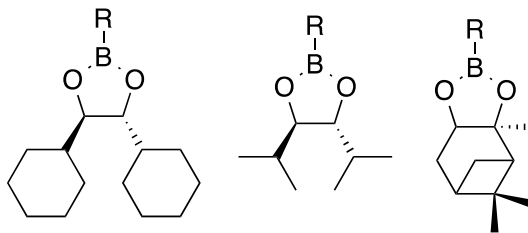
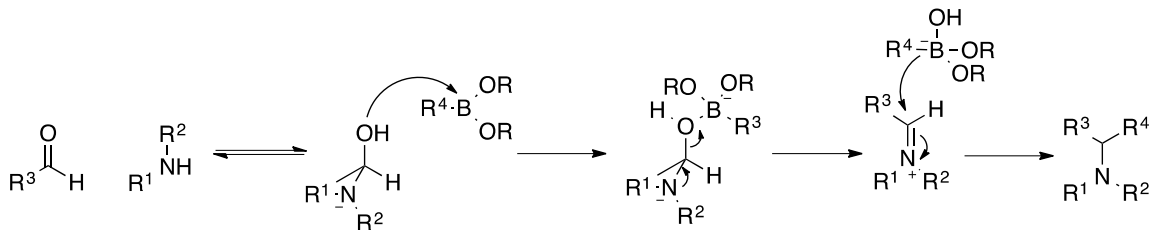


Figure 1.7 Chiral boronate esters

The Aggarwal group utilized lithiated epoxides and carbamates as pendant leaving groups in the synthesis of enantiopure 1,2 diols,⁶⁰ and tertiary alcohols.⁶¹

Boronate esters can also participate in what is known as a Petasis reaction which allows the synthesis of substituted amines.⁶² The first step is condensation to form the imminium ion (Scheme 1.36), which is catalyzed by the oxophilic character of the boronate ester. This is followed by nucleophilic attack by the tetracoordinated C-B bond to form a tertiary amine. Many of the steps for the Petasis reaction are analogous to the Mannich reaction.



Scheme 1.36 The mechanism for the Petasis reaction

Oxidation of organoboron boron compounds by H_2O_2 follows the same reaction pattern seen in Scheme 1.34. In H_2O_2 the pendant-leaving group is $-\text{OH}$ and the product is derived from

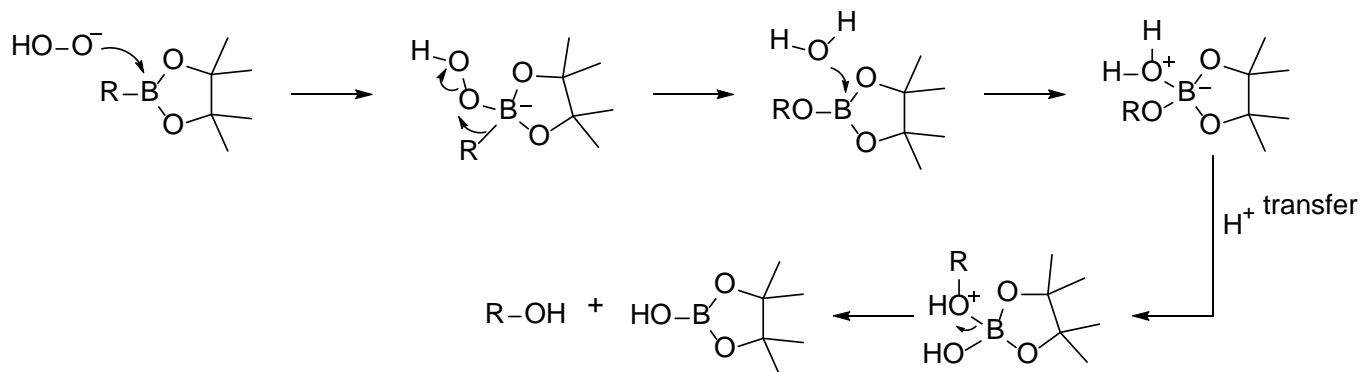
alcohol hydrolysis of the borate ester. The mechanistic details of boronate oxidation will be presented in 1.6.

1.6 BORONATE ESTERS AS PRODRUGS AND PROBES FOR H₂O₂

H₂O₂ is a non-radical oxidant that is present in aerobic organisms. Initially H₂O₂ was viewed as a detrimental byproduct of cellular respiration; however, in recent years, a large body research has determined that the concentration of H₂O₂ and other reactive oxygen species (ROS) plays a vital role in protein folding and signaling, defense response, and respiration.⁶³ The concentration of H₂O₂ in eukaryotic cells undergoing oxidative stress is disputed in the literature and shown to be organelle dependent; with higher concentrations found in the cytosol, mitochondria, and peroxisome. Reported concentrations are typically 0.1-1 μM for homeostatic base levels and 10-100 μM are typically enough to induce cells into undergoing a physiological response. The *in vivo* quantitation of H₂O₂ is a challenge due to non-specific reactivity with other reactive oxygen species (ROS) by traditional methods and the transient nature of ROS in living systems.² As a result, there has been significant effort to unravel the benefits and drawbacks of H₂O₂ within living systems.

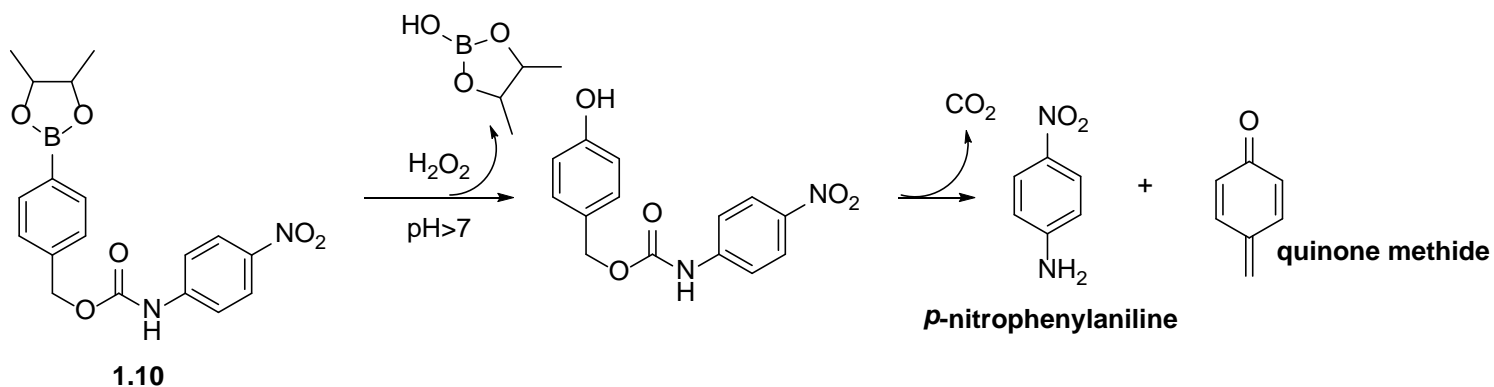
Boronate esters are attractive as probes for the detection of H₂O₂ within living systems because of their specific reactivity with H₂O₂ and no other ROS typically found within the cell such as superoxide (O₂⁻) or hydroxyl radical (•OH).² The oxidation of boronate esters to alcohols is bioorthogonal; any chemical reaction that can occur inside of living systems without interfering with native biochemical processes.⁶⁴

The mechanism for boronate oxidations begins with nucleophilic H_2O_2 reacting with the empty p-orbital on boron to form a negatively charged tetrahedral boronate complex (Scheme 1.37). This forms a nucleophilic C-B bond that undergoes a 1,2 boryl migration to give the borate ester, which rapidly undergoes hydrolysis under physiological conditions to give an alcohol.²



Scheme 1.37 Mechanism for the oxidation of boronate esters by H_2O_2

Since the discovery that the oxidation of boronate esters is compatible with biological systems, their utility as a trigger in self-immolative linkers has been demonstrated many times. The first example of a boronate ester being used as a trigger in self-immolative system was reported by Lo.⁶⁵ In this design (Scheme 1.38), boronate ester **1.10** undergoes oxidation by H_2O_2 followed by a spontaneous 1,6 benzyl elimination to release an equivalent of **quinone methide** and ***p*-nitrophenylaniline** (or the fluorescent amino coumarin reporter).



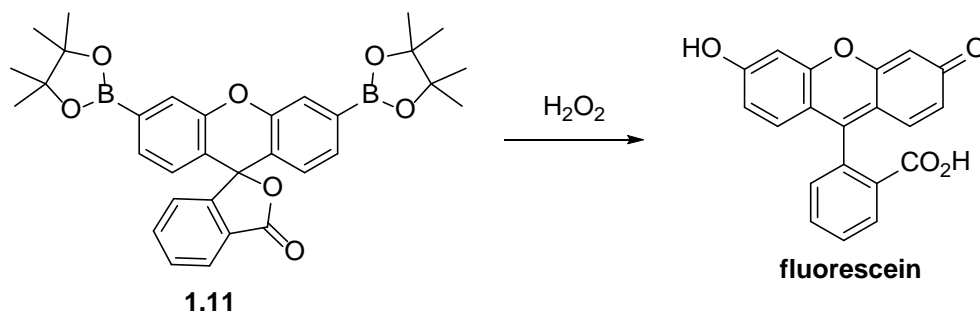
Scheme 1.38 The first report of a boronate ester based self-immolative linker.

Since this discovery several groups have utilized boronate esters as triggers for H_2O_2 . In this section, approaches that utilize boronate oxidation as a probe for H_2O_2 as well as self-immolative mechanisms for the development of targeted therapeutics will be discussed to establish the framework that led to the novel work performed by the author.

1.6.1 Boronate esters as fluorescent probes for H_2O_2

Boronate esters were first identified as excellent triggers for H_2O_2 by the Chang group.⁶³

Their initial design utilizes boronate ester **1.11** shown in Scheme 1.39.



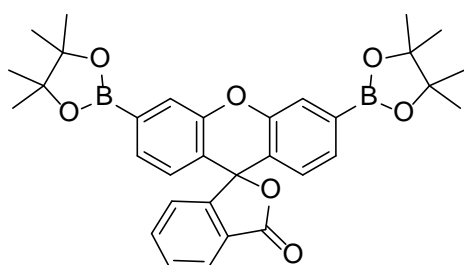
Scheme 1.39 Fluorescein Derivative as a probe for H_2O_2

In the presence of H_2O_2 , **1.11** reacts to form a phenol, which undergoes a quinone-methide elimination to open the lactone and release **fluorescein**. Since the oxidation of aryl boronate esters was found to be compatible with biological systems, the Chang group has introduced a wide pallet

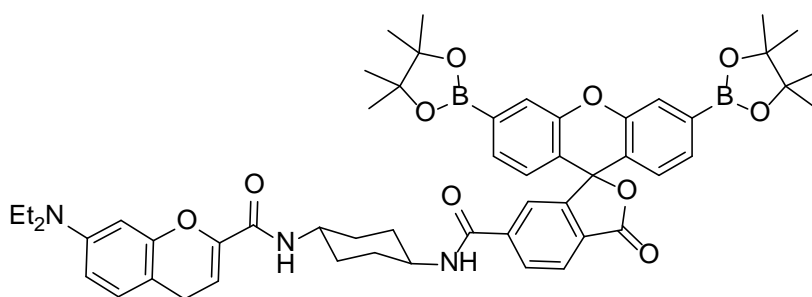
of probes to serve several purposes. This includes probes that turn on in the presence of H_2O_2 give different colors, ratiometric H_2O_2 probes, probes that localize to specific organelles such as lysosomes and mitochondria, and probes for live tissue imaging.² Figure 1.8 shows the structural variations as well as the different probes that are available for imaging of H_2O_2 in living systems.

Probe for the detection of exogenous H_2O_2

A ratiometric probe for the detection of H_2O_2



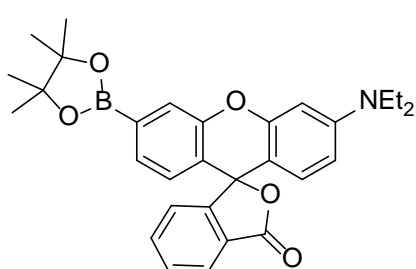
1.11



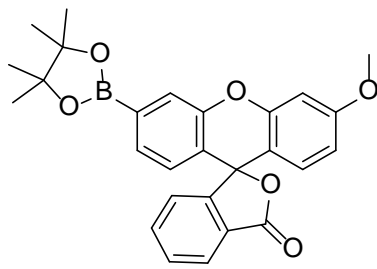
1.14

Probe for the detection of endogenous H_2O_2

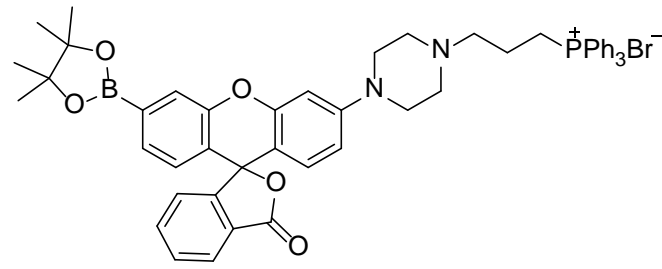
Mitochondrial localization probe for H_2O_2



1.12

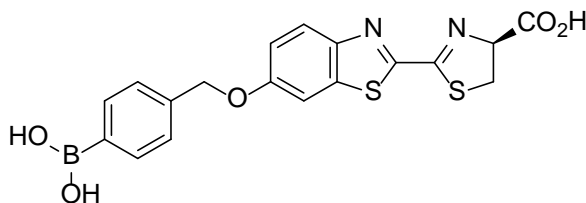


1.13



1.15

Probe for live animal imaging of H_2O_2



1.16

Figure 1.8. Probes for H_2O_2 developed by the Christopher Chang group

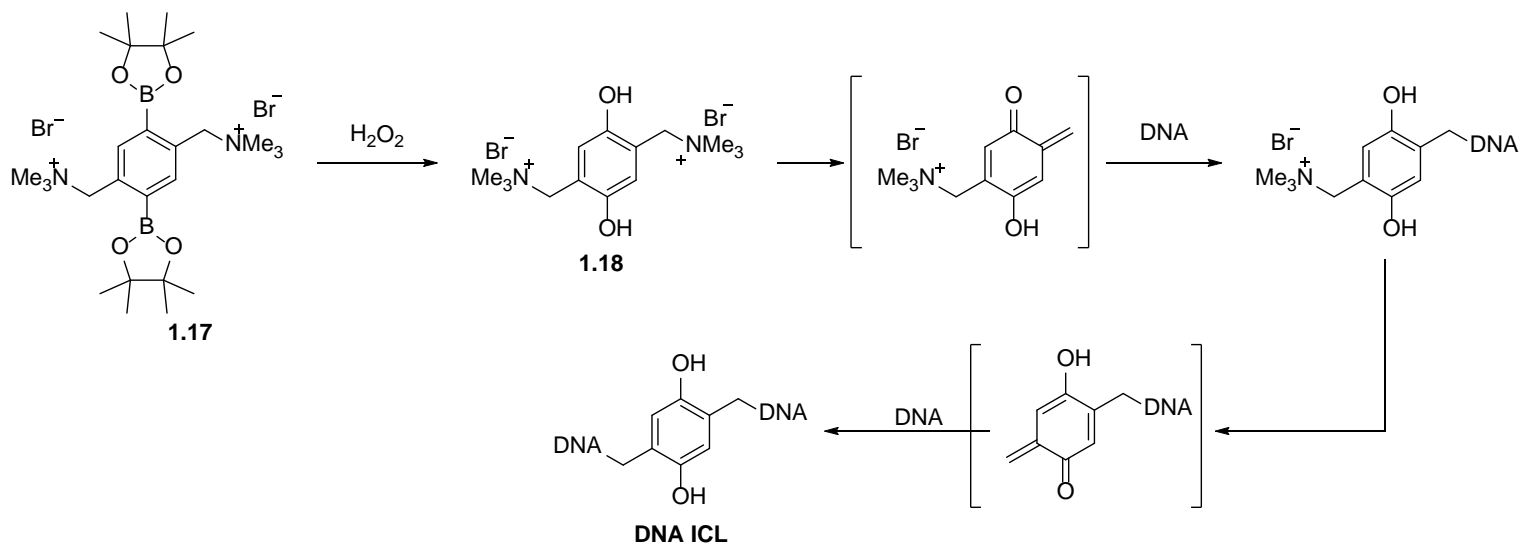
Compound **1.11** represents the first generation of probes that utilizes bis boronate esters and had the ability to detect H_2O_2 over other relevant reactive oxygen species (ROS) such as tert-

butyl hydroperoxide (TBHP), O_2^- , NO, ^-OCl , and $\bullet OH$.⁶³ **1.11** can image H_2O_2 at high micromolar ranges, a range that is relevant to states of oxidative stress. **1.11** was not sensitive enough for the detection of endogenously produced H_2O_2 , which led to the development of monoboronate probes **1.12** and **1.13**. This next generation of caged fluorophores only require a single H_2O_2 equivalent yield their fluorescent product, increasing sensitivity and allowing detection of endogenously produced H_2O_2 .⁶⁶ Once boronate ester oxidation had been established as biorthogonal, the ratiometric probe **1.14** that utilizes fluorescence resonance energy transfer (FRET) was developed.⁶⁷ FRET probe **1.14** allows for the measurement of two signals that change differentially with H_2O_2 concentrations. Probe **1.15** utilizes the triphenylphosphonium salt (known as Murphy's salt)⁶⁸ as a lipophilic cation for mitochondrial localization. Probe **1.15** allows for visualization of discrete oxidative stress changes confined to the mitochondria.⁶⁹ Finally, probe **1.16** allows for live tissue and animal imaging. **1.16** utilizes the bioluminescent luciferin fluorophore as well as a self-immolative mechanism.⁷⁰ This work demonstrates that boronate oxidation is sensitive to the micromolar concentrations of H_2O_2 found in cells and compatible with living systems.

1.6.2 Boronate Ester based Prodrugs

Several chemotherapy drugs rely on DNA interstrand crosslinking (ICL) as their primary mechanism of action; however, host toxicity continues to be a major problem. Targeted chemotherapy inspires the development of boronate ester based prodrugs; this is because several tumor cells produce higher levels of H_2O_2 than healthy cells.⁷¹ To overcome this limitation boronate ester based prodrug **1.17** was developed to release DNA alkylating agents upon oxidation

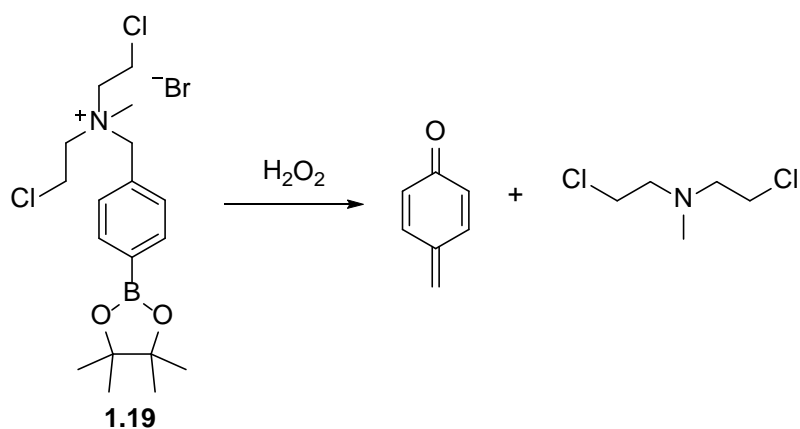
by H_2O_2 (Scheme 1.40). The primary mechanism of action occurs by oxidation of the boronate ester to phenol **1.18**, followed by a 1,4 quinone methide (QM) elimination.



Scheme 1.40 Boronate ester oxidation to induce DNA ICLs

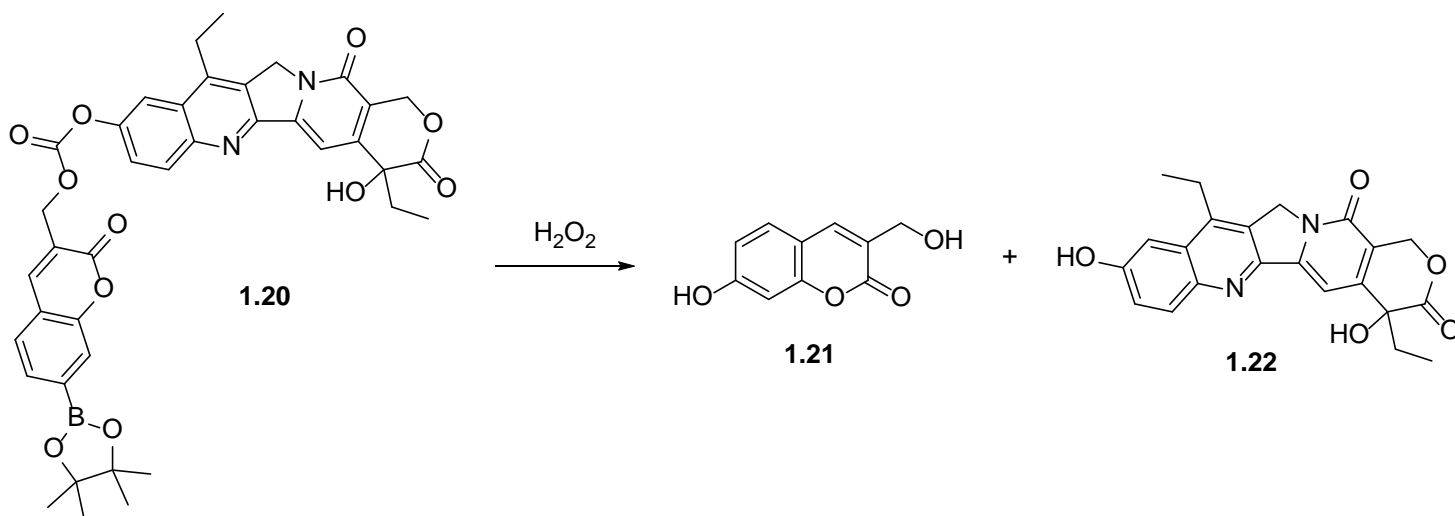
DNA rapidly reacts with this intermediate and another elimination occurs to give a QM which rapidly forms the **DNA ICL**. There are variants of these compounds that can undergo DNA cross-linking under oxidative conditions and in the presence of light; these undergo cross-linking through the formation of benzylic radicals.

Another example of a boronate ester based prodrug that releases a DNA alkylating agent is compound **1.19** (Scheme 1.41).⁷² **1.19** undergoes oxidation by H_2O_2 which causes a 1,6 elimination to release the active mustard reagent. Without H_2O_2 , the mustard reagent is not released and **1.19** does not produce host toxicity.



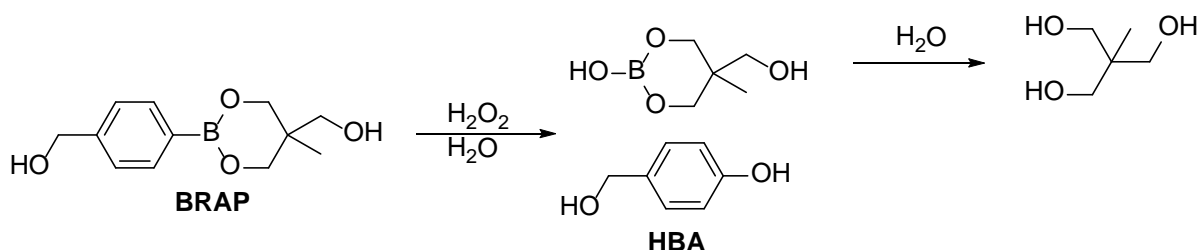
Scheme 1.41 A boronate ester based cancer prodrug

A recent example of a boronate ester based prodrug uses a different approach (Scheme 1.42).⁷³ Upon boronate oxidation, **1.20** undergoes elimination, which leads to release of fluorophore **1.21** and camptothecin derivative **1.22**. This type of approach utilizes a strategy called “theranostics” (a portmanteau of therapy and diagnostics). **1.20** was shown to selectively accumulate within metastatic tumors in mice; this strategy allows for cytotoxic agents to be tracked *in vivo*, allowing for advanced image-guided therapy strategies.



Scheme 1.42 A boronate ester based prodrug that releases cytotoxic cargo and a fluorophore

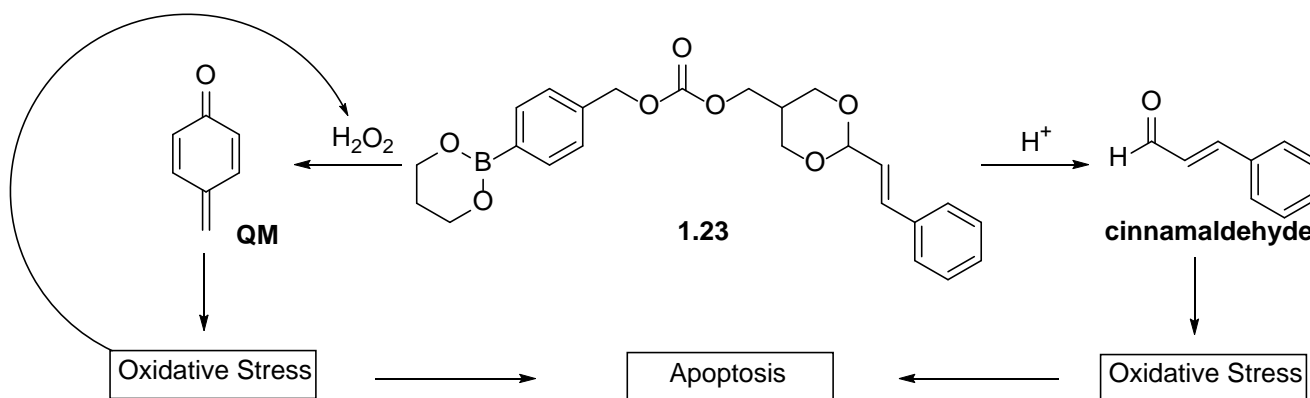
During an Ischemia-reperfusion (I/R) injury event, reperfusion of blood flow into ischemic tissues induces the formation of a large amount of H_2O_2 , which causes oxidative stress and exacerbation of tissue damage.⁷⁴ Targeted antioxidant therapy directed towards the site of an I/R injury offers advantages over classic antioxidant therapy, which suffers from off target effects and a lack of bioavailability.⁷⁵ To circumvent this issue, the boronate ester prodrug (**BRAP**) of *p*-hydroxybenzyl alcohol (**HBA**), was synthesized (Scheme 1.43).⁷⁶



Scheme 1.43 BRAP, a boronate ester prodrug for HBA, a potent antioxidant

BRAP can be specifically oxidized by H_2O_2 , limiting H_2O_2 mediated oxidative stress. The resulting oxidation also releases an equivalent of **HBA**, which has intrinsic anti-oxidant and anti-inflammatory activities; particularly in tissues undergoing oxidative stress. The boronate ester was shown to inhibit cell death and exerted anti-inflammatory activity more effectively than **HBA** alone. This work demonstrates the usefulness of boronate esters as not only a trigger for H_2O_2 but also as an effective scavenger for H_2O_2 ; a concept that the author will consider in Section 2.2.1.

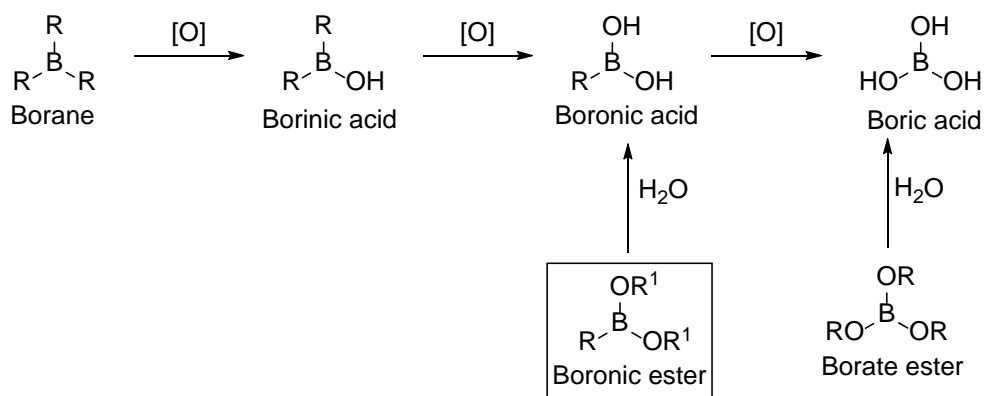
Synergy between two pharmaceutical agents occurs when a new or amplified effect can be produced that neither drug could produce on its own. Boronate ester prodrugs have been used in this fashion to amplify oxidative stress selectively in cancer cells through the release of two active agents. In the example shown in Scheme 1.44, **1.23** undergoes oxidation by H_2O_2 , which leads to the release of an equivalent of quinone-methide (**QM**), an antioxidant scavenger.⁷⁷ The low pH of the cancer cells simultaneously releases **cinnamaldehyde**, a small molecule that generates high amount of oxidative stress. This combination therapy increases oxidative stress enough to selectively kill cancer cells, while leaving healthy cells intact. More importantly, **1.23** acts in a synergistic fashion with the environment within the cancer cells.



Scheme 1.44. A dual stimuli-responsive hybrid anticancer drug

1.7 BORON CONTAINING DRUGS

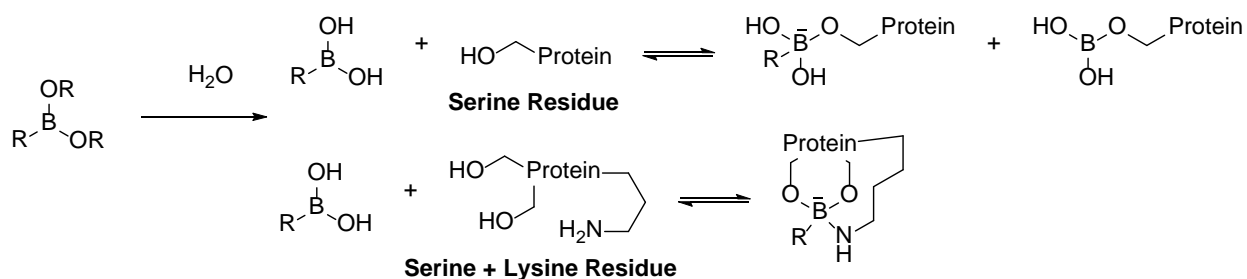
Organoboron compounds ultimately degrade by autoxidation and hydrolysis into boric acid (Scheme 1.45), a relatively non-toxic inorganic byproduct, making them useful as potential therapeutics.⁷⁸



Scheme 1.45 Ultimate degradation of organoboron compounds into boric acid.

1.7.1 Boron in Medicinal Chemistry

Pharmaceutical companies often avoid boron containing compounds because they can form reversible covalent bonds with side chains on proteins. Covalent modifications often lead to higher levels of toxicity; thus, funding of drug candidates that function through irreversible drug modification is a high risk endeavor.⁷⁹ It is tempting to assume that boron is simply another electrophile, similar to acrylates, epoxides, and aldehydes. Boron is different in that its covalent modifications are reversible. Additionally, boron has multiple coordination preferences, this differentiates its interactions from typical electrophiles (Scheme 1.46).⁸⁰ These reversible covalent interactions are what gives boron containing molecules unique interactions with their targets.



Scheme 1.46. Boron's coordination preferences with amino acids

Boronate esters can act as bioisosteres for phenols. One of the earliest examples of a boronate ester being modified in this way was the development of a boron-based 4-hydroxy tamoxifen derivative **1.24** (Figure 1.9).⁸¹ **1.24** converts to the phenol forms under oxidative conditions in breast cancer cells. Additionally, boronate ester modified Camptothecin derivative **1.25** showed increased activity against several cancer cell lines.⁸² A more recent example demonstrates that boronate oxidation can be utilized in living systems. Boronate ester **1.26**, a modified Bellinostat derivative, showed increased efficacy in treating solid tumors than Bellinostat, suggesting its potential in a clinical setting.⁸³

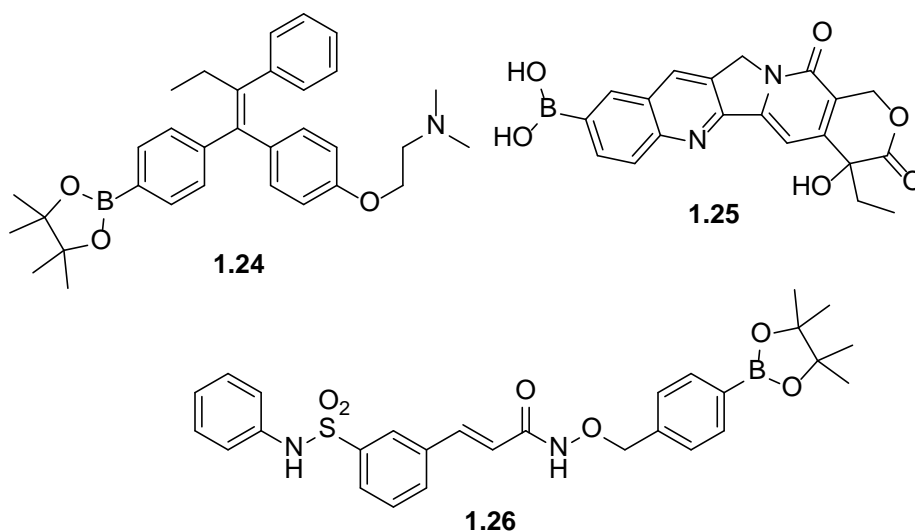


Figure 1.9. A sample of boronate esters being utilized as bioisosteres for phenols

1.7.2 Boron in pharmaceutical agents

There are four boron containing therapeutics that have been approved by the FDA (Figure 1.10). **Velcade** is widely prescribed for multiple myeloma by oncologists.⁸⁴ Thanks to a number of efforts by the biopharmaceutical company Anacor, **Tavaborole** was approved as a topical antifungal medication in July 2014.⁸⁵ **Crisaborole**, also developed by Anacor, was approved for eczema in 2016 and is currently undergoing clinical trial for psoriasis. **Vaborbactam**, discovered by Rempex pharmaceuticals, restores potency to existing antibiotics by inhibiting the beta-lactamase enzymes that would otherwise degrade them. When combined with an appropriate antibiotic it can be used for the treatment of gram negative bacterial infections.⁸⁶ **Vaborbactam** was approved for use in conjunction with Meropen for the treatment of complicated urinary tract infections and pyelonephritis in 2017.

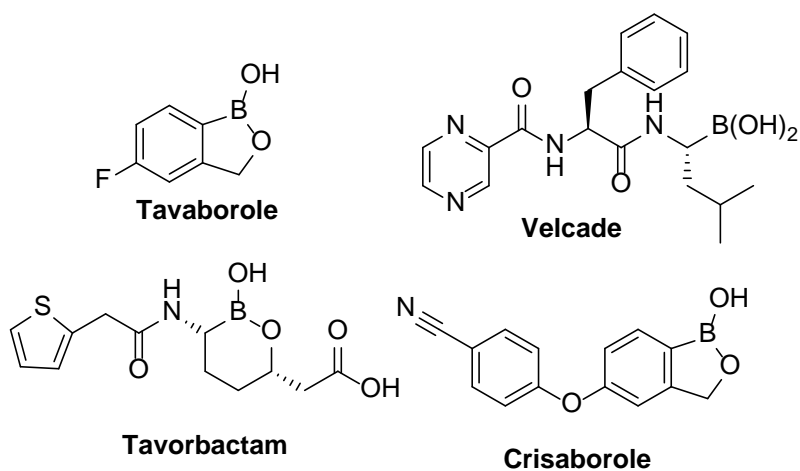
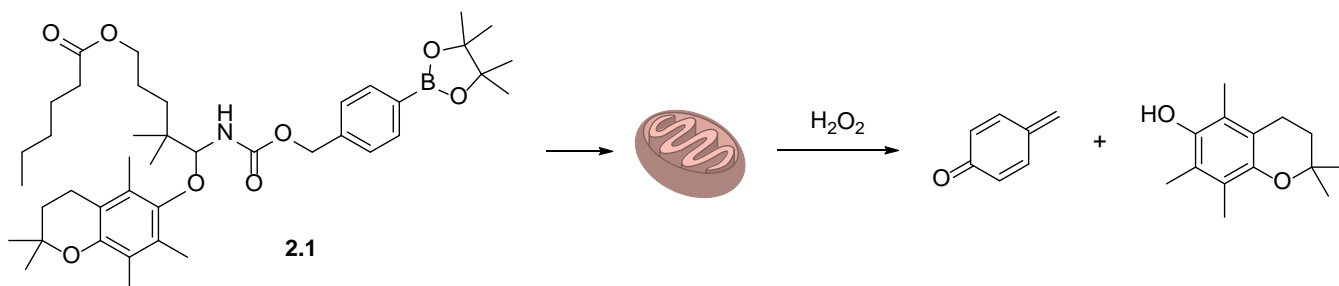


Figure 1.10 Boron-containing drugs approved by the FDA

There several other boron containing drugs going through clinical trials that have the potential to be utilized as anticancer, antiviral, and antifungal agents; however, discussing their properties is beyond the scope of this document. The next chapter of this document describes the specific contributions that that author has made to this field.

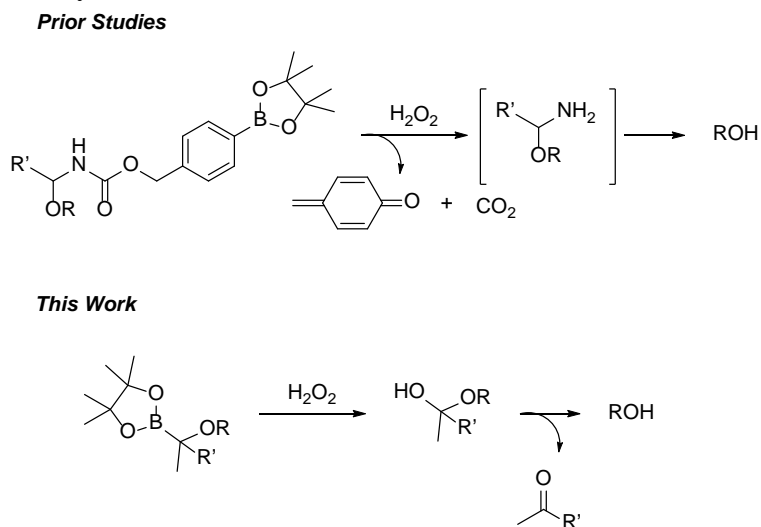
2.0 THE UTILIZATION OF BORONATE ESTERS FOR THE OXIDATIVELY TRIGGERED RELEASE OF ALCOHOLS, KETONES, AND ALDEHYDES

Previous work from the Floreancig group focused on the development of a novel carrier to deliver antioxidants to the mitochondria in an effort to mitigate damage from radiation.⁸⁷ In this work, a series of α -alkoxy carbamates were synthesized using a multicomponent reaction consisting of a nitrile hydrozirconation, acylation, and alcohol addition. These compounds were found to rapidly release their respective cargo specifically in the presence of H_2O_2 via the quinone-methide elimination discussed in 1.1.2. The arylboronates are compatible at biologically relevant concentrations, suggesting their potential for use in living systems. Using the multicomponent hydrozirconation, acylation, and alcohol addition sequence; compound **2.1** was synthesized (Scheme 2.1). Compound **2.1** was designed to act as an agent that mitigates radiation damage by suppressing the formation of ROS. Pentamethyl chromanol (PMC), was selected as a simplified Vitamin E derivative and potent antioxidant.⁸⁸ The triphenylphosphonium cation (also known as Murphy's salt) promotes mitochondrial localization.⁶⁸ Unfortunately, treatment of cells with compound **2.1** led to cell death. We reasoned that the toxicity of **2.1** resulted from the release of an equivalent of quinone methide, a potent DNA alkylator.¹⁹



Scheme 2.1 An oxidatively triggered boronate ester designed to localize in the mitochondria of cells to release an equivalent of quinone methide, and an antioxidant.

To circumvent this issue, we reasoned that new synthetic methodology for the synthesis of α -hydroxy boronate esters would enable access to novel molecular scaffold for the release of alcohols without the release of toxic byproducts. This led to the development of the first oxidatively triggered alkylboronate ester based self-immolative linker (Scheme 2.2).



Scheme 2.2 A novel scaffold for the release of alcohols that circumvents the release of quinone methide

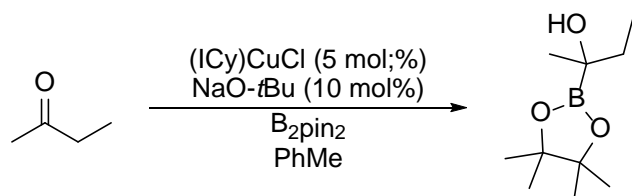
2.1 ALCOHOL, ALDEHYDE, AND KETONE LIBERATION AND INTRACELLULAR CARGO RELEASE THROUGH PEROXIDE MEDIATED α - BORYL ETHER FRAGMENTATION

The initial design envisioned for the scaffold was based on the ability to synthesize and functionalize α -hydroxy boronate esters into carbonates. We predicted that oxidation of a functionalized α -alkoxy boronate ester by H_2O_2 would give an unstable hemiacetal that would rapidly breakdown under biological condition leading to release of the desired cargo. There were several challenges that we faced in establishing a biorthogonal alkylboronate scaffold that would eventually lead to a molecular scaffold for the release of alcohols, aldehydes, and ketones.

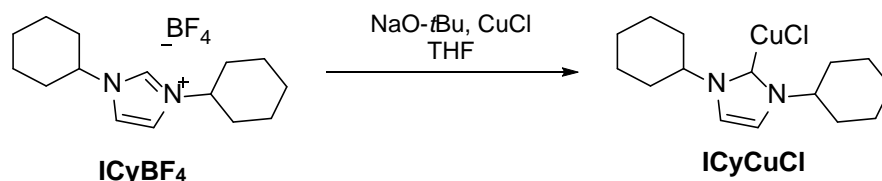
2.1.1 Facile access to α -hydroxy boronate esters

The first challenge towards the construction of a new scaffold was facile access to α -hydroxy boronate esters utilizing the diboration chemistry presented in 1.4.3. Initial attempts to access secondary α -hydroxy boronate esters from aldehydes failed due to decomposition of the diborated products into the starting aldehyde and pinB-O-Bpin upon exposure to air, as reported in the literature.⁵⁴ Thus, we turned our attention towards the synthesis of tertiary α -hydroxy boronic esters from ketones. Initial studies showed that ketones were acceptable as substrates for the synthesis of tertiary α -hydroxy boronic esters using the (ICy)Cu-*O**t*Bu catalyst system (Scheme 2.3).⁵⁸

Original Protocol



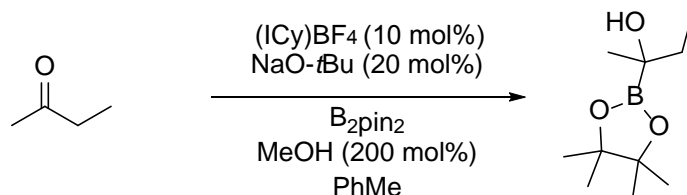
Catalyst Synthesis



- 1) Benchtop stable
- 2) Easily accessible in large amounts

- 1) Must be handled under inert conditions
- 2) Challenging to access in large amounts

Modified Protocol



Scheme 2.3 Modified protocol for the facile access of α -hydroxy boronate esters

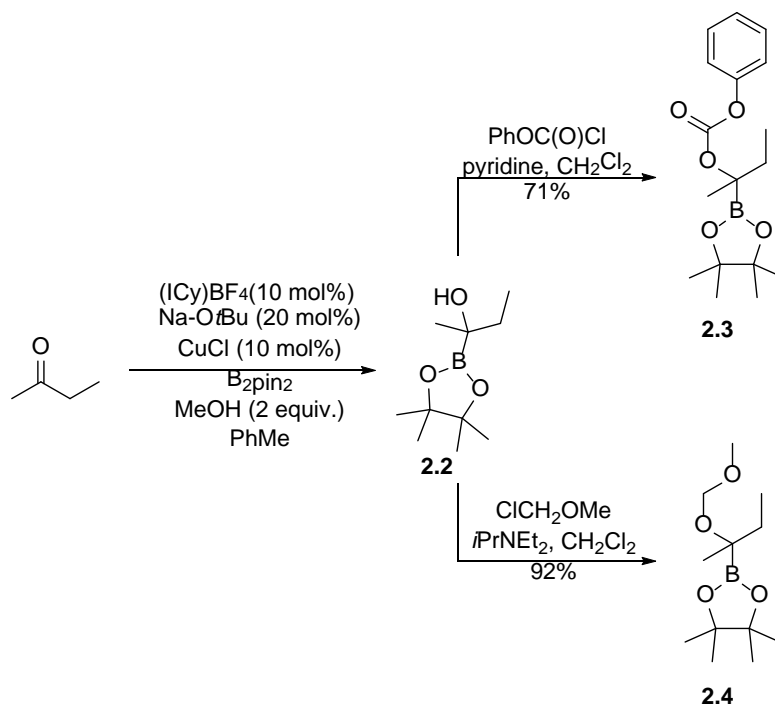
Unfortunately, (ICy)CuCl and (ICy)O-*t*Bu are not easily accessed and must be handled under inert conditions, severely limiting access to the desired substrates. Since (ICy)CuCl is normally synthesized by deprotonation of the starting imidazolium salt (ICy)BF₄ by NaO-*t*Bu, we envisioned a one pot procedure that utilized a larger mol% of NaO-*t*Bu in the presence of CuCl and (ICy)BF₄.

We predicted that this would lead to slow formation of (ICy)Cu-O*t*Bu *in situ*, and increased yields of the diborated products. Additionally, MeOH was used as an additive because it has been shown to increase catalyst efficiency by protolytic turnover in other diboration reactions.⁵⁵ This led us to the development of a novel procedure using (ICy)BF₄, CuCl, MeOH, and a larger mole

% of NaO-*t*Bu in a one pot fashion. Another advantage to this method is that the reaction can be run open to air, albeit in slightly lower yields. Facile access to tertiary α -hydroxy boronic esters allowed the synthesis of a new class of compounds for the release of alcohols in the presence of H₂O₂.

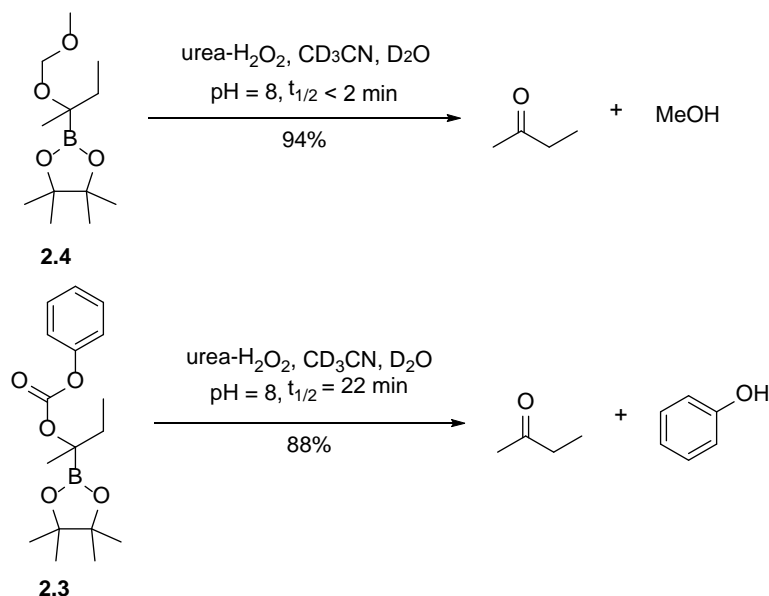
2.1.2 α -hydroxy boronate functionalized acetals and carbonates

Once facile access to α -hydroxy boronate esters was achieved, we turned our attention towards developing a scaffold that would release alcohols in the presence of H₂O₂ under biological conditions. Starting with 2-butanone, α -hydroxyboronate **2.2** was synthesized then functionalized as carbonate **2.3** with pyridine and phenyl chloroformate (Scheme 2.4).



Scheme 2.4. Synthesis of carbonate **2.3** and acetal **2.4**

We reasoned that the release of CO₂ would be entropically favored and phenol would make for a better leaving group than an alkyl group, thus promoting rapid release and oxidation. The oxidative breakdown of carbonate **2.3** was monitored in a mixture of 5:1 CD₃CN:pH 8.0 phosphate buffer to mimic the pH of the mitochondria (Scheme 2.5).



Scheme 2.5 Monitoring the fragmentation of carbonate **2.3 and acetal **2.4****

This sample was treated to achieve a final concentration of 25 mM H₂O₂ (~10 equivalents). Surprisingly, in the presence of H₂O₂ and biologically relevant conditions, the release of phenol was slower than we expected. Consumption of 50% of the starting material required 22 minutes. We predicted that due to an intramolecular bond between the C=O bond on the carbonate and the boronate ester blocking the open coordination site, preventing oxidation by H₂O₂ (Figure 2.1). Crystal structures of α -amido boronate esters show this type of coordination.⁸⁹

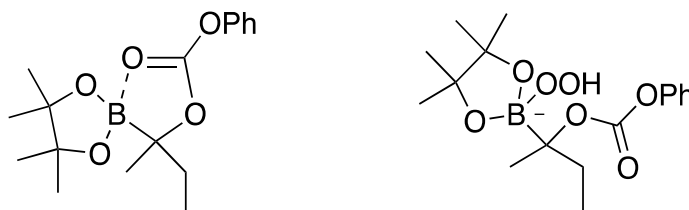


Figure 2.1 Intramolecular bond coordination between the carbonate and the boronate ester

To test our hypothesis, methoxymethyl ether **2.4** was synthesized from α -hydroxyboronate **2.2** (Scheme 2.4). As predicted, Methoxy methyl ether **2.4** fragmented rapidly in the presence of H_2O_2 to release MeOH and 2-butanone. Over 50% of the starting material was consumed in less than 2 minutes and complete conversion was achieved in 20 minutes.

The reaction progress of both methoxy methyl ether **2.4** and carbonate **2.3** were monitored by the disappearance of the diastereotopic hydrogens from the methylene group and the appearance of the corresponding enantiopic hydrogens in 2-butanone (Figure 2.2).

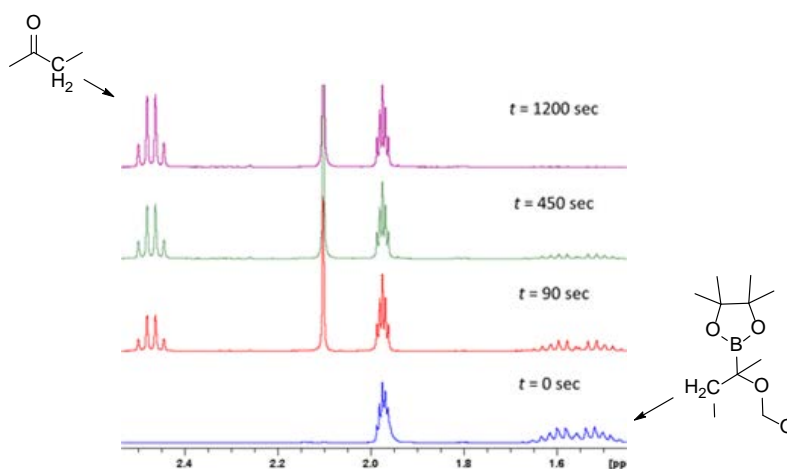


Figure 2.2 Monitoring the oxidation of methoxy methyl ether 2.4

Additionally, changing the pH from 8.0 to 7.2 (the pH of the cytosol) has a small effect on the rate of boronate ester oxidation despite the diminished peroxy anion concentration required for oxidation to occur (Figure 2.3).

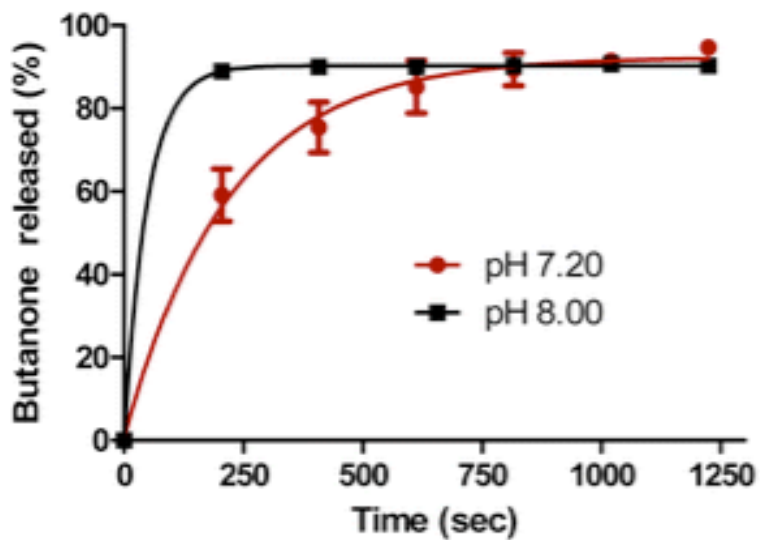
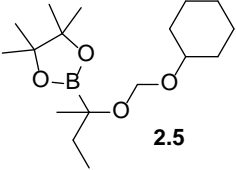
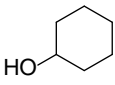
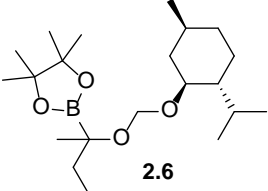
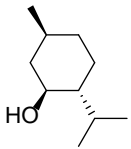
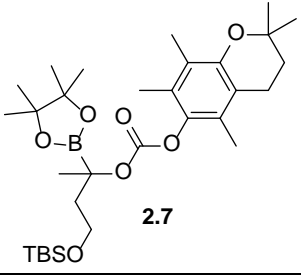
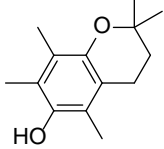
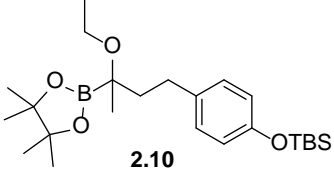
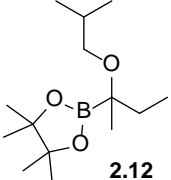
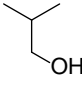
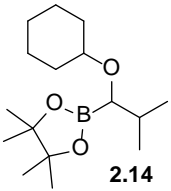
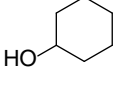
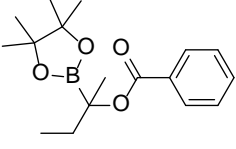
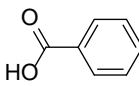


Figure 2.3 Oxidation of methoxymethyl ether 2.4 at pH 7.2 and 8.0

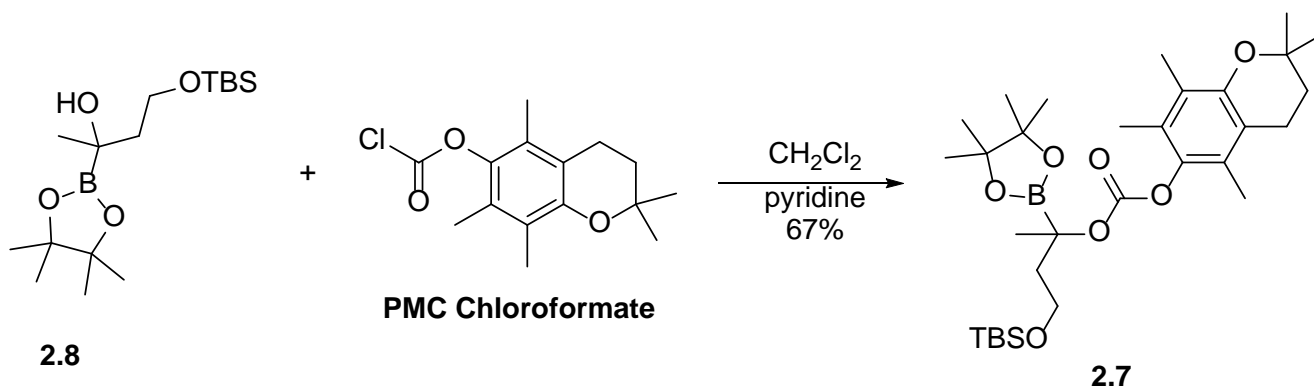
2.1.3 Defining the scope: The synthesis and fragmentation of α -boryl ethers, carbonates, and acetals

With a system for the release of alcohols established, the scope for the release of alcohols was explored. Secondary alcohols such as cyclohexanol and menthol are released quickly from substrates **2.5** and **2.6** in the presence of H_2O_2 (Table 2.1, entries 1 and 2).

Table 2.1 Scope of alcohol release for α -boryl ethers.

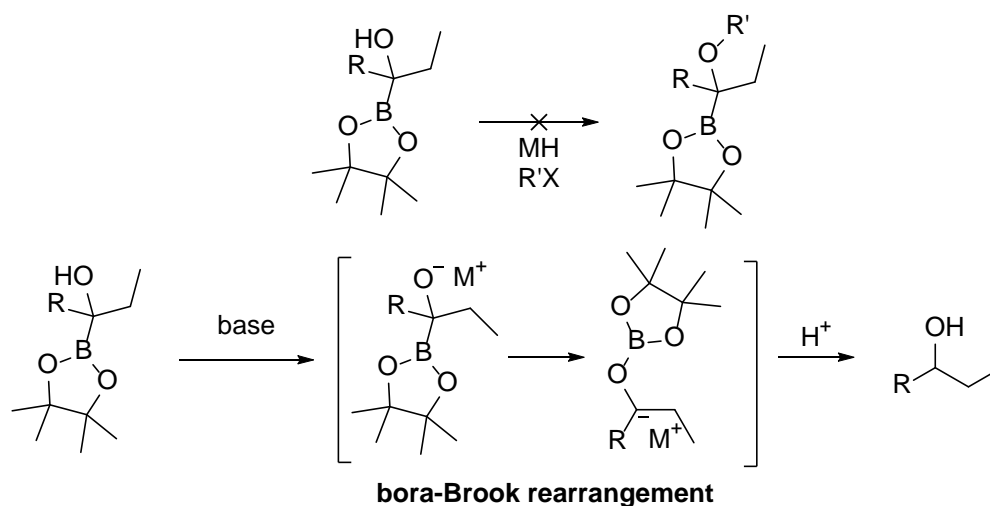
entry	substrate	product	$t_{1/2}$ (min)	yield (%)
1	 <p>2.5</p>		<2	84
2	 <p>2.6</p>		<2	85
3	 <p>2.7</p>		90	79
4	 <p>2.10</p>	EtOH	<2	89
5	 <p>2.12</p>		<2	89
6	 <p>2.14</p>		<2	83
7	 <p>2.15</p>		>936	16

It was demonstrated that a phenolic antioxidant can be released (albeit at a slower rate) from compound **2.7** (Table 2.1, entry 3). Compound **2.7** was synthesized from α -hydroxy boronate **2.8** and PMC chloroformate. (Scheme 2.6).



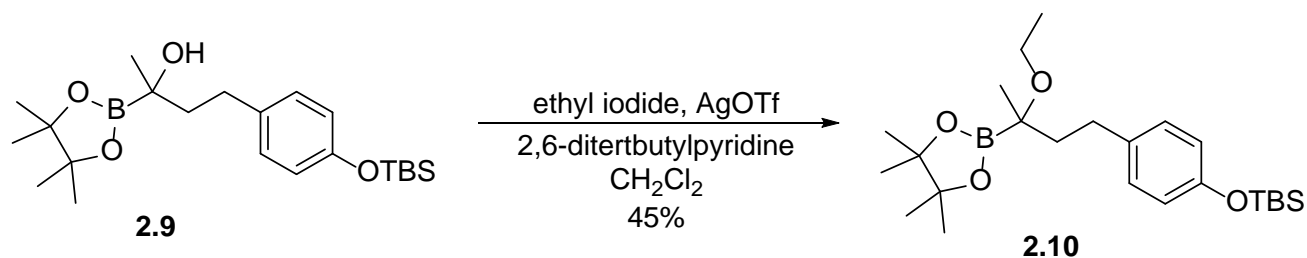
Scheme 2.6 Synthesis of carbonate **2.7** from hydroxy boronate **2.8**

Since the initial goal of the project was to avoid the release of undesired toxins, especially if the cargo is not a cytotoxin; direct release from α -boryl ethers rather than acetals was desirable (due to the release of formaldehyde). Unfortunately, direct Williamson ether synthesis with α -boryl alcohols leads to a Bora brook rearrangement; which renders the alcohol non-nucleophilic (Scheme 2.7).⁹⁰



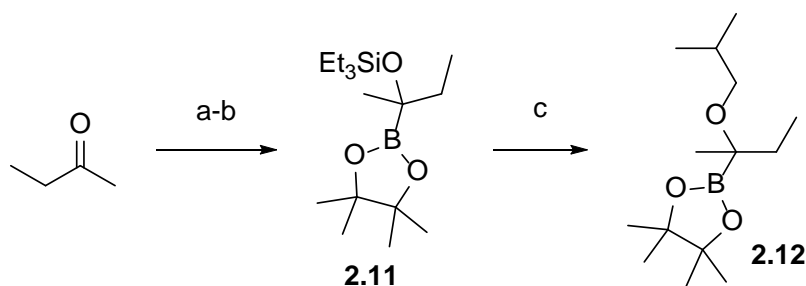
Scheme 2.7. Alkoxide generation leads to bora-Brook rearrangement rather than alkylation

To overcome this undesirable result, potent electrophiles must be used to avoid the generation of alkoxide intermediates. This can be accomplished by activating halide leaving groups with AgOTf, this allows hindered pyridines to be used as H⁺ scavengers.⁹¹ This is demonstrated in the ethylation of α -hydroxy boronate ester **2.9** to form ethyl ether **2.10**. (Scheme 2.8).



Scheme 2.8. Etherification to form boronate ester 2.10

Ethyl ether **2.10** fragments smoothly to release EtOH (Table 2.1, entry 4). If the desired halide is unavailable, reductive etherification with BiBr₃ is another method for preparing α -boryl ethers.⁹² Silyl ether **2.11** condenses with isobutyraldehyde in the presence of Et₃SiH to give α -boryl ether **2.12** (Scheme 2.9).

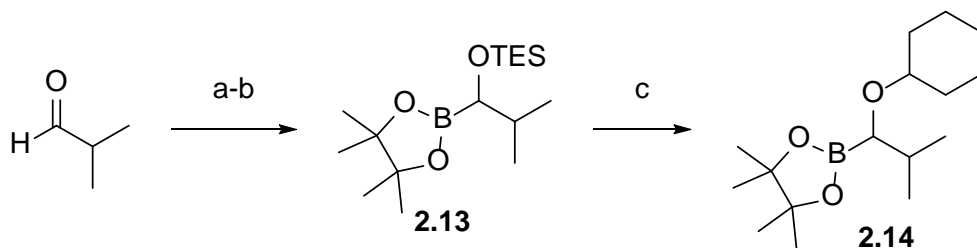


Reagents and Conditions

- a) B₂pin₂, ICyBF₄, CuCl, NaO-*t*Bu, MeOH, PhMe; b) TESCl, imidazole, CH₂Cl₂, 83% (2 steps)
c) BiBr₃, isobutyraldehyde, Et₃SiH, CH₃CN, 73%

Scheme 2.9 Reductive etherification to form α -boryl ether 2.12

α -boryl ether **2.12** fragments rapidly in H_2O_2 to release 2-methylpropanol (Table 2.1, Entry 5). Since the starting material is an ether, this allows for the borylation of aldehydes then immediate subsequent protection of 2° α -hydroxy boronate esters to give silyl ethers. Unlike the 2° α -hydroxy boronate esters, which decompose rapidly, the protected silyl ethers can be handled and purified with ease. This expanded scope was illustrated in the synthesis of α -boryl ether **2.14** from α -boryl silyl ether **2.13** (Scheme 2.10).



Reagents and Conditions

- a) B_2pin_2 , ICyBF_4 , CuCl , $\text{NaO}-t\text{Bu}$, MeOH , PhMe ; b) TESCl , imidazole, CH_2Cl_2 , 31% (2 steps)
 c) BiBr_3 , cyclohexanone, Et_3SiH , CH_3CN , 81%

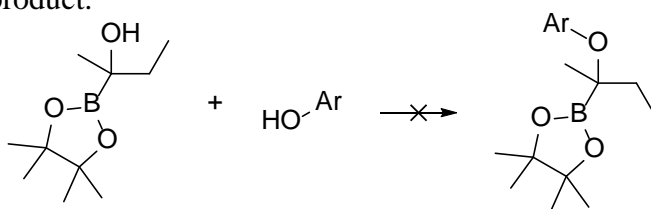
Scheme 2.10 Reductive etherification to form α -boryl ether **2.14**

α -boryl ether **2.14** fragments rapidly in the presence of H_2O_2 to release cyclohexanol (Table 2.1, entry 6). The release of a carboxylic acid from an α -boryl ester was far slower than the release of alcohols and carbonates (Table 2.1, Entry 7). Compound **2.15** does show ^{11}B shift of 27.0 ppm, slightly lower than a typical α -boryl ether (~ 30 ppm), this suggests that intramolecular coordination is likely to play a role in providing its stability.

2.1.4 Defining Limitations: Cyclic acetal discovery

With the scope defined, we looked towards finding a compound that would release a fluorophore to probe fragmentation within cells. While searching for the appropriate compound,

some of the limitations of α -boryl ether functionalization and its compatibility with low concentrations of H_2O_2 was explored. Initially we reasoned that since carbonate **2.7** fragmented so slowly in the presence of H_2O_2 , a new system could be developed that utilizes an acetal to release a fluorescent phenol compound. We reasoned that with a fluorescent phenol quenched as an acetal, release of the fluorescent species would occur upon addition of H_2O_2 . Initially attempts were made to form an ether from a fluorescent phenol using a Mitsunobu reaction.⁹³ Unfortunately (and perhaps unsurprising), the reaction was sluggish and only trace amounts of our desired product were formed, even at elevated temperatures (Scheme 2.11). Even the Mukaiyama etherification, which has been used for the synthesis of 3° ethers failed due to decomposition of the intermediate product.⁹⁴

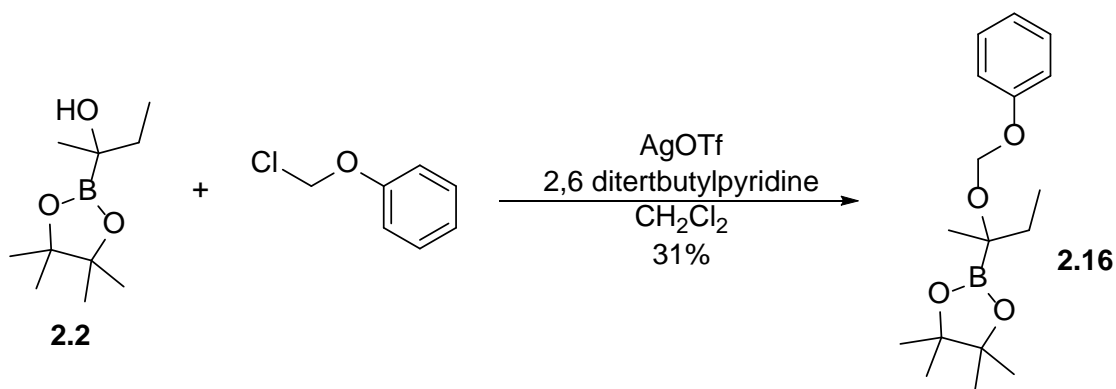


Conditions Attempted

- Mitsunobu Reaction (Low yields, elimination products)
- Mukaiyama Etherification (Decomposition of the starting alcohol)

Scheme 2.11. Attempts to synthesize a 3° aryl-alkyl α -boryl ether

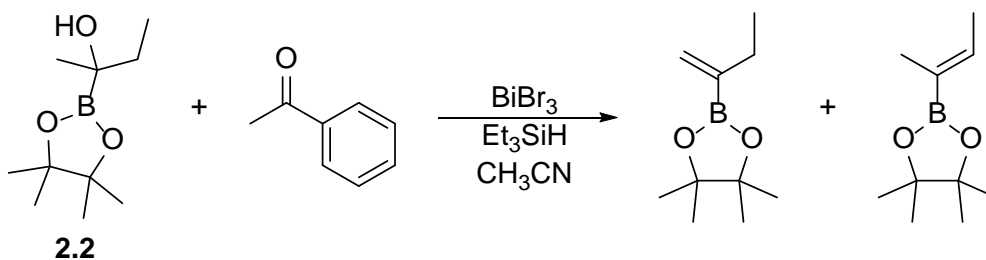
Since synthesis of the α -boryl phenolic ether was shown to be impractical, we focused our attention on the synthesis of an acetal that would release a phenol. To test our theory compound



Scheme 2.12. Synthesis of acetal **2.16** from α -hydroxy boronate **2.2**

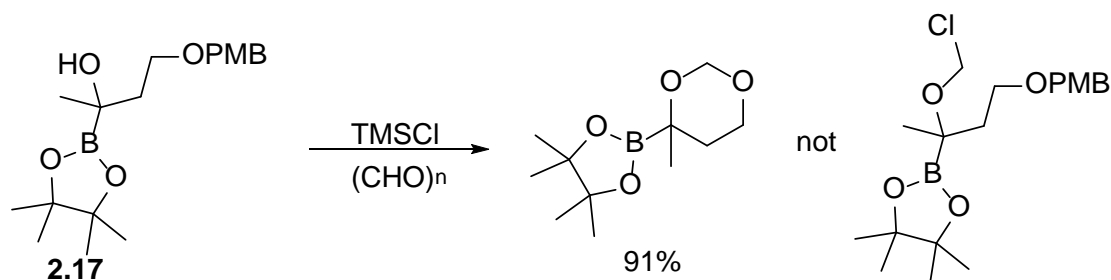
2.16 was synthesized from α -hydroxy boronate **2.2** utilizing AgOTf, 2,6 ditertbutylpyridine, and chloromethyl phenyl ether (Scheme 2.12).

Unfortunately, acetal **2.16** was not stable in pH 7.2 Buffer; thus ruling out its use in biological studies. We reasoned that the acetal was undergoing hydrolysis due to the increased leaving group ability of the phenol. Realizing that the release of a phenol was impractical and unlikely to succeed under biological conditions; we turned our attention towards substrates that would release fluorescent aldehydes and ketones in the presence of H₂O₂. Unfortunately, α -hydroxy boronates derived from aryl ketones and aldehydes are unstable and cannot be purified, limiting the scope. Even attempts to functionalize α -boryl silyl ethers using reductive etherification with aryl carbonyl compounds led exclusively to elimination products (Scheme 2.13).



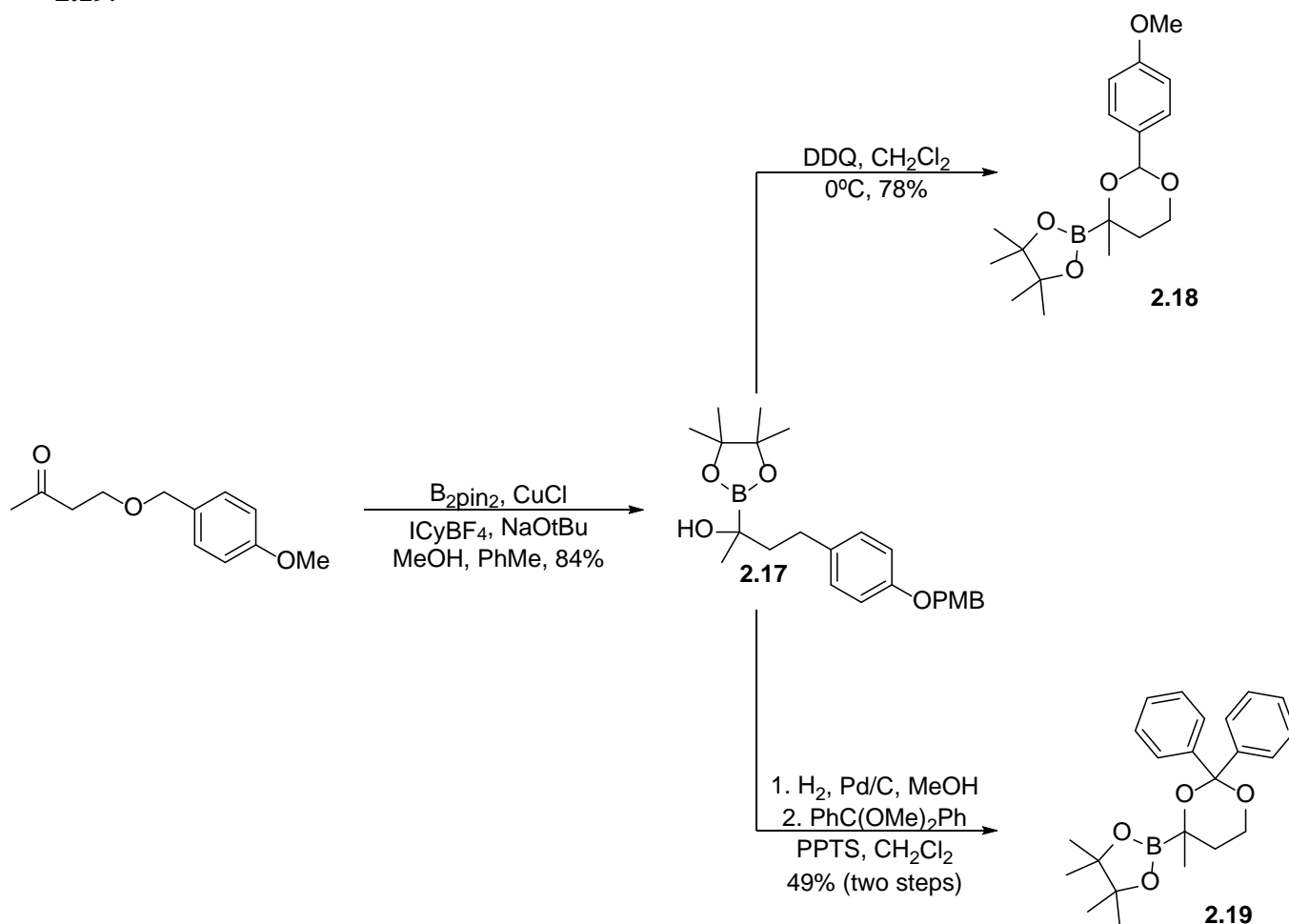
Scheme 2.13. Attempted etherification with acetophenone

To synthesize a chloromethyl ether from α -hydroxyl boronate ester **2.17**, we discovered that rather than the chloromethyl ether, a cyclic acetal was isolated in a high yield (Scheme 2.14).



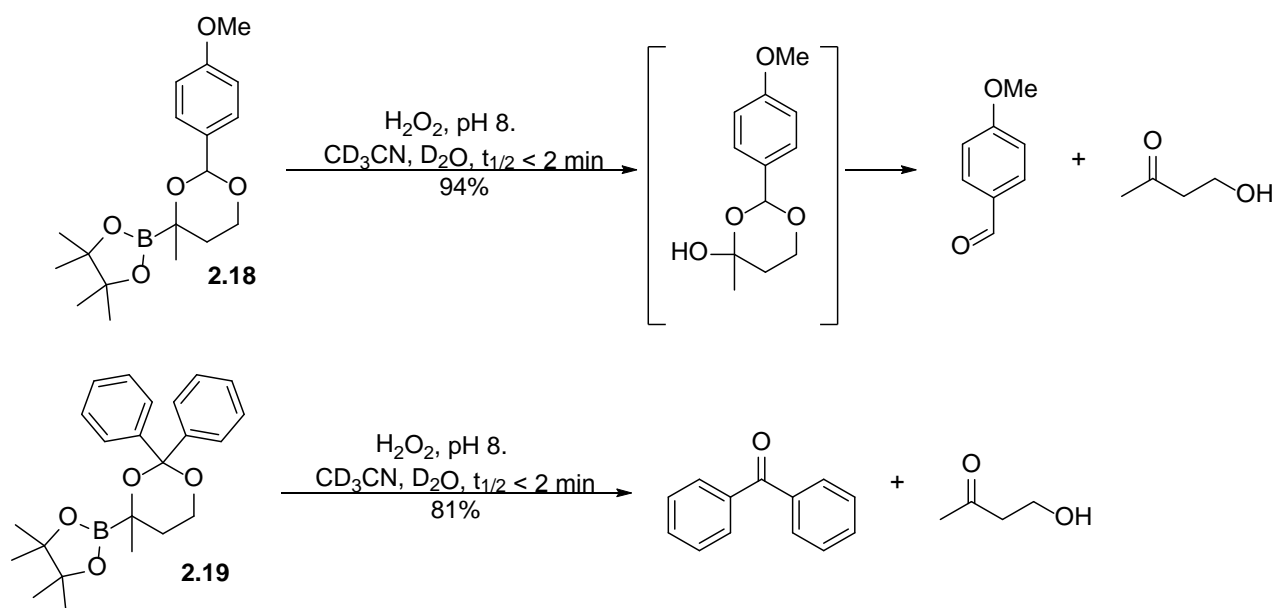
Scheme 2.14 Unintentional synthesis of a cyclic acetal

We reasoned that with the appropriate group attached to a cyclic acetal, the addition of H_2O_2 would lead to the release of a fluorescent aldehyde or ketone. Acetal **2.18** was accessed through DDQ-mediated oxidative cyclization from α -hydroxyl boronate **2.17** (Scheme 2.15).⁹⁵ Ketal **2.19** was synthesized via removal of the PMB group from **2.17** under hydrogenolytic conditions followed by acetal exchange with the dimethyl ketal of benzophenone to give ketal **2.19**.



Scheme 2.15 Synthesis of acetal **2.18** and ketal **2.19** from α -hydroxy boronate ester **2.17**

Acetal **2.18** rapidly reacts with H₂O₂ at pH 8.00 to give an equivalent of anisaldehyde and 4-hydroxy-2-butanone (Scheme 2.16). Over 50% of the starting material is consumed within 90 seconds, and complete conversion occurs in 15 minutes. Although a hemiacetal was not observed via NMR, this is the suspected intermediate. Ketal **2.19** reacts similarly, releasing an equivalent of benzophenone and 4-hydroxy-2-butanone. This advance represents a novel approach for the design of compounds that can release aldehydes and ketones under oxidative conditions; previous work on this was discussed in 1.2.^{20, 96}

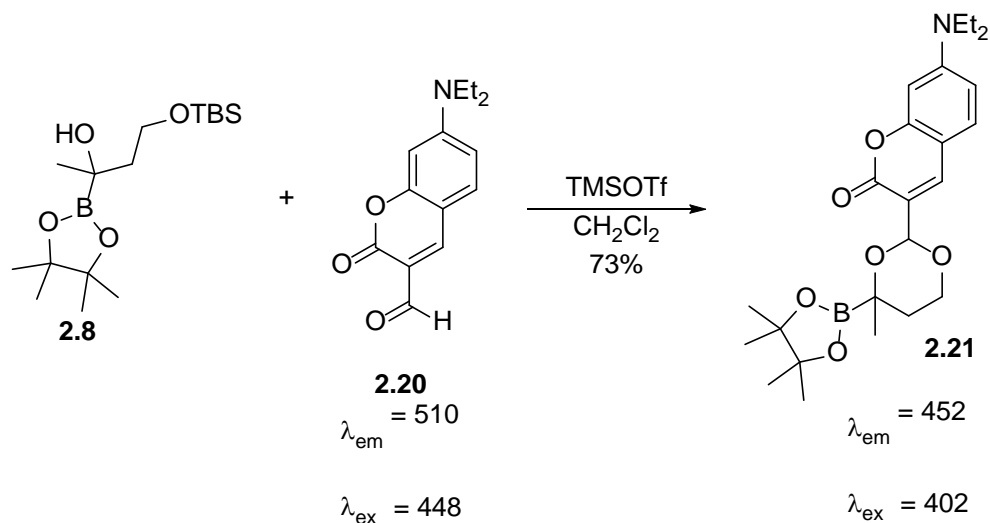


Scheme 2.16 Oxidative breakdown of cyclic acetal **2.18** and cyclic ketal **2.19**

2.1.5 A novel biorthogonal scaffold for the release of a fluorescent aldehyde.

With the scope defined, we turned our attention towards determining whether or not our scaffold would be sensitive to biologically relevant concentrations of H₂O₂. The first step towards this was to synthesize an α -boryl ether that would release a fluorescent ketone or aldehyde. Starting with α -hydroxy boronate ester **2.8**, Noyori acetalization with fluorescent coumarin

derivative **2.20** gave caged fluorophore **2.21** (Scheme 2.17).⁹⁷ Standard Brønsted acid catalyzed acetalization gave exclusively protodeboronation products. Compound **2.21** has λ_{em} and λ_{ex} values of 510 and 448 nm⁹⁸ and compound **2.20** has λ_{em} and λ_{ex} values of 452 and 402 nm, this was used to monitor the oxidative breakdown at biologically relevant concentrations of H₂O₂.



Scheme 2.17 Noyori acetalization of aldehyde **2.20** and α -hydroxy boronate ester **2.8**

Compound **2.22** was synthesized to verify the importance of the oxidative trigger in the fragmentation (Figure 2.4). Benzylic carbonate **2.23** was synthesized to compare the hydrolytic stability of **2.21** to a well-known scaffold used in several biological studies.¹⁴

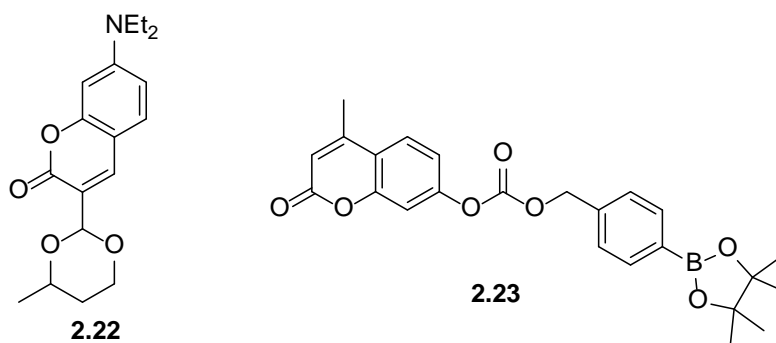


Figure 2.4 Acetal **2.22** and Carbonate **2.23**

The fragmentation of acetal **2.21** was studied at a concentration of 25 μM at pH 7.4 with H_2O_2 concentrations of 100 and 200 μM (Figure 2.5). The concentration of fluorophore **2.20** was monitored by excitation at 448 nm and emission at 499 nm (due to background from starting acetal **2.21**). The product released was quantified through comparison to a standard curve. These experiments are visualized in Figure 2.5. Compound **2.22** did not release fluorescent aldehyde **2.20** upon exposure to H_2O_2 indicating the importance of boronate oxidation for cargo release. Lowering the concentration of H_2O_2 from 200 μM to 100 μM slowed fluorophore release indicating dependency on H_2O_2 concentration. In the absence of H_2O_2 , fluorophore release is minimal. Additionally, hydrolytic stability was studied at pH 6.0 and pH 4.5. Fluorophore release was slightly inhibited at lower pH values.

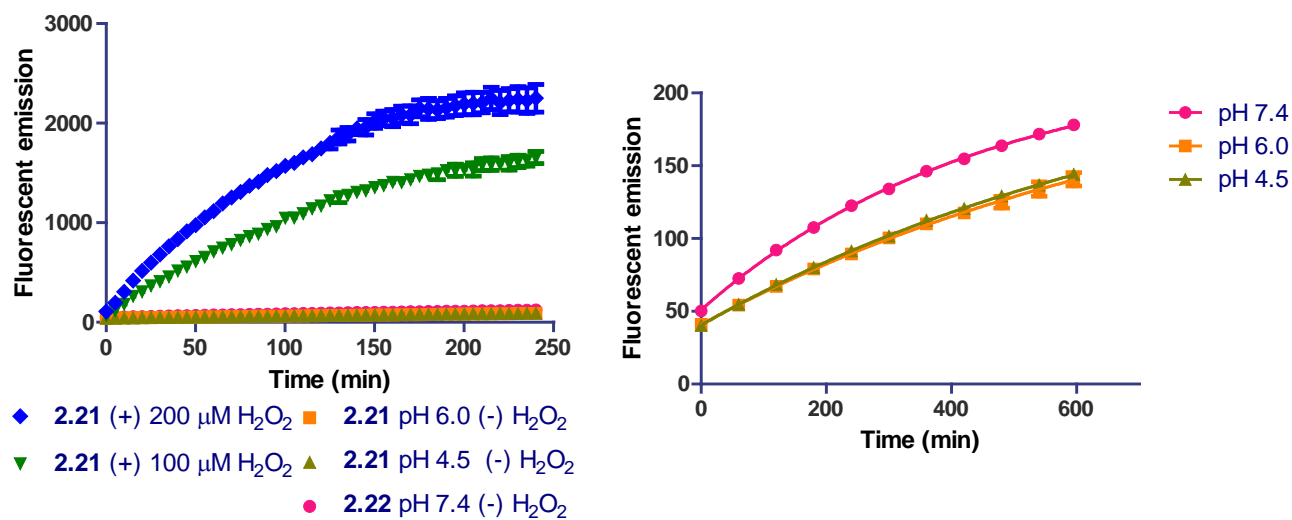


Figure 2.5 Fluorophore fragmentation at low substrate and peroxide concentration and pH stability studies.

To demonstrate that hydrolytic breakdown without H₂O₂ is minimal, the ratio of fluorophore release in the presence and absence of H₂O₂ for carbonate **2.23** and acetal **2.21** was compared; the results show that ratio is nearly equivalent (Figure 2.6).

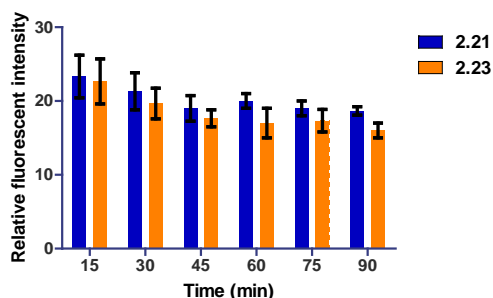


Figure 2.6. Fluorophore release from acetal **2.21** compared to carbonate **2.23**

To test the vulnerability of **2.21** to other ROS, solutions of H₂O₂, NaOCl, KO₂, and t-BuOOH were prepared and added to a 40 μM solution of acetal **2.21** in pH 7.4 buffer to give final concentrations of 200 μM for each oxidant (Figure 2.7). Additionally, solutions of hydroxyl and t-butoxyl radicals were prepared by mixing H₂O₂ with FeSO₄·5H₂O and adding catalase as a peroxide scavenger. H₂O₂ and hydroxyl radicals are the only ROS that showed any significant fluorophore release, albeit hydroxyl radical released fluorophore at a lower magnitude.

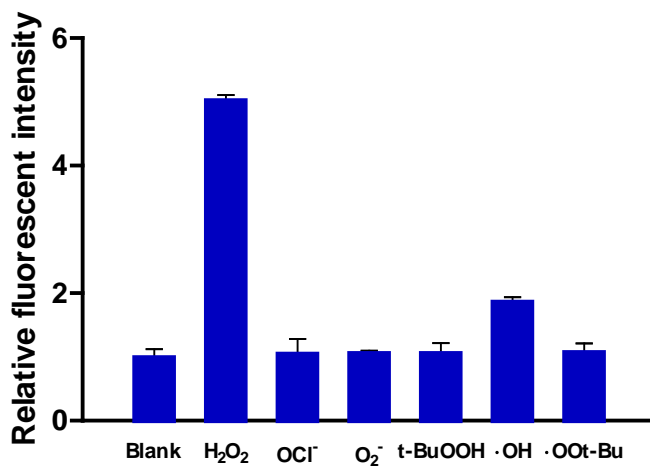


Figure 2.7. Comparison of fluorophore release by different oxidants [2.21] =40 μM [oxidant] = 200 μM

The *in vitro* results led us to investigate the fragmentation and release of fluorophore **2.20** from acetal **2.21** in a biologically relevant environment. These experiments were performed by Yuta Naro in collaboration with the Dieter's group. We chose to adapt a protocol from Chang, where HeLa cells were incubated with acetal **2.21** for 45 min, then imaged in the presence and absence of exogenous H₂O₂ (100 μM) (Figure 2.8). In the absence of H₂O₂, very little fluorophore release occurred; however, in the presence of H₂O₂, a large amount of fluorophore release was observed. These results demonstrate that α-boryl ethers are capable of crossing cell membranes and can release their cargo within cells. These studies were also conducted with acetal **2.22**, and they resulted in no release of the fluorophore in the presence and absence of H₂O₂; providing further evidence for the oxidative release mechanism.

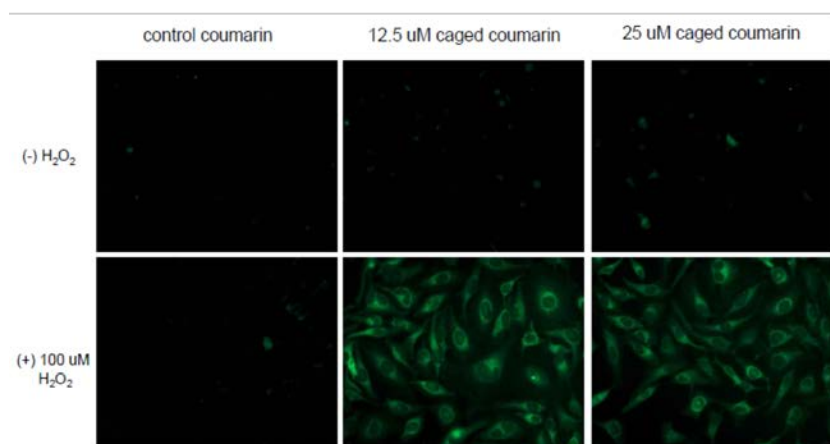


Figure 2.8 Fluorophore release from **2.21** in HeLa cells treated with exogenous H₂O₂.

Since HeLa cells are derived from cancerous tissues, they are expected to contain elevated levels of endogenous H₂O₂ and will therefore have a higher background.⁹⁹ The same experiment was performed in HEK293T cells, derived from noncancerous tissue and the background was significantly reduced in the absence of H₂O₂ for the breakdown of acetal **2.21** (Details in Appendix A). To further provide evidence that α-boryl ethers are excellent scaffold for cargo release under biological conditions, we demonstrated oxidative breakdown in the presence of endogenously

produced H_2O_2 (Figure 2.9). To achieve this, HeLa cells were incubated with 1 μM Phorbol myristate acetate (PMA) (which is known to promote intracellular H_2O_2 generation),¹⁰⁰ followed by acetal **2.21** (10 μM). Cells incubated with PMA showed increased fluorescence over cells that were not; showcasing the capacity of α -boryl ethers to act as vehicles for H_2O_2 triggered release within cells.

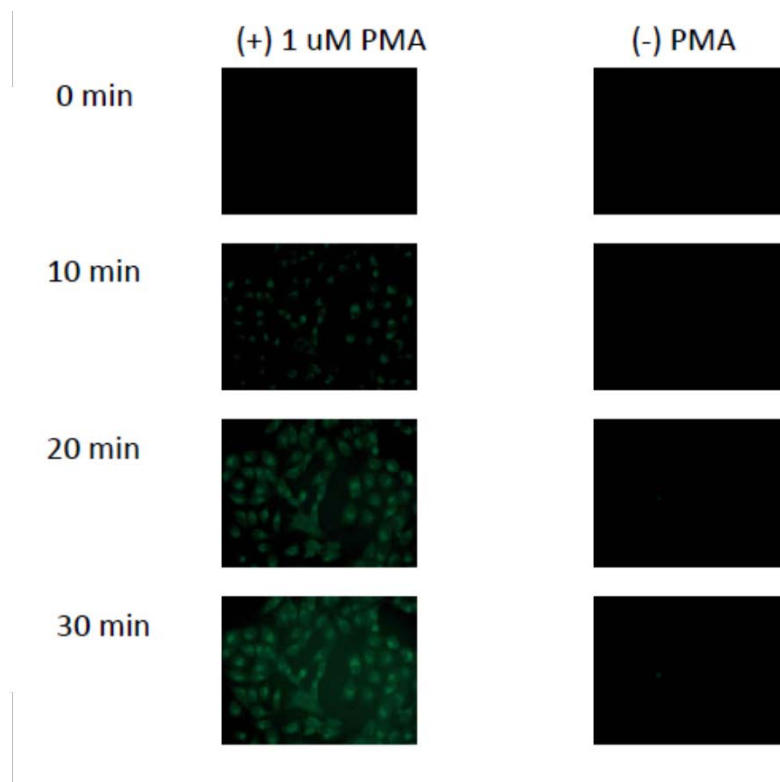


Figure 2.9 Cellular oxidative fluorophore release from acetal 2.21 in the presence of endogenously produced H_2O_2

Thus, the synthesis of α -boryl ethers their effectiveness as vehicles for the release of cargo within a biological environment was established. This advancement represents the first example of alkyl boronate esters being used in a cellular environment as triggers for H_2O_2 . Additionally, the release of cargo is not accompanied by the release of cytotoxic quinone-methides.

3.0 BISTRAMIDE A

The Bistramides are a class of bioactive small molecules isolated from the marine ascidian *Lissoclinum bistraum* in 1989.¹⁰¹ Bistramide A, B, C, D, and K all showed broad, potent antiproliferative effects towards several tumor cell lines (Figure 3.1).¹⁰² In 2005, Kozmin discovered that Actin is the primary cellular receptor for **Bistramide A**.¹⁰³ Several approaches towards its total synthesis and synthesis of potent analogues have been undertaken. In this section, previous strategies towards the synthesis of **Bistramide A** as well as previous synthesis of analogues of **Bistramide A** will be discussed. Utilizing a previous 14-step route to the synthesis of **Bistramide A**,¹⁰⁴ the author will describe the synthesis and biological activity of five analogues of **Bistramide A**.

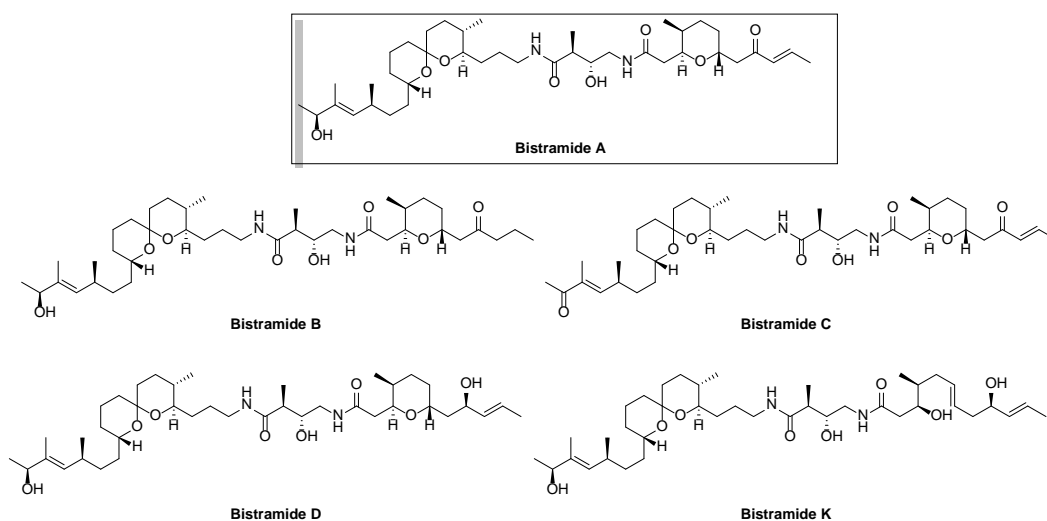
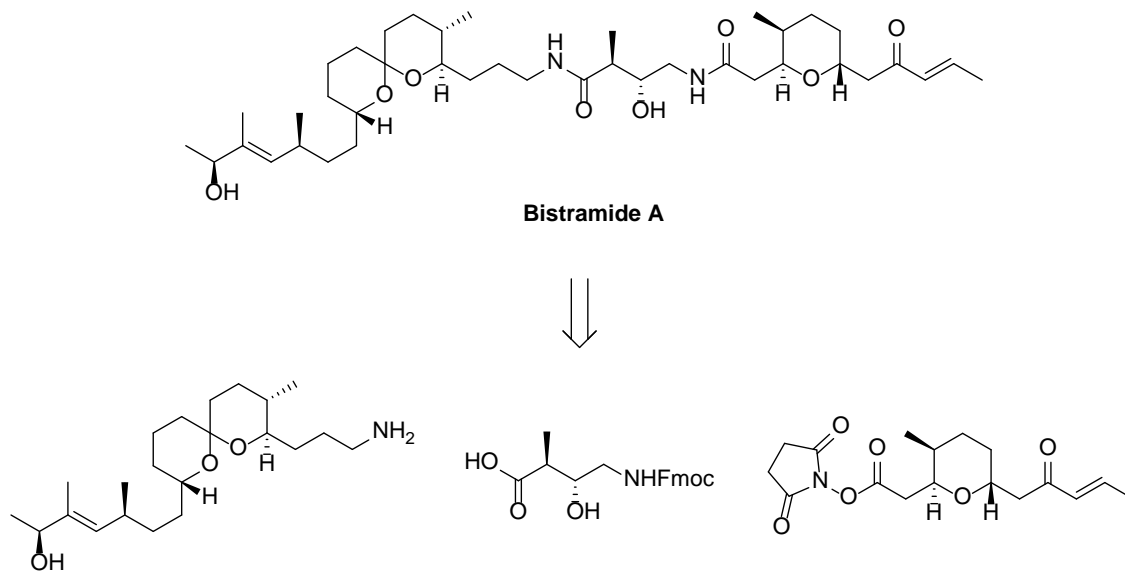


Figure 3.1. Bistramide A, B, C, D, and K

3.1 PRIOR SYNTHESIS OF BISTRAMIDE A

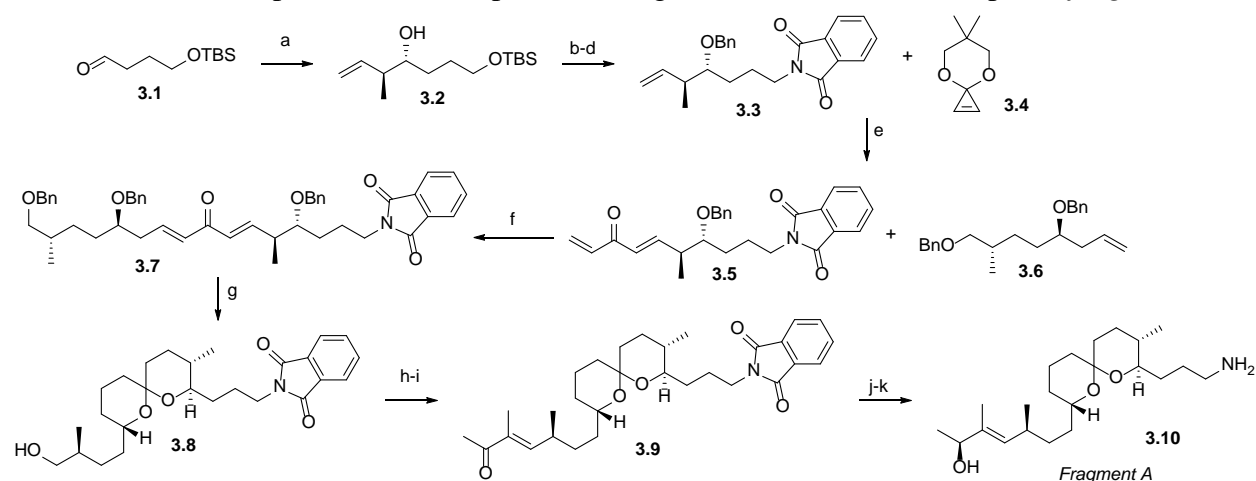
Retrosynthetically, Bistramide A can be divided into *fragment A*, *fragment B*, and *fragment C* by the 2 amide linkages (Scheme 3.1). The two major syntheses of **Bistramide A** described in this section follow this retrosynthetic pathway



Scheme 3.1 Retrosynthesis of Bistramide A

3.1.1 Kozmin's 2004 Synthesis of Bistramide A

The first total synthesis of Bistramide A was reported by Kozmin in 2004 with a longest linear sequence of 15 steps.¹⁰⁵ Kozmin's synthesis of *fragment A* is presented in Scheme 3.2. At the outset of Brown crotylation of aldehyde **3.1** gives alcohol **3.2**,¹⁰⁶ which is protected as a benzyl ether then the TBS group is removed with TBAF. A Mitsunobu reaction with phthalimide gave **3.3**,¹⁰⁷ which underwent ring-opening/cross-metathesis with strained cyclopropane acetal **3.4**.¹⁰⁸ Deprotection of the resulting acetal with H₂SO₄ gives dieneone **3.5**. Cross-metathesis with benzyl ether **3.6** gives dienone **3.7**. Deprotection of the three benzyl ethers via hydrogenolysis and the subsequent cyclization forms spiroketal **3.8** as a single diastereomer. **3.8** was oxidized to the aldehyde, then underwent Cr-mediated olefination to give enone **3.9**.¹⁰⁹ Itsuno-Corey reduction,¹¹⁰ then deprotection of the phthalimide gives amine **3.10** and completes *fragment A*.

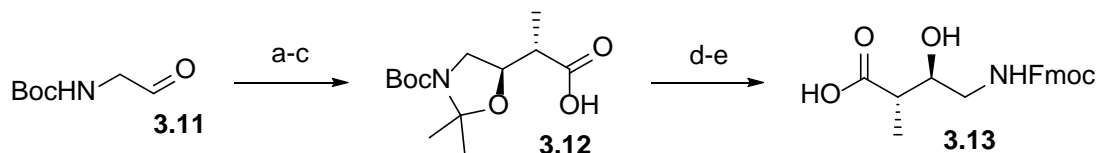


Reagents and Conditions

a) Brown Crotylation, 84%, 94% ee. b-c) KH, BnBr, Bu₄Ni then TBAF, 59% over 2 steps d) phthalimide, PPh₃, DIAD, 94% e) Grubbs Catalyst II, Benzene, then H₂SO₄, MeCN 72% f) Grubbs Catalyst II, CH₂Cl₂, 68% g) Pd(OH)₂, EtOAc/MeOH, H₂, 61% h) DMP, CH₂Cl₂, 95%, i) dibromoketone, CrCl₂, THF, 50% j) (R)-2-methyl-CBS-oxazaborolidine, Catecholborane, PhMe, 85% k) MeNH₂, MeOH, 65° C, quantitative

Scheme 3.2 Kozmin's Synthesis of the left fragment of Bistramide A

Fragment B is synthesized via brown crotylation of aldehyde **3.11**, protection of the acetonide and oxidative cleavage of the alkene to give carboxylic acid **3.12** (Scheme 3.3). Acid-mediated deprotection of the acetonide and protection of the resulting amine gives **3.13** (*fragment B*).

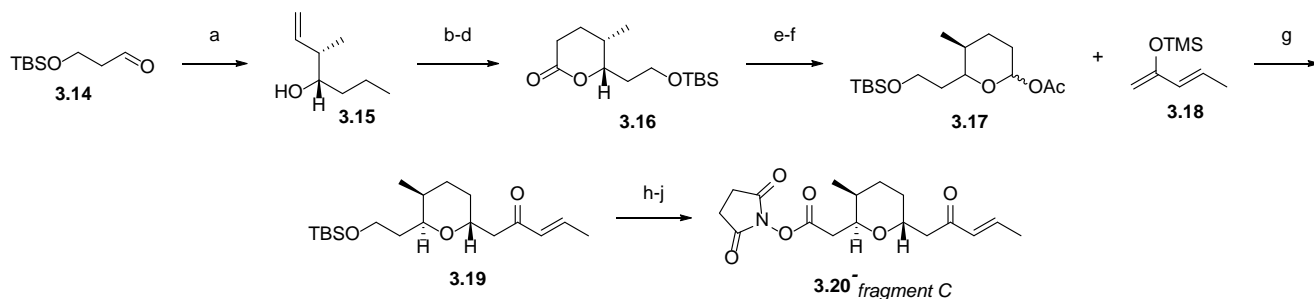


Reagents and Conditions

a) Brown Crotylation, 64%, 93% ee b) $\text{Me}_2\text{C}(\text{OMe})_2$, $\text{TsOH}\cdot\text{H}_2\text{O}$, 90% c) NaIO_4 , RuCl_3 , 62%
d) 3N HCl, EtOAc, quantitative e) FmocOSu, Na_2CO_3 , 71%

Scheme 3.3 Kozmin's synthesis of the middle fragment of Bistramide

Fragment C is assembled from Brown crotylation of TBS-protected aldehyde **3.14** gives alcohol **3.15** (Scheme 3.4). Acylation with acryloyl chloride, ring-closing metathesis, and Pd/C reduction of the double bond gives lactone **3.16**. Reduction/acylation of lactone **3.16** with DIBAL then protection of the lactol with acetic anhydride gives acetate **3.17**. ZnCl_2 mediated substitution of the acetal with silyl enol ether **3.18** affords enone **3.19**. Deprotection of the TBS ether, then oxidation of the resulting alcohol to the acid followed by DCC-mediated amide coupling with N-hydroxy succinimide provides activated ester **3.20** (*fragment C*).

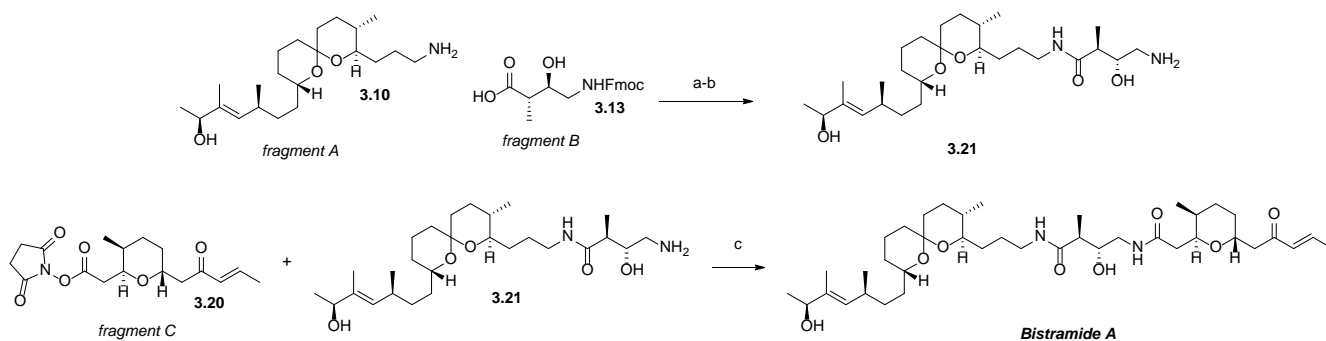


Reagents and Conditions

a) Brown Crotylation, 63%. 93% ee b) Acryloyl chloride, NEt_3 , DMAP, 88% c) Grubbs Catalyst II (13 mol%), CH_2Cl_2 , 72% d) H_2 , Pd/C, EtOAc, 99%
e) DIBAL, CH_2Cl_2 , -78°C f) Ac_2O , pyridine, DMAP, 81% over 2 steps g) CH_2Cl_2 , ZnCl_2 , -78°C h) HF, CH_3CN i) H_5IO_6 , CrO_3 , CH_3CN (0.75 % H_2O), 37% over 3 steps j) N-hydroxysuccinimide, DCC, CH_3CN , 98%

Scheme 3.4 Kozmin's synthesis of the right fragment of Bistramide A

Fragment A (3.10) and *fragment B (3.13)* are coupled via py-BOP condensation, then deprotected to afford amine **3.21** (Scheme 3.5). Deprotection followed by treatment with activated ester *fragment C (3.20)* affords **Bistramide A**. This highly convergent enantioselective synthesis is achieved in 15 steps.



Reagents and Conditions

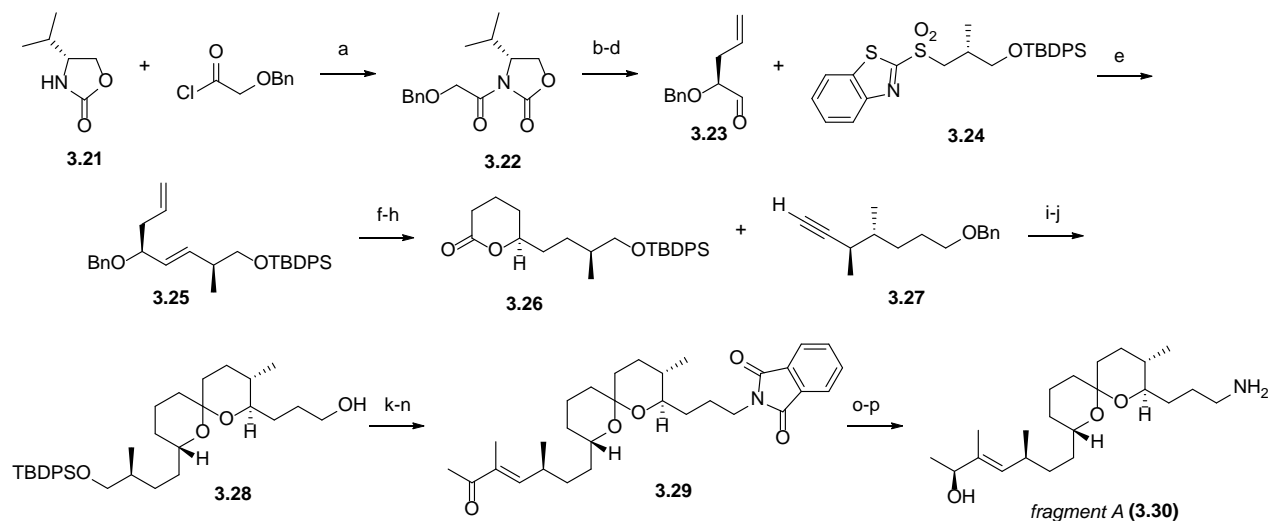
a) PyBOP, DIEA, DMF 88%; (b) Et₂NH, DMF; (c) DMF 82% (two steps)

Scheme 3.5 Kozmin's final coupling to synthesize **Bistramide A**

3.1.2 Crimmins 2006 Synthesis of Bistramide A

After the completion of Kozmin's synthesis, the Crimmins group published their own route towards Bistramide A.¹¹¹ Crimmins' synthesis differs with respect to all three fragments. *Fragment A* was constructed starting with the alkylation of valine derived oxazolidinone **3.21** with benzyloxyacetyl chloride to give benzyl glycolate **3.22** (Scheme 3.6).¹¹² The enolate of imide **3.22** was alkylated with allyl iodide, then reductively cleaved and oxidized under Swern conditions to give aldehyde **3.23**.¹¹³ A Julia olefination with sulfone **3.24** gave diene **3.25** as a mixture of isomers.¹¹⁴ Cross-metathesis with methyl acrylate, then reduction with Pd/C under H₂ and acid mediated lactonization give lactone **3.26**. The addition of the lithium acetylide of **3.27** to lactone **3.26** gives a keto alcohol, which was subsequently reduced under Pd/C and H₂ to give spiroketal

3.28. The phthalimide was installed under Mitsunobu conditions¹¹⁵ and the TBDPS ether was deprotected with HF-pyridine to give an alcohol. The alcohol was oxidized with Dess-Martin Periodinane,¹¹⁶ then subjected to Horner-Wadsworth-Emmons olefination to give enone **3.29**.¹¹⁷ Stereoselective reduction of the alcohol with Corey's oxazaborolidine gives an alcohol.¹¹⁰ Finally, cleavage of the phthalimide group with MeOH and methylamine gives *fragment A* (**3.30**).



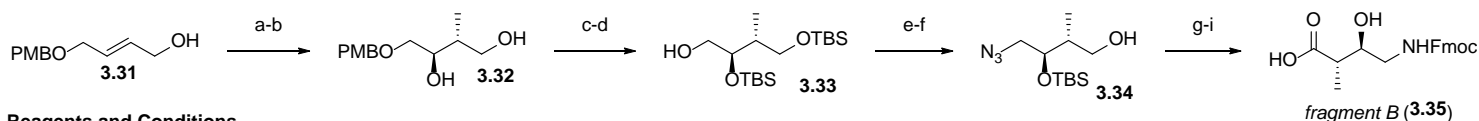
Reagents and Conditions

a) n-BuLi, then 98%; benzyloxyacetyl (b) NaHMDS, allyl iodide, THF, PhMe, 81%; (c) LiBH₄, MeOH, Et₂O, 98%; (d) Et₃N, DMSO, (COCl)₂, CH₂Cl₂ 3.24, then aldehyde 3.23, 87%; (e) LiHMDS, chloride, sulfone 86%; (f) Grubbs Catalyst II, methyl acrylate, CH₂Cl₂, 40 °C, 87%; (g) H₂, Pd/C, EtOAc; (h) p-TSA, benzene, 80 °C, 70% (two steps); (i) alkyne 3.27, n-BuLi, 3.26; (j) H₂, Pd/C, MeOH, EtOAc, 83% (two steps); (k) PPh₃, DEAD, phthalimide, THF, 0 °C; 58%; (l) HF/pyr., THF, 84% (over 2 steps) (m) Dess-Martin periodinane n) Ba(OH)₂, THF, MeCOCH(Me)P(O)(OEt)₂, 58% o) (R)-CBS, catecholborane. Toluene, 65%; p) MeOH, MeNH₂, 99%

Scheme 3.6 Crimmins synthesis of the left fragment of Bistramide A

To synthesize *fragment B*, allylic alcohol **3.31** underwent Sharpless asymmetric epoxidation, then the resulting epoxy alcohol was opened with lithium dimethyl cuprate to give 1,3 diol **3.32** as a mixture with the corresponding 1,2 diol (Scheme 3.7). Treatment with NaIO₄ removed the 1,2 diol and gave pure 1,3 diol **3.32**. Protection with TBSOTf gave bis-silyl ether, then oxidative removal of PMB with DDQ gave alcohol **3.33**. The azide was installed under Mitsunobu conditions, then the TBS ether was cleaved with catalytic camphorsulfonic acid to give

3.34. Oxidation of the primary alcohol to the carboxylic acid, reduction of the azide with Pd/C under H₂, and protection of the primary amine gave *fragment B* (**3.35**).

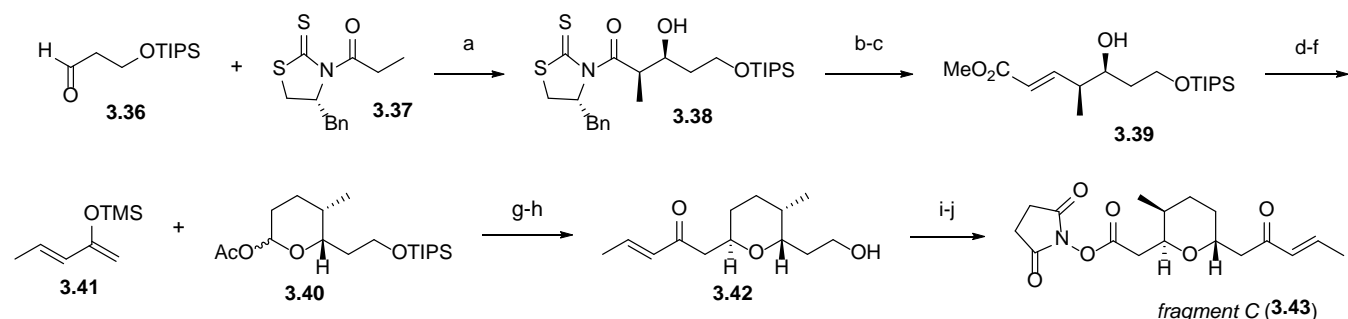


Reagents and Conditions

(a) *l*-(+)-DET, Ti(Oi-Pr)₄, *t*-BuOOH, CH₂Cl₂, 4 Å sieves, -20 °C, 95%, 98% ee; (b) Me₂CuLi, Et₂O, -50 °C to 25 °C, 6:1 of 1,3- to 1,2-diol; NaIO₄, H₂O, 71%; (c) TBSOTf, 2,6-lutidine, CH₂Cl₂, 0 °C, 97%; (d) DDQ, pH 7 buffer, CH₂Cl₂, 0 °C, 98%; (e) DEAD, PPh₃, (PhO)₂PON₃, THF, 0 °C, 90%; (f) CSA, MeOH, CH₂Cl₂, 0 °C, 85%; (g) NaClO₂, TEMPO, CH₃CN, 35 °C, 95%; (h) HF/pyr., THF, 70%; (i) H₂, Pd/C, Fmoc-OSu, THF, 70%.

Scheme 3.7 Crimmins Synthesis of the middle fragment of Bistramide A

To construct *fragment C*, aldehyde **3.36** was added to the chlorotitanium enolate of thiazolidinethione **3.37** gave aldol adduct **3.38** (Scheme 3.8).¹¹⁸ Reductive cleavage, then a Horner-Wadsworth-Emmons olefination gave unsaturated ester **3.39**. Reduction of the alkene on Pd/C and H₂, then acid-catalyzed lactonization and reductive acylation¹¹⁹ gave acetate **3.40** as a mixture of diastereomers (9:1 dr). *in situ* addition of silyl enol ether **3.41** to acetate **3.40** followed by deprotection of the TIPS ether with H₂SiF₆ gave alcohol **3.42**. Oxidation to the carboxylic acid and amide coupling with N-hydroxy succinimide gives *fragment C* (**3.43**).



Reagents and Conditions

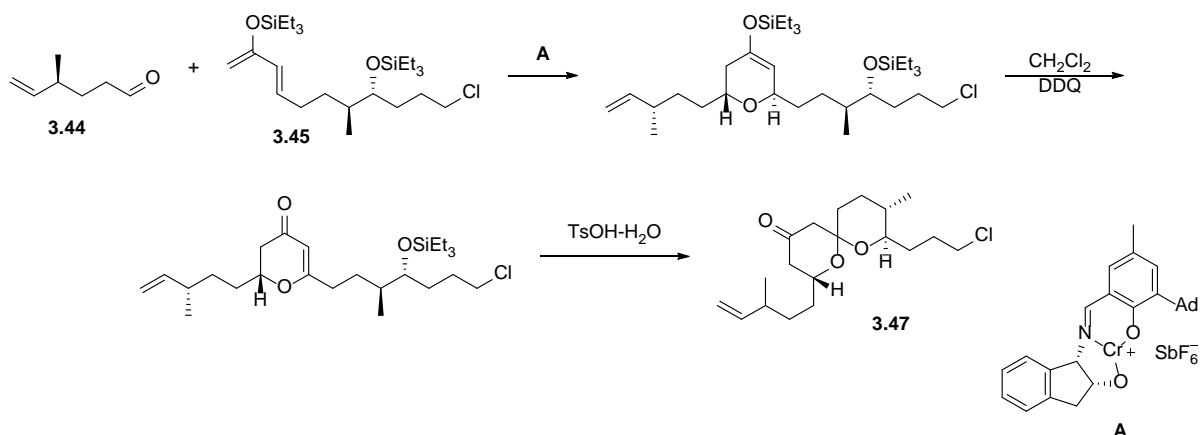
(a) TiCl₄, NMP, (-)-sparteine, CH₂Cl₂, -78 °C, 6, 87%; (b) *i*-Bu₂AlH, THF, -78 °C; (c) Ph₃PCHCO₂Et, CH₂Cl₂, 78% (two steps); (d) H₂, Raney Ni, EtOH; (e) PPTS, CH₂Cl₂, 40 °C, 81% (two steps); (f) *i*-Bu₂AlH, pyridine, DMAP, Ac₂O, CH₂Cl₂, -78 to -20 °C, 96%; (g) Et₃N, TMSOTf, 3-penten-2-one, CH₂Cl₂, 0 °C then -78 °C, then add acetate **3.40**, 87%, 9:1 dr; (h) H₂SiF₆, CH₃CN, 0 °C, 75%; (i) H₅IO₅/CrO₃, CH₃CN, 77%; (j) N-hydroxysuccinimide, EDC·HCl, CH₂Cl₂, 100%.

Scheme 3.8 Crimmins Synthesis of *Fragment C* (3.43)

Completion of Crimmins' synthesis of Bistramide A was nearly identical to Kozmin's synthesis. Overall Crimmins synthesis was 18 steps compared to Kozmin's 15.

3.1.3 Floreancig's 2014 Synthesis of Bistramide A

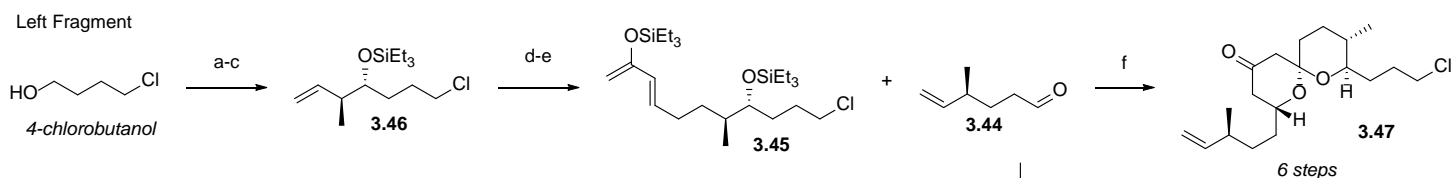
The most efficient synthesis to date of Bistramide A was reported by the Floreancig group in 2014.¹⁰⁴ The retrosynthetic plan put forth by Floreancig was quite similar to those reported by Crimmins and Kozmin. The key component of the synthetic plan was the formation of the spiroketal of *Fragment A* through a one-pot enantioselective Hetero-Diels-Alder (HDA) cycloaddition with Cr catalyst **A**,¹²⁰ C-H bond cleavage with DDQ,¹²¹ and protodesilylation/cyclization (Scheme 3.9).¹²²



Scheme 3.9. One pot synthesis of the spiroketal portion of Bistramide A

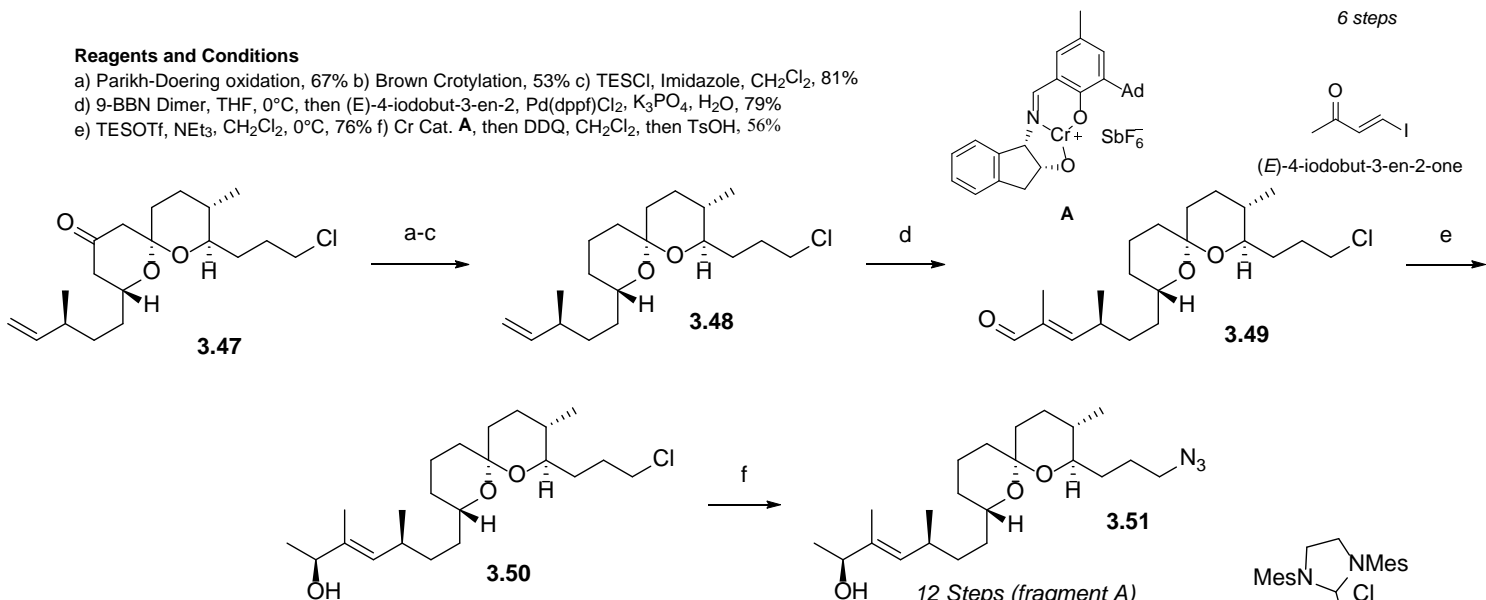
Aldehyde **3.44** was synthesized by epoxidation with *m*CPBA, then oxidation with H_5IO_6 in two steps from (+)- β -citronellene.¹²³ To synthesize siloxydiene **3.45** 4-chlorobutanol is oxidized to the aldehyde using Pahrck-doring conditions,¹²⁴ then Brown crotylation¹⁰⁶ and silyl ether protection gives alkene **3.46** (Scheme 3.10). Suzuki coupling¹²⁵ with (E)-4-iodobut-3-en-2-one yielded an enone, which was converted into siloxy diene **3.45** in the presence of NEt_3 and triethylsilyltrifluoromethanesulfonate. An enantioselective HDA reaction, DDQ treatment, and acid

mediated ring closure yielded spiroketal **3.47**. Spiroketal **3.47** was subjected to a variation of a Wolff-Kishner reduction¹²⁶ to give spirocycle **3.48**, which underwent cross-metathesis with methacrolein in the presence of Nitro-Grela catalyst to give aldehyde **3.49**. A diastereoselective addition of Me₂Zn into aldehyde **3.49** in the presence of (-)-MIB gave alcohol **3.50**. Finally, to complete azido *fragment A*, chloride displacement in the presence of NaN₃ gave azide **3.51**.



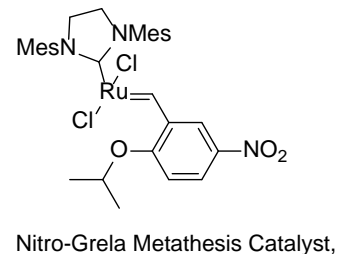
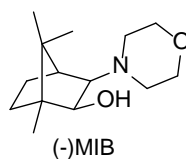
Reagents and Conditions

- a) Parikh-Doering oxidation, 67% b) Brown Crotylation, 53% c) TESCl, Imidazole, CH₂Cl₂, 81%
d) 9-BBN Dimer, THF, 0°C, then (E)-4-iodobut-3-en-2, Pd(dppf)Cl₂, K₃PO₄, H₂O, 79%
e) TESOTf, NEt₃, CH₂Cl₂, 0°C, 76% f) Cr Cat. **A**, then DDQ, CH₂Cl₂, then TsOH, 56%



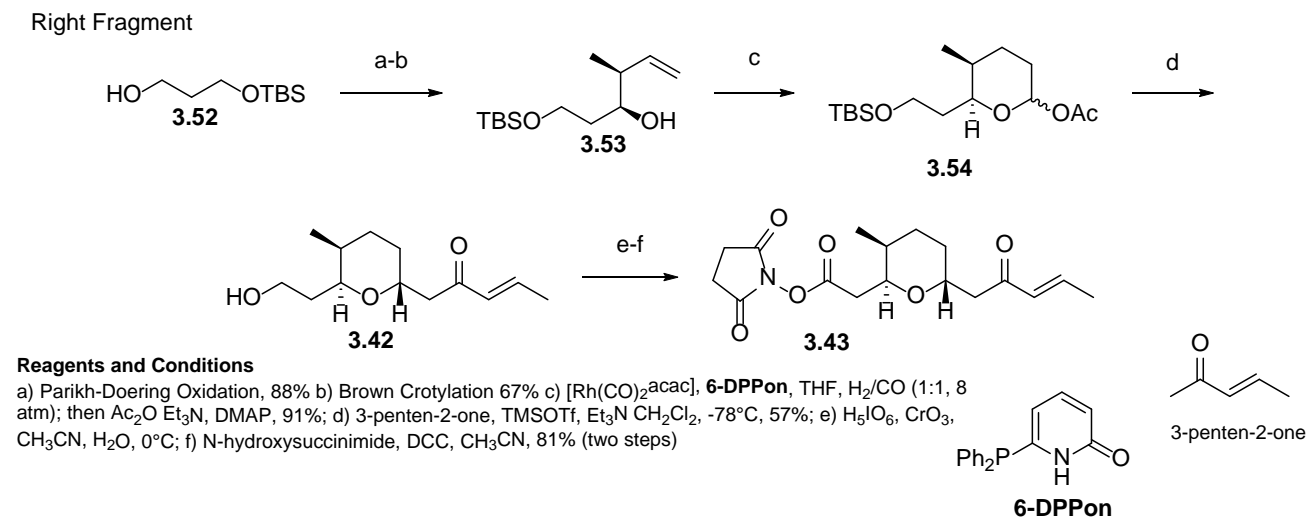
Reagents and Conditions

- a) TsNHNH₂, MeOH b) NaBH₃CN, MeOH:THF (1:1) c) EtOH:H₂O 20:1, NaOAc, 47% over three steps.) Nitro-Grela Metathesis Catalyst, methacrolein:CH₂Cl₂, 49%, e) Me₂Zn, (-)-MIB, Hexanes, 87% f) NaN₃, DMF 50°C, 95%



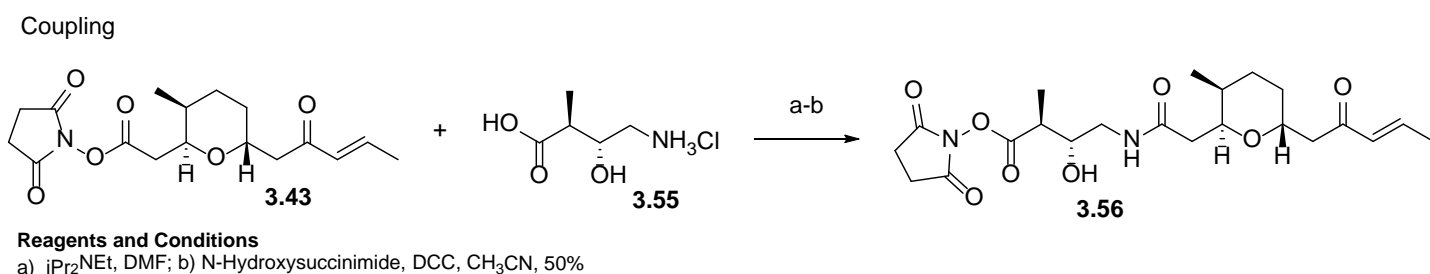
Scheme 3.10 Floreancigs synthesis of Fragment A (**3.51**)

Floreancig's approach towards *fragment C* begins with Parikh-Doering oxidation of monoprotected alcohol **3.52**, followed by Brown Crotylation to give homoallylic alcohol **3.53** (Scheme 3.11). Rhodium catalyzed hydroformylation of homoallylic alcohol **3.53** under high pressure H₂/CO (Syngas) and Breit's self-assembling supramolecular ligand (**6-DPPon**) forms a lactol,¹²⁷⁻¹²⁸ which can be protected with acetic anhydride to form acetate **3.54** as an inconsequential mixture of diastereomers. The addition of the *in situ* formed silyl enol ether derived from 3-penten-2-one into **3.54** occurs with desilylation to give alcohol **3.42** (see Kozmin synthesis). Completion of *fragment C* was performed in a manner identical to Kozmin to give succinimide **3.43**.



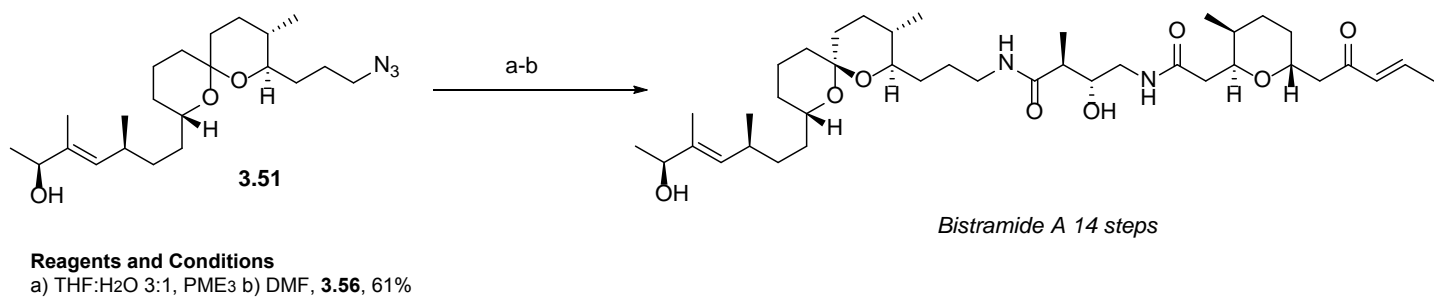
Scheme 3.11 Floreancig's synthesis of Fragment C

Succinimide **3.43** and β -amino acid fragment **3.55** (*fragment B* of Kozmin's synthesis) were coupled together in the presence of diisopropylethylamine, then DCC esterification with N-hydroxysuccinimide gives succinimide **3.56** (Scheme 3.12).



Scheme 3.12 Coupling of Fragment B and Fragment C to form BR

To complete the Synthesis, Staudinger reduction of azide **3.51**, followed by addition into succinimide **3.56** gives **Bistramide A** in 14 steps (Scheme 3.13).



Scheme 3.13 Floreancigs completion of Bistramide A

3.2 PREVIOUS ANALOGUES OF BISTRAMIDE A

Since the unexpected discovery that Bistramide A's primary cellular receptor is Actin,¹⁰³ several analogues for Bistramide A have been synthesized, primarily to determine its mode of action and increase potency. The rational design of Bistramide A analogues can be inferred from the X-ray structure of Bistramide A bound to actin, reported by Kozmin in 2006.¹²⁹ The central amino acid fragment of Bistramide A establishes several polar contacts with its target and the spiroketal fragment occupies a hydrophobic pocket (Figure 3.2).

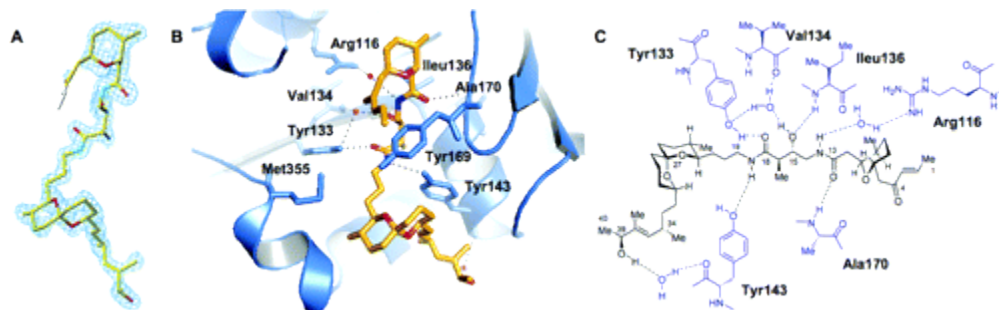


Figure 3.2 Bistramide A contacts involve with A-Actin recognition

3.2.1 Kozmin's Bistramide Analogues

Comprehensive characterization of the mode of action of Bistramide A and the structural components essential for its potency were reported in 2008 through the synthesis of several structural analogues of Bistramide A (Figure 3.3).¹³⁰ Each analogue reported was evaluated based on its ability to bind monomeric actin (K_d) and the compounds ability to inhibit cell growth of A549 (nonsmall cell lung cancer) cells (GI_{50}).

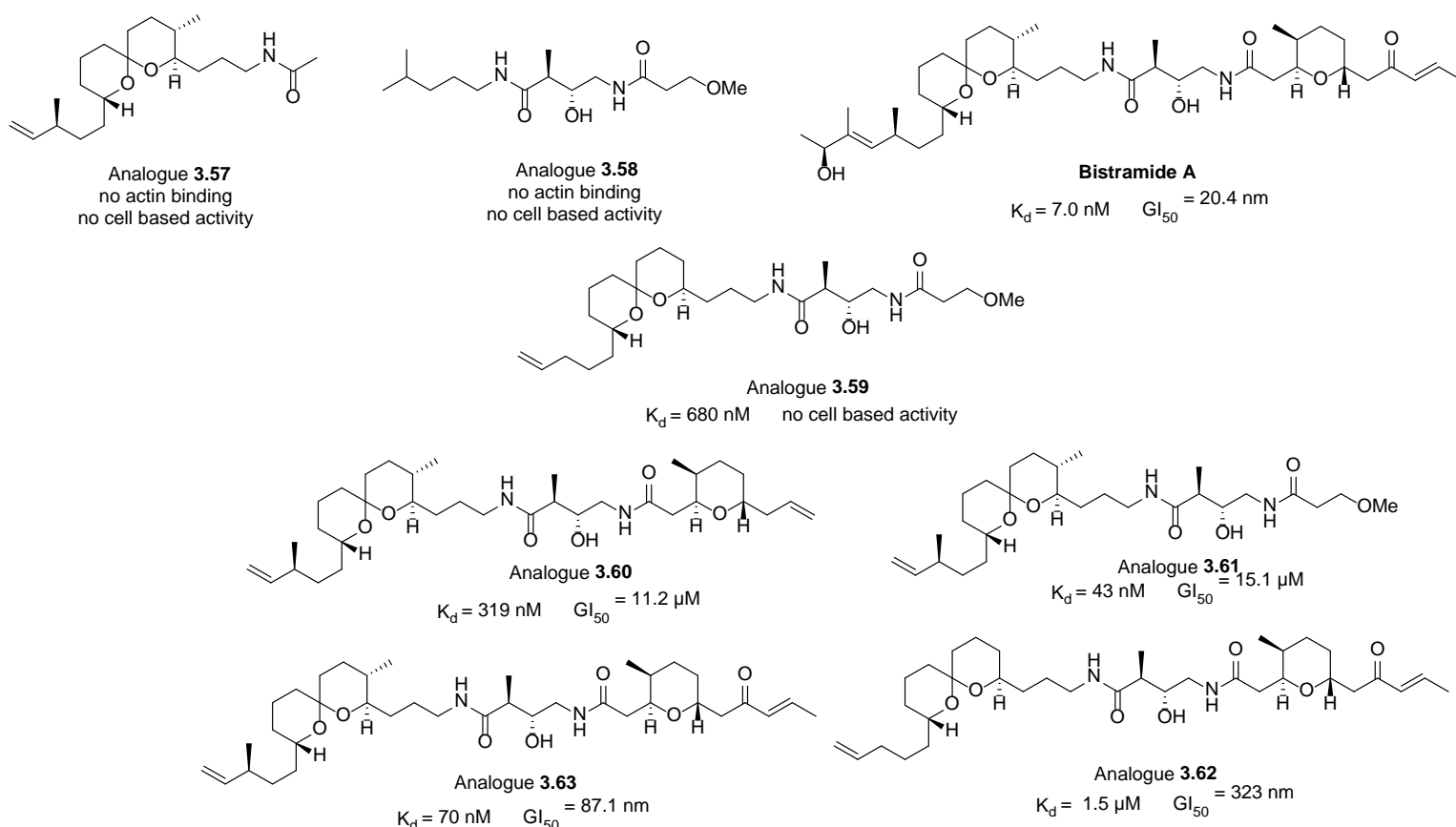


Figure 3.3. Rationally designed analogues of Bistramide A, their growth inhibition (GI_{50}) and their dissociation constants (K_d) with monomeric actin

The X-ray crystal structure of Bistramide A bound to Actin suggests that the middle amino acid fragment and the left spiroketal fragment played an influential role in establishing a hydrogen

bond-network and hydrophobic interactions with its cellular target. Analogue **3.57** and analogue **3.58**, the spiroketal fragment and the amino acid fragment respectively, showed no activity; suggesting that both fragments together are essential. When the fragments are linked (**3.61**), actin binding was restored to a partial extent; although cellular inhibition is low compared to the **Bistramide A**. Elimination of the two methyl groups on the spiroketal fragment (**3.59**) led to a sharp decrease in actin-binding efficiency, which is consistent with the hypothesis that the spiroketal interacts with a hydrophobic pocket in Actin. Adding in the pyran portion of the right fragment (**3.60**) didn't have a significant effect on the actin-binding or cell inhibition. Incorporation of the enone portion of the right fragment (**3.62** and **3.63**) dramatically increased cell-based activity. This finding suggests that the enone containing bistramide analogues **3.62** and **3.63** and **Bistramide A** suggest that Actin may be covalently modified. Monitoring the interaction of the **3.62**, **3.63**, and **Bistramide A** with Actin using MS analysis revealed the presence of high molecular weight peaks consistent with covalent modification. The unprecedented high reactivity of Cys-374 on actin¹³¹ suggests that Michael addition of the Cys-374 thiol to the enone portion of the Bistramide Analogues contributes significantly to the cytotoxic activity of **Bistramide A** and analogues **3.62** and **3.63**.

This work led to the development of rationally simplified bistramide analogue **3.64** (Figure 3.4).¹³² Compound **3.64** contains the lipophilic/hydrophobic spiroketal fragment and the hydrophilic middle fragment, both of which are essential for retaining actin-binding activity; removal of the enone minimize *in vivo* toxicity and thus makes **3.64** more appropriate for living tissue. Compared to the dissociation constant (K_d) for **Bistramide A** with Actin-G of 6.8 nM, **3.64** has a comparable K_d (9.0 nM). Analogue **3.64** depolymerizes actin *in vitro*, inhibits growth of cancer cell lines *in vitro*, and suppresses A549 (nonsmall cell lung cancer) tumor growth *in vivo*.

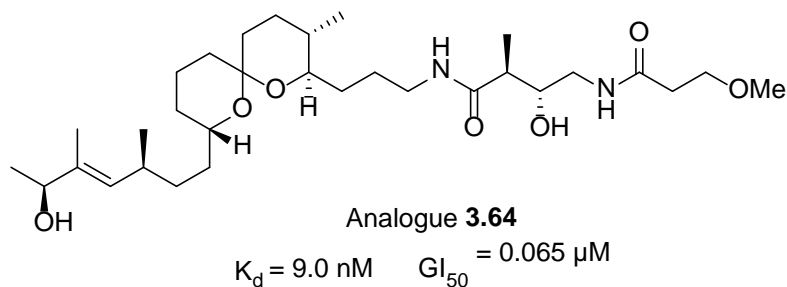
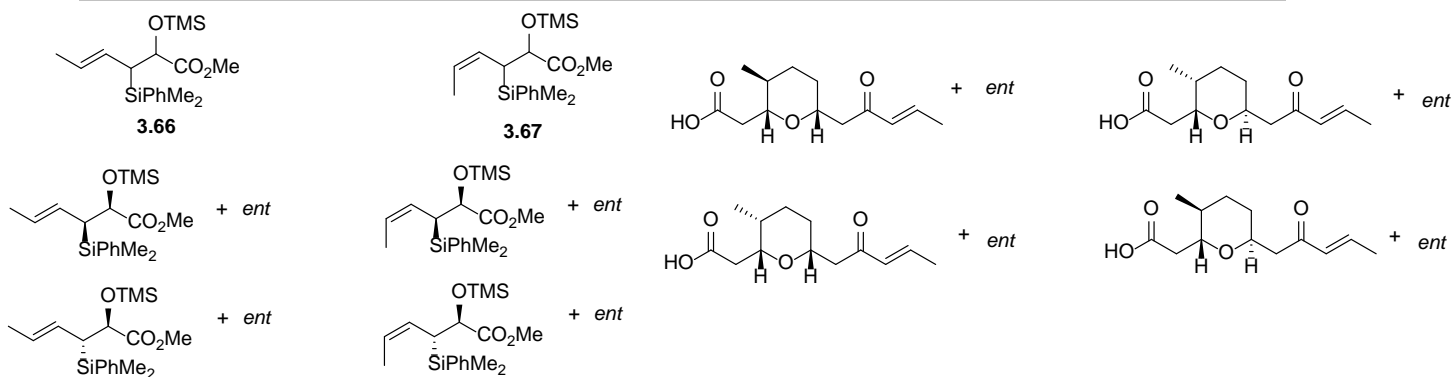
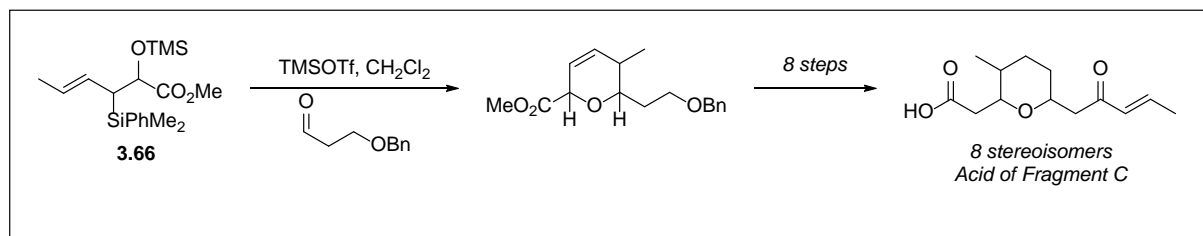


Figure 3.4 Rationally designed Bistramide Analogue for *In vivo* studies

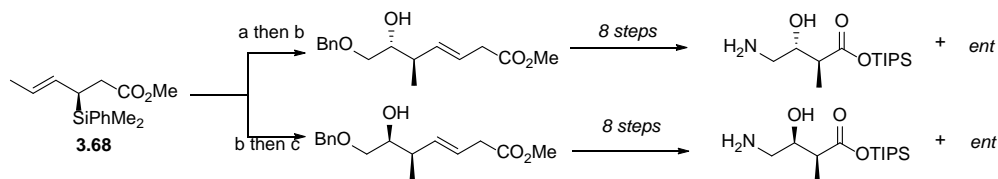
3.2.2 Panek's Bistramide A Stereoisomer Library

35 stereoisomers of Bistramide A were reported and tested by Panek in 2009, a single analogue, **3.65** had enhanced potency compared to **Bistramide A** (Figure 3.5). This work showcases the ability of crotylsilane reagents **3.66**, **3.67**, and **3.68**. In a prior synthesis of Bistramide A reported by the Panek group,¹³³ these three chiral reagents were used to establish 8 of the 11 stereoisomers of Bistramide A. Stereodifferentiation of **3.66** and **3.67** were used to provide 8 possible isomers for *fragment C* in 9 steps (Scheme 3.14). The key step in the sequence was a [4 +2]-annulation with β -benzyloxyaldehyde with each stereochemical variant of **3.66** and **3.67**. This forms the required pyran ring and establishes the relative stereochemistry of the methyl group relative to the ring junctions. An 8-step sequence was then used to synthesize the 8 stereoisomers of the carboxylic acid of *fragment C*.



Scheme 3.14 Synthesis of 8 stereoisomers of Fragment C of Bistramide A

3.68 and its corresponding enantiomer were used to provide the 4 isomers of amino acid *fragment B* (Scheme 3.15). This was achieved through a two-step sequence that consisted of [3+2]-annulation followed by a SbCl_5 mediated E_2 elimination to give homoallylic alcohols. SnCl_4 provides the *anti* relationship and $\text{BF}_3\text{-OEt}_2$ provides the *syn* relationship. An 8 step sequence provides the four isomers of TIPS protected *fragment B*.

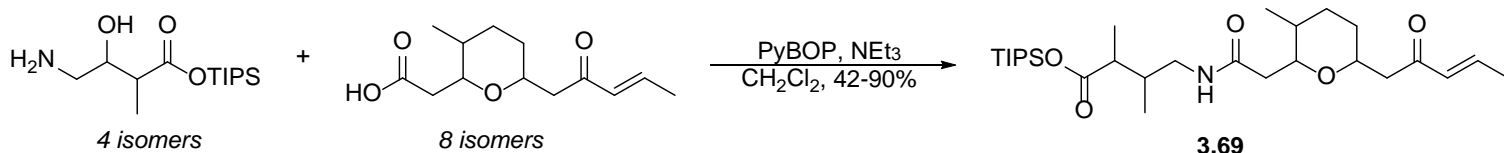


Reagents and Conditions

a) SnCl_4 , CH_2Cl_2 , -78°C , 73% dr 20:1; b) SbCl_5 , CH_2Cl_2 , -50°C , 62-85%; c) $\text{BF}_3\text{-OEt}_2$, CH_2Cl_2 , -78°C , 73% dr 20:1

Scheme 3.15 Synthesis of 4 isomers of Fragment B of Bistramide A

Coupling of the 4 diastereomers of TIPS Protected *Fragment B* and the 8 isomers of carboxylic acid *Fragment C* provides 32 different isomeric fragments of **3.69** (Scheme 3.16).



Scheme 3.16 Coupling of Fragment B and Fragment C to synthesize 32 isomers of BR

Finally, a sequence of deprotection of the TIPS ester **3.69**, followed by coupling with spiroketal *fragment A* and its corresponding epimer; then silyl ether deprotection leads to the 35 isomer library of Bistramide A analogues.

The 35-isomer library of Bistramide Analogues was screened for actin depolymerization and cytotoxicity. Only a single stereochemical isomer, **3.65**, was found to be more potent than **Bistramide A** by a factor of two (Figure 3.5). Surprisingly, **3.65** differs at the ring junction of the tetrahydropyran portion of *fragment C*, which was demonstrated by Kozmin to not have an effect on potency as much as *fragment B* and *fragment A*. Additionally, the alcohol epimer of **Bistramide A**, **3.70**, exhibited similar potency to **Bistramide A**, suggesting that the stereochemical configuration of the alcohol on *fragment A* is inconsequential for biological activity.

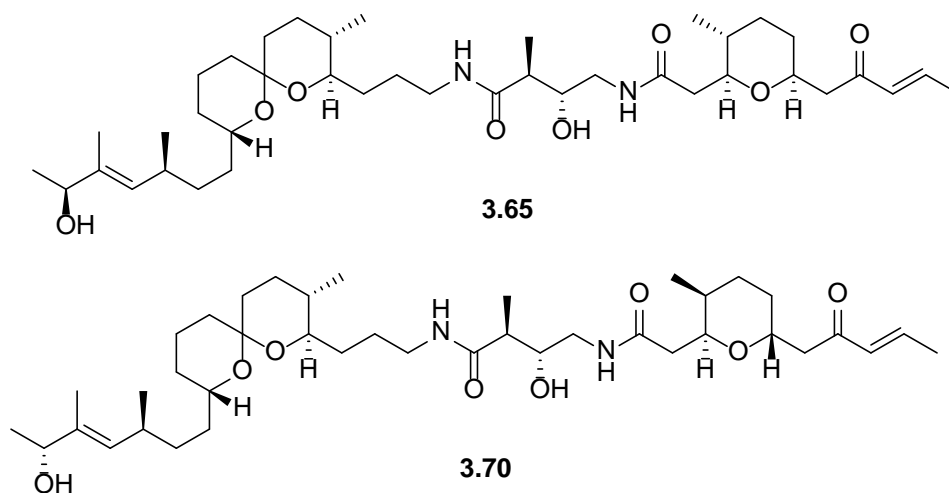
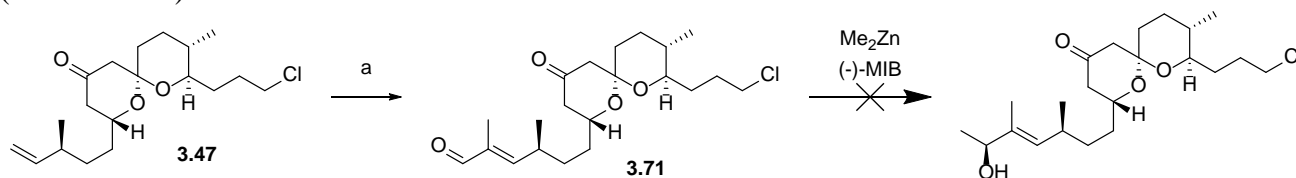


Figure 3.5 Most potent stereoisomers of Bistramide A

3.3 NOVEL ANALOGUES OF BISTRAMIDE A, SYNTHETIC OPTIMIZATION, AND BIOLOGICAL ACTIVITY

Our group currently has the shortest sequence for the synthesis of **Bistramide A** at 14 steps. In the synthesis of *fragment A*, there is a three step Wolff-Kishner reduction to remove the ketone from the spiroketal ring. We reasoned that since the spiroketal plays a central role in determining biological potency; analogues of **Bistramide A** could easily be synthesized with different levels of oxidation in the spiroketal ring in a shorter sequence than the synthesis of the natural product. Starting with spiroketal intermediate **3.47**, cross-metathesis with methacrolein in the presence of Hoveyda-Grubbs metathesis catalysis give di-carbonyl compound **3.71**. Unfortunately, the addition of Me_2Zn in the presence of (-) MIB simply led to decomposition (Scheme 3.17).



Reagents and conditions

a) Methacrolein:CH₂Cl₂ 5:1, **HG-II**, 63%

Scheme 3.17 Attempted dimethyl zinc addition into carbonyl 3.71

We reasoned that the synthesis of our desired analogues could be even further simplified by ignoring the secondary alcohol stereocenter of the spiroketal fragment. Prior work on bistramide analogues has shown that changes to the alcohol on the spiroketal fragment do not dramatically effect biological activity. We planned to make five bistramide analogues, axial and

equatorial alcohols **3.72** and **3.73**, ketone analogue **3.74**, methyl ether analogue **3.75**, and fully reduced analogue **3.76** to compare to synthetic **Bistramide A**.

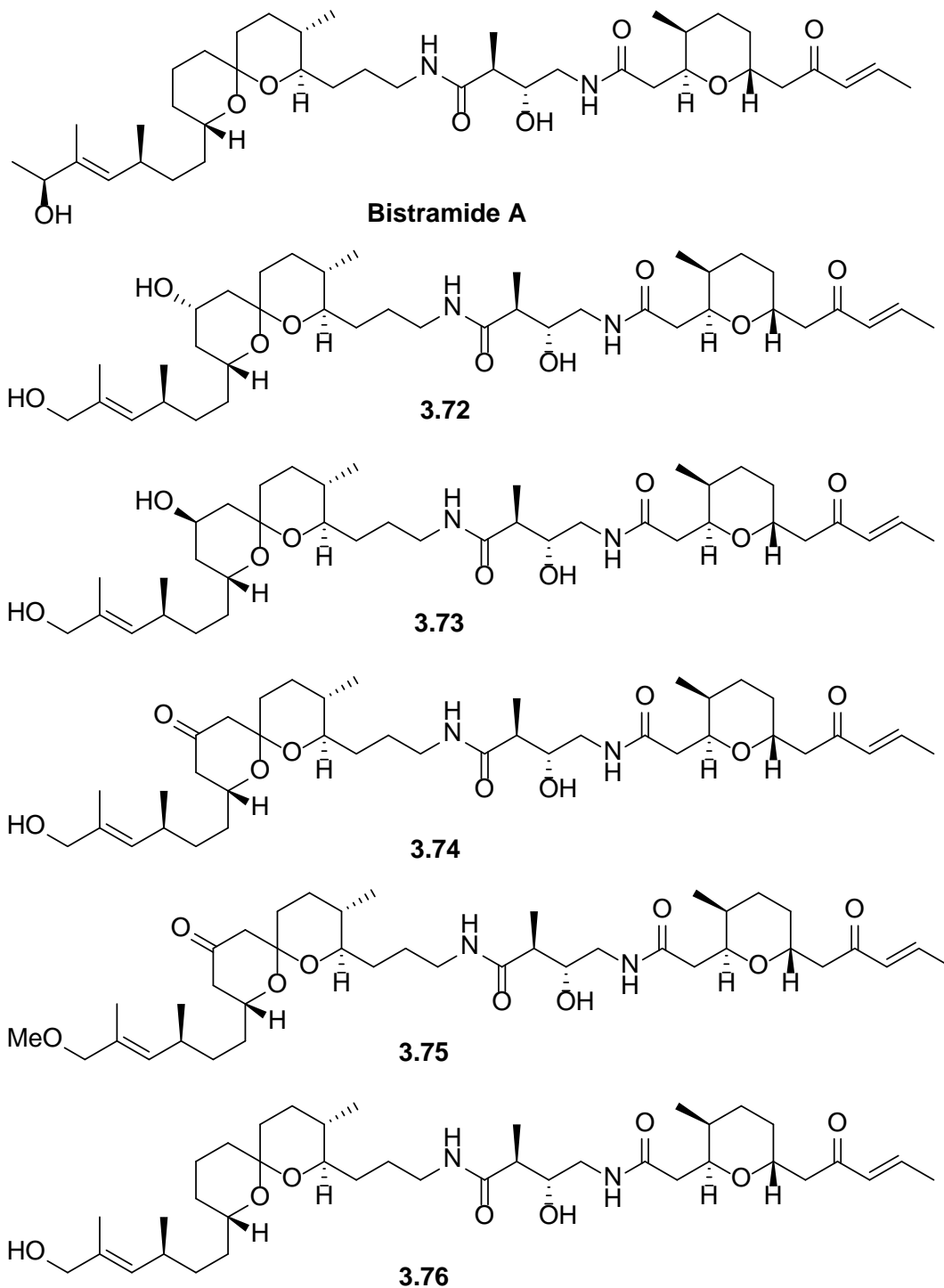
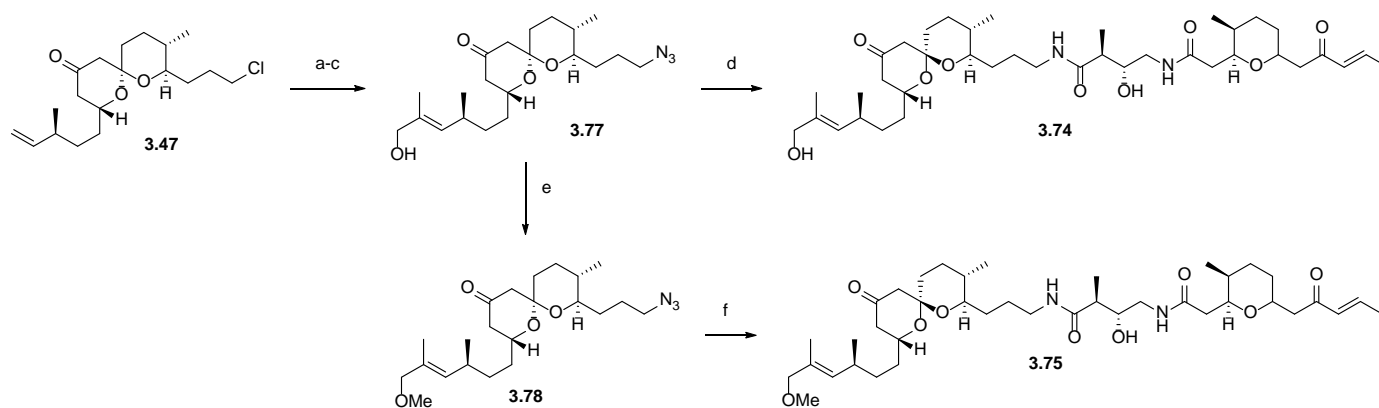


Figure 3.6 Novel analogues of Bistramide A

3.74 was synthesized by cross-metathesis between alkene **3.47** and methacrolein in the presence of **HGII** (E:Z 10:1). The E and Z isomers were inseparable and thus the synthesis of each of the analogues was completed as a mixture. Results from prior work on Bistramide analogues show that the Z isomer will not have a dramatic effect on the potency; with reported GI₅₀ values lower than **Bistramide A** by a factor of five.¹³⁴ Chemoselective reduction of aldehyde **3.71** with a single equivalent of L-selectride (Scheme 3.18) followed by chloride displacement gives azide **3.77**. Coupling with succinimide **3.56** affords ketone analogue **3.74**. To synthesized methyl ether analogue **3.75**, azide **3.77** was methylated with methyl triflate and 2,6-ditertbutylpyridine to give azide **3.78**, which was coupled with succinimide **3.56** to form methyl ether analogue **3.75**.



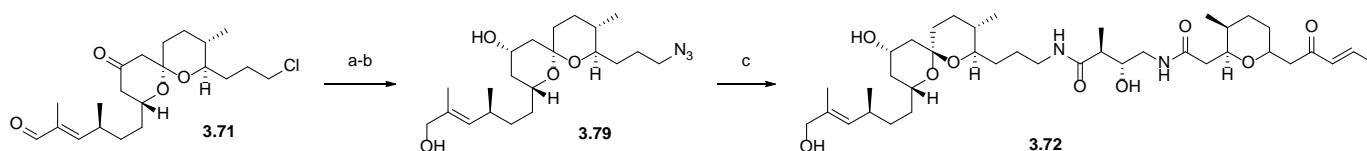
Reagents and Conditions

a) Methacrolein:CH₂Cl₂ 5:1, HG-II, 68%. b) L-selectride, THF, -78°C, 67% c) NaN₃, DMF, 50°C, 92%. d) PMe₃, THF:H₂O 3:1, then **3.56**, DMF, 41% e) 2,6 ditertbutylpyridine, MeOTf, CH₂Cl₂, 69% f) PMe₃, THF:H₂O 3:1, then **3.56**, DMF, 31%

Scheme 3.18 Synthesis of Bistramide analogues **3.74** and **3.75**

To prepare axial analogue **3.72**, dicarbonyl **3.71** was reduced with NaBH₄ to give the axial alcohol (Scheme 3.19). Chloride displacement with sodium azide in DMF give azide **3.79**. Staudinger reduction and addition into succinimide **3.56** gives axial alcohol bistramide analogue

3.72.

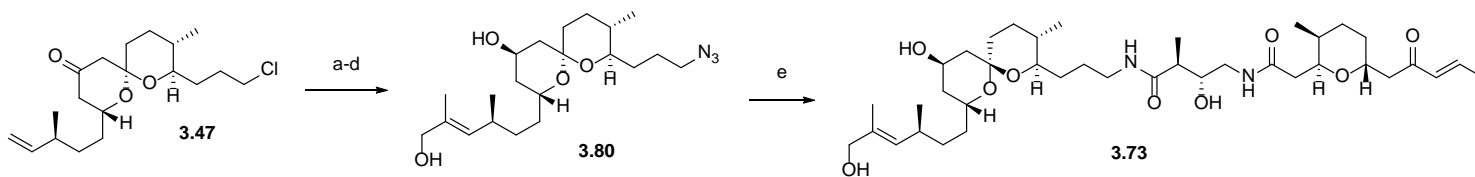


Reagents and conditions

a) NaBH₄, MeOH 0°C, 88%. b) NaN₃, DMF, 50°C, 63%.
c) PMe₃, THF:H₂O 3:1, then **3.56**, DMF, 43%

Scheme 3.19 Synthesis of **3.72**

To synthesize the equatorial analogue, alkene **3.47** was subjected to Meerwein-Ponndorf-Verley reduction conditions mediated by Sm in isopropanol delivers the hydride in the axial position to give the equatorial alcohol (Scheme 3.20). The high selectivity observed in this reduction likely results from coordination of Sm to the axial alcohol of the spiroketal ring. Cross-metathesis, NaBH₄ reduction, and chloride displacement gives azide **3.80**, which undergoes coupling with succinimide **3.56** to give equatorial bistramide analogue **3.73**.

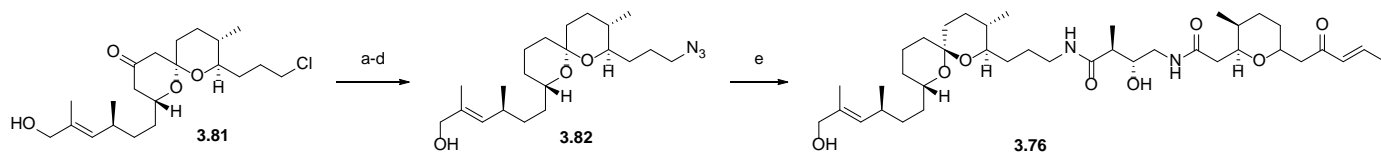


Reagents and Conditions

a) Sm, isopropanol, 75% b) Methacrolein:CH₂Cl₂ 5:1, HG-II, 68%.
c) NaBH₄, MeOH 0°C, 81%. d) NaN₃, DMF, 50°C, 90%. e) PMe₃, THF:H₂O 3:1, then **3.56**, DMF, 39%

Scheme 3.20 Synthesis of Bistramide analogue **3.73**

To synthesize the fully reduced analogue, ketone **3.81** was subjected to modified Wolff-Kishner reduction conditions and the ketone was removed over three steps. Chloride displacement provides azide **3.82**, which undergoes coupling with succinimide **3.56** to give bistramide analogue **3.76**.



Reagents and Conditions

a) MeOH, TsNHNH₂ b) MeOH:THF, NaBH₃CN c) EtOH/H₂O 20:1, NaOAc, 47% over 3 steps d) NaN₃, DMF, 50°C, 81%. e) PMe₃, THF:H₂O 3:1, then 3.56, DMF, 54%

Scheme 3.21 Synthesis of bistramide analogue **3.76**

In collaboration with the Deiter's group, Yuta Naro tested the five analogues of Bistramide A as well as synthetically prepared **Bistramide A**. Alcohol containing bistramide analogues **3.72** and **3.73** showed dramatically reduced activity compared to **Bistramide A**. This is perhaps not a surprising result, as Kozmin demonstrated that maintaining the hydrophobicity of the spiroketal core is essential for activity. Ketone and methyl ether analogues **3.74** and **3.75** showed modest decreases in activity compared to **Bistramide A**; thus the ketone is tolerated. Surprisingly, fully reduced analogue **3.76** showed increased activity compared to **Bistramide A**.

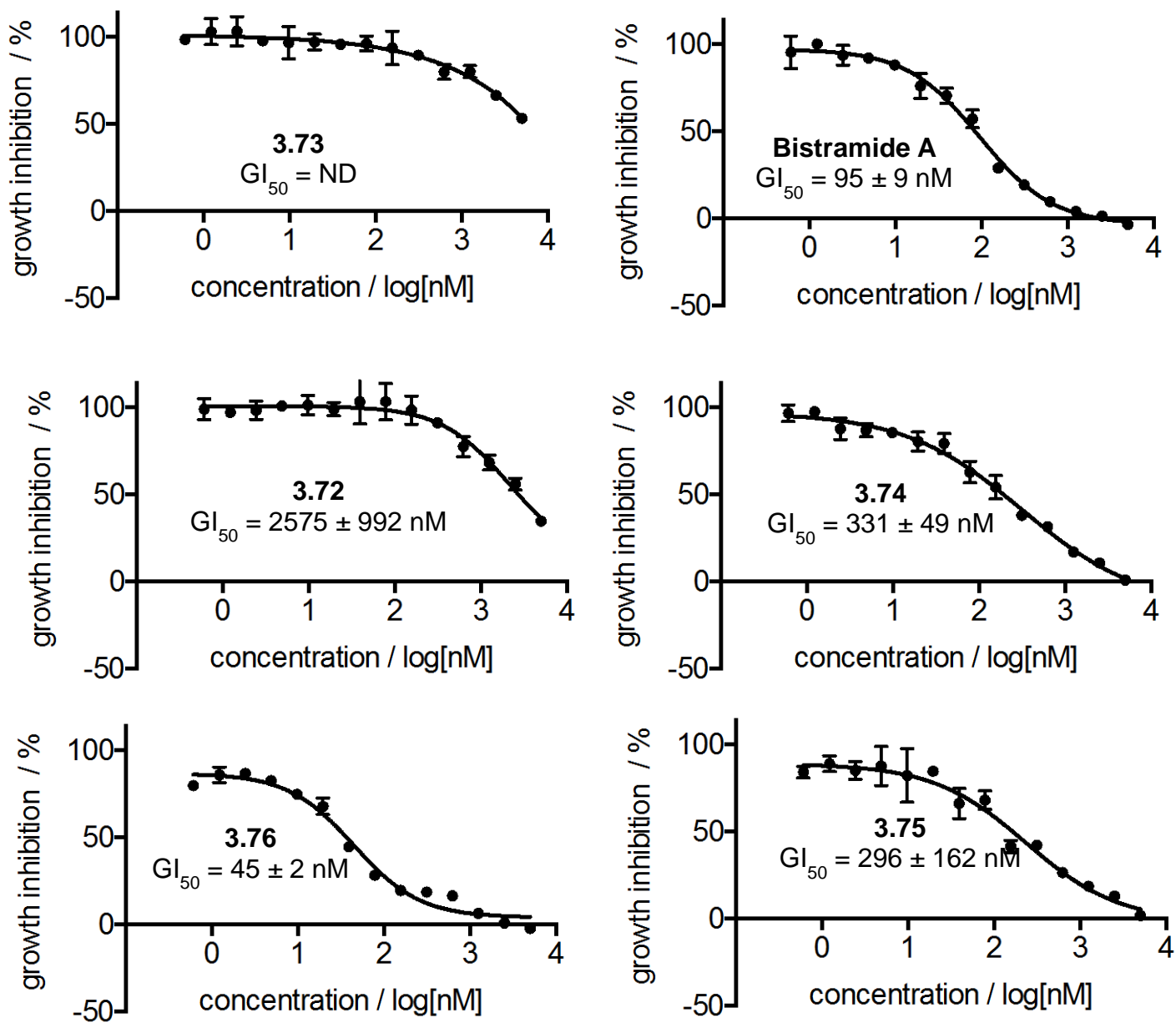
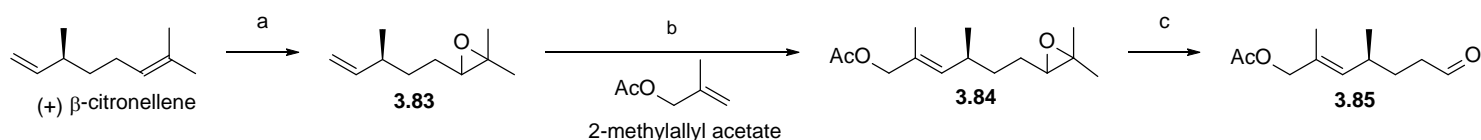


Figure 3.7 GI_{50} curves for Bistramide A, 3.73, 3.72, 3.74, 3.76, and 3.75 in small cell lung cancer (A549) cells.

Inspired by these results we envisioned a more convergent route towards the synthesis of a potent analogue of **Bistramide A**. Starting with epoxide (+) β -citronellene, **3.83** was synthesized by selective epoxidation of the more electron rich alkene. Epoxide **3.83** undergoes cross-metathesis in the presence of 2-methylallyl acetate and **HG-II** to give allyl acetate **3.84** in E:Z ratio of 5:1. Cleavage of epoxide **3.84** in the presence of H_5IO_6 gives aldehyde **3.85**.

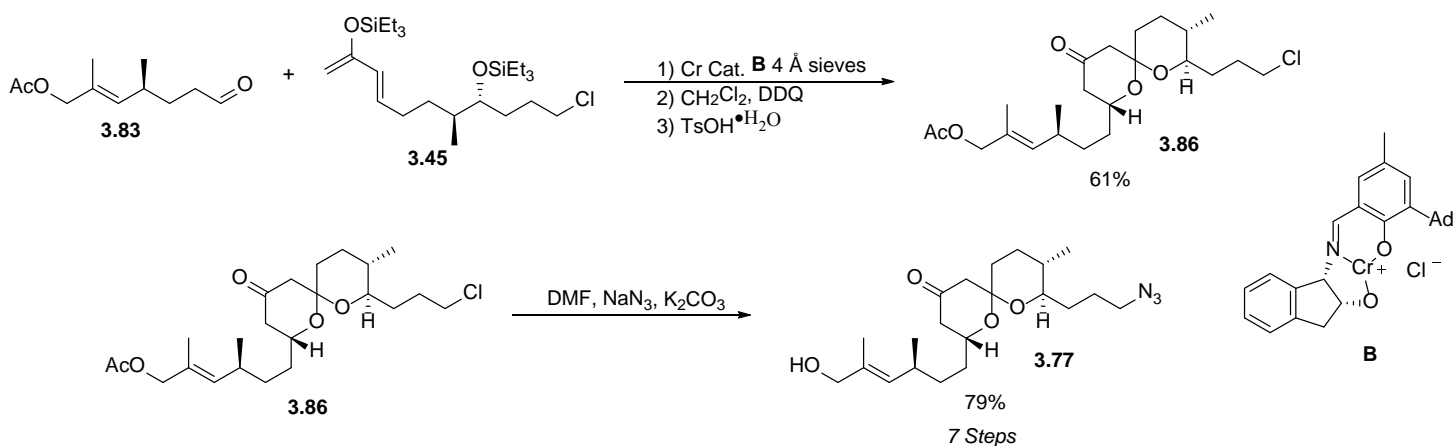


Reagents and Conditions

- a) *m*CPBA, CH_2Cl_2 , 0 C, 73% dr 1:1
 b) 5:1 2-methylallyl acetate: CH_2Cl_2 , HG-II (3 mol%), 52%, E:Z 5:1
 c) H_5IO_6 , THF, 0 C, 51%, E:Z 5:1

Scheme 3.22 Synthesis of aldehyde **3.83**

Aldehyde **3.83** and siloxydiene **3.45** undergo a one-pot HDA with Cr catalyst **B**, DDQ oxidation, and acid mediated cyclization to give spirocycle **3.86**. Spirocycle **3.86** can then undergo a one-pot acetate deprotection, azide displacement reaction to give **3.77**, the precursor to bistramide analogue **3.74**.

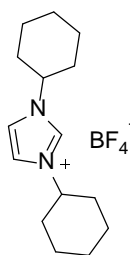


Scheme 3.23 A more convergent route towards the synthesis of a potent Bistramide Analogue

Thus completion of the synthesis of Bistramide analogue **3.74** can be accomplished in 9 steps, this is an improvement over the best prior synthesis of **Bistramide A** which is 14 steps. Obviating the need to reduce the ketone removes a three-step sequence and altering the allylic alcohol from 2° to 1° greatly expedites the synthesis.

APPENDIX A

Alcohol, Aldehyde, and Ketone Liberation and Intracellular Cargo Release through Peroxide Mediated α -boryl ether Fragmentation (Supporting Info)



1,3-dicyclohexyl-1H-imidazol-3-ium tetrafluoroborate ((ICy)BF₄). To a flame dried, 2-neck, 500 mL round bottom flask containing a stir bar was added toluene (100 mL), followed by cyclohexylamine (9.92 g, 100 mmol). Paraformaldehyde (3.16 g, 100 mmol) was added, the flask was sealed and allowed to stir under N₂ for 30 minutes. The reaction was cooled to 0 °C using an ice-water bath and cyclohexylamine (9.92 mmol, 100 mmol) was added dropwise via syringe. The reaction was allowed to stir for 15 minutes and then 48 wt% HBF₄ in H₂O (12.6 mL, 96.4 mmol) was added dropwise. The reaction was allowed to stir for 30 minutes and then glyoxal trimer dihydrate (6.93 g, 33.0 mmol) was dissolved in 20 mL of H₂O and added via syringe. The reaction was sealed and allowed to stir under N₂ at 50 °C for 16 hours. The solid precipitate was filtered off and washed with 100 mL of H₂O and 100 mL of diethyl ether. Recrystallization of the resulting off-white solid in 2:1 ethyl acetate:CH₂Cl₂ gave (ICy)BF₄ (10.8 g, 33.7 mmol, 33% yield). Characterization data is consistent with that reported in the literature.¹³⁵

Data for (ICy)BF₄

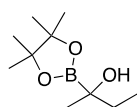
¹H NMR (400 MHz, CDCl₃)

8.93 (s, 1H), 7.44 (d, *J* = 8.0 Hz, 2H), 4.32 (tt, *J* = 3.6, 12 Hz, 2H), 2.19-2.16 (m, 4H), 1.92-1.89 (m, 4H), 1.76-1.66 (m, 6H), 1.52-1.42 (m, 4H), 1.32-1.24 (m, 2H) ppm

^{13}C NMR (125 MHz, CDCl_3)

133.18, 120.37, 60.07, 33.29, 24.93, 24.57 ppm

TLC $R_f = .2$ (10% $\text{Et}_2\text{O}/\text{CH}_2\text{Cl}_2$) [silica gel, I_2 stain]



2-(4,4,5,5-Tetramethyl-1,3,2-dioxaborolan-2-yl)butan-2-ol (2.1). To a flame dried, 250 mL round bottom flask containing a stir bar was added bis(pinacolato)diboron (1.93 g, 7.62 mmol), 1,3-bis(cyclohexyl)imidazolium tetrafluoroborate (0.22 g, 0.69 mmol), $\text{NaO}t\text{Bu}$ (0.13 g, 1.39 mmol), and CuCl (0.14 g, 1.4 mmol). Toluene (50 mL) was added, the flask was sealed, and the reaction was stirred for 30 min. 2-Butanone (0.50 g, 6.9 mmol) was added via syringe followed immediately by MeOH (0.43 g, 14 mmol). After three h the mixture was loaded directly onto a short silica plug pretreated with CH_2Cl_2 . The column was then washed with copious amounts of Et_2O and the eluent was removed under reduced pressure. The resulting residue was purified by silica gel column chromatography ($R_f = 0.4$, 5% Et_2O in CH_2Cl_2) to yield the title compound as a colorless oil (1.14 g, 5.68 mmol, 82% yield).

Data for 2.1

^1H NMR (500 MHz, CDCl_3)

δ 1.63 (m, 2H), 1.49 (m, 1H), 1.29 (s, 12H), 1.25 (s, 3H), 0.95 (t, $J = 6.5$ Hz, 3H)

^{11}B NMR (160 MHz, CDCl_3)

δ 33.1

^{13}C NMR (125 MHz, CDCl_3)

δ 84.2, 34.0, 25.7, 24.72, 24.71, 9.5

IR (thin film, NaCl)

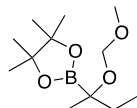
3400, 2890, 1431, 1336, 1109 cm^{-1}

HRMS (FTMS ES+)

[M+Na]⁺ Calculated for C₁₀H₂₁BO₃Na 223.1476, found 223.1473

TLC

R_f = 0.4 (5% Et₂O/CH₂Cl₂) [silica gel, p-anisaldehyde stain] [silica gel, curcumin stain]



2-(2-(Methoxymethoxy)butan-2-yl)-4,4,5,5-tetramethyl-1,3,2-dioxaborolane

(2.4). To a flame dried, 10 mL round bottom flask containing a stir bar was added

CH₂Cl₂ (5 mL), α -boryl alcohol **2.2** (0.083 g, 0.42 mmol), and (*i*Pr)₂NEt (0.107 g, 0.457 mmol).

The flask was sealed, then evacuated and refilled with Ar (3x) using a balloon equipped with a

needle and a rubber adapter. The solution was cooled to 0 °C using an ice-water bath and then

ClCH₂OMe (0.037 g, 0.46 mmol) was added dropwise via syringe. The reaction was stirred

overnight, then was quenched with saturated aqueous NaHCO₃ (5 mL). The reaction mixture was

transferred to a separatory funnel, the two layers were separated and the aqueous layer was

extracted with CH₂Cl₂ (2 x 10 mL). The combined organic layers were washed with brine (2 x 10

mL), dried over Na₂SO₄, filtered, and concentrated under reduced pressure. The resulting residue

was purified by silica gel column chromatography (R_f = 0.7, 20% Et₂O in hexanes) to yield the

title compound as a colorless oil (0.093 g, 0.38 mmol, 92% yield).

Data for 2.4

¹H NMR (400 MHz, CDCl₃)

δ 4.69 (dd, *J* = 12.9 Hz, 12.9 Hz, 2H), 3.36 (s, 3H), 1.63 (m, 2H), 1.26 (s, 12 H), 1.22 (s, 3H), 0.89

(t, *J* = 7.48 Hz, 3H)

¹¹B NMR (128 MHz, CDCl₃)

δ 32.2

¹³C NMR (100 MHz, CDCl₃)

δ 92.6, 83.6, 55.4, 31.2, 24.8, 24.7, 21.4, 21.3, 8.6

IR (thin film, NaCl)

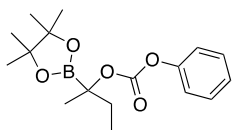
2940, 1456, 1323, 1201 cm⁻¹

HRMS (FTMS ES+)

[M+H]⁺ Calculated for C₁₂H₂₆O₄B 245.1918, found 245.1908

TLC

R_f = 0.7 (20% Et₂O in hexanes) [silica gel, p-anisaldehyde stain] [silica gel, curcumin stain]



Phenyl (2-(4,4,5,5-tetramethyl-1,3,2-dioxaborolan-2-yl)butan-2-yl) carbonate (2.3). To a flame dried, 10 mL round bottom flask containing a stir

bar was added CH₂Cl₂ (5 mL), α-boryl alcohol **2.2** (0.089 g, 0.45 mmol), and pyridine (0.073 g, 0.89 mmol). The flask was sealed, evacuated, and refilled with Ar (3x) using a balloon equipped with a needle and a rubber adapter. The solution was cooled to 0 °C using an ice-water bath and then PhOC(O)Cl (0.077 g, 0.49 mmol) was added dropwise via syringe. The reaction was stirred overnight, then was quenched with saturated aqueous NaHCO₃ (5 mL). The reaction mixture was transferred to a separatory funnel, the two layers were separated, and the aqueous layer was extracted with CH₂Cl₂ (2 x 10 mL). The combined organic layers were washed with brine (2 x 10 mL), dried over Na₂SO₄, filtered, and then concentrated under reduced pressure. The resulting residue was purified by silica gel column chromatography (R_f = 0.3, 20% Et₂O in hexanes) to yield the title compound as a colorless oil (0.101 g, 0.315 mmol, 71% yield).

Data for 2.3

¹H NMR (400 MHz, CDCl₃)

δ 7.37 (m, 2H), 7.20 (m, 3H), 1.82 (m, 2H), 1.43 (s, 3H), 1.28 (s, 6H), 1.26 (s, 6H), 0.98 (t, *J* = 7.5 Hz, 3H)

¹¹B NMR (128 MHz, CDCl₃)

δ 32.2 ppm

¹³C NMR (100 MHz, CDCl₃)

δ 154.1, 151.4, 129.3, 125.7, 121.0, 84.1, 30.2, 24.9, 24.7, 20.4, 8.2 ppm

IR (thin film, NaCl)

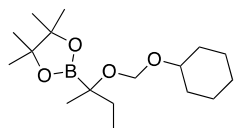
3016, 1312, 1246, 1167, 1048, 954, 837, 780, 690 cm⁻¹

HRMS (FTMS ES⁺)

[*M*+*H*]⁺ Calculated for C₁₇H₂₆O₅B 321.1868, found 321.1853

TLC

R_f = 0.3 (20% Et₂O in hexanes) [silica gel, p-anisaldehyde stain] [silica gel, curcumin stain]



2-(2-((Cyclohexyloxy)methoxy)butan-2-yl)-4,4,5,5-tetramethyl-1,3,2-dioxaborolane (2.5). To a flame dried, 10 mL round bottom flask containing

a stir bar was added CH₂Cl₂ (5 mL), α-boryl alcohol **2.2** (0.10 g, 0.50 mmol), and N(*i*Pr)₂Et (0.081 g, 1.0 mmol). The flask was sealed, evacuated and refilled with Ar (3x) using a balloon equipped with a needle and a rubber adapter. The solution was cooled to 0 °C using an ice-water bath and then ClCH₂OCy (0.129 g, 0.550 mmol) was added dropwise via syringe. The reaction was stirred overnight, then was quenched with saturated aqueous NaHCO₃ (15 mL). The reaction mixture was transferred to a separatory funnel, the two layers were separated, and the aqueous layer was extracted with CH₂Cl₂ (2 x 20 mL). The combined organic layers were washed with brine (2 x 20

mL), dried over Na₂SO₄, filtered, and then concentrated under reduced pressure. The resulting residue was purified by silica gel column chromatography (R_f = 0.8, 20% Et₂O in hexanes) to yield the title compound as a colorless oil (0.038 g, 0.12 mmol, 24% yield).

Data for 2.5

¹H NMR (400 MHz, CDCl₃)

δ 4.81 (dd, *J* = 12.2 Hz, 2H), 3.61 (m, 1H), 1.92 (m, 2H), 1.63 (m, 5H), 1.26 (s, 6H), 1.26 (s, 6H), 1.24 (s, 3H), 1.22 (m, 5H), 0.90 (t, *J* = 7.4 Hz, 3H)

¹¹B NMR (128 MHz, CDCl₃)

δ 32.5

¹³C NMR (100 MHz, CDCl₃)

δ 89.3, 83.7, 74.5, 32.9, 32.5, 25.8, 24.8, 24.7, 24.4, 24.3, 22.3, 9.0 ppm

IR (thin film, NaCl)

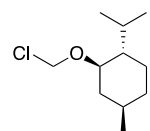
2932, 1441, 1333, 1465, 1211 cm⁻¹

HRMS (FTMS ES+)

[M+H]⁺ Calculated for C₁₇H₃₄O₄B 313.2550, found 313.2535.

TLC

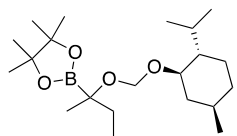
R_f = 0.8 (20% Et₂O in hexanes) [silica gel, p-anisaldehyde stain] [silica gel, curcumin stain]



(1*S*, 2*S*, 4*S*)-2-(Chloromethoxy)-1-isopropyl-4-methylcyclohexane (S1).

Trimethylsilylchloride (5 mL) was added to a flame dried flask containing menthol (0.502 g, 3.21 mmol) and paraformaldehyde (0.106 g, 3.53 mmol). The reaction was stirred for

2 h, then was filtered and concentrated under reduced pressure to give **S1** (0.558 g, 2.73 mmol, 85%), which was used as is. Characterization data are consistent with that reported in the literature.



2-(2-(((1R, 2S, 5R)-2-Isopropyl-5-methylcyclohexyl)oxy)methoxy)butan-2-yl)-4,4,5,5-tetramethyl-1,3,2-dioxaborolane (2.6). To a flame dried, 10

mL round bottom flask containing a stir bar was added CH₂Cl₂ (5 mL), α -boryl alcohol **2.2** (0.200 g, 1.00 mmol), and N(*i*Pr)₂Et (0.322 g, 2.00 mmol). The flask was sealed, evacuated and refilled with Ar (3x) using a balloon equipped with a needle and a rubber adapter. The solution was cooled to 0 °C using an ice-water bath and then freshly prepared **S1** (0.226 g, 1.10 mmol) was added dropwise via syringe. The reaction was stirred overnight, then was quenched with saturated aqueous NaHCO₃ (15 mL). The reaction mixture was transferred to a separatory funnel, the two layers were separated and the aqueous layer was extracted with CH₂Cl₂ (2 x 20 mL). The combined organic layers were washed with brine (2 x 20 mL), dried over Na₂SO₄, filtered, and concentrated under reduced pressure. The resulting residue was purified by silica gel column chromatography (R_f = 0.8, 20% Et₂O in hexanes) to yield the title compound as a colorless oil (0.040 g, 0.109 mmol, 11% yield, 1:1 mixture of diastereomers).

Data for 2.6

¹H NMR (400 MHz, CDCl₃)

δ 4.91 (d, *J* = 7.0 Hz, 0.5H), 4.84 (d, *J* = 7.0 Hz, 0.5H), 4.76 (d, *J* = 7.0 Hz, 0.5H), 4.69 (d, *J* = 7.0 Hz, 0.5H), 3.47 (m, 2H), 2.20 (m, 2H), 1.62 (m, 4H), 1.25 (m, 18H), 0.88 (m, 12H), 0.76 (d, *J* = 6.9 Hz, 3H)

¹¹B NMR (128 MHz, CDCl₃)

δ 32.5

^{13}C NMR (100 MHz, CDCl_3)

δ 90.1, 83.7, 76.9, 48.5, 48.38, 42.0, 41.6, 34.5, 31.7, 31.6, 31.4, 25.1, 25.01, 24.9, 24.8, 24.7, 24.6, 23.0, 22.4, 22.0, 21.9, 21.2, 15.93, 15.90, 9.21, 9.18 ppm

IR (thin film, NaCl)

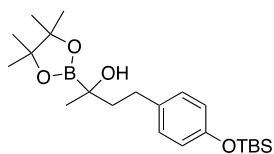
2938, 1439, 1341, 1375, 1464, 1210 cm^{-1}

HRMS (FTMS ES+)

$[\text{M}+\text{H}]^+$ Calculated for $\text{C}_{21}\text{H}_{42}\text{O}_4\text{B}$ 369.3171, found 369.3173

TLC

$R_f = 0.7$ (20% Et_2O in hexanes) [silica gel, p-anisaldehyde stain] [silica gel, curcumin stain]



4-(4-((*tert*-Butyldimethylsilyl)oxy)phenyl)-2-(4,4,5,5-tetramethyl-1,3,2-dioxaborolan-2-yl)butan-2-ol (2.9). To a flame dried, 250 mL

round bottom flask containing a stir bar was added bis(pinacolato)diboron (0.547 g, 2.16 mmol), 1,3-bis(cyclohexyl)imidazolium tetrafluoroborate (0.058 g, 0.18 mmol), NaOtBu (0.035 g, 0.36 mmol), and CuCl (0.036 g, 0.36 mmol). The flask was sealed, then evacuated and refilled with Ar (3x) using a balloon equipped with a needle and a rubber adapter. Toluene (10 mL) was added to the flask via syringe and the reaction was stirred for 30 min. The appropriate ketone (0.500 g, 1.80 mmol) was added via syringe followed immediately by MeOH (0.112 g, 3.60 mmol). After three h the mixture was loaded directly onto a short silica plug pretreated with CH_2Cl_2 . The column was then washed with copious amounts of Et_2O and the eluent was removed under reduced pressure. The resulting residue was purified by silica gel column chromatography ($R_f = 0.5$, 5% Et_2O in CH_2Cl_2) to yield the title compound as a colorless oil (0.575 g, 1.42 mmol, 78% yield).

Data for 2.9

¹H NMR (400 MHz, CDCl₃)

δ 7.04 (d, *J* = 8.4 Hz, 2H), 6.74 (d, *J* = 8.4 Hz, 2H), 2.76 (ddd, *J* = 4.8, 12.8, 12.8 Hz, 1H), 2.49 (ddd, *J* = 4.8, 12.8, 12.8 Hz, 1H), 1.89 (ddd, *J* = 4.8, 13.2, 13.2 Hz, 1H), 1.76-1.68 (m, 1H), 1.75 (s, 1H), 1.28 (s, 12H), 1.27 (s, 3H), 0.98 (s, 9H), 0.18 (s, 9H)

¹¹B NMR (128 MHz, CDCl₃)

δ 34.3

¹³C NMR (100 MHz, CDCl₃)

δ 153.6, 135.3, 129.1, 119.8, 84.4, 53.4, 43.6, 31.0, 26.1, 25.7, 25.7, 25.0, 24.8, 24.7, 18.2, 17.99, -4.4

IR (thin film, NaCl)

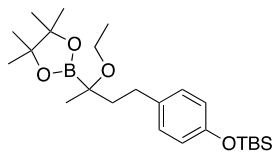
3456, 3015, 1312, 1439, 1167, 1143, 912, 837, 780, 690 cm⁻¹

HRMS (FTMS ES+)

[M+H]⁺ Calculated for C₂₂H₄₀BO₄Si 407.2784, found 407.2766

TLC

R_f = 0.5 (5% Et₂O in CH₂Cl₂) [silica gel, p-anisaldehyde stain] [silica gel, curcumin stain]



***tert*-Butyl(4-(3-ethoxy-3-(4,4,5,5-tetramethyl-1,3,2-dioxaborolan-2-yl)butyl)phenoxy)dimethylsilane (2.10).** To a flame dried, 25 mL round

bottom flask containing a stir bar was added silver trifluoromethane sulfonate (0.174 g, 0.677 mmol). The flask was sealed, then evacuated and refilled with Ar (3x) using a balloon equipped with a needle and a rubber adapter. Alcohol **2.9** (0.250 g, 0.615 mmol) in CH₂Cl₂ (15 mL) was added to the flask via syringe. The solution was cooled to 0 °C using an

ice-water bath and 2,6-di-*tert*-butylpyridine (0.176 g, 0.923 mmol) was added dropwise via syringe followed immediately by ethyl iodide (0.115 g, 0.738 mmol). The mixture was slowly warmed to room temperature, stirred for 1 h, filtered through a pad of Celite® 545, and concentrated under reduced pressure. The resulting residue was dissolved in diethyl ether (20 mL), washed with H₂O (3 X 30 mL), dried over Na₂SO₄, filtered, and concentrated under reduced pressure. The resulting oily yellow residue was purified by silica gel column chromatography ($R_f = 0.4$, 30% Et₂O in hexanes) to yield the title compound as a yellow oil (0.121 g, 0.279 mmol, 45% yield).

Data for 2.10

¹H NMR (400 MHz, CDCl₃)

δ 7.05 (d, $J = 8.4$ Hz, 2H), 6.73 (d, $J = 8.4$ Hz), 3.46 (q, $J = 7.0$ Hz, 2H), 2.58 (m, 2H), 1.84 (m, 2H), 1.29 (s, 12H), 1.27 (s, 3H), 0.98 (s, 9H), 0.18 (s, 6H)

¹¹B NMR (128 MHz, CDCl₃)

δ 33.8

¹³C NMR (100 MHz, CDCl₃)

δ 153.4, 135.8, 129.1, 119.8, 83.8, 59.6, 39.8, 29.8, 25.7, 24.8, 24.7, 21.4, 18.2, 16.3, -4.4

IR (thin film, NaCl)

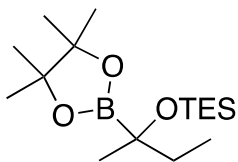
3013, 1309, 1434, 1156, 1141, 986, 834, 777, 682 cm⁻¹

HRMS (TOF MS ES+)

[M+Na]⁺ Calculated for C₂₄H₄₃BO₄SiNa 457.2921, found 457.2783

TLC

$R_f = 0.7$ (20% Et₂O in hexanes) [silica gel, p-anisaldehyde stain] [silica gel, curcumin stain]



Triethyl((2-(4,4,5,5-tetramethyl-1,3,2-dioxaborolan-2-yl)butan-2-yl)oxy)silane (2.11).

To a flame dried, 25 mL round bottom flask containing a stir bar was added CH_2Cl_2 (10 mL), α -boryl alcohol **2.2** (0.150 g, 0.750 mmol), and imidazole (0.102 g, 1.50 mmol). The flask was sealed, then evacuated and refilled with Ar (3x) using a balloon equipped with a needle and a rubber adapter. The solution was cooled to 0 °C using an ice-water bath, and then tritethylsilylchloride (0.150 g, 1.00 mmol) was added dropwise via syringe. The reaction was stirred overnight, then was quenched with saturated aqueous NH_4Cl (15 mL). The reaction mixture was transferred to a separatory funnel, the two layers were separated, and the aqueous layer was extracted with CH_2Cl_2 (2 x 15 mL). The combined organic layers were washed with brine (2 x 15 mL), dried over Na_2SO_4 , filtered, and concentrated under reduced pressure. The resulting residue was purified by silica gel column chromatography ($R_f = 0.8$, 5% Et_2O in hexanes) to yield the title compound as a colorless oil (0.186 g, 0.592 mmol, 79% yield).

Data for 2.11

$^1\text{H NMR}$ (400 MHz, CDCl_3)

δ 1.44 (q, $J = 7.5$ Hz, 2H), 1.18 (s, 12H), 1.13 (s, 3H), 0.87 (t, $J = 8.0$ Hz, 9H), 0.80 (t, $J = 7.5$ Hz), 0.50 (m, 6H)

$^{11}\text{B NMR}$ (128 MHz, CDCl_3)

δ 33.0

$^{13}\text{C NMR}$ (100 MHz, CDCl_3)

δ 83.5, 77.2, 35.0, 25.6, 24.8, 9.3, 7.2, 6.8

IR (thin film, NaCl)

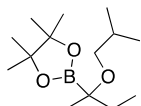
2940, 1456, 1323, 1255, 1201, 1145 cm^{-1}

HRMS (TOF MS ES+)

[M-C₂H₅]⁺ Calculated for C₁₄H₃₀BO₃Si 285.2057, found 285.2034

TLC

R_f = 0.7 (20% Et₂O in hexanes) [silica gel, p-anisaldehyde stain] [silica gel, curcumin stain]



2-(2-Isobutoxybutan-2-yl)-4,4,5,5-tetramethyl-1,3,2-dioxaborolane (2.12). To a

10 mL scintillation vial containing a stir bar was added CH₃CN (4 mL), compound **2.11** (0.100 g, 0.318 mmol), and isobutyraldehyde (0.048 g, 0.64 mmol). To the reaction mixture was added a solution of BiBr₃ dissolved in CH₃CN (1.5 g/mL, 0.016 mmol, 53 μL), immediately followed by triethylsilane (0.184 g, 1.59 mmol). The vial was sealed and stirred for 2 h, then was run through a short plug of celite which was flushed with diethyl ether. The eluent was concentrated and the resulting residue was purified by silica gel column chromatography (R_f = 0.8, 5% Et₂O in hexanes) to yield the title compound as a colorless oil (0.063 g, 0.24 mmol, 77% yield).

Data for 2.12

¹H NMR (500 MHz, CDCl₃)

δ 3.02 (d, *J* = 6.7 Hz, 2H), 1.73 (m, *J* = 6.7 Hz, 1H), 1.51 (m, 2H), 1.19 (s, 6H), 1.18 (s, 6H), 1.09 (s, 3H), 0.81 (m, 9H)

¹¹B NMR (160 MHz, CDCl₃)

δ 32.9

¹³C NMR (125 MHz, CDCl₃)

δ 83.5, 71.7, 30.6, 29.3, 24.9, 24.7, 20.7, 19.7, 19.6, 8.5 ppm

IR (thin film, NaCl)

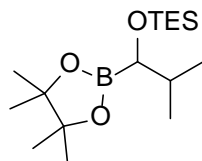
2930, 1452, 1325, 1254, 1200 cm⁻¹

HRMS (TOF MS ES+)

[M+H]⁺ Calculated for C₁₄H₃₀BO₃ 257.2288, found 257.2276

TLC

R_f = 0.7 (20% Et₂O in hexanes) [silica gel, p-anisaldehyde stain] [silica gel, curcumin stain]



triethyl(2-methyl-1-(4,4,5,5-tetramethyl-1,3,2-dioxaborolan-2-yl)propoxy)silane (2.13). To a flame dried, 25 mL round bottom flask

containing a stir bar was added bis(pinacolato)diboron (0.920 g, 3.63 mmol), 1,3-Bis(cyclohexyl)imidazolium tetrafluoroborate (0.111 g, 0.346 mmol), NaOtBu (0.067 g, 0.692 mmol), and CuCl (0.069 g, 0.692 mmol). Toluene (15 mL) was added to the flask and the flask was sealed, then the reaction was stirred for 30 minutes. isobutyraldehyde (0.250 g, 3.46 mmol) was added via syringe followed immediately by MeOH (0.214 g, 6.92 mmol). After three hours, the reaction was loaded directly onto a short silica plug pretreated with CH₂Cl₂. The column was then washed with copious amounts of Et₂O and the eluent was removed under reduced pressure. The resulting residue was dissolved in CH₂Cl₂ (10 mL) and transferred to a flame dried, 25 mL round bottom flask containing a stirbar. Imidazole (0.707 g, 10.4 mmol) was added and the flask was sealed, then evacuated and refilled with Ar (3x) using a balloon equipped with a needle and a rubber adapter. The solution was cooled to 0 °C using an ice-water bath and then tritethylsilylchloride (0.782 g, 5.19 mmol) was added dropwise via syringe. The reaction was allowed to stir overnight, then quenched with saturated aqueous NH₄Cl (15 mL). The reaction mixture was transferred to a separatory funnel, the two layers were separated and the aqueous layer was extracted with CH₂Cl₂ (2 x 15 mL). The combined organic layers were washed with brine (2 x 15 mL), dried over Na₂SO₄, gravity filtered, and then concentrated under reduced pressure. The

resulting residue was purified by silica gel column chromatography ($R_f = 0.7$, 5% Et₂O:hexanes) to yield the title compound as a colorless oil (0.338 g, 0.311 mmol, 31% yield). The column should be run as quickly as possible, as the boronate group is prone to degradation when it is left on silica gel for too long.

Data for 2.13

¹H NMR (400 MHz, CDCl₃)

3.18 (d, $J = 6.4$ Hz, 1H), 1.76 (m, 1H), 1.20 (s, 6H), 1.19 (s, 6H), 0.87 (m, 15H), 0.52 (m, 6H) ppm

¹¹B NMR (128 MHz, CDCl₃)

32.44

¹³C NMR (100 MHz, CDCl₃)

83.62, 32.74, 25.1, 24.81, 19.43, 19.33, 7.07, 4.82 ppm

IR (thin film, NaCl)

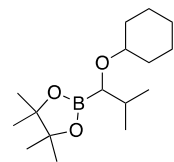
2934 1456, 1321, 1253, 1200, 1144 cm⁻¹

HRMS (TOF MS ES+)

[M-29]²⁺ Calculated for C₁₄H₃₀BO₃Si : 285.2057 found 285.2052

TLC

$R_f = 0.4$ (5% Et₂O/CH₂Cl₂) [silica gel, p-anisaldehyde stain] [silica gel, curcumin stain]



2-(1-(Cyclohexyloxy)-2-methylpropyl)-4,4,5,5-tetramethyl-1,3,2-

dioxaborolane (2.14). To a 10 mL scintillation vial containing a stir bar was added

CH₃CN (4 mL), compound **2.13** (0.018 g, 0.079 mmol), and cyclohexanone (0.008

g, 0.083 mmol). To the reaction mixture was added a solution of BiBr₃ in CH₃CN (1.5 g/mL, 0.004

mmol, 12 μL), immediately followed by triethylsilane (0.028 g, 0.24 mmol). The vial was sealed

and the reaction mixture was stirred for 2 h. The mixture was run through a short plug of Celite

then was flushed with diethyl ether. The eluent was concentrated and the resulting residue was purified by silica gel column chromatography ($R_f = 0.6$, 5% Et₂O in hexanes) to yield the title compound as a colorless oil (0.018 g, 0.063 mmol, 81% yield).

Data for 2.14

¹H NMR (500 MHz, CDCl₃)

δ 3.04 (m, 1H), 2.82 (d, 7.45 Hz), 1.81 (m, 3H), 1.65 (m, 2H), 1.41 (m, 1H), 1.20 (s, 6H), 1.19 (s, 6H), 1.20-1.07 (m, 18H), 0.88 (d, $J = 6.7$ Hz, 3H), 0.84 (d, $J = 6.7$ Hz, 3H) ppm

¹¹B NMR (128 MHz, CDCl₃)

δ 31.9 ppm

¹³C NMR (125 MHz, CDCl₃)

δ 83.5, 33.2, 32.3, 30.9, 25.9, 25.0, 24.5, 24.4, 19.9, 19.4 ppm

IR (thin film, NaCl)

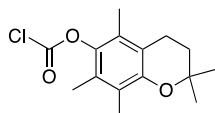
2932, 1465, 1446, 1321, 1252, 1199, 1148 cm⁻¹

HRMS (TOF MS ES⁺)

[M+H]⁺ Calculated for C₁₆H₃₂BO₃ 283.2444 found 283.2431

TLC

$R_f = 0.4$ (5% Et₂O in CH₂Cl₂) [silica gel, p-anisaldehyde stain] [silica gel, curcumin stain]



2,2,5,7,8-Pentamethylchroman-6-yl carbonochloridate (S2). To a flame

dried, 2-neck 25 mL round bottom flask containing a stir bar was added triphosgene (1.09 g, 3.70 mmol). The flask was sealed, then evacuated and refilled with Ar (3x) using a balloon equipped with a needle and a rubber adapter. A solution of 2,2,5,6,8-pentamethylchroman-7-ol (2.20 g, 10.0 mmol) dissolved in CH₂Cl₂ (5 mL) was added to the flask

via syringe. The solution was cooled to 0 °C using an ice-water bath and pyridine (0.79 g, 10.0 mmol) was added dropwise via syringe. The reaction was slowly warmed to rt, stirred for 3 h, and then diluted with ethyl acetate (25 mL). The resulting mixture was partitioned with 1M HCl (15 mL) and the resulting biphasic mixture was placed into a separatory funnel. The organic layer was washed with brine (2 X 20 mL) and H₂O (2 x 20 mL), dried over Na₂SO₄, filtered, and concentrated under reduced pressure. The resulting yellow oil (2.14 g, 7.59 mmol, 76% yield) was used as is.

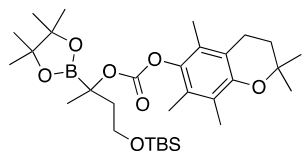
Data for S2

¹H NMR (400 MHz, CDCl₃)

δ 2.63 (t, *J* = 7.2 Hz, 2H), 2.12 (s, 3H), 2.11 (s, 3H), 2.08 (s, 3H), 2.11 (s, 3H), 1.81 (t, *J* = 7.2 Hz, 2H), 1.31 (s, 6H)

¹³C NMR (100 MHz, CDCl₃)

δ 150.4, 142.7, 126.1, 124.5, 123.6, 117.6, 73.6, 32.5, 26.8, 20.9, 12.8, 12.0, 11.8



4-((*tert*-Butyldimethylsilyl)oxy)-2-(4,4,5,5-tetramethyl-1,3-dioxaborolan-2-yl)butan-2-yl (2,2,5,7,8-pentamethylchroman-6-yl) carbonate (2.7). To a flame dried, 5 mL round bottom flask containing

a stir bar was added the appropriate boryl alcohol (0.200 mg, 0.550 mmol) in CH₂Cl₂ (5 mL) and pyridine (0.087 g, 1.1 mmol). The flask was sealed, then evacuated and refilled with Ar (3x) using a balloon equipped with a needle and a rubber adapter. The solution was cooled to 0 °C using an ice-water bath, and freshly prepared chloroformate (0.310 g, 1.1 mmol) was added dropwise via syringe. The reaction was stirred for 1 h, then was quenched with saturated aqueous NH₄Cl (5 mL). The reaction mixture was transferred to a separatory funnel, the two layers were separated and the aqueous layer was extracted with CH₂Cl₂ (2 x 5 mL). The combined organic layers were

washed with brine (2 x 5 mL), dried over Na₂SO₄, filtered, and concentrated under reduced pressure. The resulting residue was purified by silica gel column chromatography (R_f = 0.5, 20% Et₂O in hexanes) to provide the desired compound as a yellow oil (0.210 g, 0.370 mmol, 67% yield).

Data for 2.7

¹H NMR (400 MHz, CDCl₃)

δ 3.81 (ddd, *J* = 6.0, 6.0, 10.0 Hz, 2H), 2.61 (t, *J* = 6.8 Hz, 2H), 2.12-2.02 (m, 2H), 2.09 (s, 6H), 2.05 (s, 3H), 1.78 (t, *J* = 6.4 Hz, 2H), 1.47 (s, 3H), 1.30 (s, 6H), 1.24 (s, 6H), 1.23 (s, 6H), 0.90 (s, 9H), 0.07 (s, 9H)

¹¹B NMR (128 MHz, CDCl₃)

δ 32.8

¹³C NMR (100 MHz, CDCl₃)

δ 154.5, 149.5, 141.2, 126.9, 125.2, 122.9, 117.0, 84.0, 73.0, 59.0, 40.2, 32.7, 26.9, 25.96, 24.9, 24.8, 21.6, 20.9, 18.3, 12.7, 11.9, 11.8, -5.26, -5.28

IR (thin film, NaCl)

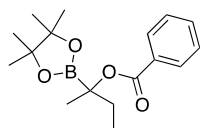
3023, 1739, 1446, 1288, 1368, 1165, 1217, 1091, 894, 834, 775, 638 cm⁻¹

HRMS (TOF MS ES⁺)

[M+H]⁺ Calculated for C₃₁H₅₄BO₇Si 577.3752, found 577.3732

TLC

R_f = 0.5 (20% Et₂O in hexanes) [silica gel, p-anisaldehyde stain] [silica gel, curcumin stain]



2-(4,4,5,5-tetramethyl-1,3,2-dioxaborolan-2-yl)butan-2-yl benzoate (2.15).

To a flame dried, 10 mL round bottom flask containing a stir bar was added

CH₂Cl₂ (5 mL), α -boryl alcohol **2.2** (0.050 g, 0.25 mmol), and pyridine (0.023 g, 0.30 mmol). The flask was sealed, then evacuated and refilled with Ar (3x) using a balloon equipped with a needle and a rubber adapter. The solution was cooled to 0 °C using an ice-water bath, then PhC(O)Cl (0.039 g, 0.27 mmol) was added dropwise via syringe. The reaction was stirred overnight, then was quenched with saturated aqueous NaHCO₃ (5 mL). The reaction mixture was transferred to a separatory funnel, the two layers were separated and the aqueous layer was extracted with CH₂Cl₂ (2 x 10 mL). The combined organic layers were washed with brine (2 x 10 mL), dried over Na₂SO₄, filtered, and concentrated under reduced pressure. The resulting residue was purified by silica gel column chromatography (R_f = 0.2, 20% Et₂O in hexanes) to yield the title compound as a colorless oil (0.051 g, 0.17 mmol, 67% yield).

Data for 2.15

¹H NMR (400 MHz, CDCl₃)

δ 8.03 (d, *J* = 7.1 Hz, 2H), 7.56 (t, *J* = 7.4 Hz, 1H), 7.43 (t, *J* = 7.9 Hz, 2H) 1.88 (dq, *J* = 7.6, 14.8 Hz, 1H), 1.76 (dq, *J* = 7.6, 14.8 Hz, 1H), 1.39 (s, 3H), 1.28 (s, 6H), 1.27 (s, 3H), 1.01 (t, *J* = 7.5 Hz).

¹¹B NMR (128 MHz, CDCl₃)

δ 27.0

¹³C NMR (100 MHz, CDCl₃)

δ 169.5, 133.6, 130.6, 129.9, 129.0, 128.3, 82.9, 24.9, 24.8, 20.6, 8.2

IR (thin film, NaCl)

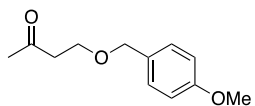
3012, 1720, 1333, 1246, 1167, 1043, 952, 834, 777, 681 cm⁻¹

HRMS (TOF MS ES+)

[M+H]⁺ Calculated for C₁₇H₂₆BO₄ 305.1924 found 305.1910

TLC

$R_f = 0.7$ (20% Et₂O in hexanes) [silica gel, p-anisaldehyde stain] [silica gel, curcumin stain]



4-((4-methoxybenzyl)oxy)butan-2-one (S3). To a flame dried, wide neck

100 mL round bottom flask containing a stir bar was added 4-hydroxy-2-butanone (4.12 g, 46.5 mmol), *p*-methoxybenzyl bromide (8.00 g, 51.1 mmol), and *i*PrNEt (13.2 g, 102 mmol). A flame dried reflux condenser was attached, and the reaction mixture was refluxed under N₂ for 6 h. The reaction mixture was cooled to rt, then was diluted with ethyl acetate (100 mL). A saturated aqueous solution of sodium bisulphate was added to the reaction mixture dropwise via pipette (40 mL). The resulting biphasic mixture was transferred to a separatory funnel the two layers were separated and the aqueous layer was extracted with ethyl acetate (3 x 50 mL). The combined organic layers were dried over Na₂SO₄, filtered, and concentrated under reduced pressure. The resulting yellow oil was purified by silica gel column chromatography ($R_f = 0.5$, 20% ethyl acetate in hexanes) to yield the title compound as a colorless oil (4.21 g, 20.2 mmol, 40% yield). Characterization data are consistent with those reported in the literature.

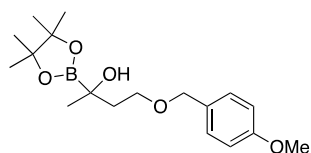
Data for S3

¹H NMR (400 MHz, CDCl₃)

δ 7.30-7.20 (m, 5H), 4.46 (s, 2H), 3.68 (t, $J = 6.4$ Hz, 2H), 2.67 (t, $J = 6.0$ Hz, 2H), 2.12 (s, 3H)

TLC

$R_f = 0.5$ (20% ethyl acetate in hexanes) [silica gel, p-anisaldehyde stain]



4-((4-Methoxybenzyl)oxy)-2-(4,4,5,5-tetramethyl-1,3,2-dioxaborolan-2-yl)butan-2-ol (2.17). To a flame dried, 100 mL round

bottom flask containing a stir bar was added bis(pinacolato)diboron (2.92 g, 11.5 mmol), 1,3-bis(cyclohexyl)imidazolium tetrafluoroborate (0.319 g, 0.960 mmol), NaOtBu (0.184 g, 1.92 mmol), and CuCl (0.188 g, 1.92 mmol). The flask was sealed, then evacuated and refilled with Ar (3x) using a balloon equipped with a needle and a rubber adapter. Toluene (25 mL) was added to the flask via syringe and the reaction was stirred for 30 min. Ketone **27** (2.00 g, 9.60 mmol) was added via syringe followed immediately by MeOH (0.595 g, 19.2 mmol). After three h, the mixture was loaded directly onto a short silica plug pretreated with CH₂Cl₂. The column was washed with copious amounts of Et₂O and the eluent was removed under reduced pressure. The resulting residue was purified by silica gel column chromatography (R_f = 0.6, 10% Et₂O in CH₂Cl₂) to yield the title compound as a colorless oil (2.71 g, 8.06 mmol, 84% yield).

Data for 2.17

¹H NMR (400 MHz, CDCl₃)

δ 7.28 (d, *J* = 8.6 Hz, 2H), 6.88 (d, *J* = 8.6 Hz, 2H), 4.46 (d, *J* = 12.0 Hz, 2H), 3.81 (s, 3H), 3.63 (m, 1H), 3.45 (m, 1H), 2.37 (s, 1H), 1.96 (ddd, *J* = 5.6, 5.9, 14.0 Hz, 1H), 1.71 (dt, *J* = 5.6, 5.6, 14.0 Hz), 1.26 (s, 3H), 1.25 (s, 12H) ppm

¹¹B NMR (400 MHz, CDCl₃)

δ 33.2

¹³C NMR (125 MHz, CDCl₃)

δ 159.2, 130.4, 129.3, 113.8, 84.1, 72.7, 67.1, 55.3, 40.1, 26.1, 24.7, 24.7

IR (thin film, NaCl)

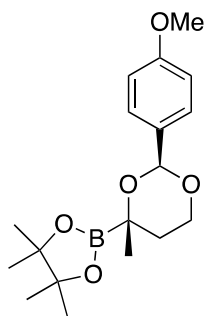
3446, 3015, 1312, 1433, 1145, 910, 834, 779, 686 cm⁻¹

HRMS (TOF MS ES⁺)

[M+H]⁺ Calculated for C₁₈H₃₀BO₅ 337.2180, found 337.2175

TLC

$R_f = 0.6$ (5% Et₂O in CH₂Cl₂) [silica gel, p-anisaldehyde stain] [silica gel, curcumin stain]



2-((2S,4R)-2-(4-Methoxyphenyl)-4-methyl-1,3-dioxan-4-yl)-4,4,5,5-tetramethyl-1,3,2-dioxaborolane (2.18). To a flame dried, 10 mL round

bottom flask containing a stir bar was added CH₂Cl₂ (5 mL) and α -boryl alcohol **2.17** (0.100 g, 0.297 mmol). The reaction flask was cooled to 0 °C using an ice-water bath, then 2,3-dichloro-5,6-dicyano-1,4-benzoquinone (0.067 g, 0.30 mmol) was added. The reaction was stirred for 1 h at 0 °C, then for 30 min at rt. The reaction was quenched with saturated aqueous NaHCO₃ (5 mL) then was transferred to a separatory funnel. The two layers were separated and the aqueous layer was extracted with CH₂Cl₂ (2 x 10 mL). The combined organic layers were washed with brine (2 x 10 mL), dried over Na₂SO₄, filtered, and concentrated under reduced pressure. The resulting residue was purified by silica gel column chromatography ($R_f = 0.4$, 20% Et₂O in hexanes) to yield the title compound as a white solid (0.079 g, 0.23 mmol, 78% yield).

Data for 2.18

¹H NMR (400 MHz, CDCl₃)

δ 7.44 (d, $J = 8.7$ Hz, 2H), 6.87 (d, $J = 8.7$ Hz, 2H), 5.56 (s, 1H), 4.18 (m, 1H), 3.88 (m, 1H), 3.80 (s, 3H), 1.79 (m, 2H), 1.33 (s, 3H), 1.31 (s, 12H)

¹¹B NMR (128 MHz, CDCl₃)

δ 33.3

¹³C NMR (100 MHz, CDCl₃)

δ 159.8, 132.0, 127.5, 113.5, 100.1, 84.2, 77.2, 68.8, 55.3, 35.2, 25.4, 24.9, 24.6

IR (thin film, NaCl)

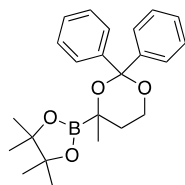
3011, 1314, 1434, 1097, 913, 837, 781, 698 cm^{-1}

HRMS (FTMS ESI)

$[\text{M}+\text{H}]^+$ Calculated for $\text{C}_{18}\text{H}_{28}\text{BO}_5$ 335.2024, found 335.2023

TLC

$R_f = 0.4$ (20% Et_2O in hexanes) [silica gel, *p*-anisaldehyde stain] [silica gel, curcumin stain]



4,4,5,5-Tetramethyl-2-(4-methyl-2,2-diphenyl-1,3-dioxan-4-yl)-1,3,2-dioxaborolane (2.19). To a flame dried, 25 mL Schlenk flask containing a stir bar was added Pd/C (0.096 g, 0.090 mmol), then small amounts of CH_2Cl_2 were run down the sides of the flask. α -Boryl alcohol **2.17** (0.200 g, 0.594 mmol) was dissolved in 10 mL of methanol and added to the flask. The flask was sealed, then evacuated and refilled with H_2 (3x). The reaction was stirred under H_2 for 8 h, then the mixture was run through a short plug of Celite, washed with copious amounts of ethyl acetate, and concentrated under reduced pressure to yield the crude diol. The crude product was used without further purification. To a flame dried, 10 mL round bottom flask containing a stir bar was added the crude alcohol in CHCl_3 (1 mL) followed by benzophenone dimethyl ketal (0.134 g, 0.594 mmol). A trace amount of pyridinium *p*-toluene sulfonate was added to the flask and the flask was sealed. The reaction was stirred for 12 h, then was quenched with saturated aqueous NaHCO_3 (10 mL). The reaction mixture was transferred to a separatory funnel, the two layers were separated, and the aqueous layer was extracted with CH_2Cl_2 (2 x 15 mL). The combined organic layers were washed with brine (2 x 15 mL), dried over Na_2SO_4 , filtered, and then concentrated under reduced pressure. The resulting residue was purified by silica

gel column chromatography ($R_f = 0.2$, 10% Et₂O in hexanes) to yield the title compound as a white solid (0.112 g, 0.291 mmol, 49 % yield over two steps).

Data for 2.19

¹H NMR (400 MHz, CDCl₃)

δ 7.59 (d, $J = 7.3$ Hz, 2H), 7.51 (d, $J = 7.3$ Hz, 2H), 7.23 (m, 6H), 4.19 (ddd, $J = 4.4, 10.9, 10.9$ Hz, 1H), 4.00 (ddd, $J = 3.1, 5.5, 10.9$ Hz, 1H), 1.89 (ddd, $J = 4.4, 4.4, 7.5$ Hz, 1H), 1.70 (ddd, $J = 5.6, 10.9$ Hz, 12.8 Hz, 1H), 1.40 (s, 3H), 1.10 (s, 6H), 0.92 (s, 6H)

¹¹B NMR (128 MHz, CDCl₃)

δ 33.1

¹³C NMR (100 MHz, CDCl₃)

δ 146.1, 143.0, 127.9, 127.9, 127.8, 127.4, 127.2, 125.9, 100.2, 83.7, 77.2, 60.5, 33.9, 26.4, 25.1, 23.8

IR (thin film, NaCl)

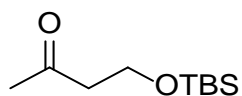
3111, 1314, 1431, 1108, 918, 826, 797, 712 cm⁻¹

HRMS (FTMS ESI)

[M+H]⁺ Calculated for C₂₃H₃₀BO₄ 381.2232, found 381.2230

TLC

$R_f = 0.2$ (10% Et₂O in hexanes) [silica gel, p-anisaldehyde stain] [silica gel, curcumin stain]



4-((*tert*-butyldimethylsilyl)oxy)butan-2-one (S4). To a flame dried, 500 mL round bottom flask containing a stir bar was added CH₂Cl₂ (200 mL), followed by 4-hydroxy-2-butanone (10.0 g, 114 mmol) and imidazole (9.30 g, 137 mmol). The reaction was allowed to stir until all the imidazole had dissolved, and then tert-

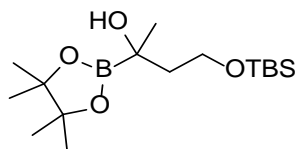
butyldimethylsilyl chloride (18.0 g, 119 mmol) was added. The flask was sealed and allowed to stir under N₂ for 1.5 hours. The reaction was quenched with saturated aqueous NH₄Cl (80 mL). The mixture was transferred to a separatory funnel, the two layers were separated, and the aqueous layer was extracted with CH₂Cl₂ (2 x 50 mL). The combined organic layers were washed with brine (2 x 100 mL) and H₂O (2 x 100 mL), dried over MgSO₄, gravity filtered, and concentrated under reduced pressure to yield the title compound as a colorless oil (22.5 g, 111 mmol, 98% yield). Characterization data is consistent with that reported in the literature.

Data for S4

¹H NMR (400 MHz, CDCl₃)

3.89 (t, *J* = 6.4 Hz, 2H), 2.62 (t, *J* = 6.4 Hz, 2 H), 0.88 (s, 9H), .06 (s, 6H) ppm

TLC R_f = .9 (20% Et₂O/Hexanes) [silica gel, p-anisaldehyde stain]



4-((*tert*-butyldimethylsilyloxy)-2-(4,4,5,5-tetramethyl-1,3,2-dioxaborolan-2-yl)butan-2-ol (2.8). To a flame dried, 250 mL round bottom flask containing a stir bar was added bis(pinacolato)diboron

(0.690 g, 2.72 mmol), 1,3-Bis(cyclohexyl)imidazolium tetrafluoroborate (0.082 g, 0.245 mmol), NaOtBu (0.474 g, 0.494 mmol), and CuCl (0.489 g, 0.494 mmol). The flask was sealed, then evacuated and refilled with Ar (3x) using a balloon equipped with a needle and a rubber adapter. Toluene (10 mL) was added to the flask via syringe and the reaction was stirred for 30 minutes. Ketone **S6** (0.500 g, 2.47 mmol) was added via syringe followed immediately by MeOH (0.153 g, 4.94 mmol). After three hours, the reaction was loaded directly onto a short silica plug pretreated with CH₂Cl₂. The column was then washed with copious amounts of Et₂O and the eluent was removed under reduced pressure. The resulting residue was purified by silica gel column

chromatography ($R_f = 0.6$, 10% Et₂O:CH₂Cl₂) to yield the title compound as a colorless oil (0.646 g, 1.96 mmol, 79% yield). The column should be run as quickly as possible, as the boronate group is prone to degradation when it is left on silica gel for too long.

Data for 2.8

¹H NMR (400 MHz, CDCl₃)

3.89-3.85 (m, 2H), 3.23 (s, 1H), 1.87 (ddd, $J = 5.6, 5.6, 14.2$ Hz, 1H), 1.73 (ddd, $J = 6.8, 6.8, 13.6$ Hz), 1.27 (s, 12H), 1.26 (s, 3H), .90 (s, 9H), .08 (s, 6H) ppm

¹¹B NMR (128 MHz, CDCl₃)

33.39 ppm

¹³C NMR (100 MHz, CDCl₃)

83.99, 61.98, 41.47, 25.89, 25.54, 25.02, 24.75, 24.69, 18.14, -5.52 ppm

IR (thin film, NaCl)

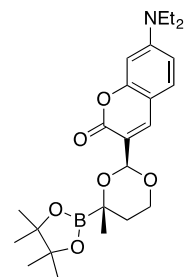
3503, 3012, 1367, 1436, 1228, 1084, 1005, 834, 773 cm⁻¹

HRMS (TOF MS ES+)

[M+H]⁺ Calculated for C₁₆H₃₆BO₄Si: 331.2476, found 331.2478

TLC

$R_f = 0.6$ (5% Et₂O/CH₂Cl₂) [silica gel, p-anisaldehyde stain] [silica gel, curcumin stain]



7-(Diethylamino)-3-(4-methyl-4-(4,4,5,5-tetramethyl-1,3,2-dioxaborolan-2-yl)-1,3-dioxan-2-yl)-2H-chromen-2-one (2.21). To a flame dried, 10 mL round

bottom flask containing a stir bar was added CH₂Cl₂ (5 mL), TBS protected boryl alcohol **2.8** (0.050 g, 0.151 mmol), and aldehyde **2.20** (0.025 g, 0.102 mmol). The

flask was sealed, then evacuated and refilled with Ar (3x) using a balloon equipped with a needle and a rubber adapter. The solution was cooled to -78 °C using an acetone-dry ice bath and then a

single drop of trimethylsilyl trifluoromethane sulfonate diluted in CH₂Cl₂ (1 mL) was added dropwise via syringe, followed by .025 mL of methanol. The reaction was allowed to warm to room temperature, and then was quenched with triethylamine (0.5 mL), then concentrated under reduced pressure. The resulting crude oil purified by silica gel column chromatography (R_f = 0.2, 40% hexanes in Et₂O) to yield the title compound as a pale yellow solid (0.033 g, 0.73 mmol, 73% yield).

Data for 2.21

¹H NMR (500 MHz, CD₃CN)

δ 7.88 (s, 1H), 7.41 (d, *J* = 8.9 Hz, 1H), 6.69 (dd, *J* = 2.5, 8.9 Hz, 1H), 6.53 (d, *J* = 2.5 Hz, 1H), 5.61 (s, 1H), 4.07 (ddd, *J* = 1.6, 4.7, 11.6 Hz, 1H), 3.84 (ddd, *J* = 2.9, 11.6, 11.6 Hz, 1H), 3.46 (q, *J* = 7.1 Hz, 4H), 1.73 (m, 2H), 1.31 (s, 12H), 1.29 (s, 3H), 1.19 (t, *J* = 7.1 Hz, 6 H)

¹¹B NMR (128 MHz, CDCl₃)

δ 34.1

¹³C NMR (125 MHz, CDCl₃)

δ 161.1, 156.5, 150.8, 141.1, 129.5, 118.8, 108.7, 108.3, 97.1, 95.2, 84.5, 66.9, 44.7, 35.2, 25.4, 24.9, 24.5, 12.5 ppm

IR (thin film, NaCl)

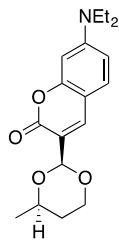
3101, 3021, 1751, 1432, 1316, 1302, 1102, 912, 860 cm⁻¹

HRMS (TOF MS ES⁺)

[M+H]⁺ Calculated for C₂₄H₃₅BO₆N 444.2552, found 444.2537

TLC

R_f = 0.2 (40% hexanes in Et₂O) [silica gel, *p*-anisaldehyde stain] [silica gel, curcumin stain]



7-(Diethylamino)-3-(4-methyl-1,3-dioxan-2-yl)-2H-chromen-2-one (2.22). To a flame dried, 10 mL round bottom flask containing a stir bar was added CH₂Cl₂ (5 mL), 1,3 butanediol (0.50 mL), and the dimethyl acetal of the **2.20** (0.100 g, 0.343 mmol). A trace amount of pyridinium *p*-toluenesulfonate was added and the flask was sealed, stirred under argon for 6 hours, and quenched with saturated aqueous NaHCO₃ (5 mL). The reaction mixture was transferred to a separatory funnel, the two layers were separated and the aqueous layer was extracted with CH₂Cl₂ (2 x 10 mL). The combined organic layers were washed with brine (2 x 10 mL), dried over Na₂SO₄, filtered, and concentrated under reduced pressure. The resulting residue was purified by silica gel column chromatography (R_f = 0.8, 40% ethyl acetate in hexanes) to yield the title compound as a white solid (0.102 g, 0.316 mmol, 92% yield).

Data for 2.22

¹H NMR (400 MHz, CDCl₃)

δ 7.83 (s, 1H), 7.19 (s, 1H), 6.47 (dd, *J* = 2.4, 8.8 Hz, 1H), 6.40 (d, *J* = 2.4 Hz, 1H), 5.57 (s, 1H), 4.14 (dd, *J* = 4.6, 11.5 Hz, 1H), 3.91 (m, 2H), 3.32 (q, *J* = 7.1 Hz, 4H), 1.69 (dddd, *J* = 5.1, 13.0, 13.0, 13.0 Hz, 1H), 1.45 (dd, *J* = 1.1, 13.4 Hz, 1H), 1.23 (d, *J* = 6.2 Hz, 3H), 1.13 (t, *J* = 7.1 Hz, 6H)

¹³C NMR (100 MHz, CDCl₃)

δ 161.2, 156.5, 150.9, 141.0, 118.4, 108.9, 108.3, 97.2, 96.4, 73.6, 67.2, 44.8, 33.1, 21.8, 12.4

IR (thin film, NaCl)

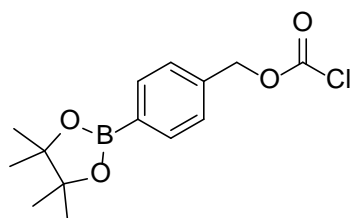
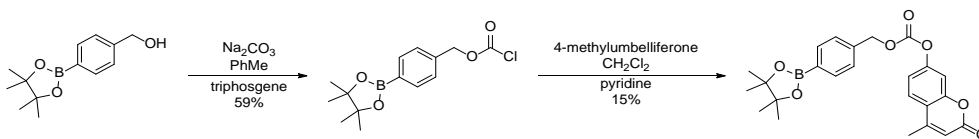
3103, 3011, 1749, 1302, 1104, 916, 890 cm⁻¹

HRMS (TOF MS ES⁺)

[M+H]⁺ Calculated for C₁₈H₂₄O₄N 318.1699, found 318.1721

TLC

$R_f = 0.8$ (40% ethyl acetate in hexanes) [silica gel, UV]



4-(4,4,5,5-tetramethyl-1,3,2-dioxaborolan-2-yl)benzyl

carbonochloridate (S5). A flask containing Na_2CO_3 (3.51 g, 33.0 mmol) and a stir bar was flame dried then allowed to cool to room temperature in a dessicator. The flask was cooled to 0°C under a

positive pressure of N_2 , then triphosgene (2.20 g, 7.42 mmol) dissolved in toluene (15 mL) was added via syringe. The reaction was stirred at 0°C for 30 minutes, then the (4-(4,4,5,5-tetramethyl-1,3,2-dioxaborolan-2-yl)phenyl)methanol (0.87 g, 3.72 mmol) dissolved in toluene was added via syringe. The reaction was allowed to warm to room temperature and stirred for three hours. The reaction was filtered and concentrated under reduced pressure to give the crude chloroformate which was used as is (0.651 g, 2.13 mmol, 59 % yield). Characterization data is consistent with that reported in the literature.

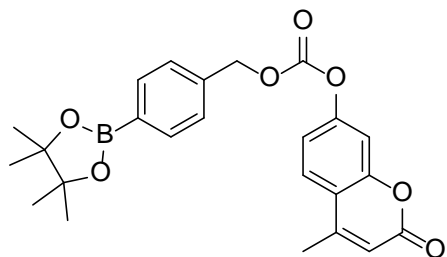
Data for S5

^1H NMR (500 MHz, CDCl_3)

7.83 (d, $J = 8.0$ Hz, 2H), 7.38 (d, $J = 8.0$ Hz, 2 H), 5.31 (s, 2H), 1.35 (s, 12H) ppm

TLC

$R_f = 0.7$ (20% ethyl acetate/Hexanes) [silica gel, p-anisaldehyde stain]



4-methyl-2-oxo-2H-chromen-7-yl (4-(4,4,5,5-tetramethyl-1,3,2-dioxaborolan-2-yl)benzyl) carbonate (2.23).

4-methyl umbelliferone (0.100 g, 0.56 mmol), was added to a flame dried flask containing a stir bar. Dichloromethane (15 mL) was added to the flask, followed by pyridine (0.27 g, 3.36 mmol). The reaction was sealed, cooled to 0°C, and placed under a positive pressure of N₂. Chlororoformate **S5** (0.33 g, 1.12 mmol) was added dropwise via syringe. The reaction was allowed to stir for three hours at room temperature, then was quenched with saturated aqueous NaHCO₃ (10 ml). The reaction was transferred to a separatory funnel, and the organic layer was washed with brine (2 x 10 mL), dried over Na₂SO₄, filtered and concentrated under reduced pressure to give a crude residue. The residue was purified by column chromatography on silica gel (20% ethyl acetate/hexanes) to give the product (0.036 g, .083 mmol, 15 % yield) as a white solid.

Data for 2.23

¹H NMR (500 MHz, CDCl₃)

7.85 (d, *J* = 8.0 Hz, 2H), 7.60 (d, *J* = 8.7 Hz, 1H), 7.43 (d, *J* = 8.0 Hz, 2H), 7.22 (d, *J* = 2.3 Hz, 1H), 7.16 (dd, *J* = 2.3, 8.7 Hz, 1H), 6.28 (d, *J* = 1.2 Hz, 1H), 5.31 (s, 2H), 2.43 (d, *J* = 1.2 Hz, 3H), 1.35 (s, 12H).

¹¹B NMR (160 MHz, CDCl₃)

30.47 ppm

¹³C NMR (125 MHz, CDCl₃)

160.40, 154.15, 153.26, 152.78, 151.79, 137.22, 135.18, 127.83, 127.61, 125.49, 118.02, 117.39, 114.70, 109.96, 83.97, 70.66, 24.88, 18.75 ppm

HRMS (TOF MS ES+)

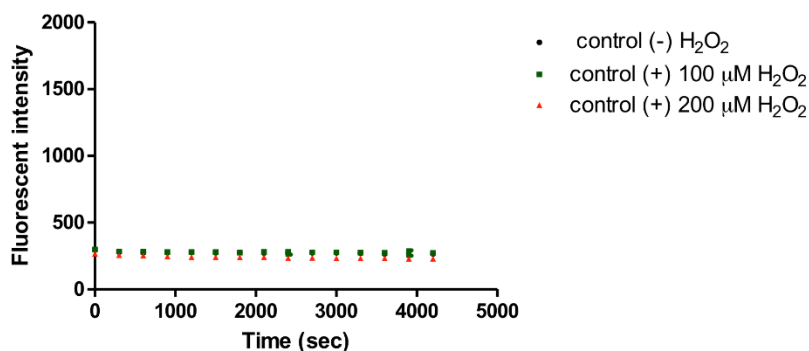
[M+H]⁺ Calculated for C₂₄H₂₆BO₇: 437.1766, found 437.1766

TLC

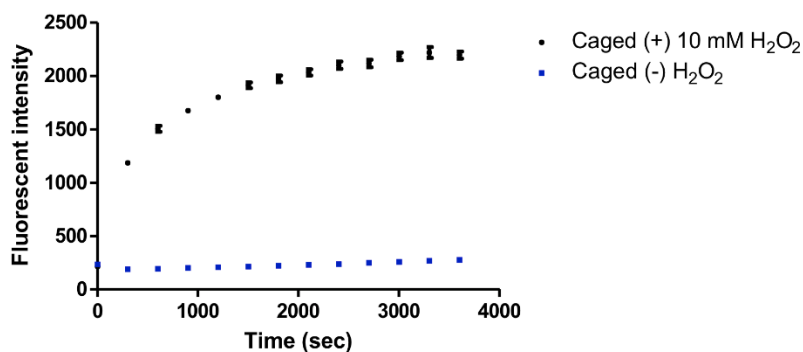
R_f = 0.3 (20% ethyl acetate/Hexanes) [silica gel, KMnO₄ stain, UV]

Fluorophore release response of 2.21 to H₂O₂.

The same procedure was used to monitor fluorophore release response of **2.21**. The results of these release studies are shown in Figure 1.

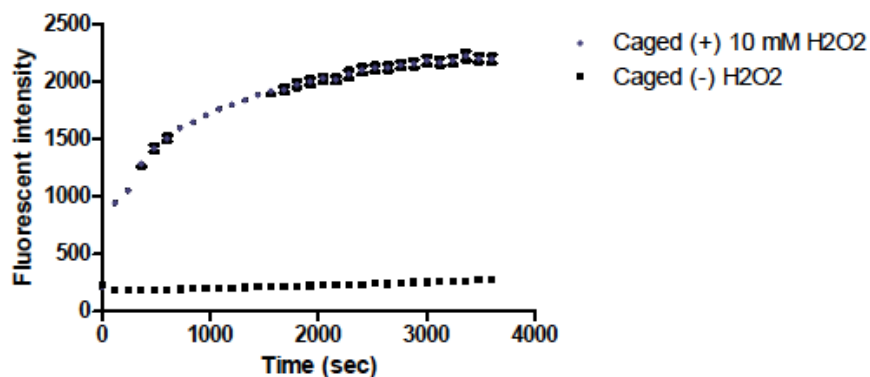


The above procedure was followed except that the 25 μM solution of **2.21** was treated with 2 μL of a 1 M aqueous solution of H₂O₂ to provide a final [H₂O₂] of 10 mM. The results of these release studies are shown in Figure 2.



Fluorophore release response of **2.21** to Reactive Oxygen Species.

4 mL of a 40 μM solution of **2.21** was prepared by diluting a 8 mM DMSO stock solution of **2.21** with PBS (pH 7.4). Experiments employed a final concentration of 10 mM O_2 and 200 μM for all other ROS. Superoxide (O_2^-) was added as solid KO_2 . Hydrogen peroxide (H_2O_2), *tert*-butyl hydroperoxide (TBHP), and hypochlorite (OCl^-) were delivered from commercially available solutions of 30%, 70%, and 5% aqueous solutions, respectively. Hydroxyl radical ($\cdot\text{OH}$) and *tert*-butoxy radical ($\cdot\text{O}^t\text{Bu}$) were generated by reaction of 1 mM Fe^{2+} with 200 μM H_2O_2 or 200 μM TBHP, respectively (prior to administration of these solutions to **2.21**, 200 units of catalase was also added as a scavenger for any remaining H_2O_2). Fluorescence was measured using a plate reader ($\lambda_{\text{ex}} = 448 \text{ nm}$, $\lambda_{\text{em}} = 499 \text{ nm}$) every minute. Temperature was maintained at 27 $^\circ\text{C}$.



Cell culture

HeLa cells were grown at 37 $^\circ\text{C}$ and 5% CO_2 in Dulbecco's modified Eagle's medium (Hyclone), supplemented with 10% fetal bovine serum (Seradigm). Dulbecco's phosphate buffered saline (DPBS) solution was formulated according to manufacturer's protocol (Sigma-Aldrich) at pH 7.3.

Ultra pure dimethylsulfoxide (DMSO) was purchased from Sigma-Aldrich, hydrogen peroxide (37%) was purchased from Fisher Scientific, and phorbol 12-myristate 13-acetate (PMA) was purchased from Acros Organics.

Fluorophore release from 2.21 in HeLa cells with exogenous H₂O₂

HeLa cells were plated at 35,000 cells/well in a black 96-well plate (Greiner Bio-one) and incubated overnight. Media was replaced with **2.21** (10 μ M, 0.5% DMSO) diluted in DPBS (100 μ L). Cells were incubated with **2.21** for 45 min at 37 °C, before removing treatment and washing cells with DPBS (2 x 50 μ L). Fresh DPBS was added (90 μ L), and initial fluorescence (F_i) was imaged on a Zeiss Axio Observer Z1 microscope using a 20x objective and GFP (Set 38 HE) filter (ex. 470 nm, em. 525 nm). Next, 10 μ L of aq. hydrogen peroxide (1 mM) or 10 μ L of water (vehicle) was added and cells were incubated for an additional 45 min at 37 °C before imaging final fluorescence (F). Next, fresh DPBS containing 2 μ M Hoeschst 33258 (100 μ L) was added to cells and incubated for 15 min before imaging using a DAPI (Set 68) filter (ex. 377 nm, em. 464 nm).

Fluorophore 2.21 in HeLa cells with exogenous H₂O₂

HeLa cells were plated at 35,000 cells/well in a black 96-well plate (Greiner Bio-one) and incubated overnight. Media was replaced with **2.21** (25 μ M, 0.5% DMSO) diluted in DPBS (100 μ L). Cells were incubated with **2.21** for 45 min at 37 °C, before removing treatment and washing cells with DPBS (2 x 50 μ L). Fresh DPBS was added (90 μ L), and initial fluorescence (F_i) was

imaged on a Zeiss Axio Observer Z1 microscope using a 20x objective and GFP (Set 38 HE) filter (ex. 470 nm, em. 525 nm). Next, 10 μ L of aq. hydrogen peroxide (1 mM) or 10 μ L of water (vehicle) was added and cells were incubated for an additional 45 min at 37 °C before imaging final fluorescence (F).

Fluorophore release from 2.21 in HeLa cells by endogenous PMA-stimulated H₂O₂ generation

HeLa cells were plated at 35,000 cells/well in a black 96-well plate (Greiner Bio-one) and incubated overnight. Media was refreshed with PMA-treated DMEM (1 μ M, 0.1% DMSO) or DMSO (0.1%) and cells were incubated for 1 h before removing treatment and washing cells with DPBS (2 x 50 μ L). Fresh DPBS (100 μ L) containing **2.21** (10 μ M, 0.5% DMSO) was added to the wells and cells were imaged for initial fluorescence (F_i) on a Zeiss Axio Observer Z1 microscope using a 20x objective and GFP (Set 38 HE) filter (ex. 470 nm, em. 525 nm). Cells were subsequently incubated for an additional 60 min before imaging final fluorescence (F), then fresh DPBS containing 2 μ M Hoeschst 33258 (100 μ L) was added to cells and incubated for 15 min before imaging using a DAPI (Set 68) filter (ex. 377 nm, em. 464 nm).

Fluorescence intensity calculations and statistical analysis

ImageJ software (National Institutes of Health) was utilized for image analysis and quantification. A region-of-interest (ROI) was selected around individual HeLa cells ($n = 3$) and mean fluorescent intensity of each cell was calculated using the ImageJ “Measure” tool. ROIs containing no cells

were used to calculate background mean fluorescent intensity and were subsequently background subtracted from the mean fluorescent intensities of cell. For each condition, three cells were quantified and the final fluorescence (F) was set relative to the initial fluorescence (F_i) for each individual cell (F/F_i). Statistical analysis was conducted via an unpaired t-test in the GraphPad Prism software.

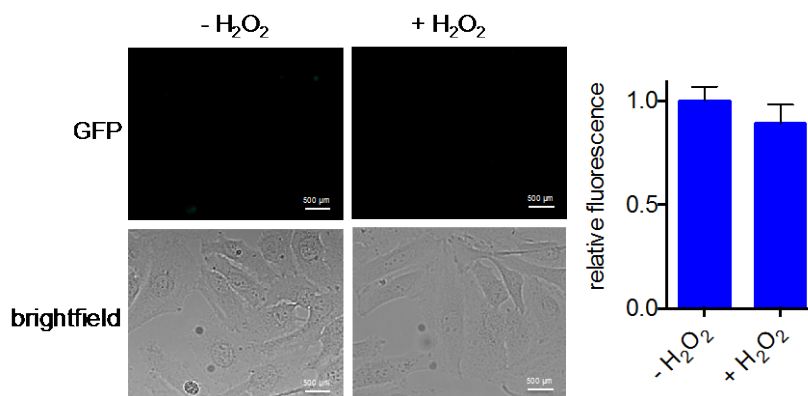


Figure 3. Control fluorophore acetal **2.22** in HeLa cells. Cells were treated with 25 μM **2.22** in DPBS buffer for 45 min at 37 °C, followed by replacement with fresh DPBS containing vehicle or 100 μM H₂O₂. Following 30 min incubation, cellular fluorescence was imaged on a Zeiss Axio Observer Z1 microscope using a 20x objective and GFP (Set 38 HE) filter (ex. 470 nm, em. 525 nm). Mean fluorescence intensities were calculated from individual HeLa cells (*n* = 3) and set relative to vehicle control. Error bars denote SD.

General procedure for monitoring alcohol release via ¹H NMR spectroscopy.

The NMR spectrometer was programmed to acquire a spectrum every 32 scans (3 minutes, 24 seconds) with a relaxation time of 2 seconds to ensure accurate integration values. Buffer solutions were prepared according to and using D₂O instead of H₂O.

Representative procedure for sample preparation.

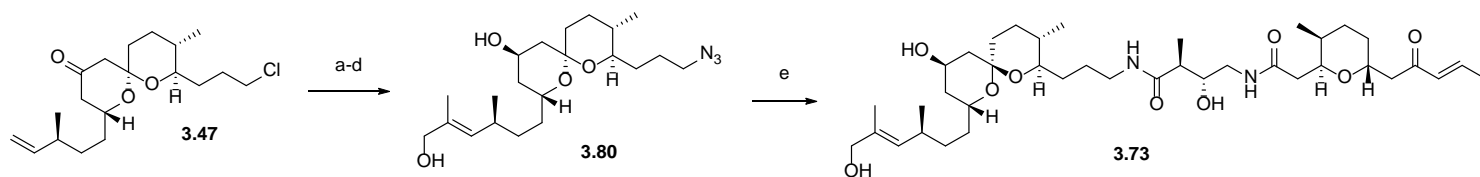
Compound **2.3** (2.9 mg, 0.012 mmol) was dissolved in CD₃CN (475 μL) and D₂O (50 μL) was added followed by pH 8.00 phosphate buffer (25 μL, 0.1 M, D₂O) and dimethoxy ethane (internal standard, 25 μL, 1.5 M, CD₃CN). The resulting solution was transferred to an NMR tube. This sample preparation is modeled after Phillip's Protocol.

Representative procedure for alcohol release in response to H₂O₂.

The release of butanone from **2.3** was monitored via ¹H NMR spectroscopy at 300 K. NMR samples were prepared according to the representative procedure for sample preparation. An initial ¹H NMR scan was taken to obtain baseline integration values relative to the internal standard (1,2-dimethoxyethane). The NMR sample was treated with a solution of H₂O₂•urea (3.0 M, 25 μL, 6.25 equivalents), and mixing was achieved by inverting the NMR tube three times. The final concentration of **2.3** was 20 mM and the final concentration of H₂O₂ was 125 mM. The release of alcohol was either directly measured by integration of alcohol or measured based on integration of the known ketone or aldehyde by products.

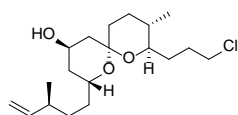
APPENDIX B

Novel Analogues of Bistramide A, synthetic Optimization, and Biological Activity (Supporting Info)



Reagents and conditions

- a) Sm, isopropanol, 75% b) Methacrolein:CH₂Cl₂ 5:1, HG-II, 68%.
c) NaBH₄, MeOH 0°C, 81%. d) NaN₃, DMF, 50°C, 90%.
e) PMe₃, THF:H₂O 3:1, then 3.56, DMF, 39%



(2R,4R,6S,8S)-8-(3-chloropropyl)-2-((S)-3-methylpent-4-en-1-yl)-

1,7-dioxaspiro[5.5]undecan-4-ol (**S6**). To a flame dried, 10 mL schlenk

flask containing a stir bar was added samarium (0.15 g, 1.00 mmol) and I₂ (6 mg, 0.039 mmol). The flask was back filled with Ar (3x), then degassed, dry, isopropanol (3 mL) was added via syringe. The reaction was stirred for 30 minutes, then ketone **3.47** (40 mg, 0.11 mmol) dissolved in isopropanol (1 mL) was added via syringe and allowed to stir overnight. The reaction was quenched with 1M HCl (5 mL) and extracted with diethyl ether (3x). The combined organic layers were dried over Na₂SO₄, filtered, and concentrated under reduced pressure. The resulting residue was purified by silica gel chromatography (R_f = 0.3, 20% ethyl acetate in hexanes) to give alcohol **S6** (31 mg, 0.086 mmol, 75% yield).

Data for S6

Optical Rotation (*c* = 0.14, CHCl₃)

[α]_D²⁵ = -9.3

¹H NMR (500 MHz, CDCl₃)

δ 5.72 (ddd, *J* = 7.5, 10.3, 17.5 Hz, 1H), 4.99-4.93 (m, 2H), 4.12-4.07 (m, *J*_{tot} = 26 Hz, axial, 1H), 3.62-3.52 (m, 2H), 3.49-3.43 (m, 1H), 3.13 (t, 1H, *J* = 9.7 Hz), 2.15 (sep, *J* = 5.6 Hz, 1H), 2.05-2.12 (m, 1H), 2.05-1.92 (m, 3H), 1.83-1.67 (m, 3H), 1.47-1.11 (m, 12H), 1.02 (d, *J* = 6.8 Hz, 3 H), 0.85 (d, *J* = 6.6 Hz, 3H).

Meerwein-Ponndorf-Verley reduction of similar cyclic ketones is known to give the alcohol in the equatorial position.¹³⁶

¹³C NMR (125 MHz, CDCl₃)

δ 144.51, 112.68, 97.18, 74.38, 68.01, 65.02, 45.46, 44.99, 41.05, 37.61, 35.77, 34.70, 33.48, 32.64, 30.54, 29.09, 27.89, 20.15, 17.88

IR (ATR)

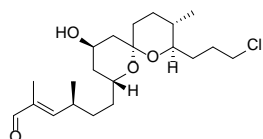
3416, 2911, 1493, 1361, 1321, 1249, 1093, 1081, 1033, 981, 911 cm⁻¹

HRMS (FTMS ES+)

[M+H]⁺ Calculated for C₁₉H₃₄O₃Cl 345.2191, found 345.2204

TLC

R_f = 0.3, 20% ethyl acetate in hexanes [silica gel, anisaldehyde stain]



(S,E)-6-((2R,4R,6R,8R,9S)-8-(3-chloropropyl)-4-hydroxy-9-methyl-1,7-dioxaspiro[5.5]undecan-2-yl)-2,4-dimethylhex-2-enal (S7). To a

flame dried, 25 mL round bottom flask containing a stir bar was added alkene **S7** (20 mg, 0.056 mmol) dissolved in CH₂Cl₂ (1 mL). Methacrolein (5 mL) was added, then Nitro-Grela catalyst (3.8 mg, 5.6 μmol) and the flask was sealed and placed under an argon balloon. The reaction was heated at 40 °C for 4 hours, then concentrated under reduced pressure. The resulting residue was

purified by silica gel chromatography ($R_f = 0.3$, 40% ethyl acetate in hexanes) to give aldehyde **S7** (.014 g, 0.037 mmol, 67%, E:Z (10:1)).

Data for **S7**

Optical Rotation ($c = 0.28$, CHCl_3)

$[\alpha]_D^{25} = +11.82$

^1H NMR (500 MHz, CDCl_3)

δ 9.42 (s, 1H), 6.28 (dd, $J = 1.1, 9.9$ Hz), 4.12-4.08 (m, 1H), 3.61-3.52 (m, 2H), 3.48-3.45 (m, 1H), 3.10 (td, $J = 2.3, 9.7$ Hz, 1H), 2.73-2.69 (m, 1H), 2.08-1.98 (m, 2H), 1.94-1.91 (m, 1H), 1.83-1.78 (m, 1H), 1.77 (d, $J = 1.2$ Hz, 3H), 1.75-1.59 (m, 3H), 1.54-1.15 (m, 10 H), 1.11 (d, $J = 5.8$ Hz, 3H), 0.85 (d, $J = 6.5$ Hz, 3H)

^{13}C NMR (100 MHz, CDCl_3)

δ 195.63, 159.98, 138.20, 97.25, 77.23, 74.45, 67.78, 64.88, 60.42, 45.47, 40.92, 35.68, 34.67, 33.79, 33.59, 32.83, 30.52, 29.15, 27.87, 19.93, 17.95, 14.21, 9.49

IR (ATR)

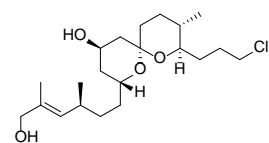
3412, 2901, 1681, 1632, 1493, 1361, 1316, 1243, 1099, 1074, 1011, 979, 907 cm^{-1}

HRMS (FTMS ES+)

$[\text{M}+\text{H}]^+$ Calculated for $\text{C}_{21}\text{H}_{36}\text{O}_4\text{Cl}$ 387.2296, found 345.2304

TLC

$R_f = 0.3$, 40% ethyl acetate in hexanes [silica gel, anisaldehyde stain]



(2R,4R,6R,8R,9S)-8-(3-chloropropyl)-2-((S,E)-6-hydroxy-3,5-dimethylhex-4-en-1-yl)-9-methyl-1,7-dioxaspiro[5.5]undecan-4-ol (S8).

To a flame dried, 10 mL round bottom flask, containing stir bar was added aldehyde **S8** (15 mg,

0.040 mmol) dissolved in MeOH (3 mL). The reaction was cooled to 0°C using an ice-water bath, then NaBH₄ (5 mg, 0.14 mmol) was added in a single portion. The reaction stirred at 0°C for 30 minutes, then quenched with H₂O and extracted with diethyl ether (3x). The combined organic layers were dried over Na₂SO₄, filtered, and concentrated under reduced pressure. A column was run on the resulting residue (R_f = 0.15, 40% ethyl acetate in hexanes) to give diol **S8** (12 mg, 0.032 mmol, 81%).

Data for S8

Optical Rotation (c = 0.18, CHCl₃)

[α]²⁵_D = +10.0

¹H NMR (500 MHz, CDCl₃)

δ 5.20 (dd, *J* = 1.0, 9.4 Hz, 1H), 4.16-4.07 (m, 1H), 4.01 (s, 2H), 3.61-3.52 (m, 2H), 3.47-3.43 (m, 1H), 3.13 (td, *J* = 2.3, 9.7 Hz, 1H), 2.44-2.37 (m, 1H), 2.06-1.98 (m, 2H), 1.94-1.91 (m, 1H), 1.83-1.71 (m, 2H), 1.68 (d, *J* = 1 Hz, 3H), 1.59-1.25 (m, 12 H), 0.97 (d, *J* = 6.7 Hz, 3H), 0.85 (d, *J* = 6.6 Hz, 3H).

¹³C NMR (125 MHz, CDCl₃)

δ 133.6, 132.37, 97.19, 74.40, 68.97, 67.95, 65.02, 45.44, 44.98, 41.06, 35.76, 34.71, 33.75, 33.52, 31.99, 30.53, 29.13, 27.88, 21.03, 17.89, 13.91

IR (ATR)

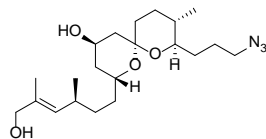
3407, 2877, 1490, 1332, 1211, 1076, 1062, 1001, 986, 907 cm⁻¹

HRMS (FTMS ES+)

[M+H]⁺ Calculated for C₂₁H₃₈O₄Cl 389.2453, found 389.2462

TLC

R_f = 0.15, 40% ethyl acetate in hexanes [silica gel, anisaldehyde stain]



(2R,4R,6R,8R,9S)-8-(3-azidopropyl)-2-((S,E)-6-hydroxy-3,5-

dimethylhex-4-en-1-yl)-9-methyl-1,7-dioxaspiro[5.5]undecan-4-ol

(3.80). To a flame dried, 1 dram vial mL containing stir bar was added diol **3.80** (9.0 mg , 0.023 mmol) in DMF (1 mL). Sodium azide (15 mg, 0.23 mmol) was added in a single portion and the reaction was sealed then heated to 50°C and stirred overnight. The reaction was allowed to cool to room temperature, then diluted with H₂O and extracted with diethyl ether (3x). The combined organic layers were dried over Na₂SO₄, filtered, and concentrated under reduced pressure. A column was run on the resulting residue (R_f = 0.15, 40% ethyl acetate in hexanes) to give diol **3.80** (8.1 mg, 0.020 mmol, 88%).

Data for 3.80

Optical Rotation (c = 0.21, CHCl₃)

[α]²⁵_D = +10.1

¹H NMR (500 MHz, CDCl₃)

δ 5.20 (d, J = 9.5, 1H), 4.16-4.07 (m, 1H), 4.02 (s, 2H), 3.47-3.43 (m, 1H), 3.39-3.26 (m, 2H), 3.13 (td, J = 2.2, 9.7 Hz, 1H), 2.43-2.35 (m, 1H), 1.99 (dd, J = 4.6, 12.3 Hz, 1H), 1.95-1.91 (m, 1H), 1.88-1.81 (m, 2H), 1.77-1.26 (m, 15H), 0.97 (d, J = 6.7 Hz, 3H), 0.84 (d, J = 6.6 Hz, 3H)

¹³C NMR (100 MHz, CDCl₃)

δ 133.61, 132.37, 97.20, 74.47, 68.97, 67.99, 65.02, 51.87, 44.98, 41.05, 35.76, 34.70, 33.76, 33.55, 32.02, 30.19, 29.68, 27.87, 25.32, 17.89, 13.89

IR (ATR)

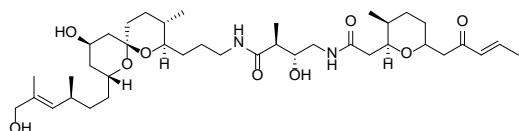
3419, 2873, 2080, 1487, 1331, 1307, 1215, 1077, 1064, 999, 981, 900 cm⁻¹

HRMS (FTMS ES+)

[M+H]⁺ Calculated for C₂₁H₃₈O₄N₃ 396.2857, found 396.2860

TLC

R_f = 0.15, 40% ethyl acetate in hexanes [silica gel, anisaldehyde stain] Note: Starting material and product have identical R_f



(2S,3R)-3-hydroxy-N-(3-((2R,3S,6R,8R,10R)-10-hydroxy-8-((S,E)-6-hydroxy-3,5-dimethylhex-4-en-

1-yl)-3-methyl-1,7-dioxaspiro[5.5]undecan-2-yl)propyl)-2-methyl-4-(2-((2S,3S)-3-methyl-6-((E)-2-oxopent-3-en-1-yl)tetrahydro-2H-pyran-2-yl)acetamido)butanamide (3.73). To a

flame dried 5 mL flask containing a stir bar was added azide **3.80** (7.0 mg, 0.018 mmol) dissolved in THF (1mL), then H₂O (0.3 mL) was added. The reaction was sealed under Ar, then PMe₃ (1.00 M in THF, 0.10 mL, 0.10 mmol) was added via syringe. The reaction was stirred for 1 hour, then diluted with diethyl ether and H₂O. The resulting mixture was extracted with diethyl ether (3x) and the combined organic layers were dried over Na₂SO₄, filtered, and concentrated under reduced pressure. The resulting residue was then dissolved in dimethylformamide (1 ml) and sealed under argon. Succinimide **3.56** (5.1 mg, 0.011 mmol) dissolved in dimethylformamide (0.3 ml) was added via syringe. The reaction was stirred at room temperature overnight, then diluted with CH₂Cl₂ and H₂O. The resulting mixture was extracted with CH₂Cl₂ (3x), dried over Na₂SO₄, filtered, and concentrated under reduced pressure. A column was run on the resulting residue (R_f = 0.15, 5% methanol in CH₂Cl₂) to give bisamide analogue **3.73** (3.1 mg, 0.0044 mmol, 39%).

Data for 3.73

Optical Rotation (c = 0.12, CHCl₃)

[α]_D²⁵ = +2.1

¹H NMR (500 MHz, CDCl₃)

δ 7.30 (br. t, 1H), 6.99 (br. t, 1H), 6.91 (dd, 1H, *J* = 6.8, 15.7 Hz), 6.12 (dd, 1H, *J* = 1.6, 15.8 Hz), 5.21 (d, 1H, *J* = 9.4 Hz), 4.58 (br. d, 1H), 4.22-4.19 (m, 1H), 4.11-4.09 (m, 1H), 4.05-4.04 (m, 1H), 3.99 (s, 2H), 3.81-3.77 (m, 1H), 3.72 (q, 1H, *J* = 5.2 Hz), 3.45 (dd, 1H, *J* = 5.3, 14 Hz), 3.37-3.22 (m, 4H), 2.90 (dd, 1H, *J* = 8.75, 16.9 Hz), 2.75 (dd, 1H, *J* = 11.7, 15.2 Hz), 2.54 (dd, 1H, *J* = 3.15, 16.9 Hz), 2.42-2.36 (m, 2H), 2.15 (d, 1H, *J* = 15.1 Hz), 1.92 (dd, 3H, *J* = 1.6, 6.8 Hz), 1.85-1.74 (m, 3H), 1.68 (s, 3H), 1.57-1.19 (m, 24H), 0.96 (d, 3H, *J* = 6.7 Hz), 0.86 (d, 3H, *J* = 7 Hz), 0.83 (d, 3H, *J* = 6.5 Hz)

¹³C NMR (125 MHz, CDCl₃)

δ 198.98, 174.97, 173.71, 144.68, 135.58, 132.32, 132.06, 97.12, 74.98, 74.45, 74.07, 68.90, 68.04, 64.63, 45.25, 44.90, 43.63, 40.91, 39.18, 35.79, 34.62, 33.65, 33.49, 33.32, 32.31, 31.99, 31.91, 30.82, 30.02, 29.69, 27.89, 26.53, 25.87, 20.93, 18.39, 17.92, 17.15, 15.64, 13.95

IR (ATR)

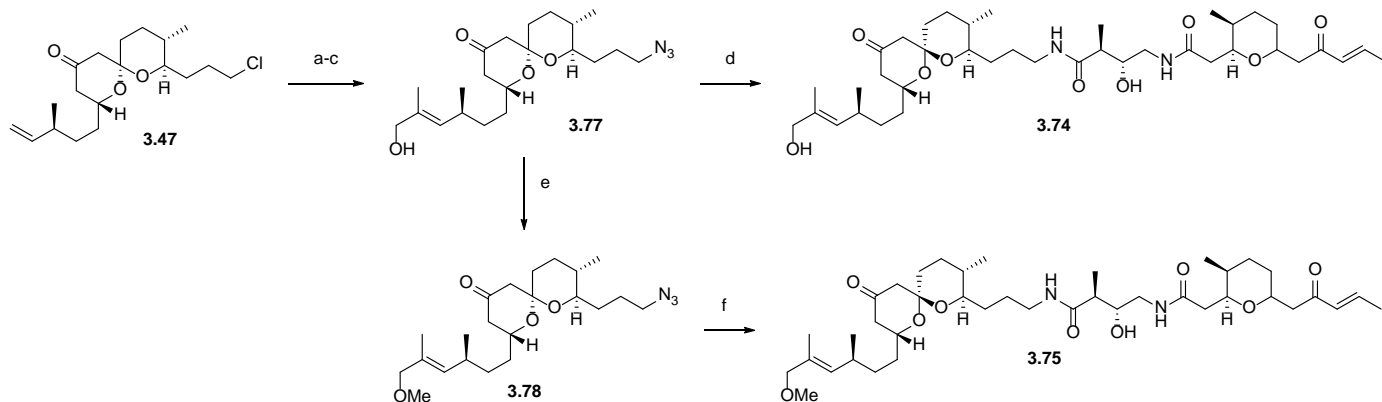
3600-3200 (brs), 2937, 2861, 1651, 1549, 1379, 1298, 1201, 986, 731 cm⁻¹

HRMS (FTMS ES+)

[M+H]⁺ Calculated for C₃₉H₆₇O₉N₂ 707.4841, found 707.4821

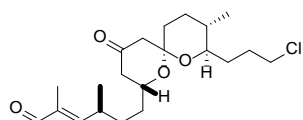
TLC

R_f = 0.15 5% methanol in dichloromethane [silica gel, p-anisaldehyde stain]



Reagents and conditions

- a) Methacrolein:CH₂Cl₂ 5:1, HG-II, 68%.
 b) L-selectride, THF, -78°C, 67%. c) NaN₃, DMF, 50°C, 92%.
 d) PMe₃, THF:H₂O 3:1, then **3.56**, DMF, 41% e) 2,6 ditertbutylpyridine, MeOTf, CH₂Cl₂, 69%
 f) PMe₃, THF:H₂O 3:1, then **3.56**, DMF, 31%



(S,E)-6-((2R,6S,8S)-8-(3-chloropropyl)-4-oxo-1,7-

dioxaspiro[5.5]undecan-2-yl)-2,4-dimethylhex-2-enal (3.71). To a

flame dried, 25 mL round bottom flask containing a stir bar was added alkene **3.47** (0.040 g, 0.11 mmol) dissolved in CH₂Cl₂ (1 mL). Methacrolein (5 mL) was added, then Nitro-Grela catalyst (.014 g, .021 mmol) and the flask was sealed and placed under an argon balloon. The reaction was heated at 40 °C for 4 hours, then concentrated under reduced pressure. The resulting residue was purified by silica gel chromatography (R_f = 0.3, 20% ethyl acetate in hexanes) to give aldehyde **3.71** (.031 g, 0.083 mmol, 68% E:Z 20:1).

Data for 3.71

Optical Rotation (c = 0.41, CHCl₃)

[α]²⁵_D = +12.2

¹H NMR (400 MHz, CDCl₃)

δ 9.43 (s, 1H), 6.30 (d, J = 9.8 Hz, 1H), 3.75 (m, 1H), 3.58-3.46 (m, 2H), 3.13 (t, J = 9.4 Hz, 1H), 2.73 (m, 1H), 2.58-2.42 (m, 1H), 2.39 (s, 2H), 2.36-2.32 (m, 1H), 2.18 (t, J = 13.8 Hz, 1H), 1.86-1.81 (m, 2H), 1.78 (s, 3H), 1.69-1.36 (m, 10H), 1.13 (d, J = 6.4 Hz, 3H), 0.86 (d, J = 6.2 Hz, 3H)

^{13}C NMR (100 MHz, CDCl_3)

δ 205.71, 195.48, 159.41, 138.41, 99.03, 75.43, 68.67, 51.83, 47.05, 45.51, 35.23, 34.10, 33.87, 33.56, 32.57, 30.27, 28.52, 27.90, 19.55, 17.82, 9.53

IR (ATR)

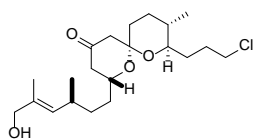
2901, 1701, 1681, 1626, 1498, 1349, 1316, 1241, 1099, 1052, 1000, 976 cm^{-1}

HRMS (FTMS ES+)

$[\text{M}+\text{H}]^+$ Calculated for $\text{C}_{21}\text{H}_{34}\text{O}_4\text{Cl}$ 385.2140, found 385.2144

TLC

$R_f = 0.3$ 20% ethyl acetate in hexanes [silica gel, p-anisaldehyde stain]



(2R,6S,8S)-8-(3-chloropropyl)-2-((S,E)-6-hydroxy-3,5-dimethylhex-4-en-1-yl)-1,7-dioxaspiro[5.5]undecan-4-one (3.81). To a flame dried flask

containing a stir bar was added aldehyde **3.71** (0.051 g, 0.13 mmol)

dissolved in THF (10 ml). The flask was placed under argon, cooled to $-78\text{ }^\circ\text{C}$, then L-selectride

(1M in THF, 0.17 ml, 0.17 mmol) was added dropwise. The reaction was stirred for 30 minutes

at $-78\text{ }^\circ\text{C}$ then cooled to room temperature. The reaction was quenched with H_2O and extracted

with diethyl ether (3x). The combined organic layers were dried over Na_2SO_4 , filtered, and

concentrated under reduced pressure. The resulting residue was purified by silica gel column

chromatography ($R_f = 0.15$, 30% ethyl acetate in hexanes) to give title compound **3.81** (0.031 g,

.081 mmol, 62%) as well as diol **S8** (0.015 g, .039 mmol, 30%).

Data for 3.81

Optical Rotation ($c = 0.18$, CHCl_3)

$[\alpha]_{\text{D}}^{25} = +10.4$

¹H NMR (500 MHz, CDCl₃)

δ 5.20 (dd, *J* = 9.5, 1.1 Hz, 1H), 4.03 (s, 2H), 3.74 (ddt, *J* = 11.4, 8.5, 3.2 Hz, 1H), 3.58-3.47 (m, 2H), 3.15 (td, *J* = 9.4, 2.4 Hz, 1H), 2.43-2.40 (m, 1H), 2.39 (s, 2H), 2.36-2.32 (m, 1H), 2.34 (dd, *J* = 13.7, 1.7 Hz, 1H), 2.18 (dd, *J* = 14.1, 11.5 Hz, 1H), 1.99-1.93 (m, 1H), 1.87-1.76 (m, 2H), 1.68 (d, *J* = 1 Hz, 3H), 1.66-1.26 (m, 13H), 0.98 (d, *J* = 6.7 Hz, 3H), 0.87 (d, *J* = 5.6 Hz, 3H)

¹³C NMR (125 MHz, CDCl₃)

δ 205.71, 133.87, 131.90, 98.96, 75.29, 68.86, 68.82, 51.86, 47.19, 45.53, 35.30, 34.08, 33.90, 33.22, 31.97, 30.27, 28.52, 27.89, 21.11, 17.79, 13.96

IR (ATR)

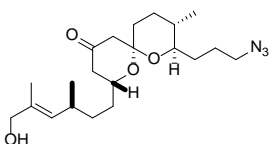
3311, 2901, 1701, 1640, 1498, 1349, 1299, 1254, 1081, 1042, 999, 979, 652 cm⁻¹

HRMS (FTMS ES+)

[M+H]⁺ Calculated for C₂₁H₃₆O₄Cl 387.2297, found 387.2298

TLC

R_f = 0.15 30% ethyl acetate in hexanes) [silica gel, p-anisaldehyde stain]



(2R,6R,8R,9S)-8-(3-azidopropyl)-2-((S,E)-6-hydroxy-3,5-dimethylhex-4-en-1-yl)-9-methyl-1,7-dioxaspiro[5.5]undecan-4-one

(3.77). To a flame dried, 1 dram vial mL containing stir bar was added

ketone **3.81** (12 mg, 0.030 mmol) in DMF (1 mL). Sodium azide (30 mg, 0.46 mmol) was added in a single portion and the reaction was sealed then heated to 50°C and stirred overnight. The reaction was cooled to room temperature, then diluted with H₂O and extracted with diethyl ether (3x). The combined organic layers were dried over Na₂SO₄, filtered, and concentrated under

reduced pressure. The resulting residue was purified by silica gel column chromatography ($R_f = 0.15$, 30% ethyl acetate in hexanes) to give azide **3.77** (9.0 mg, 0.023 mmol, 75%).

Data for 3.77

Optical Rotation ($c = 0.10$, CHCl_3)

$[\alpha]_D^{25} = +3.5$

$^1\text{H NMR}$ (500 MHz, CDCl_3)

δ 5.20 (d, $J = 9.2$ Hz, 1H), 4.02 (s, 2H), 3.77-3.73 (m, 1H), 3.32-3.21 (m, 2H), 3.17-3.13 (m, 1H), 2.43-2.40 (m, 1H), 2.38 (s, 2H), 2.36-2.33 (m, 1H), 2.19 (dd, $J = 14.1, 11.5$ Hz, 1H), 1.87-1.82 (m, 2H), 1.78-1.36 (m, 15H), 0.99 (d, $J = 6.7$ Hz, 3H), 0.86 (d, $J = 6.6$ Hz, 3H)

$^{13}\text{C NMR}$ (125 MHz, CDCl_3)

δ 205.96, 133.88, 131.90, 98.96, 75.40, 68.84, 61.89, 51.84, 47.17, 45.91, 35.32, 34.06, 33.91, 33.24, 31.97, 30.15, 29.68, 27.89, 24.92, 21.06, 17.78, 13.91, 8.61

IR (ATR)

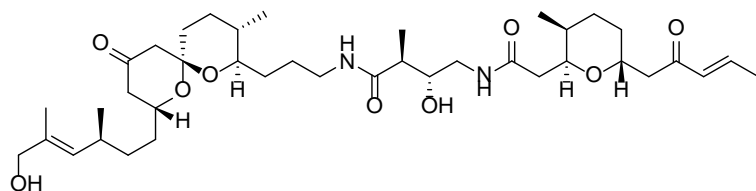
3211, 2899, 2121, 1699, 1630, 1498, 1356, 1278, 1243, 1077, 1045, 976 cm^{-1}

HRMS (FTMS ES+)

$[\text{M}+\text{H}]^+$ Calculated for $\text{C}_{21}\text{H}_{36}\text{O}_4\text{N}_3$ 394.2700, found 394.2697

TLC

$R_f = 0.15$ 30% ethyl acetate in hexanes [silica gel, p-anisaldehyde stain]



**(2S,3R)-3-hydroxy-N-(3-
((2R,3S,6R,8R)-8-((S,E)-6-
hydroxy-3,5-dimethylhex-4-en-1-**

yl)-3-methyl-10-oxo-1,7-dioxaspiro[5.5]undecan-2-yl)propyl)-2-methyl-4-(2-((2S,3S)-3-methyl-6-((E)-2-oxopent-3-en-1-yl)tetrahydro-2H-pyran-2-yl)acetamido)butanamide (3.74).

To a flame dried 5 mL flask containing a stir bar was added azide **3.77** (7.0 mg, 0.018 mmol) dissolved in THF (1mL), then H₂O (0.3 mL) was added. The reaction was sealed under Ar, then PMe₃ (1.00 M in THF, 0.10 mL, 0.10 mmol) was added via syringe. The reaction was stirred for 1 hour, then diluted with diethyl ether and H₂O. The resulting mixture was extracted with diethyl ether (3x) and the combined organic layers were dried over Na₂SO₄, filtered, and concentrated under reduced pressure. The resulting residue was then dissolved in dimethylformamide (1 ml) and sealed under argon. Succinimide **3.56** (5.0 mg, 0.011 mmol) dissolved in dimethylformamide (0.3 ml) was added via syringe. The reaction was stirred at room temperature overnight, then diluted with CH₂Cl₂ and H₂O. The resulting mixture was extracted with CH₂Cl₂ (3x), dried over Na₂SO₄, filtered, and concentrated under reduced pressure. A column was run on the resulting residue (R_f = 0.20, 5% methanol in CH₂Cl₂) to give bistramide analogue **3.74** (3.2 mg, 0.0045 mmol, 41%).

Data for 3.74

Optical Rotation (c = 0.10, CHCl₃)

$$[\alpha]_D^{25} = +3.6$$

¹H NMR (500 MHz, CDCl₃)

δ 7.29 (br.t, 1H), 6.91 (dd, 1H, J = 6.85, 15.9 Hz), 6.82 (br.t, 1H), 6.13 (dd, 1H, J = 1.5, 15.8 Hz), 5.21 (d, 1H, J = 9.35 Hz), 4.21 (m, 1H), 4.10 (m, 1H), 4.01 (s, 2H), 3.77 (m, 1H), 3.72 (d, 1H J = 5.25 Hz), 3.51-3.46 (m, 1H), 3.25-3.22 (m, 2H), 3.14 (t, 1H, J = 10 Hz), 2.91 (dd, 1H, J = 8.75, 16.9 Hz), 2.76 (dd, 1H, J = 11.9, 15.0 Hz), 2.55 (dd, 1H, J = 3.05, 17 Hz), 2.38 (s, 2 H), 2.41 (m, 1H), 2.37-2.33 (m, 1H), 2.20-2.13 (m, 3H), 1.92 (dd, 3H, J = 1.4, 6.8 Hz), 1.85-1.81 (m, 1H), 1.67-

1.31 (m, 19H), 1.29- 1.22 (m, 8H), 0.98 (d, 3H, $J = 6.7$ Hz), 0.86 (d, 3H, $J = 7.05$ Hz), 0.83 (d, 3H, $J = 6.6$ Hz)

^{13}C NMR (125 MHz, CDCl_3)

δ 206.32, 198.91, 175.27, 173.34, 144.40, 133.92, 132.16, 131.78, 98.92, 98.89, 75.32, 74.77, 73.73, 70.60, 68.92, 68.75, 51.96, 47.13, 45.29, 44.57, 43.31, 39.13, 35.35, 33.96, 33.80, 33.32, 33.15, 32.48, 31.98, 30.74, 29.76, 27.93, 26.54, 25.21, 20.98, 18.37, 17.80, 17.05, 15.49, 13.97.

IR (ATR)

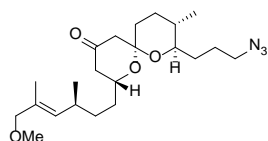
3600-3200 (brs), 2937, 2861, 1721, 1650, 1520, 1386, 1298, 1201, 977, 722 cm^{-1}

HRMS (FTMS ES+)

$[\text{M}+\text{H}]^+$ Calculated for $\text{C}_{39}\text{H}_{65}\text{O}_9\text{N}_2$ 705.4685, found 705.4667

TLC

$R_f = 0.20$ 5% methanol in dichloromethane [silica gel, p-anisaldehyde stain]



(2R,8R,9S)-8-(3-azidopropyl)-2-((S,E)-6-methoxy-3,5-dimethylhex-4-en-1-yl)-9-methyl-1,7-dioxaspiro[5.5]undecan-4-one (3.78). To a flame

dried, 5 mL round bottom flask containing a stir bar was added azide **3.77**

(6.0 mg, 0.015 mmol) in CH_2Cl_2 (1 mL). The flask was sealed under Ar and 2,6-ditertbutylpyridine

(0.2 mL) and methyl trifluoromethanesulfonate (0.1 mL) were added *via* syringe sequentially. The

reaction was allowed to stir at room temperature overnight, then concentrated under reduced

pressure. The resulting residue was purified by silica gel column chromatography ($R_f = 0.6$, 20%

ethyl acetate in hexanes) to give methyl ether **3.78** (4.1 mg, 0.010 mmol, 69% yield).

Data for 3.78

Optical Rotation ($c = 0.071$, CHCl_3)

$[\alpha]_D^{25} = -11.3$

$^1\text{H NMR}$ (500 MHz, CDCl_3)

δ 5.20 (d, $J = 9.6$ Hz, 1H), 3.81 (s, 2H), 3.71-3.73 (m, 1H), 3.33-3.21 (m, 2H), 3.29 (s, 3H), 3.14 (t, $J = 9.2$ Hz, 1H), 2.44-2.41 (m, 1H), 2.38 (s, 2H), 2.36-2.32 (m, 1H), 2.18 (dd, $J = 14.05, 11.4$ Hz, 1H), 1.86-1.73 (m, 4H), 1.65 (s, 3H), 1.63-1.26 (m, 10 H), 0.99 (d, $J = 6.6$ Hz, 3H), 0.86 (d, $J = 6.5$ Hz, 3H)

$^{13}\text{C NMR}$ (125 MHz, CDCl_3)

δ 205.97, 133.98, 131.12, 98.94, 78.62, 75.39, 68.82, 57.33, 51.84, 47.16, 35.32, 34.06, 33.89, 33.19, 32.07, 30.12, 29.98, 27.88, 24.92, 21.03, 17.77, 14.02

IR (ATR)

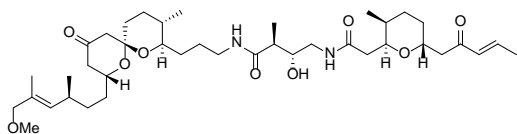
2890, 2119, 1715, 1640, 1490, 1353, 1279, 1247, 1099, 1049, 966 cm^{-1}

HRMS (FTMS ES+)

$[\text{M}+\text{H}]^+$ Calculated for $\text{C}_{22}\text{H}_{37}\text{N}_3\text{O}_4$ 408.2857, found 408.2864

TLC

$R_f = 0.6$, 20% ethyl acetate in hexanes [silica gel, anisaldehyde stain]



(2*S*,3*R*)-3-hydroxy-*N*-(3-((2*R*,3*S*,8*R*)-8-((*S*,*E*)-6-methoxy-3,5-dimethylhex-4-en-1-yl)-3-methyl-10-oxo-1,7-dioxaspiro[5.5]undecan-2-yl)propyl)-2-

methyl-4-(2-((2*S*,3*S*,6*R*)-3-methyl-6-((*E*)-2-oxopent-3-en-1-yl)tetrahydro-2*H*-pyran-2-yl)acetamido)butanamide (3.76). To a flame dried 5 mL flask containing a stir bar was added

azide **3.78** (4.0 mg, 0.0098 mmol) dissolved in THF (1mL), then H_2O (0.3 mL) was added. The reaction was sealed under Ar, then PMe_3 (1.00 M in THF, 0.10 mL, 0.10 mmol) was added via

syringe. The reaction was stirred for 1 hour, then diluted with diethyl ether and H₂O. The resulting mixture was extracted with diethyl ether (3x) and the combined organic layers were dried over Na₂SO₄, filtered, and concentrated under reduced pressure. The resulting residue was then dissolved in dimethylformamide (1 ml) and sealed under argon. Succinimide **3.56** (8.0 mg, 0.018 mmol) dissolved in dimethylformamide (0.3 ml) was added via syringe. The reaction was stirred at room temperature overnight, then diluted with CH₂Cl₂ and H₂O. The resulting mixture was extracted with CH₂Cl₂ (3x), dried over Na₂SO₄, filtered, and concentrated under reduced pressure. A column was run on the resulting residue (R_f = 0.20, 5% methanol in CH₂Cl₂) to give bistramide analogue **3.76** (1.8 mg, 0.0025 mmol, 31% yield).

Data for **3.76**

Optical Rotation (c = 0.053, CHCl₃)

[α]²⁵_D = +1.3

¹H NMR (700 MHz, CDCl₃)

δ 7.42 (br. t, 1H), 6.91 (dd, 1H, J = 6.9, 15.8 Hz), 6.82 (br. t, 1H), 6.13 (dd, 1H, J = 1.4, 15.6 Hz), 5.20 (d, 1H, J = 9.4 Hz), 4.21 (m, 1H), 4.10 (m, 1H), 3.81 (m, 2H), 3.77-3.67 (m, 2H), 3.53-3.49 (m, 1H), 3.29 (s, 3H), 2.72-3.19 (m, 2H), 3.13 (t, 1H, J = 8.8 Hz), 2.95-2.88 (m, 1H), 2.77 (dd, 1H, J = 11.6, 15.0 Hz), 2.58-2.54 (m, 1H), 2.42-2.40 (m, 1H), 2.38 (s, 2H), 2.34-2.33 (m, 1H), 2.20-2.12 (m, 2H), 1.92 (s, 3H), 1.85-1.83 (m, 1H), 1.65 (s, 3H), 1.69-1.52 (m, 6H), 1.48-1.44 (m, 2H), 1.40-1.30 (m, 6H), 1.29-1.18 (m, 6H), 0.98 (d, 3H, J = 6.7 Hz), 0.87 (d, 3H, J = 6.8 Hz), 0.83 (d, 3H, J = 6.5 Hz)

¹³C NMR (175 MHz, CDCl₃)

δ 206.55, 199.00, 175.31, 173.35, 144.54, 134.20, 132.05, 130.97, 98.96, 78.66, 75.45, 74.79, 73.66, 68.84, 57.32, 51.96, 47.20, 45.27, 44.52, 43.25, 39.30, 35.29, 34.16, 33.62, 33.32, 33.11, 33.13, 32.17, 30.79, 29.86, 29.71, 27.87, 26.51, 25.17, 21.22, 18.47, 17.82, 17.14, 15.52, 14.07

IR (ATR)

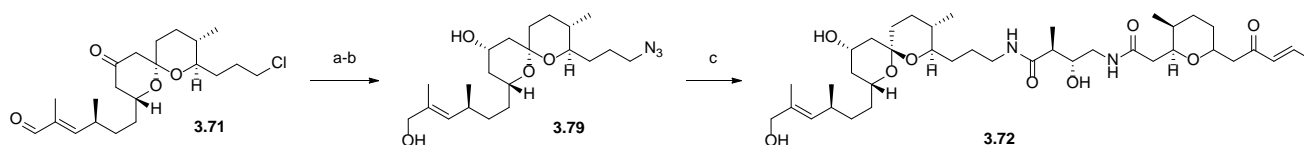
3600-3200 (brs), 2941, 2731, 1660, 1391, 1301, 1200, 976, 721 cm^{-1}

HRMS (FTMS ES+)

$[\text{M}+\text{H}]^+$ Calculated for $\text{C}_{40}\text{H}_{67}\text{O}_9\text{N}_2$ 719.4841, found 719.48476

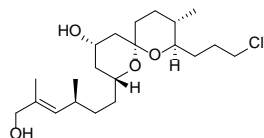
TLC

$R_f = 0.35$ 5% methanol in dichloromethane [silica gel, p-anisaldehyde stain]



Reagents and conditions

a) NaBH_4 , MeOH 0°C , 88%. b) NaN_3 , DMF, 50°C , 63%.
c) PMe_3 , THF: H_2O 3:1, then **3.56**, DMF, 43%



(2R,4S,6R,8R,9S)-8-(3-chloropropyl)-2-((S,E)-6-hydroxy-3,5-dimethylhex-4-en-1-yl)-9-methyl-1,7-dioxaspiro[5.5]undecan-4-ol (S8**).**

To a flame dried, 10 mL round bottom flask, containing stir bar was added aldehyde **3.71** (21 mg, 0.050 mmol) dissolved in MeOH (3 mL). The reaction was cooled to 0°C using an ice-water bath, then NaBH_4 (5 mg, 0.14 mmol) was added in a single portion. The reaction stirred at 0°C for 30 minutes, then quenched with H_2O and extracted with diethyl ether (3x). The combined organic layers were dried over Na_2SO_4 , filtered, and concentrated under reduced pressure. A column was run on the resulting residue ($R_f = 0.25$, 40% ethyl acetate in hexanes) to give diol **S8** (18 mg, 0.045 mmol, 88%).

Data for **S8**

Optical Rotation ($c = 0.14$, CHCl_3)

$[\alpha]_D^{25} = +14.3$

$^1\text{H NMR}$ (500 MHz, CDCl_3)

δ 5.21 (dd, $J = 9.5, 1.2$ Hz, 1H), 4.07-4.04 (m, $J_{\text{tot}} = 15.2$ Hz, 1H), 4.02 (s, 1H), 4.01 (s, 1H), 3.95 (d, $J = 9.7$ Hz, 1H), 3.80-3.76 (m, 1H), 3.59-3.56 (m, 2H), 3.34-3.39 (m, 1H), 2.44-2.39 (m, 1H), 1.97-1.90 (m, 1H), 1.86-1.75 (m, 4H), 1.68 (d, $J = 1.2$ Hz, 3H), 1.65-1.57 (m, 4H), 1.54-1.31 (m, 10H), 0.98 (d, $J = 6.7$ Hz, 3H), 0.87 ($J = 6.5$ Hz, 3H)

$^{13}\text{C NMR}$ (125 MHz, CDCl_3)

δ 133.65, 132.34, 97.98, 75.39, 69.95, 65.21, 63.94, 45.30, 40.27, 38.30, 35.76, 33.96, 33.78, 33.41, 32.07, 30.06, 28.56, 27.32, 21.11, 17.89, 13.93

IR (ATR)

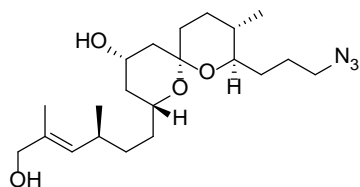
3300-3200 (brs), 2899, 1643, 1496, 1359, 1301, 1243, 1076, 1039, 999, 652 cm^{-1}

HRMS (FTMS ES+)

$[\text{M}+\text{H}]^+$ Calculated for $\text{C}_{21}\text{H}_{38}\text{O}_4\text{Cl}$ 389.2453, found 389.2456

TLC

$R_f = 0.25$, 40% ethyl acetate in hexanes [silica gel, anisaldehyde stain]



(2R,4S,6R,8R,9S)-8-(3-azidopropyl)-2-((S,E)-6-hydroxy-3,5-dimethylhex-4-en-1-yl)-9-methyl-1,7-dioxaspiro[5.5]undecan-

4-ol (3.79). To a flame dried, 1 dram vial mL containing stir bar was

added diol **3.79** (14 mg, 0.036 mmol) in DMF (1 mL). Sodium azide (23 mg, 0.36 mmol) was added in a single portion and the reaction was sealed then heated to 50°C and stirred overnight.

The reaction was cooled to room temperature, then diluted with H_2O and extracted with diethyl

ether (3x). The combined organic layers were dried over Na₂SO₄, filtered, and concentrated under reduced pressure. A column was run on the resulting residue (R_f = 0.25, 40% ethyl acetate in hexanes) to give azide **3.79** (9 mg, 0.023 mmol, 63%).

Data for 3.79

Optical Rotation (c = 0.11, CHCl₃)

[α]²⁵_D = +28.2

¹H NMR (500 MHz, CDCl₃)

δ 5.21 (dd, J = 1.05 Hz, 1H), 4.06-4.04 (m, 1H), 4.01 (s, 2H), 3.94 (d, J = 9.6 Hz, 1H), 3.80-3.77 (m, 1H), 3.36-3.29 (m, 3H), 2.45-2.37 (m, 1H), 1.86-1.73 (m, 4H), 1.67 (d, J = 1 Hz, 3H), 1.65-1.34 (m, 14H), 0.98 (d, J = 6.7 Hz, 3H), 0.86 (d, J = 6.6 Hz, 3H)

¹³C NMR (125 MHz, CDCl₃)

δ 133.60, 132.22, 97.98, 75.47, 68.94, 65.20, 63.97, 57.17, 40.27, 38.29, 35.76, 34.00, 33.78, 33.44, 32.08, 29.91, 29.68, 27.31, 25.06, 17.91, 13.91

IR (ATR)

3300-3200 (brs), 2877, 2111, 1641, 1498, 1361, 1299, 1243, 1077, 1041, 978 cm⁻¹

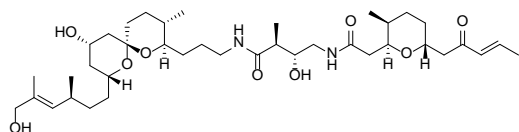
HRMS (FTMS ES+)

[M+H]⁺ Calculated for C₂₁H₃₈O₄N₃ 396.2856, found 396.2856

TLC

R_f = 0.25, 40% ethyl acetate in hexanes [silica gel, anisaldehyde stain]

(2S,3R)-3-hydroxy-N-(3-((2R,3S,6R,8R,10S)-10-hydroxy-8-((S,E)-6-hydroxy-3,5-dimethylhex-4-en-1-yl)-3-methyl-1,7-dioxaspiro[5.5]undecan-2-yl)propyl)-2-methyl-4-(2-((2S,3S)-3-methyl-6-((E)-2-oxopent-3-en-1-yl)tetrahydro-2H-pyran-2-



yl)acetamido)butanamide (3.72). To a flame dried 5 mL flask containing a stir bar was added azide **3.79** (6.2

mg, 0.016 mmol) dissolved in THF (1mL), then H₂O (0.3 mL) was added. The reaction was sealed under Ar, then PMe₃ (1.00 M in THF, 0.10 mL, 0.10 mmol) was added via syringe. The reaction was stirred for 1 hour, then diluted with diethyl ether and H₂O. The resulting mixture was extracted with diethyl ether (3x) and the combined organic layers were dried over Na₂SO₄, filtered, and concentrated under reduced pressure. The resulting residue was then dissolved in dimethylformamide (1 ml) and sealed under argon. Succinimide **3.56** (5.9 mg, 0.013 mmol) dissolved in dimethylformamide (0.3 ml) was added via syringe. The reaction was stirred at room temperature overnight, then diluted with CH₂Cl₂ and H₂O. The resulting mixture was extracted with CH₂Cl₂ (3x), dried over Na₂SO₄, filtered, and concentrated under reduced pressure. A column was run on the resulting residue (R_f = 0.15, 5% methanol in CH₂Cl₂) to give bistramide analogue **3.72** (5.1 mg, 0.0072 mmol, 55%).

Data for 3.72

Optical Rotation (c = 0.07, CHCl₃)

$$[\alpha]_D^{25} = +14.3$$

¹H NMR (500 MHz, CDCl₃)

δ 7.31 (br. t, 1H), 6.97 (br. t, 1H), 6.91 (dd, 1H, J = 6.8, 15.8 Hz), 6.14 (dd, 1H, J = 1.7, 15.9 Hz), 5.21 (d, 1H, J = 9.5 Hz), 4.57 (d, 1H, J = 4.3 Hz), 4.22-4.18 (m, 1H), 4.15-4.09 (m, 1H), 4.05 (m, 2H), 4.00 (s, 2H), 3.80-3.78 (m, 1H), 3.73 (m, 1H), 3.75 (dt, 1H, J = 6.3, 14 Hz), 3.39-3.22 (m, 3H), 2.90 (dd, 1H, J = 8.8, 17 Hz), 2.76 (dd, 1H, J = 6.0, 15.0 Hz), 2.54 (dd, 1H, J = 3.0, 16.8 Hz), 2.41-2.37 (m, 2H), 2.15 (d, 1H, J = 15.2 Hz), 1.93 (dd, 3H, J = 1.5, 6.8 Hz), 1.84-1.72 (m, 3H),

1.69-1.28 (m, 18H), 1.68 (s, 3H), 1.26-1.19 (m, 6H), 0.97 (d, 3H, $J = 6.7$ Hz), 0.87 (d, 3H, $J = 7.0$ Hz), 0.83 (d, 3H, $J = 6.5$ Hz)

^{13}C NMR (125 MHz, CDCl_3)

δ 197.92, 174.31, 172.30, 143.40, 132.60, 131.28, 131.18, 96.80, 74.45, 73.76, 73.67, 72.62, 67.85, 64.19, 62.93, 44.30, 43.51, 42.22, 39.36, 38.10, 37.22, 34.80, 32.97, 32.73, 32.38, 32.30, 31.47, 31.10, 29.77, 28.74, 26.37, 25.54, 24.63, 20.01, 17.36, 16.91, 16.06, 14.51, 12.97

IR (ATR)

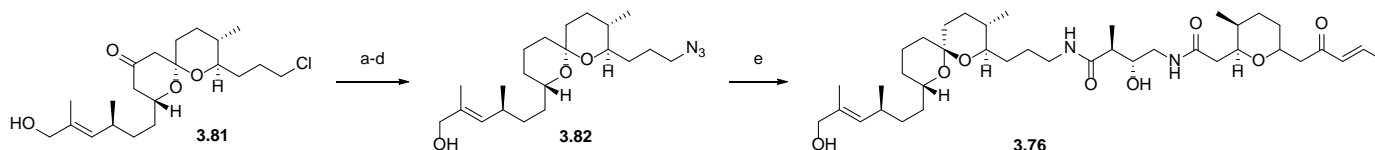
3600-3200 (brs), 2937, 2861, 1651, 1519, 1382, 1295, 1200, 977, 724 cm^{-1}

HRMS (FTMS ES+)

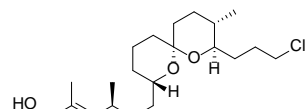
$[\text{M}+\text{H}]^+$ Calculated for $\text{C}_{39}\text{H}_{67}\text{O}_9\text{N}_2$ 707.4841, found 707.4842

TLC

$R_f = 0.20$ 5% methanol in dichloromethane [silica gel, p-anisaldehyde stain]



Reagents and conditions
a) MeOH , TsNHNH_2
b) $\text{MeOH}:\text{THF}$, NaBH_3CN
c) $\text{EtOH}:\text{H}_2\text{O}$ 20:1, NaOAc , 47% over 3 steps
d) NaN_3 , DMF , 50°C , 81%.
e) PMe_3 , $\text{THF}:\text{H}_2\text{O}$ 3:1, then **3.56**, DMF , 54%



(*S,E*)-6-((*2S,6S,8R,9S*)-8-(3-chloropropyl)-9-methyl-1,7-

dioxaspiro[5.5]undecan-2-yl)-2,4-dimethylhex-2-en-1-ol (**S9**). To a

solution of ketone **S9** (.031 g, .078 mmol) in MeOH (1.2 mL) was added TsNHNH_2 (0.029 g, 0.16 mmol) in one portion. The resulting solution was stirred at room temperature for 6 hours then was concentrated under reduced pressure. The residue was diluted with 30% ethyl acetate in hexanes and filtered through a short silica plug. The filtrate was concentrated and re-dissolved in MeOH and THF (1:1, 3 mL). A solution of NaBH_3CN (6.3 mg, 0.10 mmol) in MeOH (0.10 mL) was added dropwise via syringe at 0°C . To the resulting solution was carefully added a 1 M HCl stock

solution in EtOH dropwise at 0°C until TLC analysis indicated completion (0.5 mL). The reaction was diluted with diethyl ether and washed with H₂O, saturated aqueous NaHCO₃, and brine. The organic layer was dried over Na₂SO₄, filtered, and concentrated under reduced pressure. The residue was dissolved in EtOH (4 mL), the NaOAc (0.161 g, 1.94 mmol) was added followed by H₂O (0.20 ml). The reaction was heated to 75°C for 1 hour, cooled to room temperature, diluted with diethyl ether, and washed with H₂O and brine. The organic layer was dried over Na₂SO₄, filtered, and concentrated under reduced pressure. The resulting residue was purified by silica gel column chromatography (R_f = 0.5, 20% ethyl acetate in hexanes) to give alcohol **S9** (.021 g, 0.055 mmol, 47% yield over 3 steps).

Data for S9

Optical Rotation (c = 0.10, CHCl₃)

$[\alpha]_D^{25} = +20.4$

¹H NMR (500 MHz, CDCl₃)

δ 5.20 (d, J = 9.4 Hz, 1H), 4.01 (s, 2H), 3.65-3.54 (m, 2H), 3.43 (m, 1H), 3.17 (t, J = 9.7 Hz, 1H), 2.39-2.34 (m, 1H), 2.16-2.09 (m, 1H), 1.87-1.73 (m, 4H), 1.68 (s, 3H), 1.64-1.29 (m, 10H), 1.20-1.11 (m, 15H), 0.96 (d, J = 6.6 Hz, 3H), 0.85 (d, J = 6.5 Hz, 3H)

¹³C NMR (125MHz,CDCl₃)

δ 133.44, 132.65, 95.50, 74.11, 69.12, 69.05, 45.61, 35.10, 35.47, 35.01, 34.19, 33.53, 32.05, 31.39, 30.69, 29.69, 29.29, 27.91, 21.03, 19.20, 17.94, 13.91

IR (ATR)

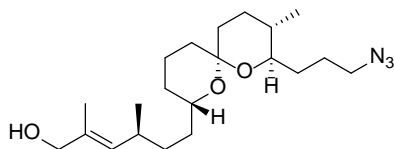
3412, 2929, 2863, 1451, 1381, 1269, 1221, 1175, 1090, 1032, 986, 676 cm⁻¹

HRMS (FTMS ES+)

$[M+H]^+$ Calculated for C₂₁H₃₈O₃Cl 373.2504, found 373.2512

TLC

$R_f = 0.5$ 20% ethyl acetate in hexanes [silica gel, p-anisaldehyde stain]



(*S,E*)-6-((*2S,6S,8R,9S*)-8-(3-azidopropyl)-9-methyl-1,7-dioxaspiro[5.5]undecan-2-yl)-2,4-dimethylhex-2-en-1-ol

(3.82). To a flame dried, 1 dram vial mL containing stir bar was

added compound **3.82** (10 mg, 0.026 mmol) in DMF (1 mL). Sodium azide (30 mg, 0.46 mmol)

was added in a single portion and the reaction was sealed then heated to 50°C and stirred overnight.

The reaction was cooled to room temperature, then diluted with H₂O and extracted with diethyl

ether (3x). The combined organic layers were dried over Na₂SO₄, filtered, and concentrated under

reduced pressure. The resulting residue was purified by silica gel column chromatography ($R_f =$

0.50, 20% ethyl acetate in hexanes) to give azide **3.82** (8.0 mg, 0.021 mmol, 81%).

Data for 3.82

Optical Rotation ($c = 0.11$, CHCl₃)

$$[\alpha]_D^{25} = +27.3$$

¹H NMR (500 MHz, CDCl₃)

δ 5.19 (d, $J = 9.4$ Hz, 1H), 4.00 (s, 2H), 3.47-3.44 (m, 1H), 3.38-3.27 (m, 2H), 3.17 (td, $J = 9.7, 1.9$ Hz, 1H), 2.39-2.32 (m, 1H), 1.97-1.90 (m, 2H), 1.84-1.72 (m, 4H), 1.67 (s, 3H), 1.63-1.28 (m, 10H), 1.22-1.14 (m, 15H), 0.96 (d, $J = 6.7$ Hz, 3H), 0.85 (d, $J = 6.5$ Hz, 3H)

¹³C NMR (125 MHz, CDCl₃)

δ 133.43, 132.64, 95.51, 74.18, 69.17, 69.02, 51.94, 36.09, 35.46, 35.02, 34.20, 33.57, 32.07, 31.38, 30.33, 29.69, 27.90, 25.46, 21.02, 19.20, 17.95, 13.89

IR (ATR)

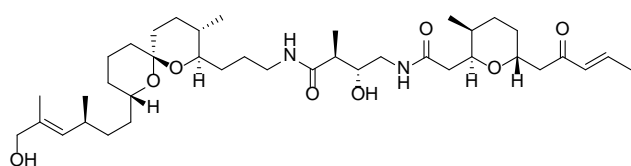
3425, 2929, 2863, 2121, 1443, 1377, 1267, 1219, 1089, 1029, 984 cm⁻¹

HRMS (FTMS ES+)

[M+H]⁺ Calculated for C₂₁H₃₈O₃N₃ 380.2908, found 380.2909

TLC

R_f = 0.5 20% ethyl acetate in hexanes [silica gel, p-anisaldehyde stain]



(2S,3R)-3-hydroxy-N-(3-((2R,3S,6S,8S)-8-

((S,E)-6-hydroxy-3,5-dimethylhex-4-en-1-

yl)-3-methyl-1,7-dioxaspiro[5.5]undecan-2-

yl)propyl)-2-methyl-4-(2-((2S,3S)-3-methyl-6-((E)-2-oxopent-3-en-1-yl)tetrahydro-2H-

pyran-2-yl)acetamido)butanamide (**3.78**). To a flame dried 5 mL flask containing a stir bar was

added azide **3.82** (7.0 mg, 0.018 mmol) dissolved in THF (1mL), then H₂O (0.3 mL) was added.

The reaction was sealed under Ar, then PMe₃ (1.00 M in THF, 1.5 mL, 0.15 mmol) was added via syringe. The reaction was stirred for 1 hour, then diluted with diethyl ether and H₂O. The resulting

mixture was extracted with diethyl ether (3x) and the combined organic layers were dried over Na₂SO₄, filtered, and concentrated under reduced pressure. The resulting residue was then dissolved

in dimethylformamide (1 ml) and sealed under argon. Succinimide **3.56** (5.0 mg, 0.011 mmol)

dissolved in dimethylformamide (0.3 ml) was added via syringe. The reaction was stirred at room

temperature overnight, then diluted with CH₂Cl₂ and H₂O. The resulting mixture was extracted

with CH₂Cl₂ (3x), dried over Na₂SO₄, filtered, and concentrated under reduced pressure. A column

was run on the resulting residue (R_f = 0.20, 5% methanol in CH₂Cl₂) to give bistramide analogue

3.78 (4.1 mg, 0.0059 mmol, 54%).

Data for 3.78

Optical Rotation (c = 0.21, CHCl₃)

$[\alpha]_D^{25} = +1.5$

$^1\text{H NMR}$ (500 MHz, CDCl_3)

δ 7.32 (br.t, 1H), 6.96 (br.t, 1H), 6.91 (dd, 1H, $J = 6.95, 13.8$ Hz), 6.15 (dd, 1H, $J = 1.5, 15.9$ Hz), 5.20 (d, 1H, $J = 9.1$ Hz), 4.20 (m, 1H), 4.07 (dd, 1H, $J = 4.75, 11.5$ Hz), 3.99 (s, 2H), 3.72 (d, 1H, $J = 4.55$ Hz), 3.53-3.46 (m, 2H), 3.35-3.21 (m, 3H), 3.18 (t, 1H, $J = 8.0$ Hz), 2.91 (dd, 1H, $J = 9.0$ Hz, 17.1 Hz), 2.76 (dd, 1H, $J = 11.6$ Hz, 15.1 Hz), 2.53 (dd, 1H, $J = 2.8, 17.0$ Hz), 2.38 (m, 2H), 2.14 (d, 1H, $J = 15$ Hz), 1.92 (dd, 3H, $J = 1.35, 6.8$ Hz), 1.84-1.81 (m, 4H), 1.66-1.56 (m, 13H), 1.47-1.10 (m, 25H), 0.95 (d, 3 H, $J = 6.7$ Hz), 0.86 (d, 3H, $J = 6.9$ Hz), 0.81 (d, 3H, $J = 6.4$ Hz)

$^{13}\text{C NMR}$ (175 MHz, CDCl_3)

δ 198.98, 175.20, 173.53, 144.59, 133.43, 132.42, 132.11, 95.49, 74.85, 74.17, 73.85, 69.21, 68.87, 45.27, 44.68, 43.31, 39.40, 36.11, 35.51, 34.96, 34.09, 33.52, 33.33, 32.06, 31.32, 30.33, 29.71, 27.93, 26.51, 25.85, 22.70, 20.97, 19.24, 18.44, 18.02, 17.18, 15.59, 14.14, 13.97

IR (ATR)

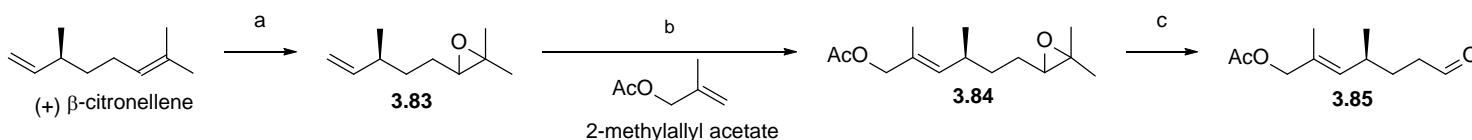
3600-3200 (brs), 2927, 2857, 1651, 1545, 1455, 1367, 1299, 1219, 988, 733 cm^{-1}

HRMS (FTMS ES+)

$[\text{M}+\text{H}]^+$ Calculated for $\text{C}_{39}\text{H}_{67}\text{O}_8\text{N}_2$ 691.4892, found 691.4904

TLC

$R_f = 0.30$ 5% methanol in dichloromethane [silica gel, p-anisaldehyde stain]

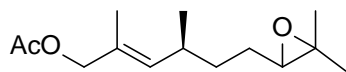


Reagents and Conditions

a) *m*CPBA, CH_2Cl_2 , 0 C, 73% dr 1:1

b) 5:1 2-methylallyl acetate: CH_2Cl_2 , HG-II (3 mol%), 52%, E:Z 5:1

c) H_5IO_6 , THF, 0 C, 51%, E:Z 5:1



(4*S*,*E*)-6-(3,3-dimethyloxiran-2-yl)-2,4-dimethylhex-2-en-1-yl

acetate (**3.84**). To a flame dried, 250 mL round bottom flask, was

added (+)- β -Citronellene (4.04 g, 29.3 mmol), followed by CH_2Cl_2 (150 mL). The reaction was cooled to 0°C using an ice bath, then *meta*-Chloroperoxybenzoic acid (50%, 11.2 g, 32.3 mmol) was added portion wise over 30 minutes. The reaction was allowed to warm to room temperature and then was stirred for 1 hour. The reaction was filtered through a celite plug eluting with CH_2Cl_2 , then the filtrate was concentrated under reduced pressure. The resulting residue was dissolved in diethyl ether (150 mL), then washed with saturated aqueous NaHCO_3 (3 x 100 mL) and brine (2 x 100 mL). The organic layer was dried over Na_2SO_4 filtered and concentrated. The resulting oil was purified by silica gel chromatography ($R_f = 0.5$, 10% ethyl acetate in hexanes) to give epoxide **3.83** (3.61 g, 26.1 mmol, 79%, dr 1:1). To a flame dried, 25 mL round bottom flask containing a stir bar was added epoxide **3.83** (2.01 g, 13.05 mmol) dissolved in CH_2Cl_2 (2 mL). 2-methylallyl acetate (10 mL) was added then HG-II catalyst (0.254 g, 0.405 mmol). The flask was sealed under an argon balloon and heated to 90°C overnight. The reaction was cooled to room temperature, then concentrated under reduced pressure. The resulting brown oil was purified by silica gel column chromatography ($R_f = 0.3$, 10% ethyl acetate in hexanes) to give acetate **3.84** (1.63 g, 6.78 mmol, 51%, E:Z 5:1, d.r. 1:1).

Data for 3.84

Optical Rotation ($c = 0.6$, CHCl_3)

$$[\alpha]_D^{25} = +35.2$$

^1H NMR (500 MHz, CDCl_3)

δ 5.26-5.22 (m, 1H, E isomer), 5.19-5.16 (m, 1H, Z isomer), 4.66-4.56 (m, 2H, Z isomer), 4.46 (s, 2H, E isomer), 2.72-2.69 (m, 1H), 2.53-2.40 (m, 1H), 2.09-2.08 (m, 3H), 1.77 (d, $J = 1$ Hz, 3H, E

isomer), 1.67 (s, 3H, E isomer), 1.61-1.41 (m, 4H), 1.32 (s, H), 1.26 (d, $J = 3.6$ Hz), 0.99 (d, $J = 6.7$ Hz, 3H)

^{13}C NMR (100 MHz, CDCl_3)

δ 170.91, 135.42, 135.38, 129.25, 129.14, 70.20, 70.17, 64.48, 64.27, 63.34, 58.22, 58.14, 34.08, 33.85, 32.21, 32.05, 26.92, 26.74, 24.88, 20.97, 20.91, 20.83, 20.64, 20.97, 20.92, 20.83, 20.64, 18.63, 18.61, 14.15

IR (ATR)

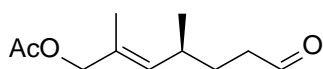
3083, 2866, 1721, 1644, 1245, 1055, 981 cm^{-1}

HRMS (FTMS ES+)

$[\text{M}+\text{H}]^+$ Calculated for $\text{C}_{14}\text{H}_{25}\text{O}_3$ 241.1798, found 241.1838

TLC

$R_f = 0.3$ 10% ethyl acetate in hexanes [silica gel, p-anisaldehyde stain]



(E)-2,4-dimethyl-7-oxohept-2-en-1-yl acetate (3.85). To a

flame dried, 50 mL round bottom flask containing a stir bar was added epoxide **3.84** (0.502 g, 2.02 mmol) dissolved in THF (10 mL). The reaction was cooled to 0°C using an ice bath and placed under argon. H_5IO_6 (0.915 g, 4.03 mmol) dissolved in THF (5 mL) was added dropwise *via* syringe. The reaction was allowed to warm to room temperature and stirred for 2 hours. The reaction was (slowly) quenched with saturated aqueous NaHCO_3 (5 mL), then the mixture was transferred to a separatory funnel and extracted with diethyl ether (3 x 20 mL). The combined organic layers were dried over Na_2SO_4 , filtered and concentrated under reduced pressure. The resulting oil was purified by silica gel column chromatography ($R_f = 0.25$, 10% ethyl acetate in hexanes) to give aldehyde **3.85** (0.227 g, 1.15 mmol, 56%, E:Z 5.5:1)

Data for 3.85

Optical Rotation ($c = 0.9, \text{CHCl}_3$)

$[\alpha]_D^{25} = +21.0$

$^1\text{H NMR}$ (400 MHz, CDCl_3)

δ 9.77 (bt, 1H, Z isomer), 9.75 (bt, 1H, E isomer), 5.18 (d, $J = 9.7$ Hz, 1H, E isomer), 5.11 (d, $J = 10.1$ Hz, Z isomer), 4.58-4.52 (m, 2H, Z isomer), 4.47-4.42 (m, 2H, E isomer), 2.48-2.36 (m, 3H), 2.08 (s, 3H, E isomer), 2.07 (s, 3H, Z isomer), 1.79-1.65 (m, 1H), 1.64 (s, 3H, E isomer), 1.60-1.47 (m, 1H), 1.00-0.98 (m, 3H)

$^{13}\text{C NMR}$ (100 MHz, CDCl_3)

δ 202.40, 202.34, 170.86, 135.92, 134.24, 130.03, 129.84, 69.92, 63.20, 42.02, 41.95, 31.97, 31.74, 29.48, 29.37, 21.49, 21.35, 20.97, 20.89, 20.76, 14.15

IR (ATR)

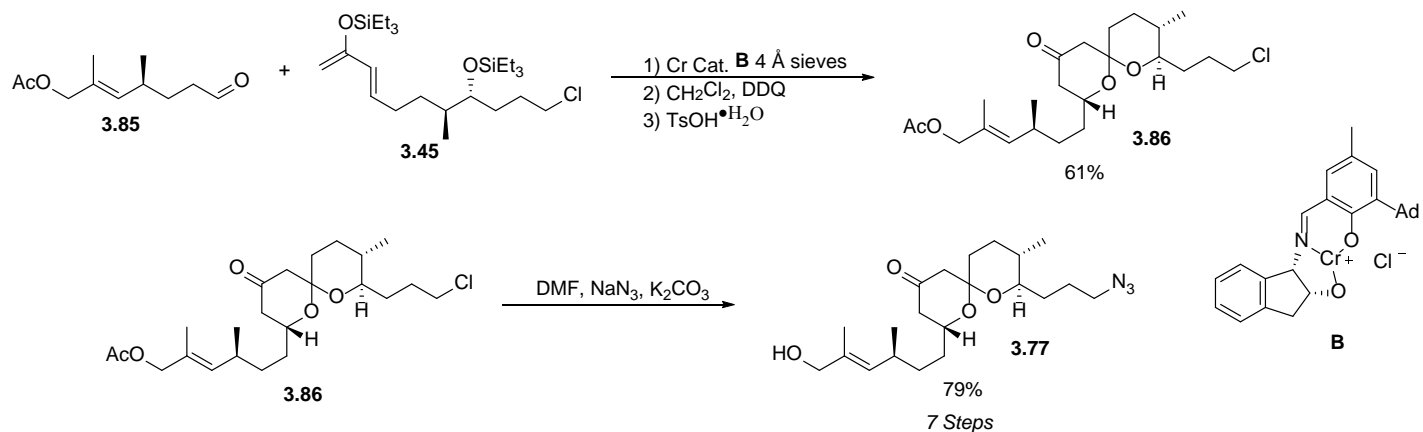
3079, 2721, 1752, 1731, 1043, 991 cm^{-1}

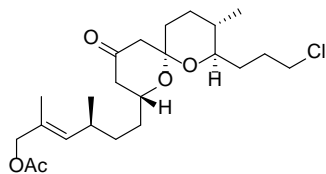
HRMS (FTMS ES+)

$[\text{M}+\text{H}]^+$ Calculated for $\text{C}_{11}\text{H}_{19}\text{O}_3$ 199.1329, found 199.1334

TLC

$R_f = 0.20$ 10% ethyl acetate in hexanes [silica gel, p-anisaldehyde stain]





(4*S*,*E*)-6-((2*R*,8*R*,9*S*)-8-(3-chloropropyl)-9-methyl-4-oxo-1,7-dioxaspiro[5.5]undecan-2-yl)-2,4-dimethylhex-2-en-1-yl acetate

(3.86). A flame dried 10 mL Schlenck tube containing a stir bar was charged with Cr catalyst **B** (0.030 g, 0.060 mmol) and 4 Å molecular sieves (0.050 g) then sealed and back filled with Ar (3x). Aldehyde (0.303 g, 1.53 mmol) was added via syringe and the reaction was allowed to stir for 5 minutes, then diene **3.45** (0.203 g, 0.44 mmol) was added *via* syringe and the reaction was allowed to stir for 3 days. An additional aliquot of aldehyde **3.85** (0.101 g, 0.51 mmol) was added *via* syringe and the reaction was allowed to stir another 3 days. The reaction was diluted with CH₂Cl₂ (5 mL) then 2,3-Dichloro-5,6-dicyano-1,4-benzoquinone (0.0990 g, 0.44 mmol) was added. The reaction was stirred for 1 hour, then TsOH-H₂O (0.151 g, 0.880 mmol) was added. The reaction was stirred for 2 hours then was quenched with NEt₃ (1 mL) and filtered through a silica plug eluting with a copious amount of ethyl acetate. The filtrate was concentrated under reduced pressure, then purified by silica gel column chromatography (*R_f* = 0.4, 20% ethyl acetate in hexanes) to give acetate **3.86** (0.112 g, 0.261 mmol, 61% yield)

Data for **3.86**

Optical Rotation (*c* = 0.14, CHCl₃)

[α]²⁵_D = +14.3

¹H NMR (500 MHz, CDCl₃)

δ 5.25 (d, 1H, *J* = 9.5 Hz), 4.47 (s, 2H), 3.76-3.72 (m, 1H), 3.57-3.47 (m, 2H), 3.15 (td, 1H, *J* = 2.45, 9.55 Hz), 2.43-2.40 (m, 1H), 2.38 (s, 2H), 2.34 (dd, 1H, *J* = 14.05, 2.00 Hz), 2.19 (dd, 1H, *J* = 14.05, 11.3, Hz), 2.08 (s, 3H), 1.99-1.92 (m, 1H), 1.87-1.74 (m, 3H), 1.66 (d, 3H *J* = 1Hz), 1.59-1.32 (m, 7H), 0.99 (d, 3H, *J* = 6.65), 0.87 (d, 3H, *J* = 6.55 Hz)

^{13}C NMR (100 MHz, CDCl_3)

δ 205.97, 170.91, 135.40, 129.24, 98.94, 75.30, 70.21, 68.74, 51.84, 47.15, 45.48, 35.31, 33.95, 33.88, 33.03, 32.08, 30.29, 28.52, 27.89, 21.01, 20.82, 17.77, 14.19

IR (ATR)

3211, 2901, 1749, 1701, 1622, 1501, 1352, 1289, 1247, 1091, 1032, 989, 652

HRMS (FTMS ES+)

$[\text{M}+\text{H}]^+$ Calculated for $\text{C}_{23}\text{H}_{38}\text{O}_5\text{Cl}$ 429.2402, found 429.2423

TLC

$R_f = 0.40$ 20% ethyl acetate in hexanes [silica gel, p-anisaldehyde stain]

One Pot Acetate Deprotection/Chloride Displacement Deprotection Protocol

To a flame dried, 1 dram vial mL containing stir bar was added compound **3.86** (10 mg , 0.026 mmol) in DMF (1 mL) and MeOH (0.1 mL). K_2CO_3 (25 mg, 0.18 mmol) and Sodium azide (30 mg, 0.46 mmol) was added in a single portion and the reaction was sealed then heated to 50°C and stirred overnight. The reaction was cooled to room temperature, then diluted with H_2O and extracted with diethyl ether (3x). The combined organic layers were dried over Na_2SO_4 , filtered, and concentrated under reduced pressure. The resulting residue was purified by silica gel column chromatography ($R_f = 0.50$, 20% ethyl acetate in hexanes) to give azide **3.77** (8.0 mg, 0.023 mmol, 79%).

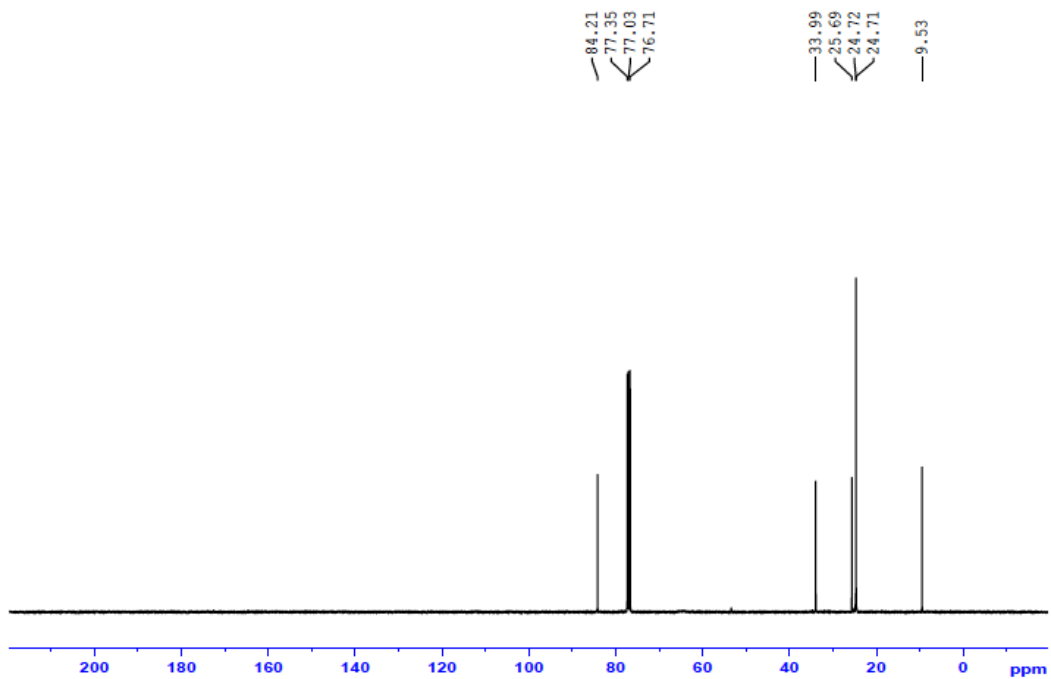
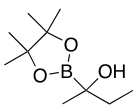
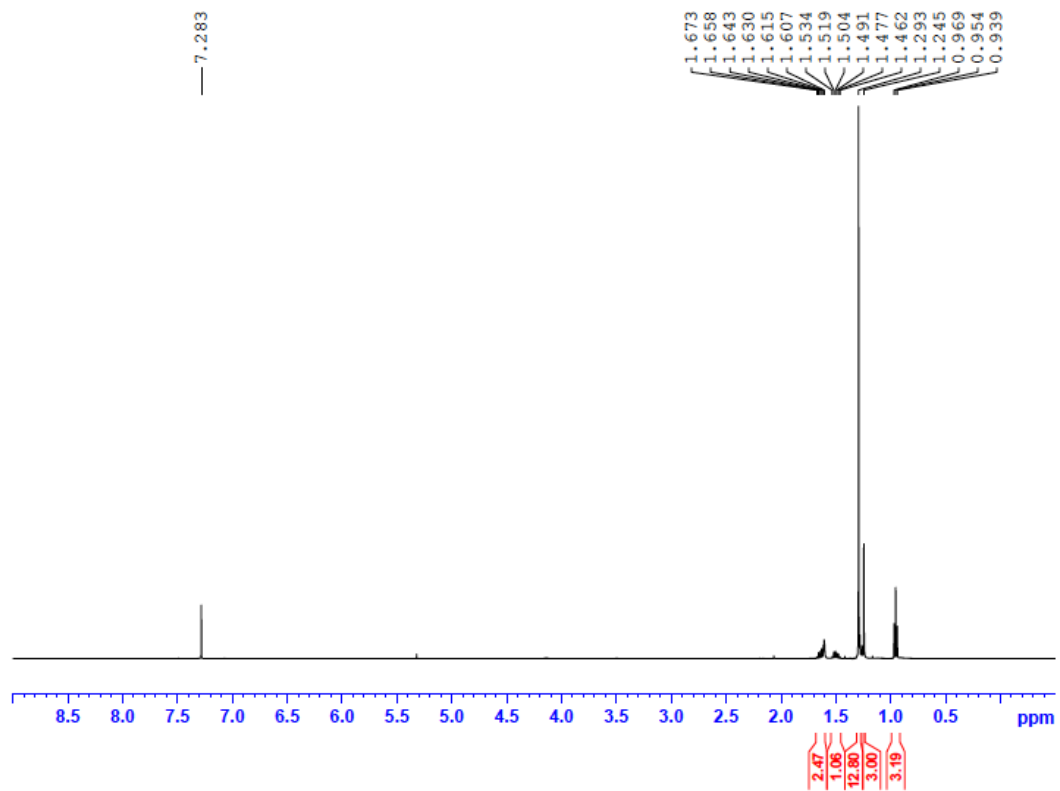
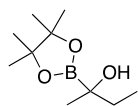
Cell culture. Experiments were performed using A549 (ATCC) cells cultured in Dulbecco's Modified Eagle Medium (DMEM; Gibco). All media was supplemented with 10% Fetal Bovine Serum (FBS; Sigma-Adrich) and 5% penicillin/streptomycin (VWR) and maintained at 37°C in a 5% CO_2 atmosphere. Cell line is tested for mycoplasma contamination every three months.

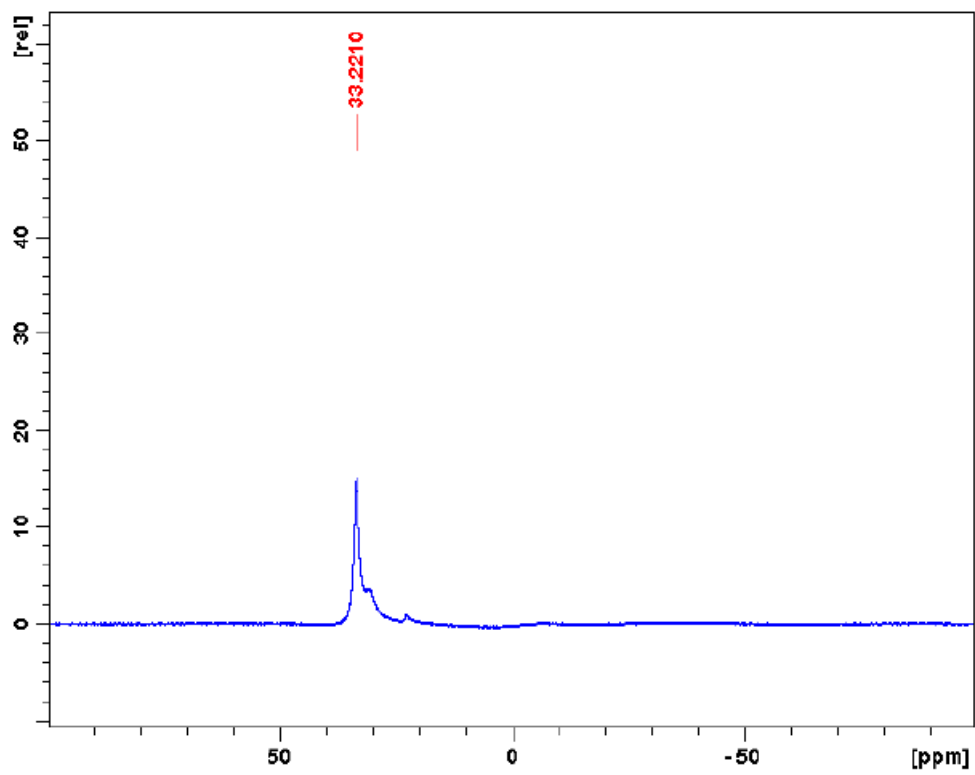
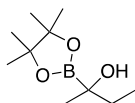
Cell viability assays. A549 cells were seeded at 500 cells per well in white, clear-bottom, 384-well plates (Greiner). After overnight incubation, cells were treated with increasing concentrations of compounds or a DMSO control (0.1% DMSO final concentration) in triplicate followed by incubation for an additional 48 h. After incubation, cell viability was measured using a luminescence-based kit (CellTiter-Glo, Promega) according to manufacturers protocol. Luminescence was measured using a Tecan M1000 plate reader. To determine growth inhibition, cell viability assays were performed at the time of initial treatment (T_0) and after 48 h incubation (T_{48}). Data was normalized to DMSO control (C) and growth inhibition (GI) was calculated using the equation $GI = (T_{48} - T_0)/(C - T_0)$. Data was fit to a sigmoidal plot using GraphPad Prism in order to determine GI_{50} values. Errors bars represent standard deviations from three independent experiments.

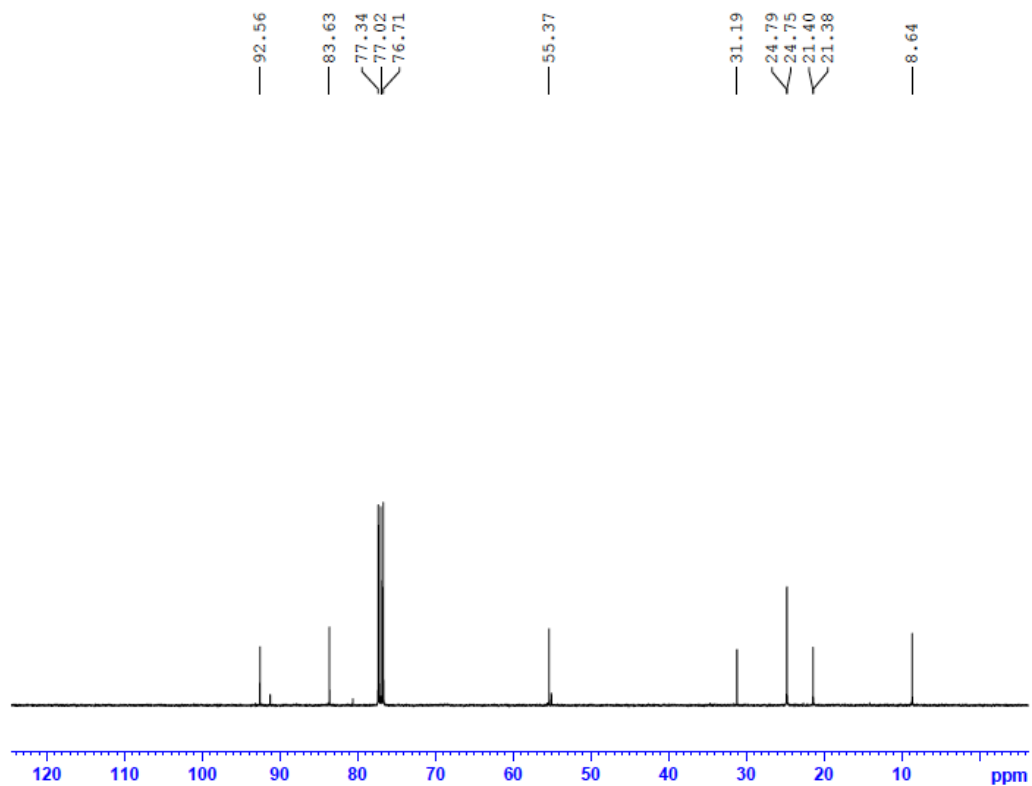
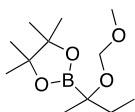
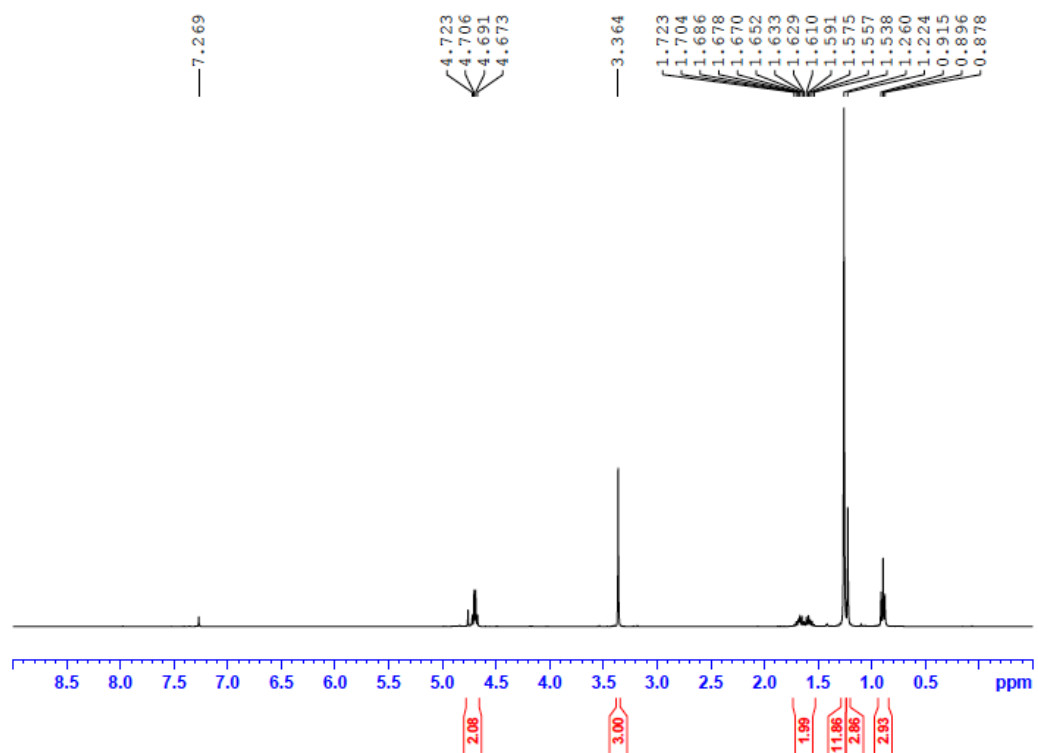
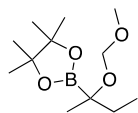
Fluorescent visualization of actin in cells. A549 cells were seeded at 10,000 cells per well in black, clear-bottom, 96-well plates (Greiner). After overnight incubation, cells were treated with either DMSO control (0.1% DMSO) or 400 nM compound for 2 h. Following incubation, media was removed and cells were fixed with 5% formaldehyde in PBS buffer for 10 minutes at room temperature and permeabilized with 0.1% Triton X-100 in PBS buffer at room temperature for 20 minutes. After thorough washing with PBS buffer, cells were co-stained with Rhodamine Phalloidin (Invitrogen) and Hoechst 33342 (Sigma Aldrich) stains according to manufacturers protocols and visualized on an Axio Observer Z1 microscope (Zeiss).

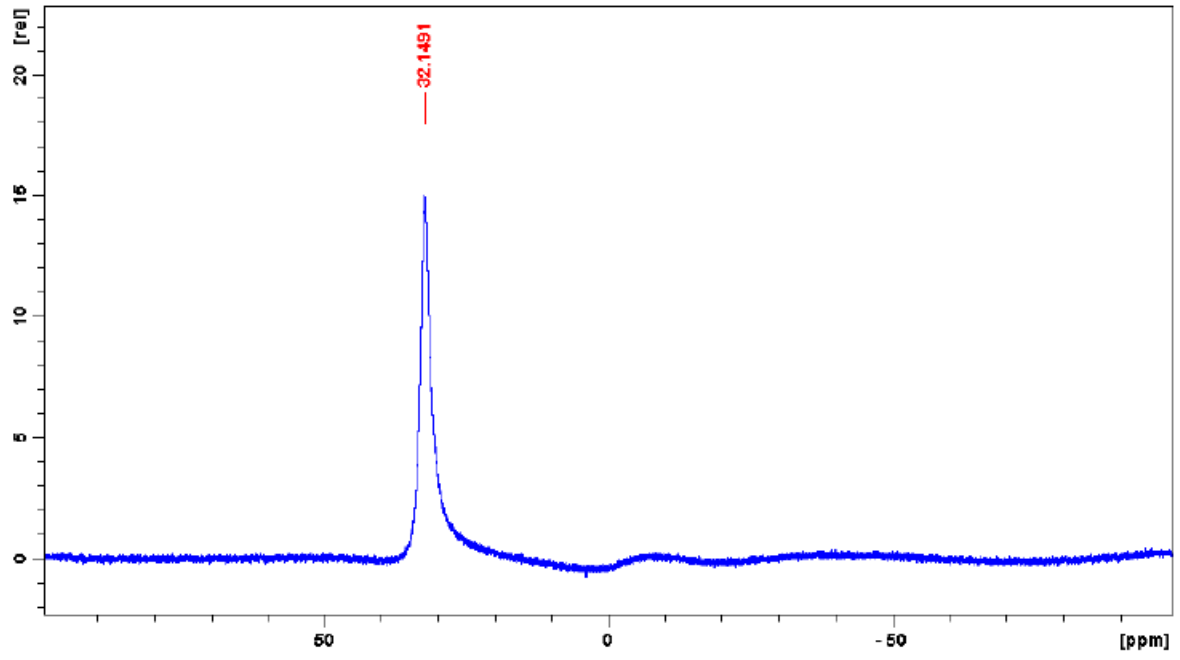
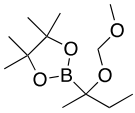
APPENDIX C

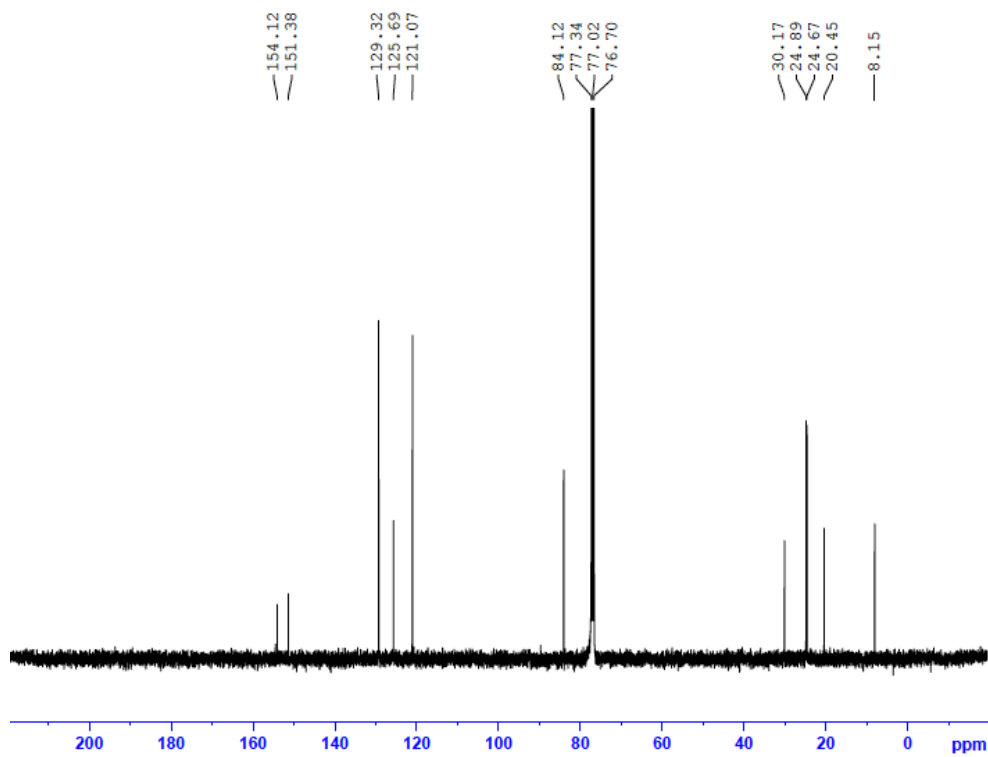
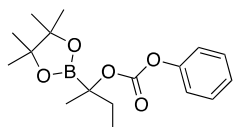
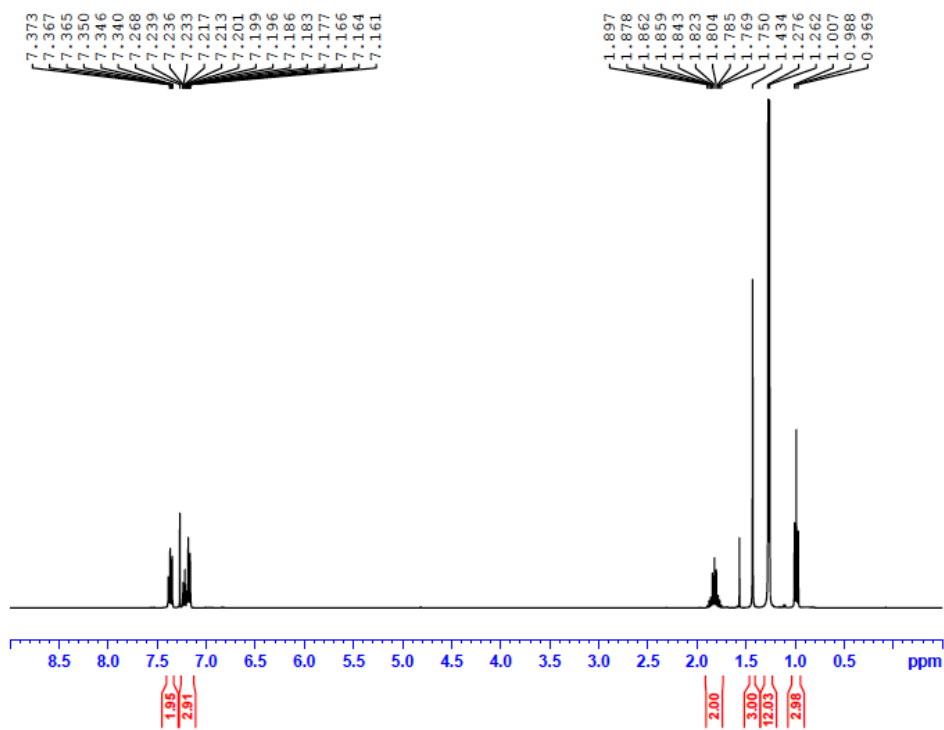
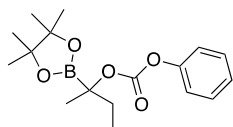
^1H , ^{13}C , and ^{11}B NMR Spectra for 2.1

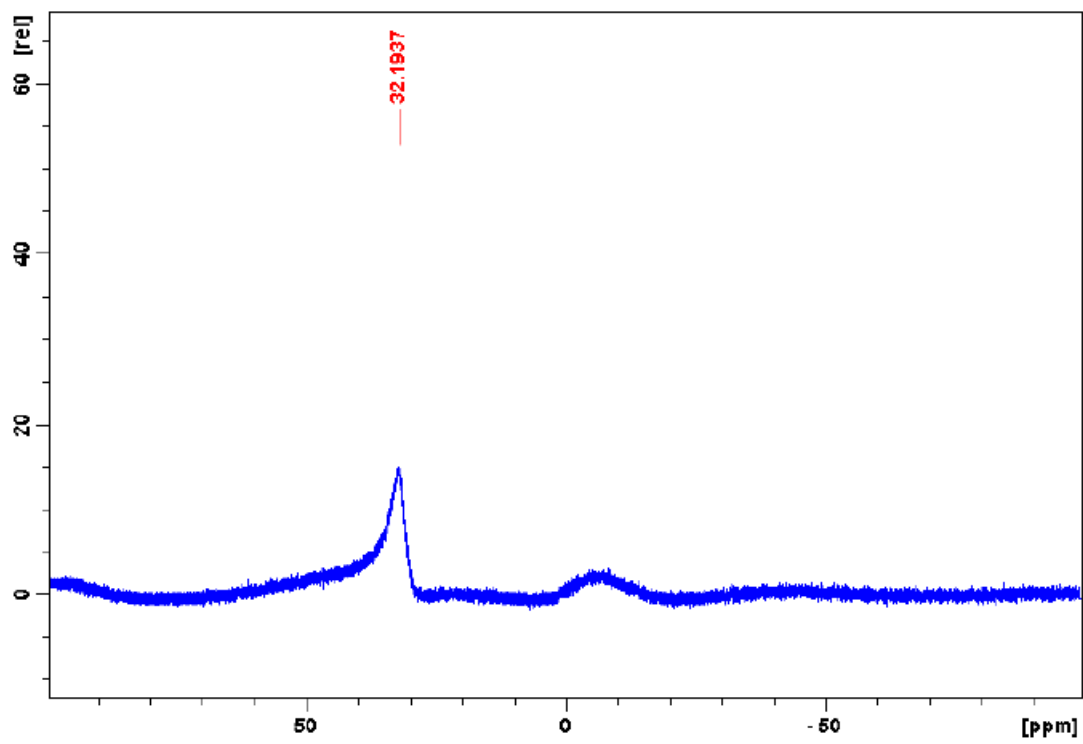
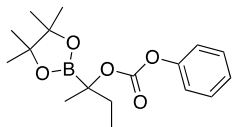


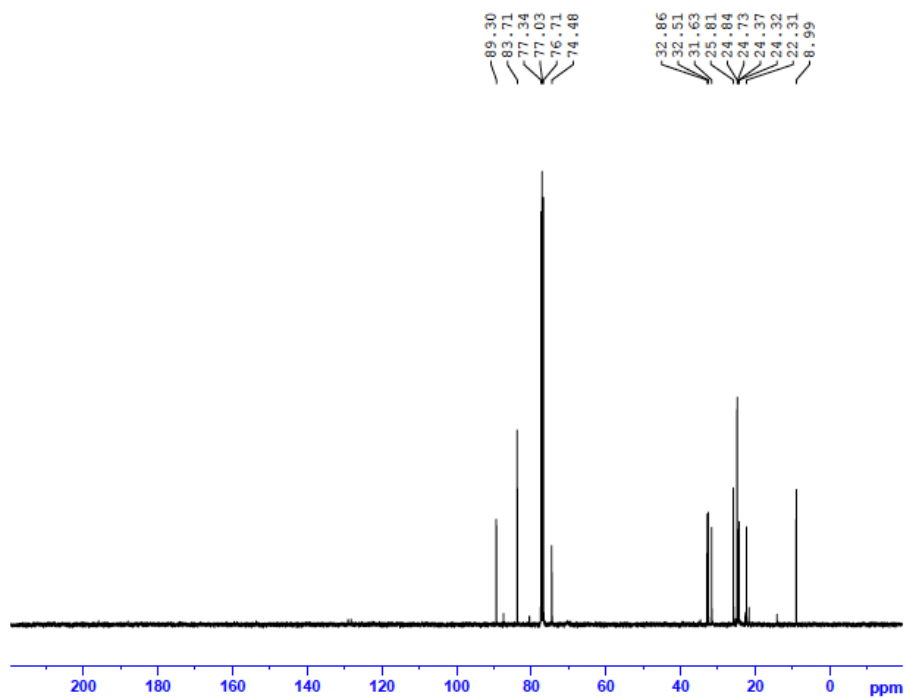
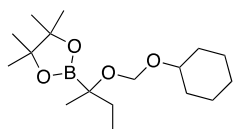
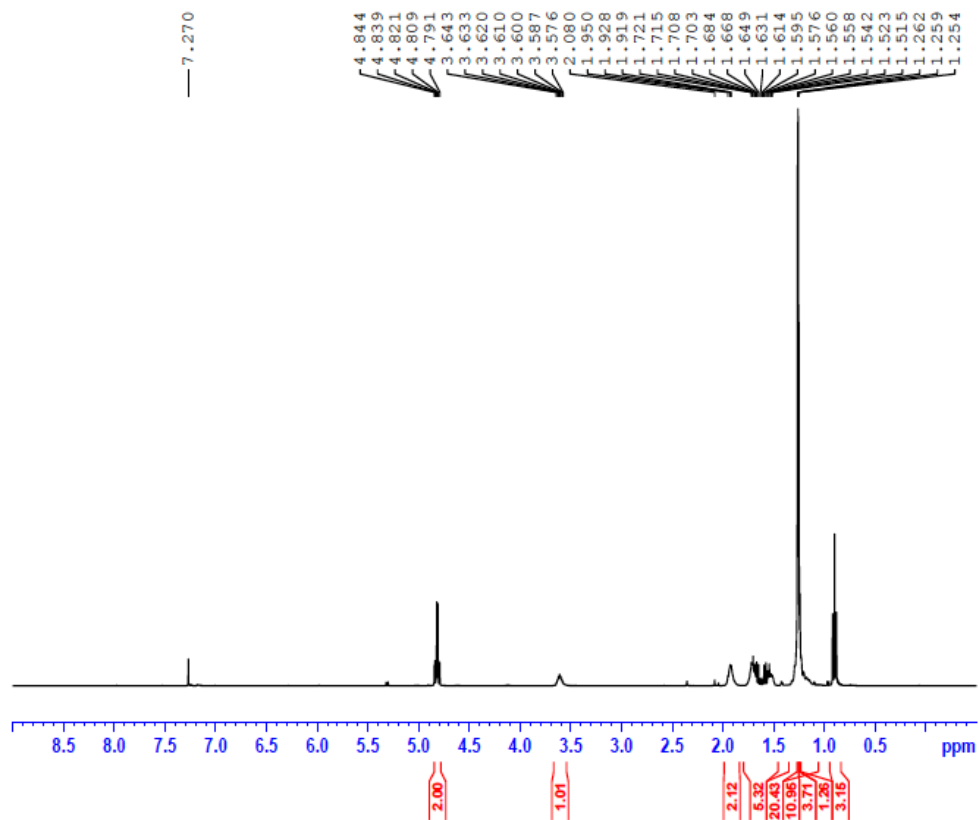
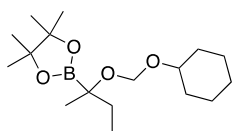


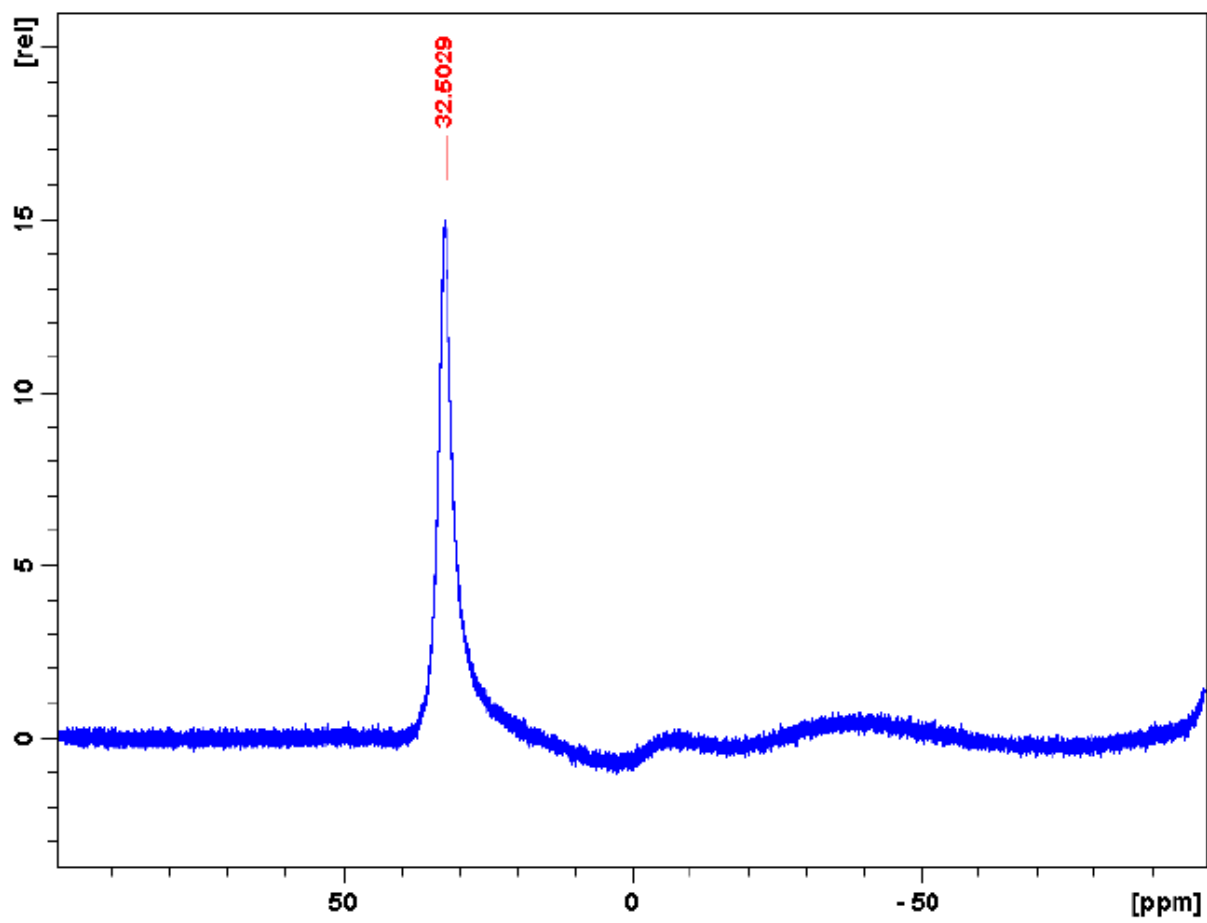
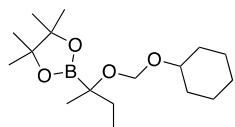


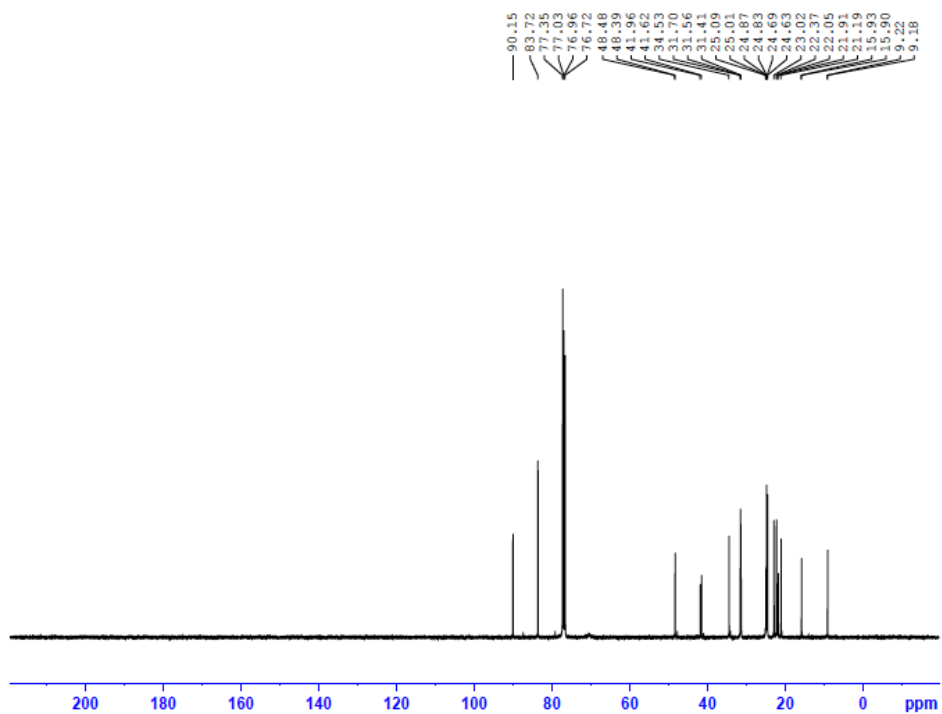
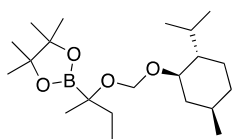
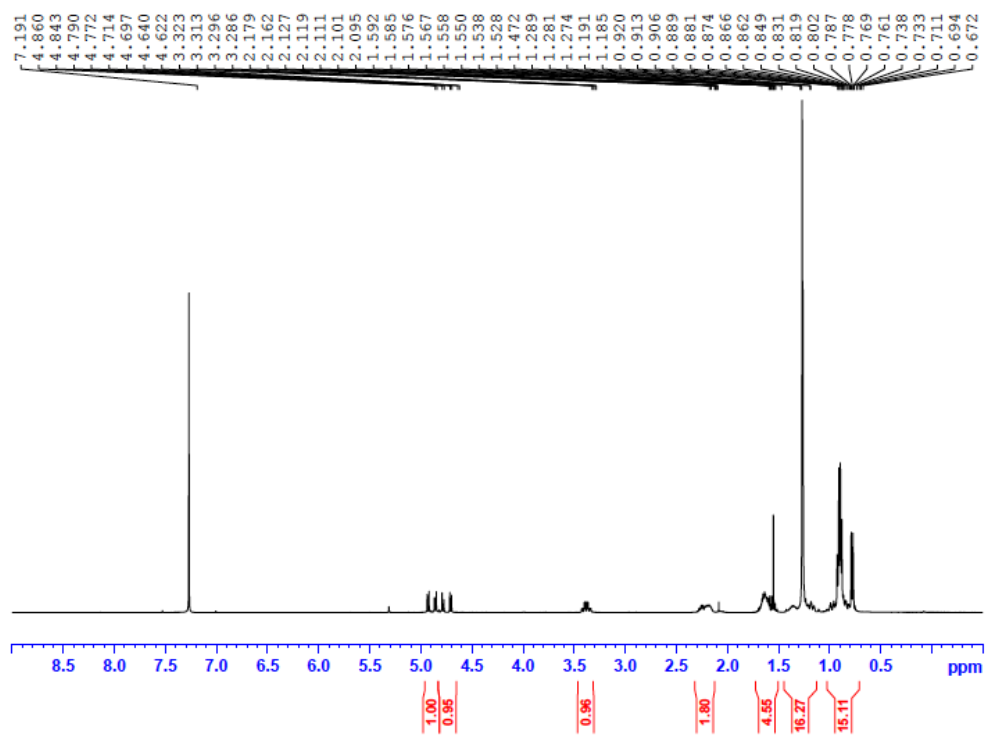
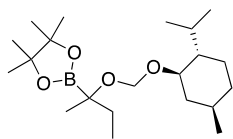


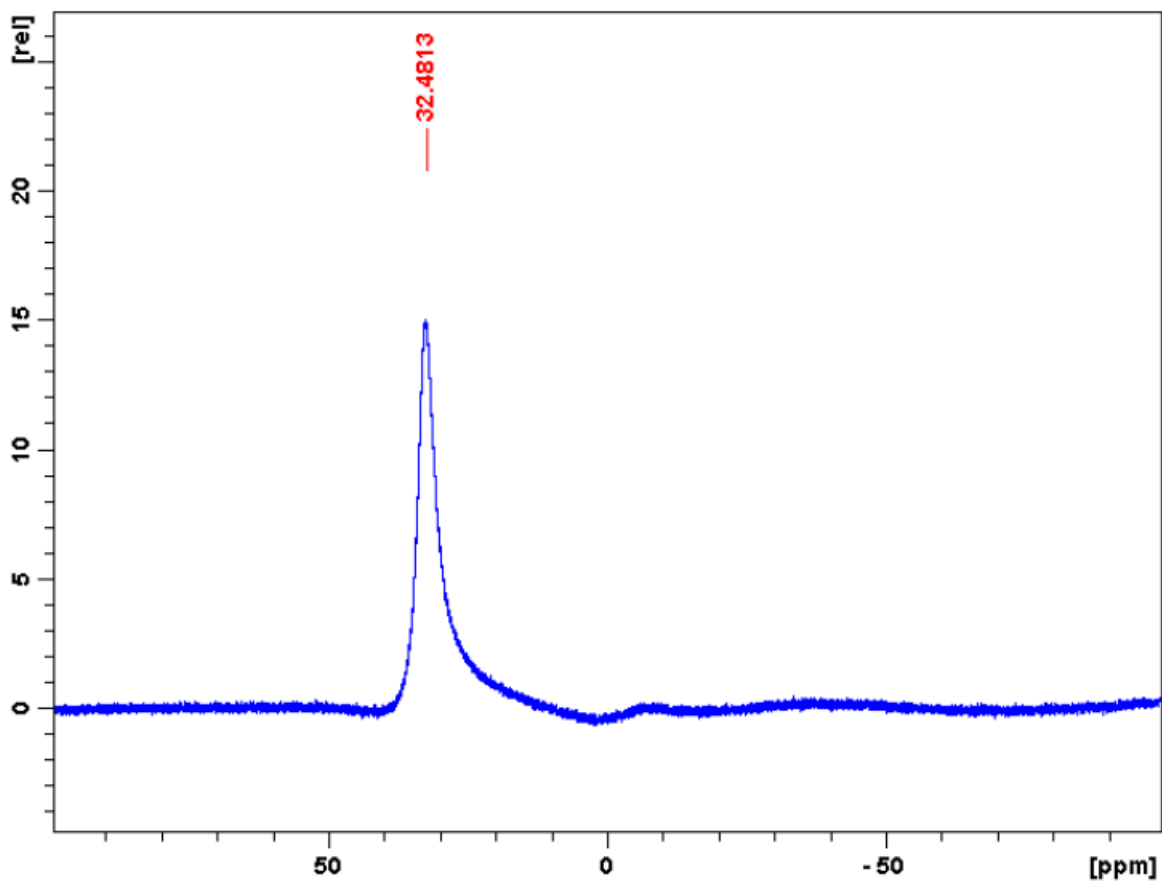
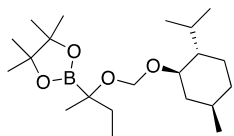


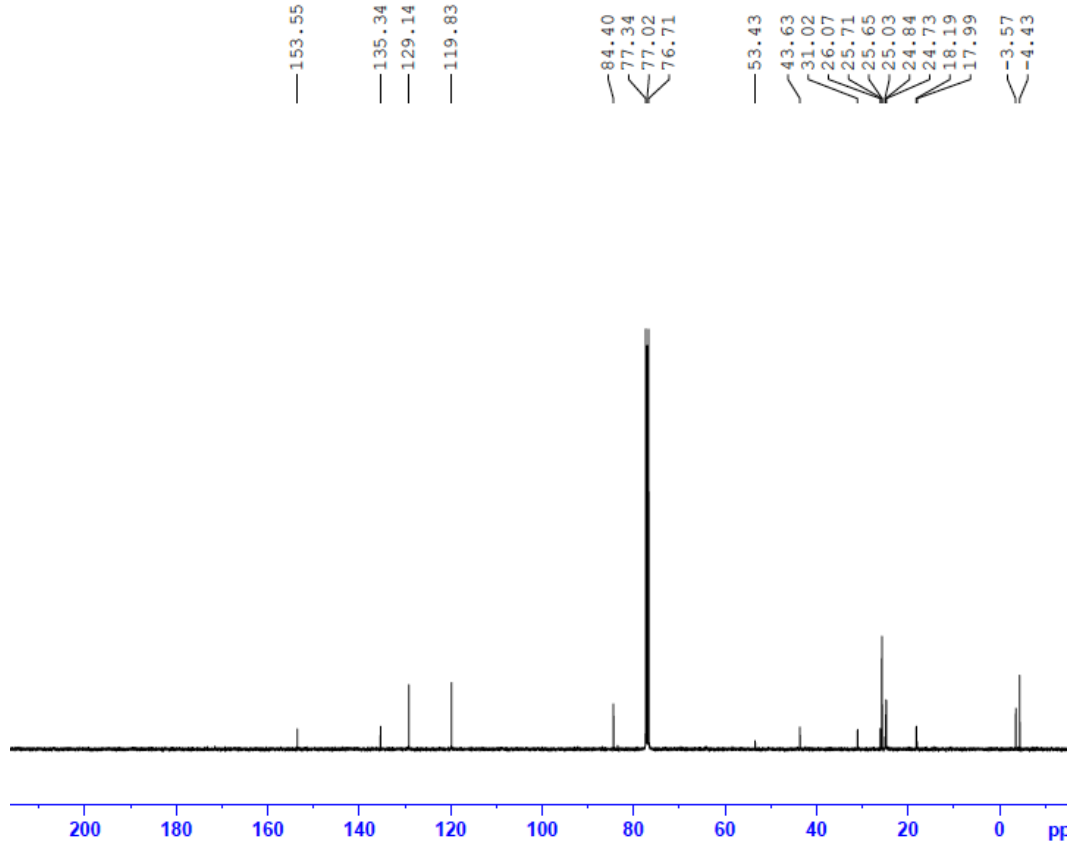
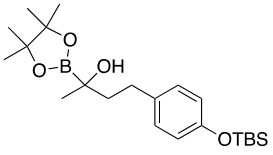
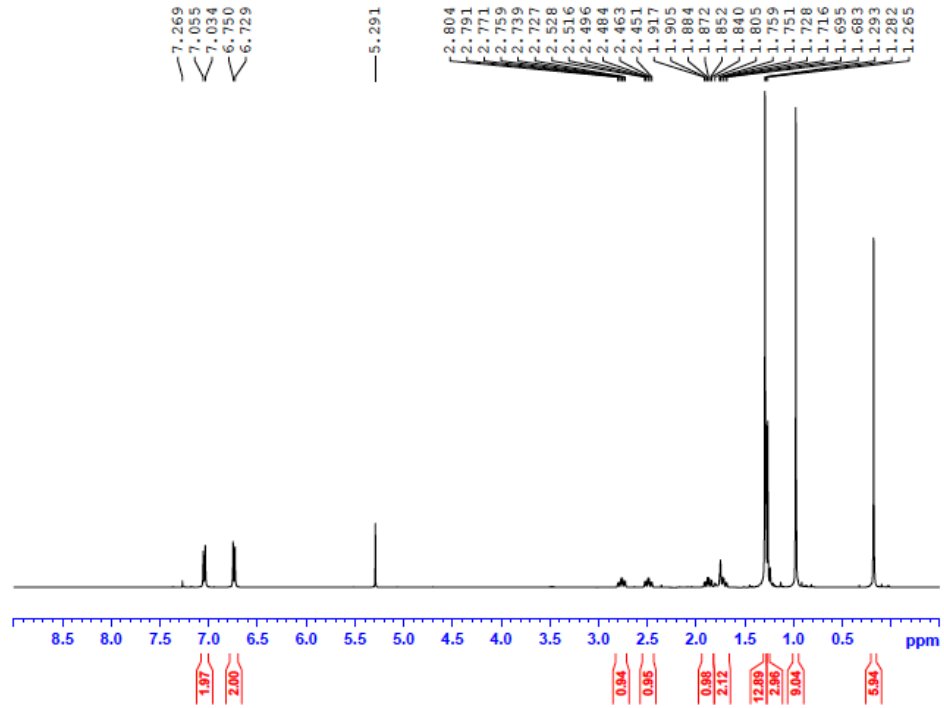
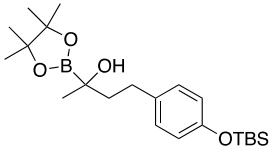


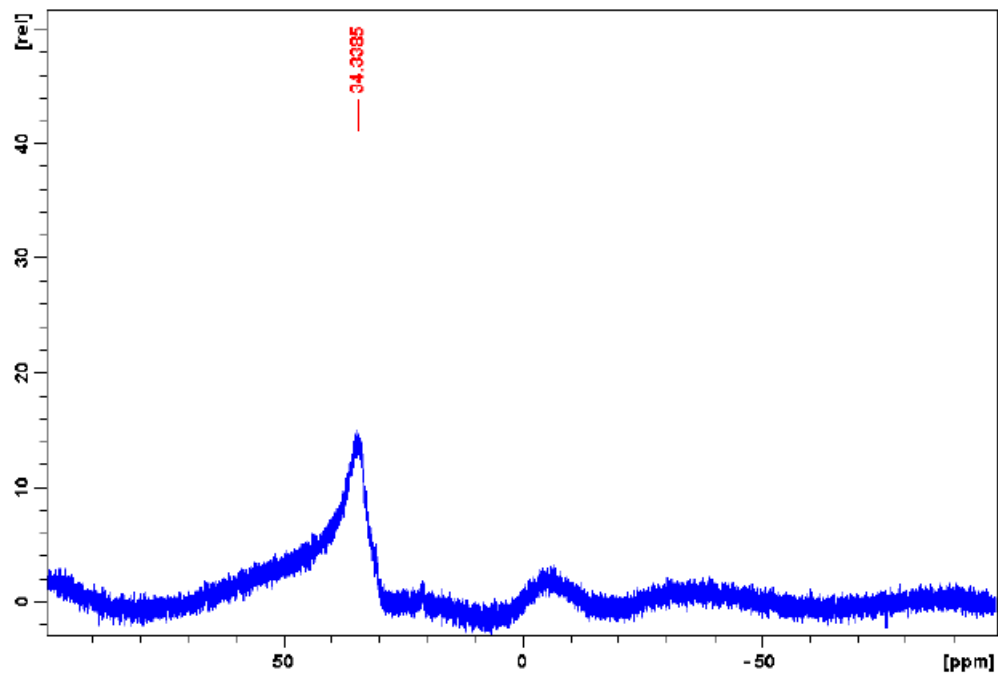
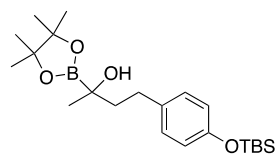


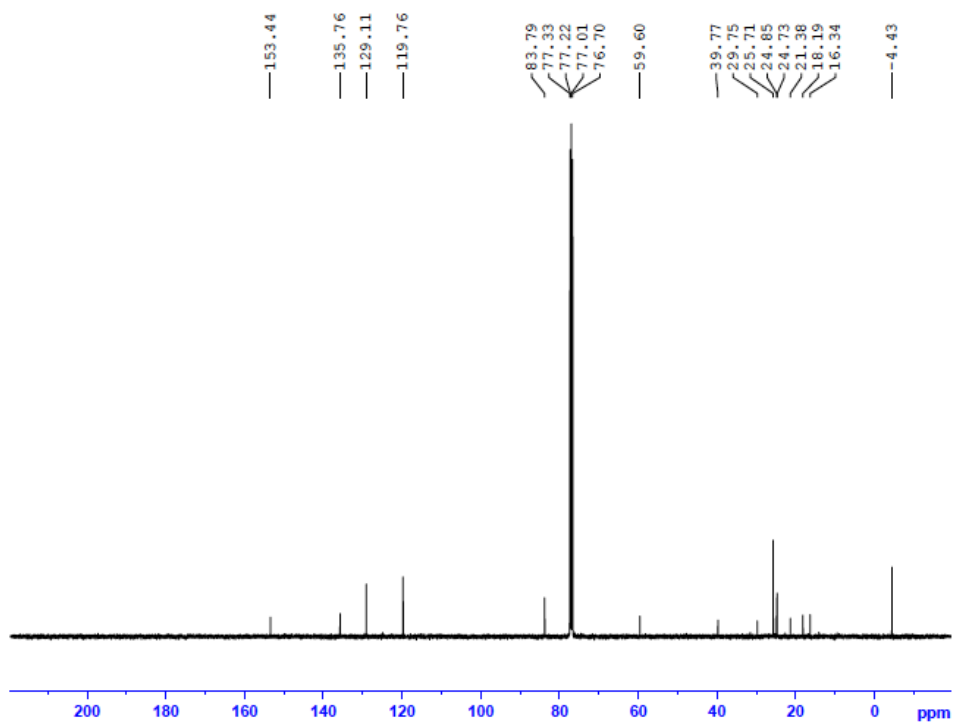
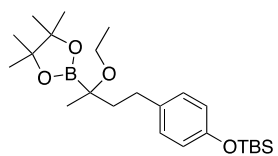
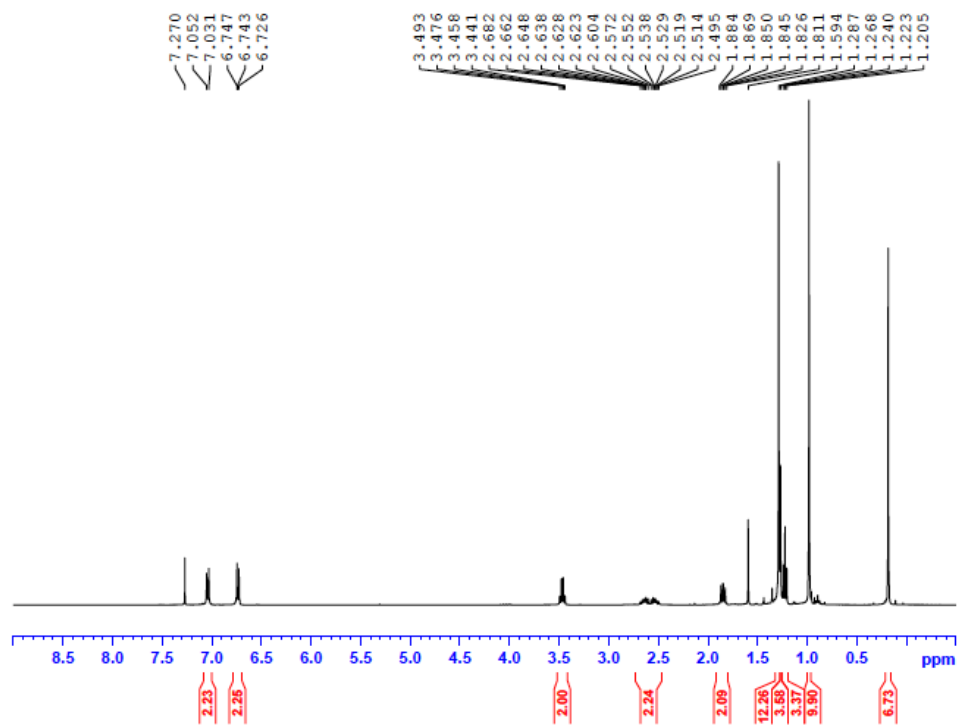
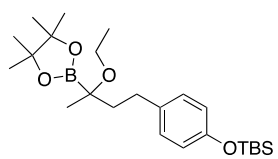


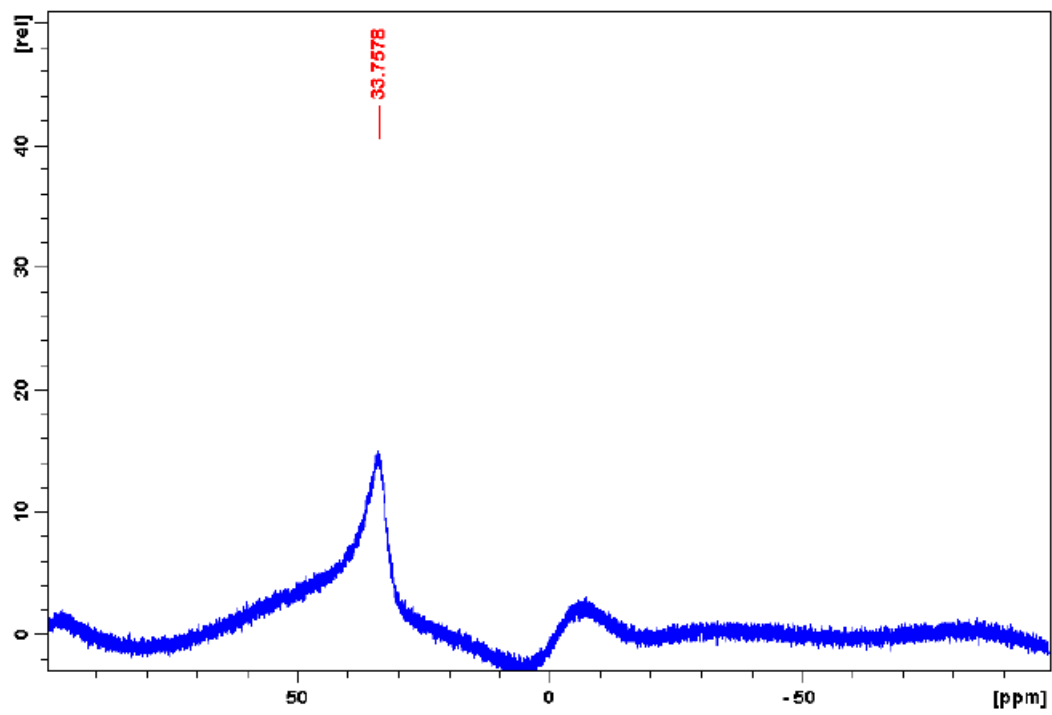
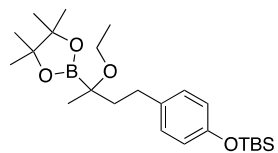


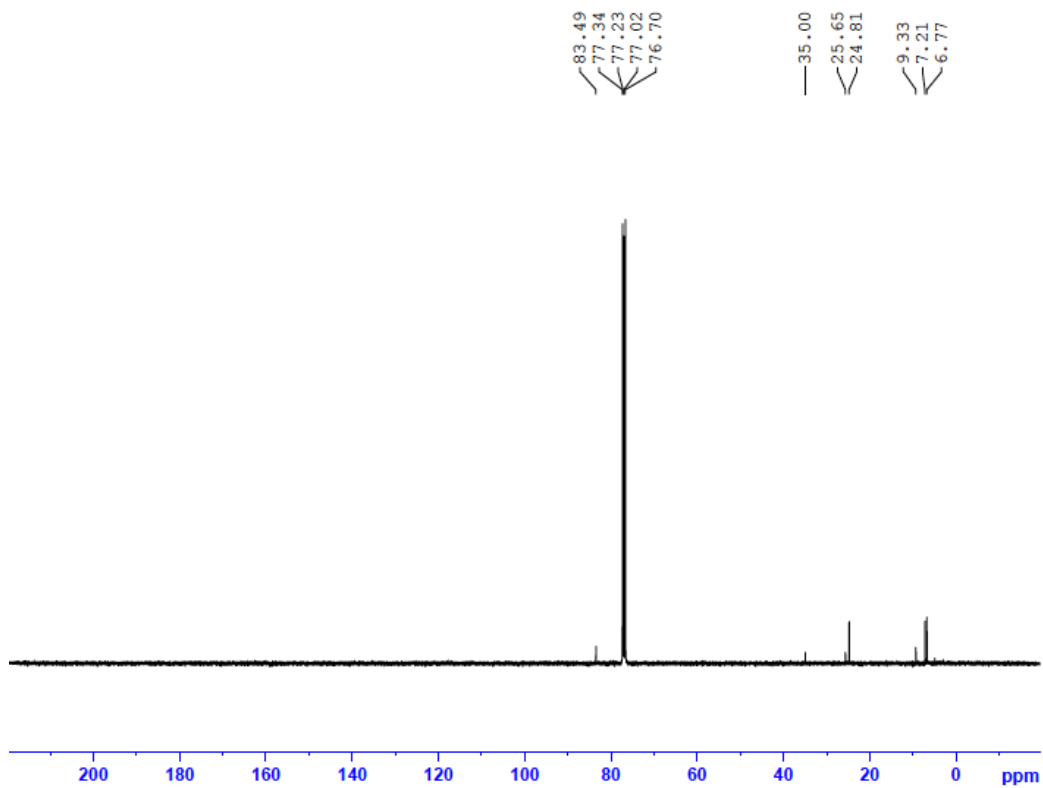
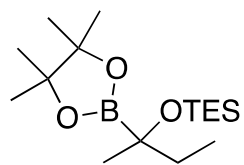
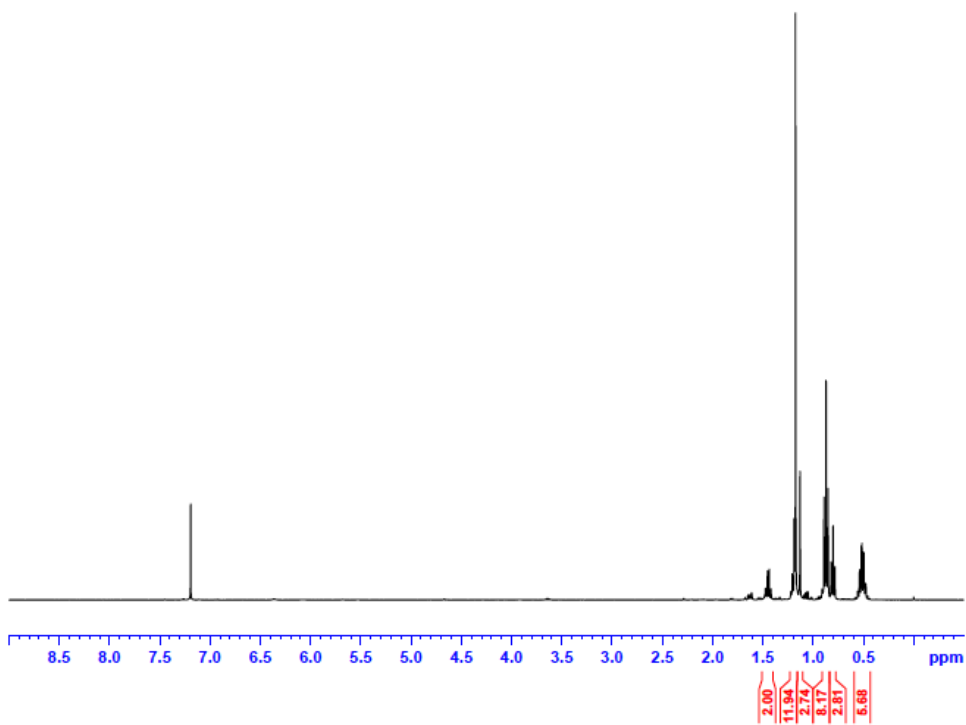
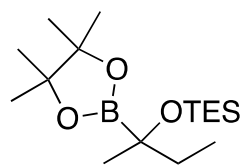


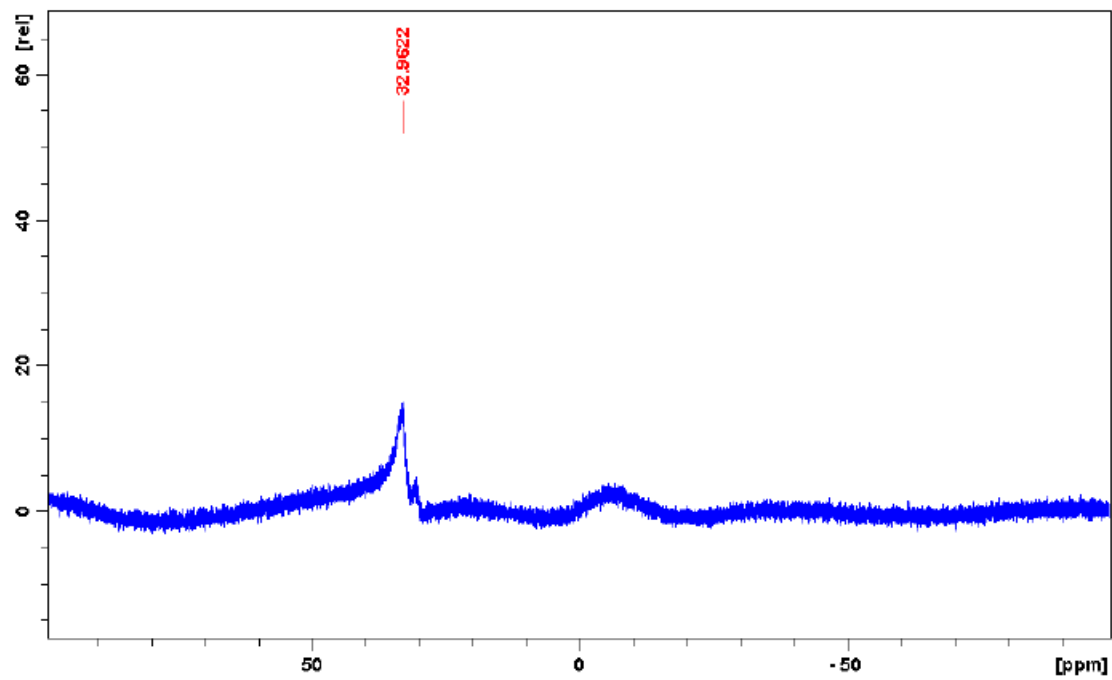
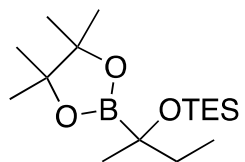


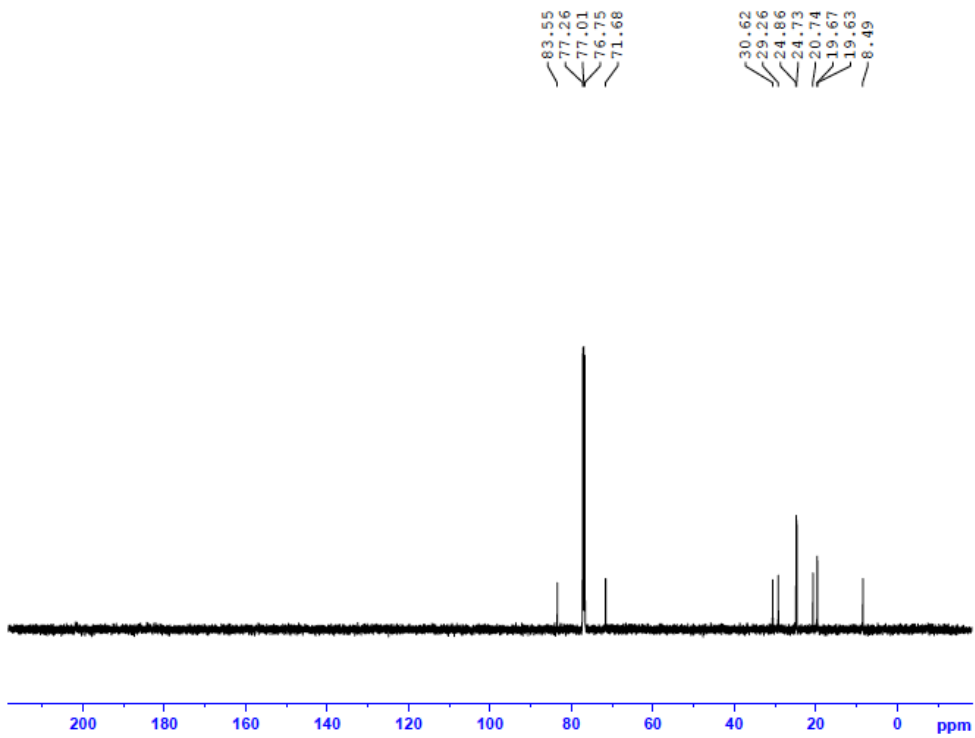
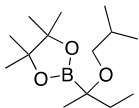
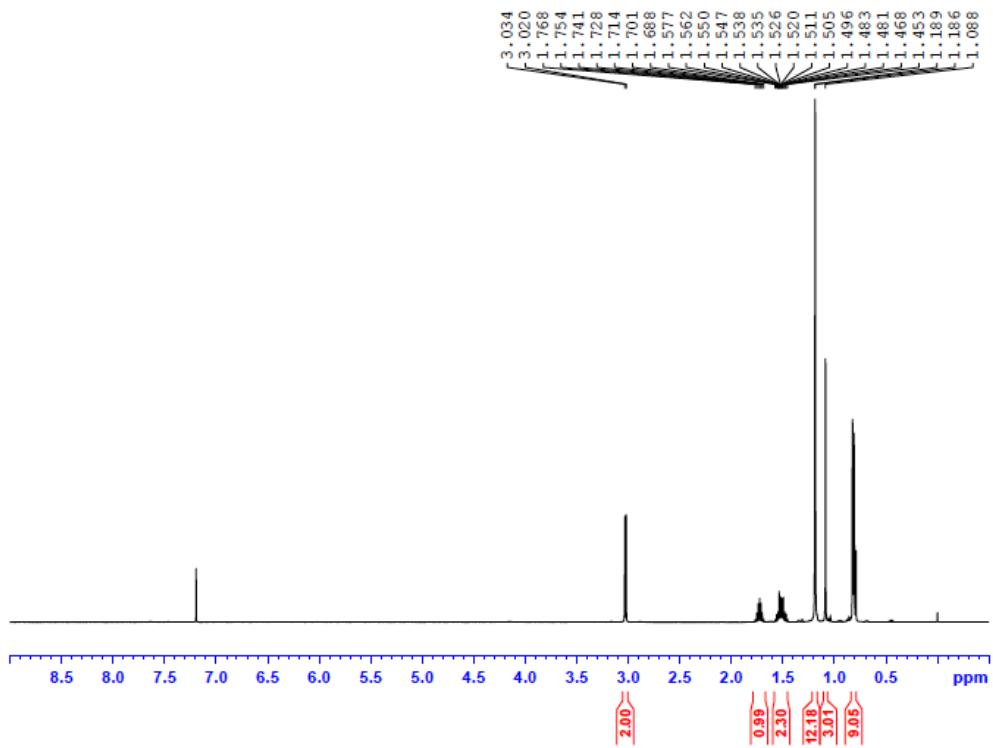
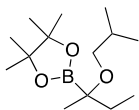


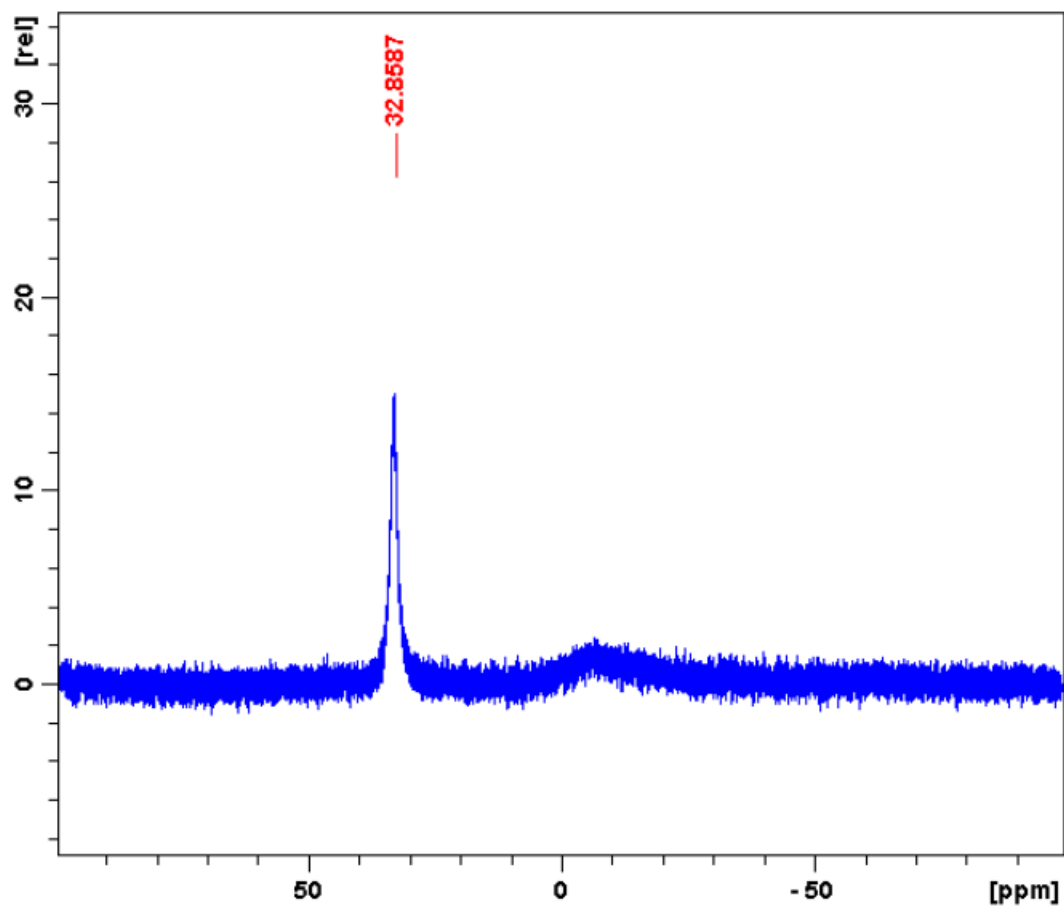
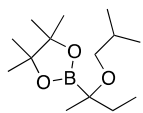


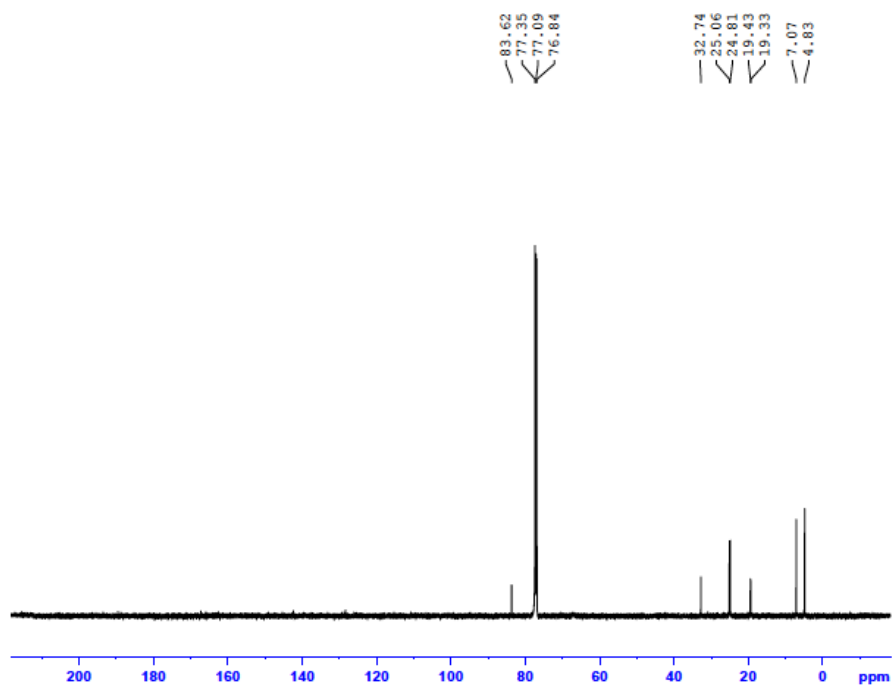
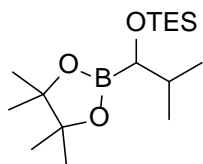
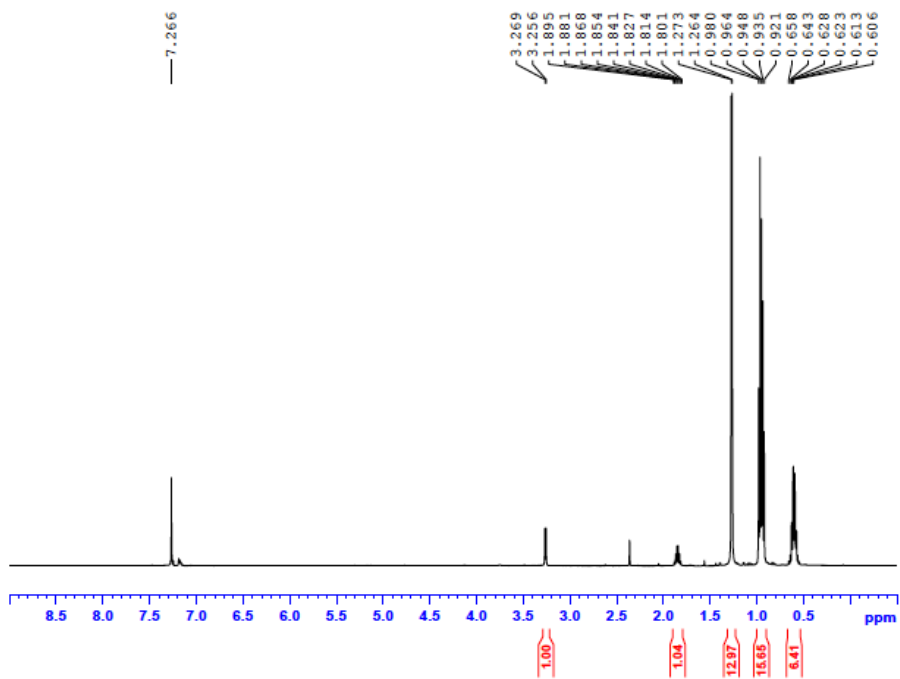
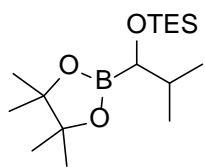


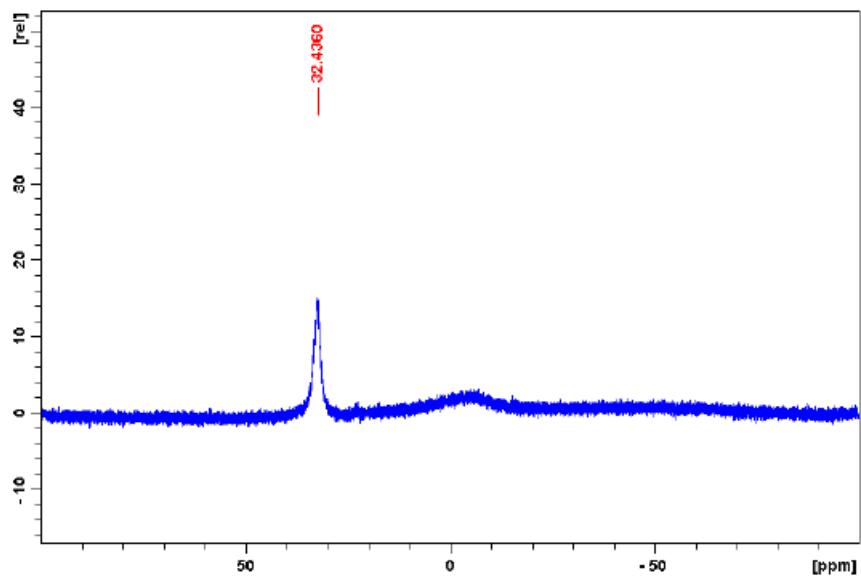
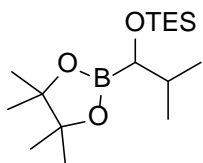


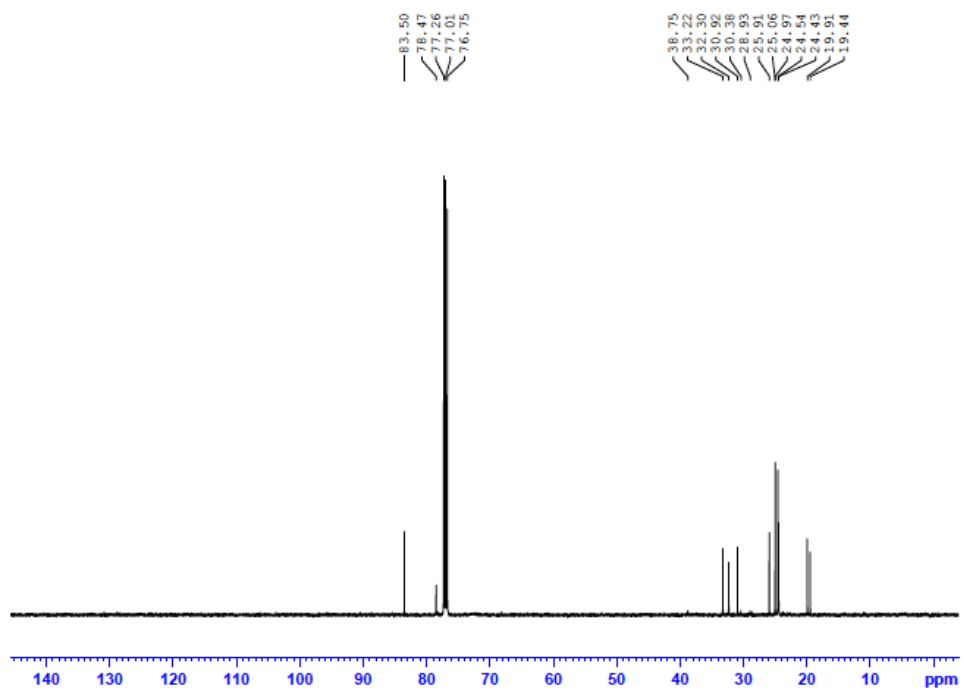
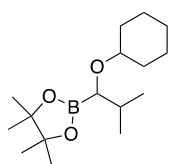
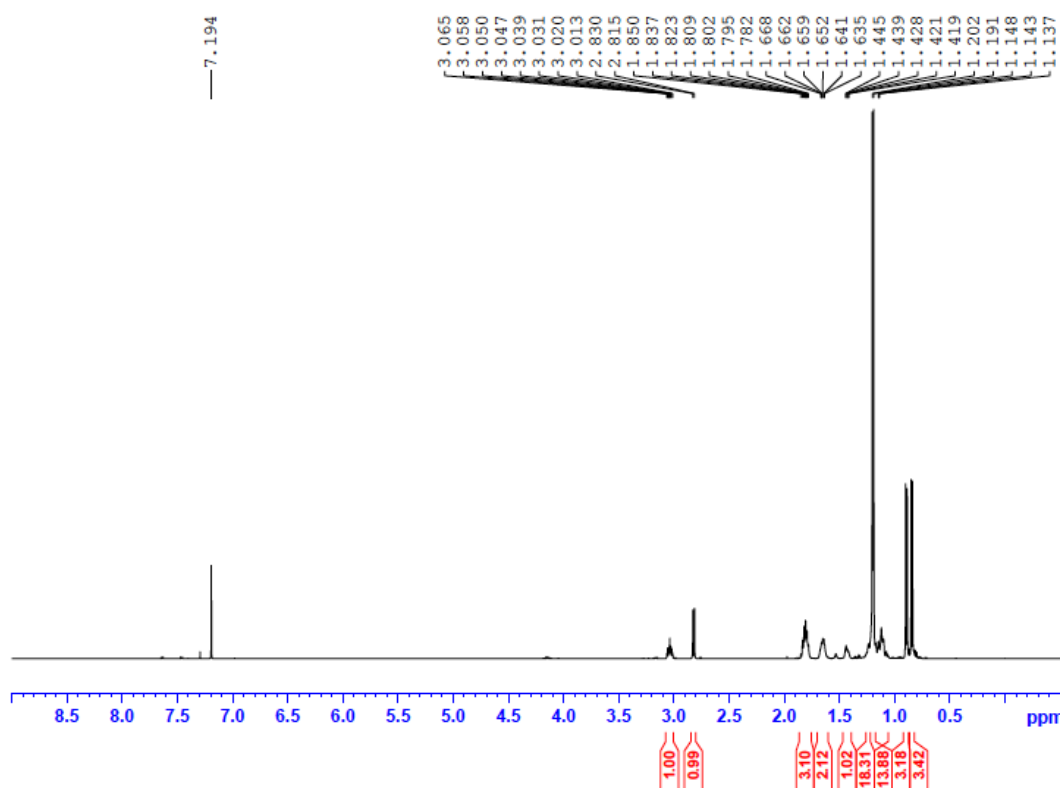
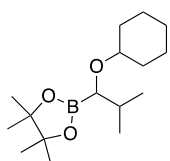


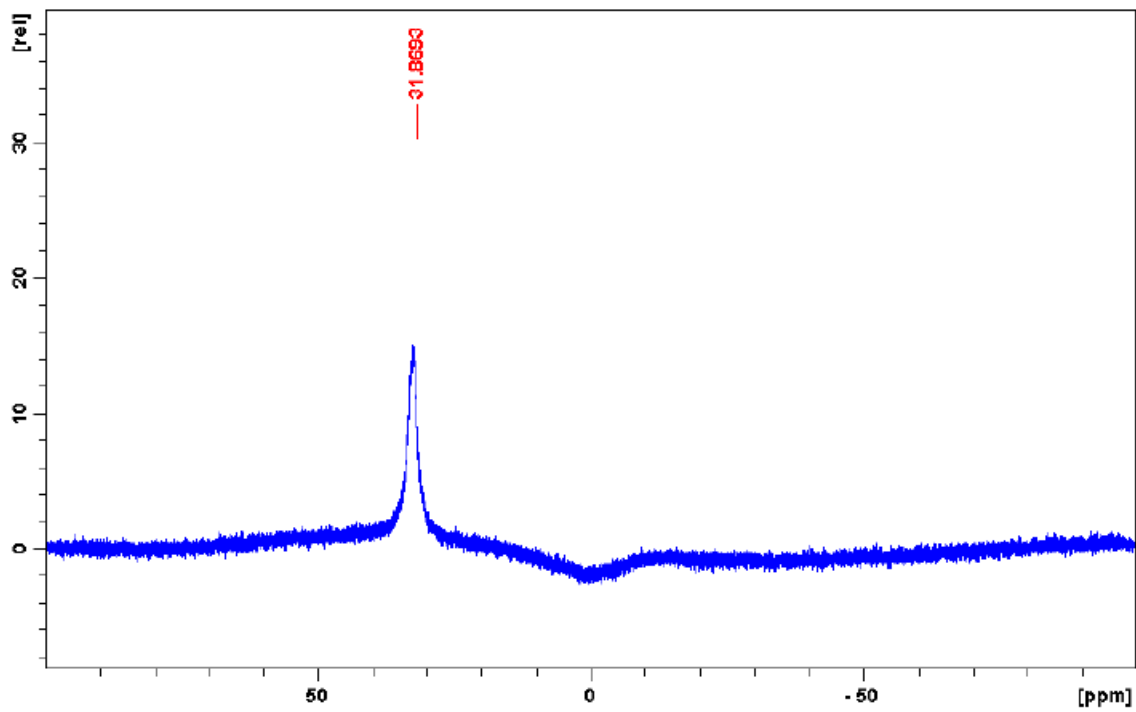
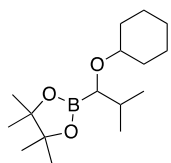


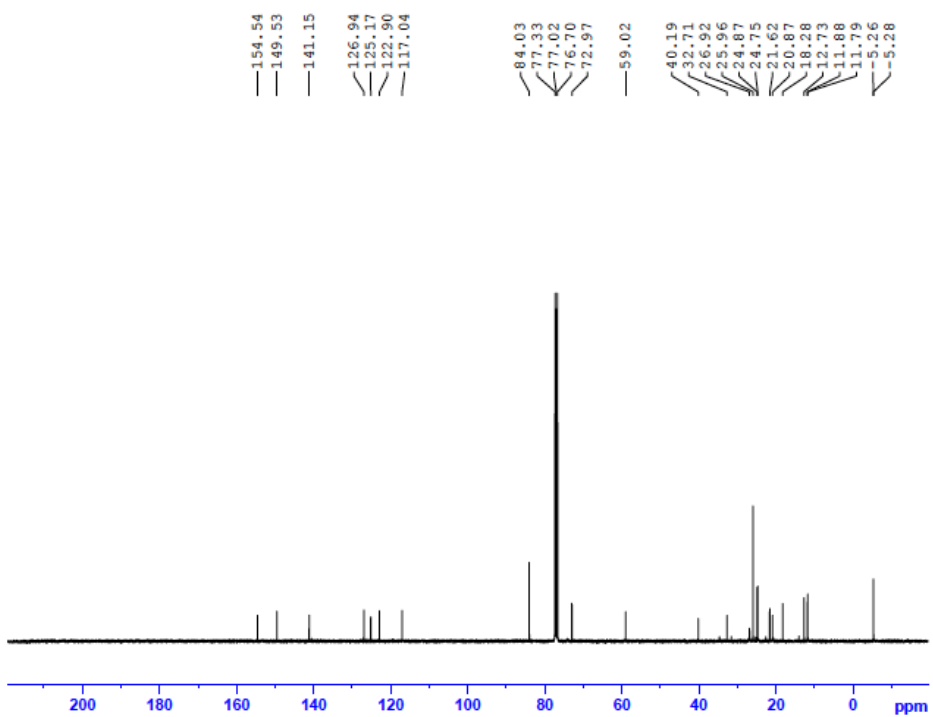
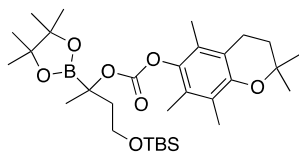
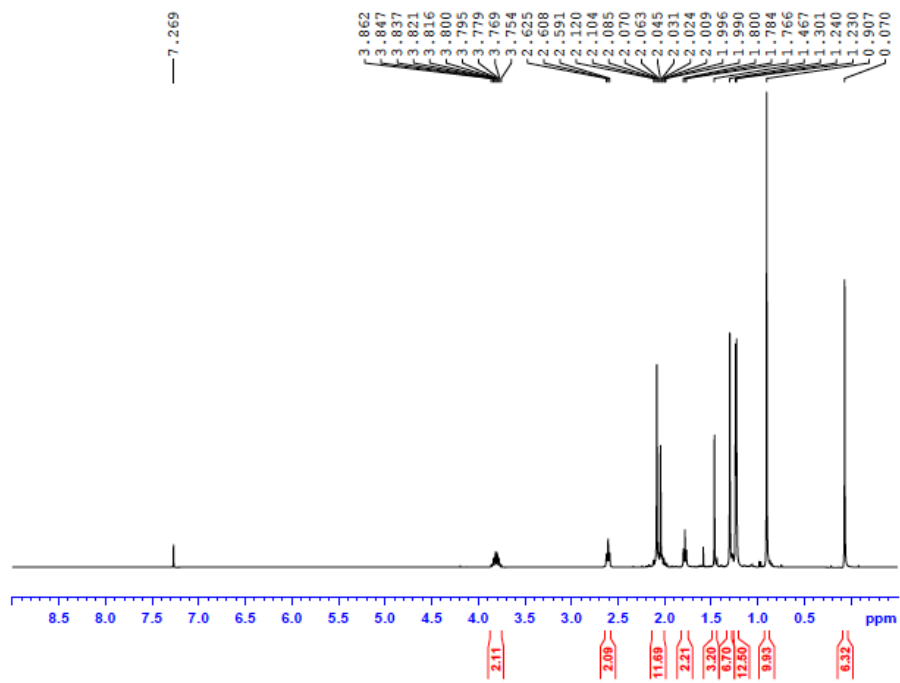
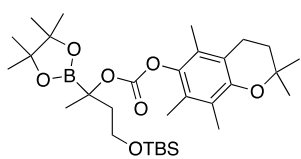


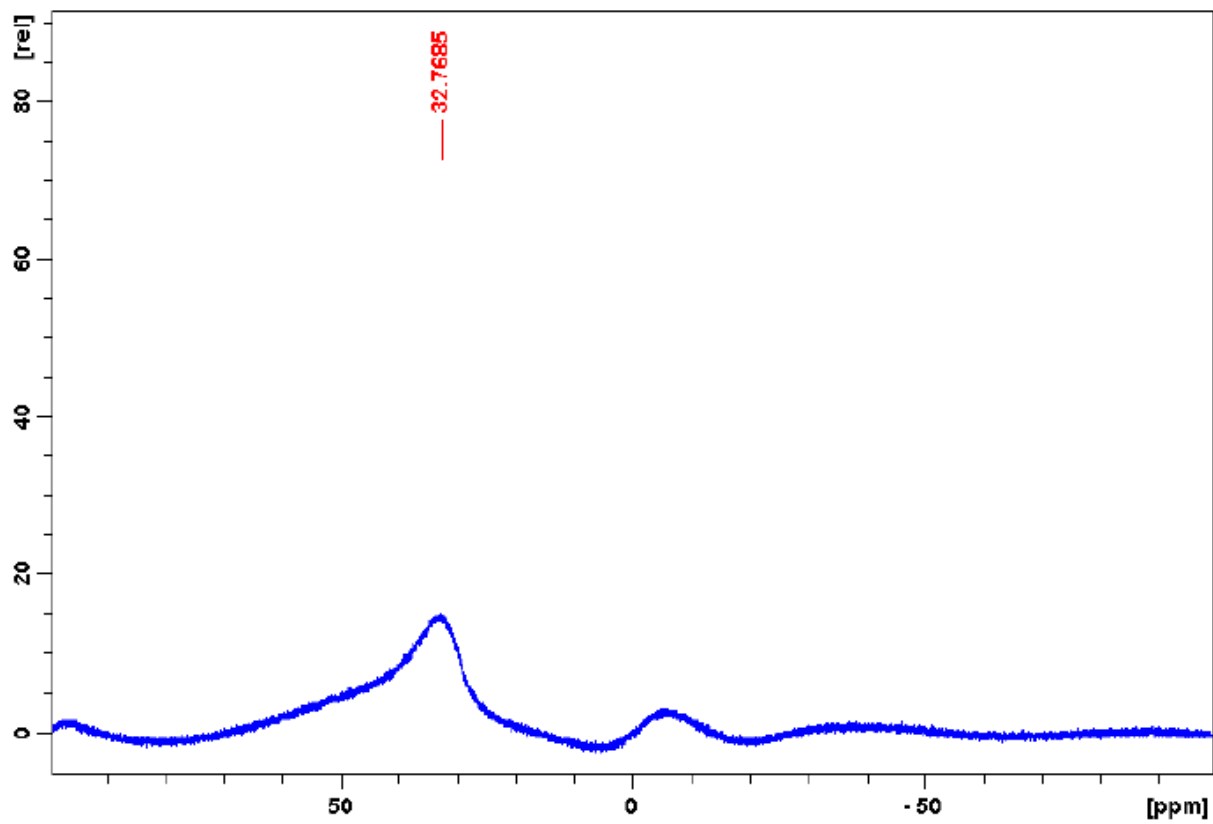
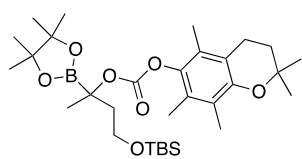


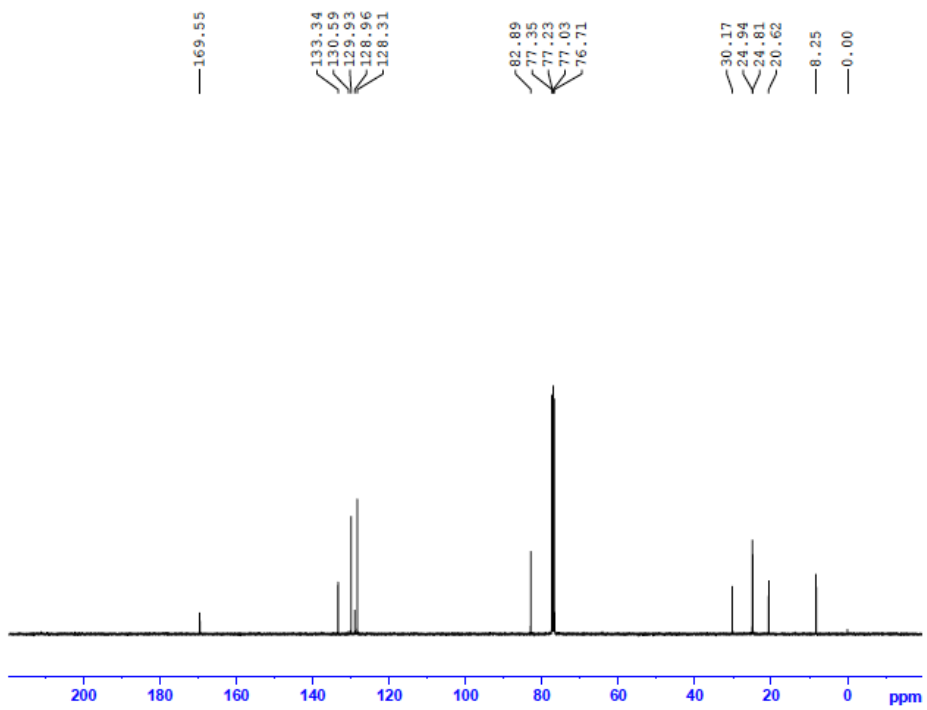
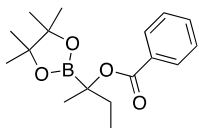
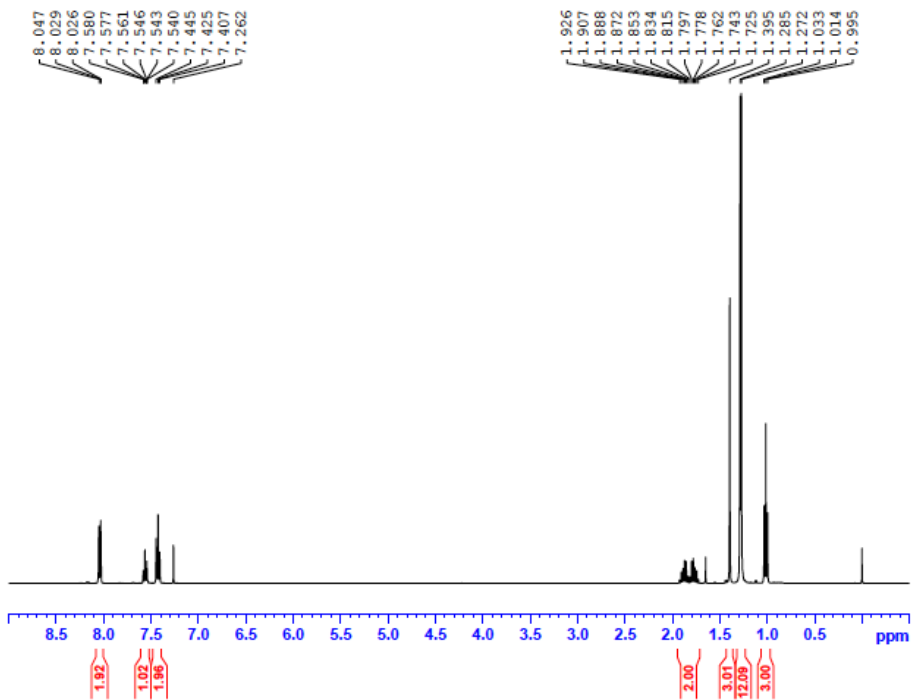
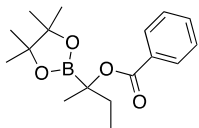


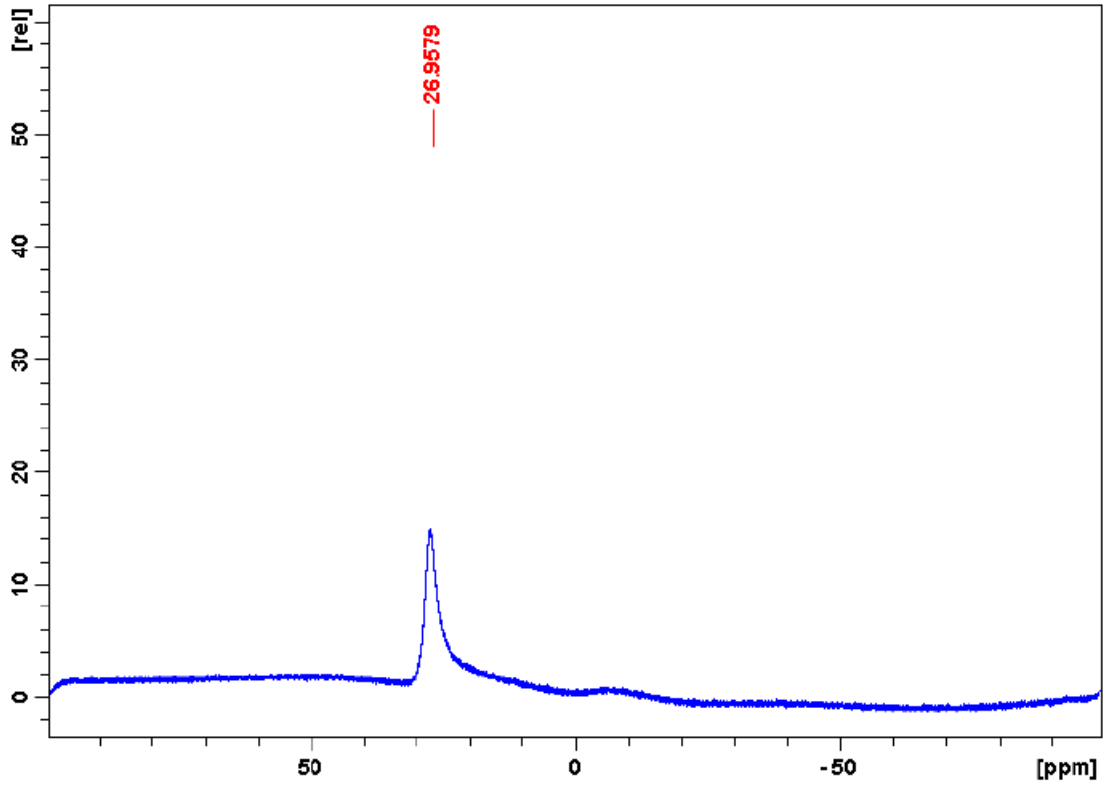
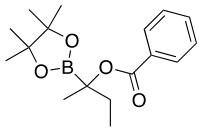


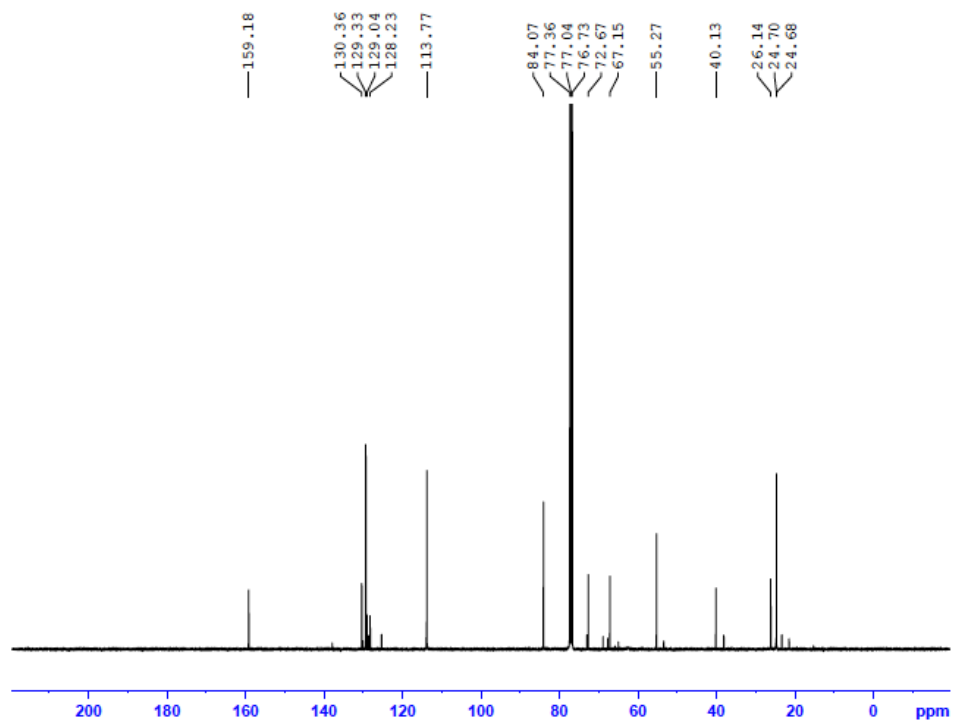
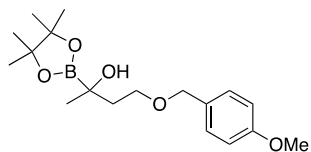
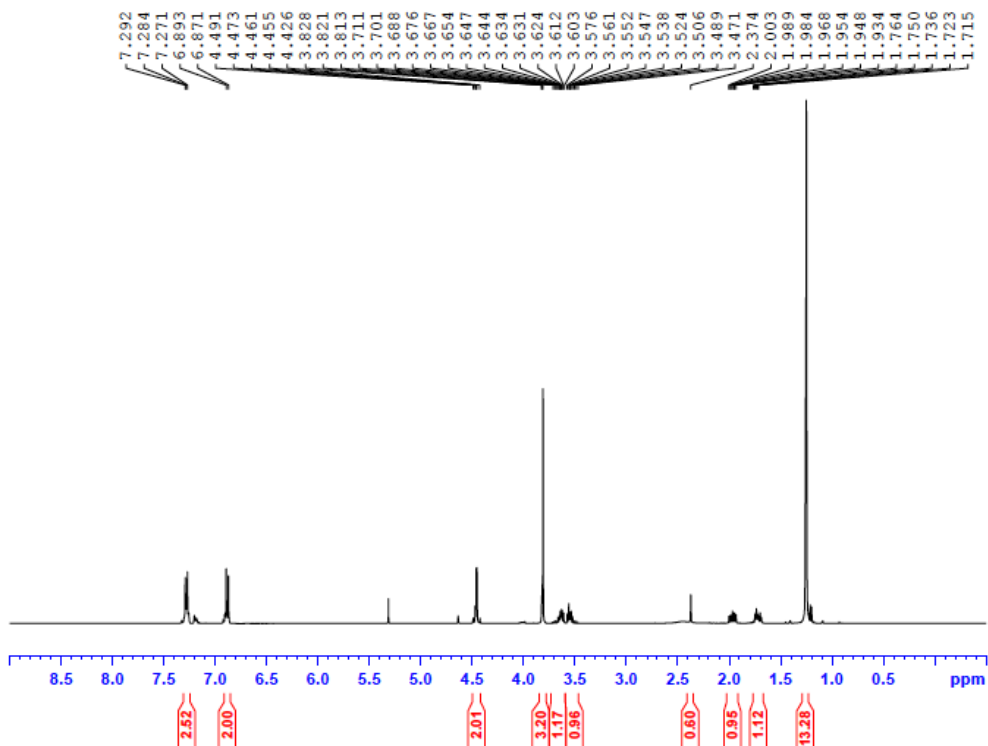
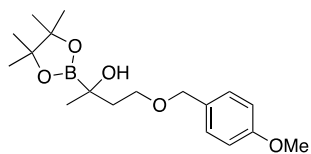


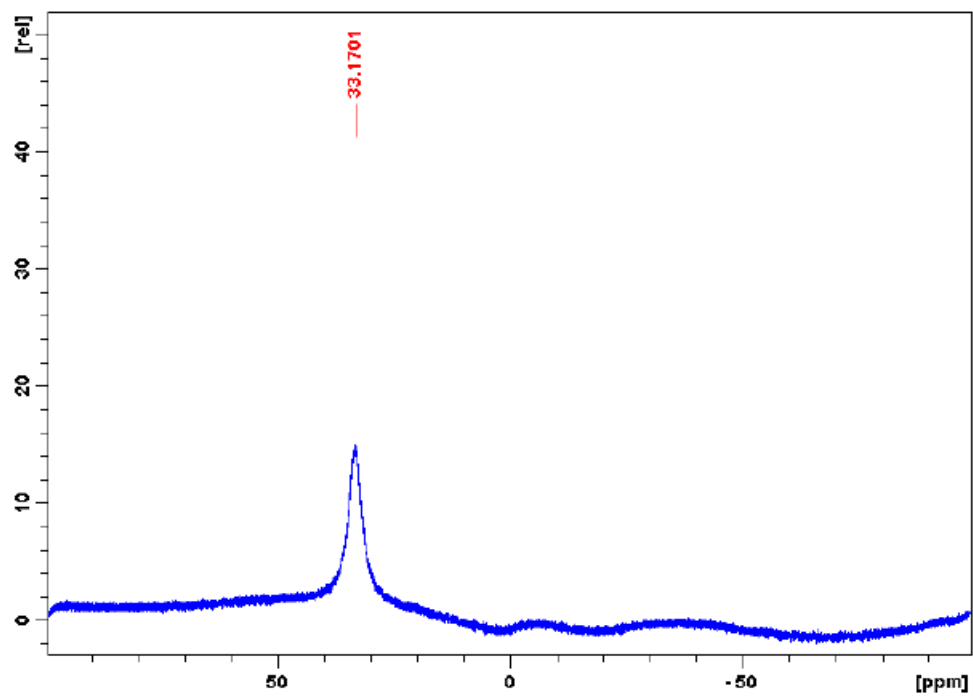
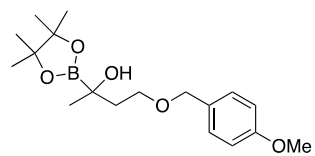


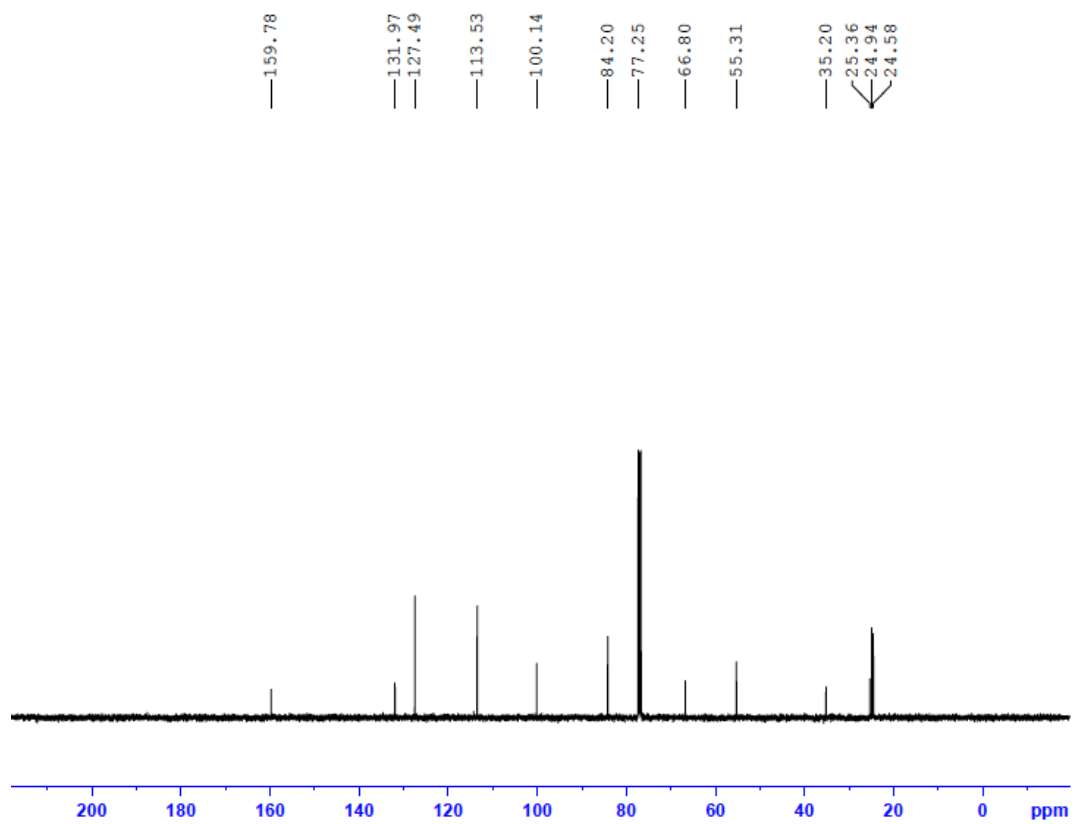
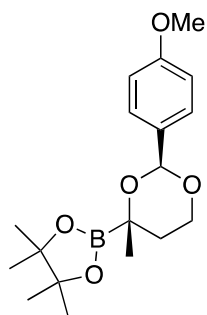
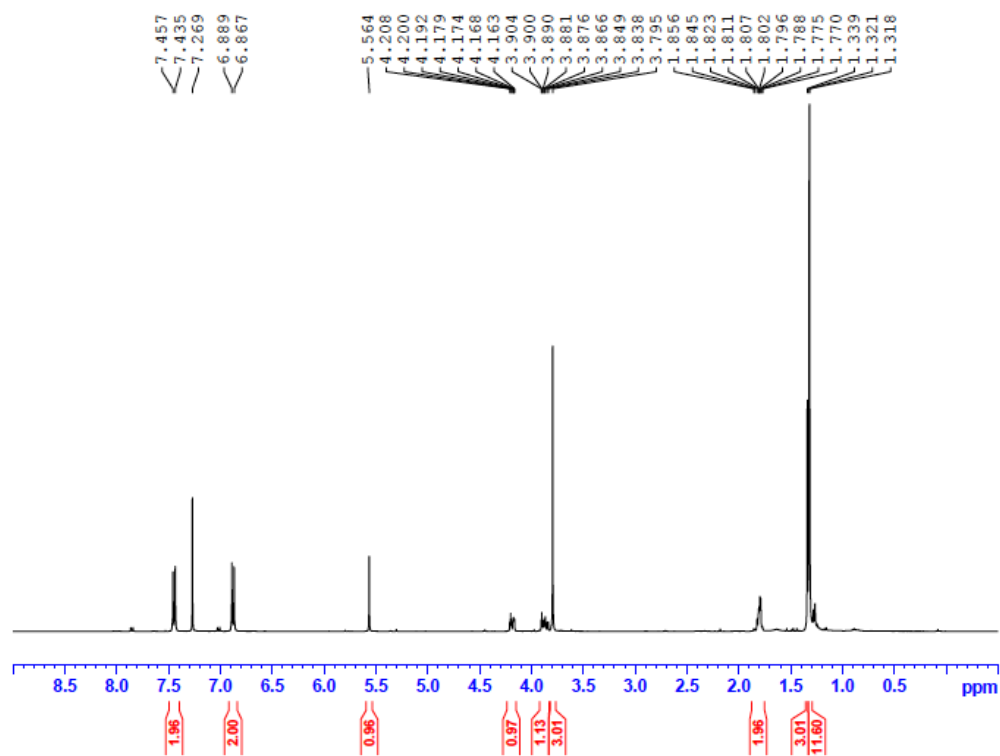
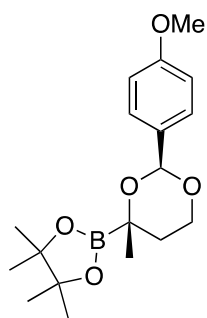


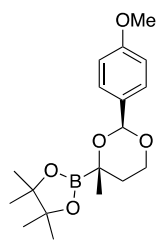




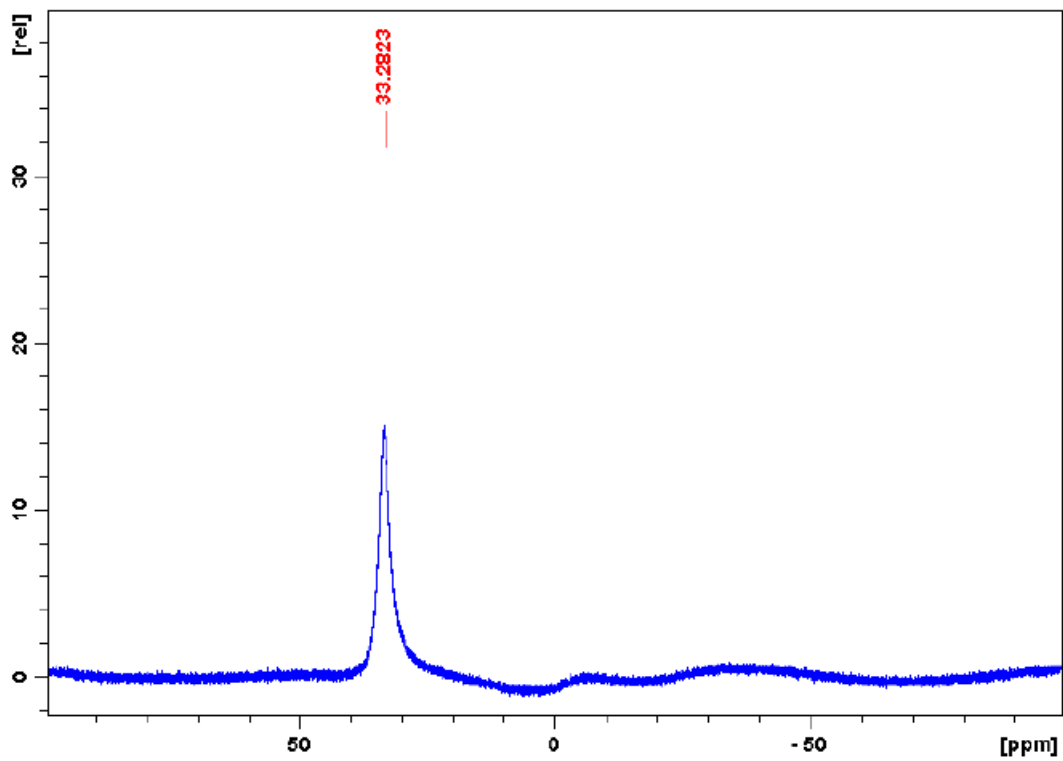


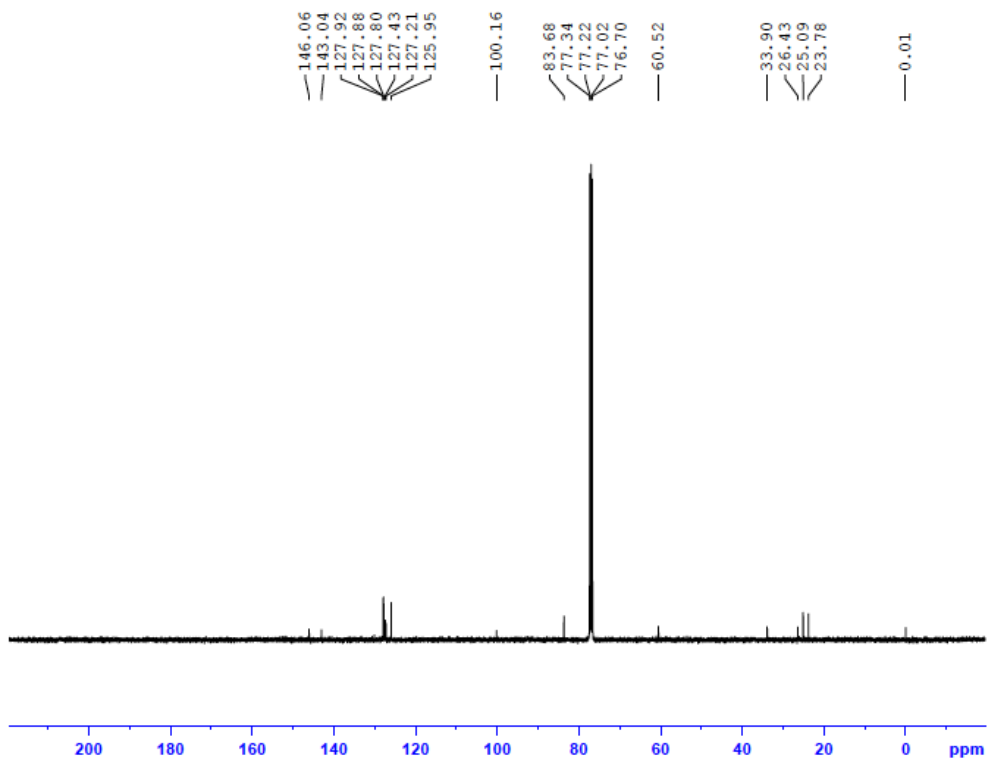
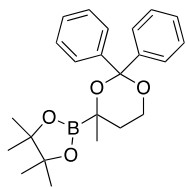
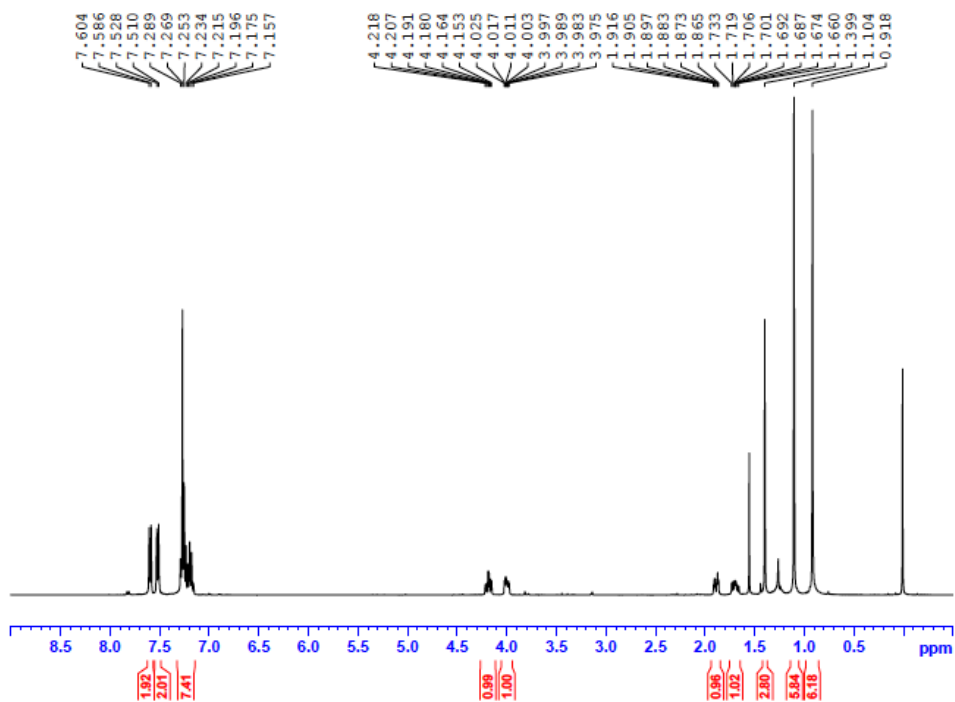
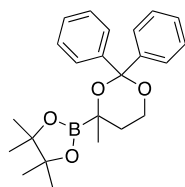


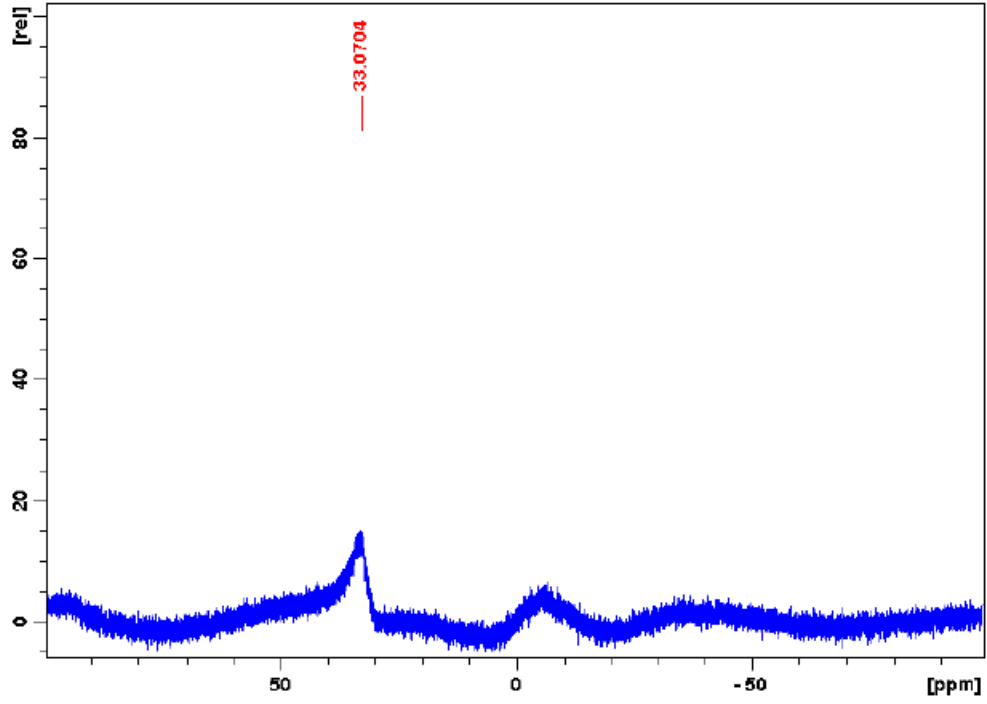
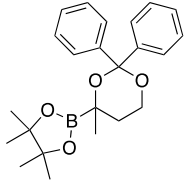


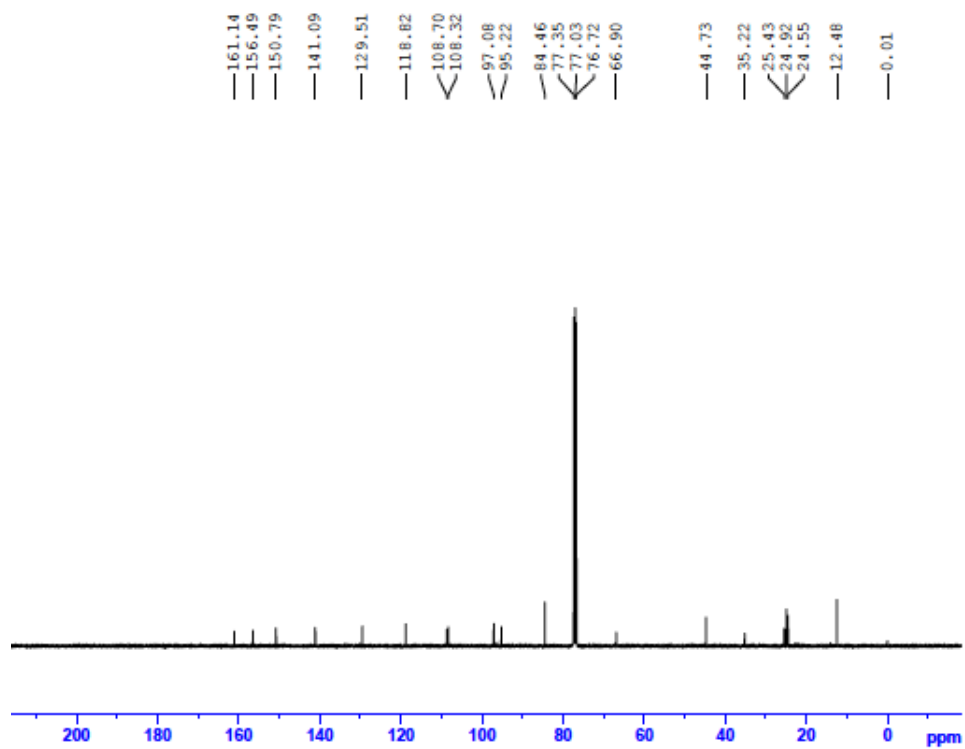
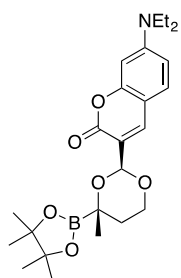
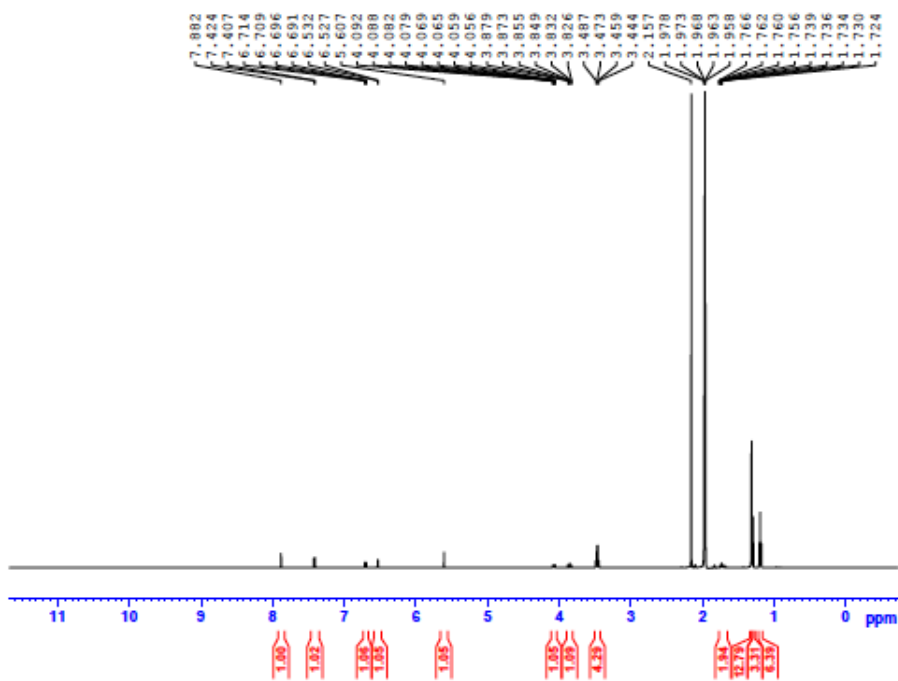
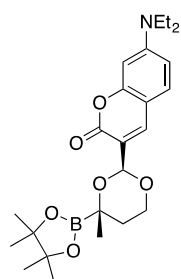


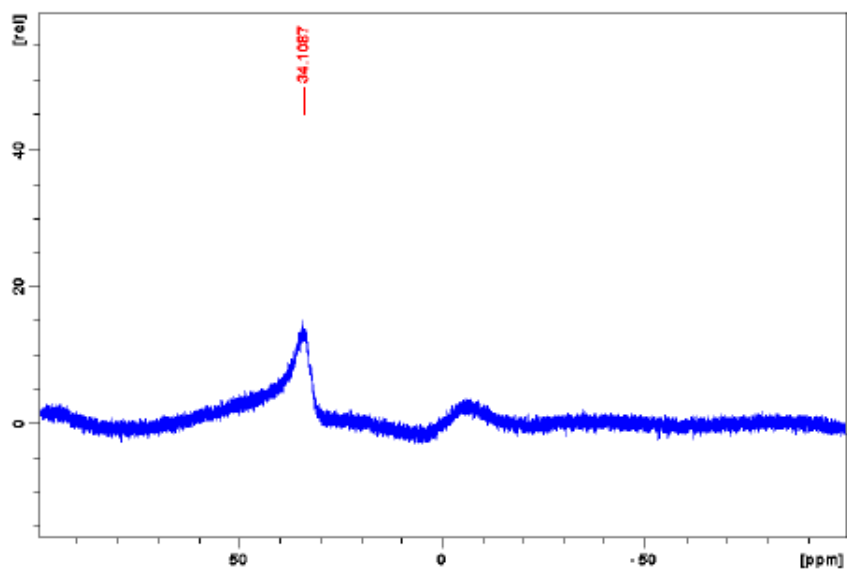
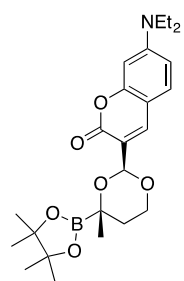
28

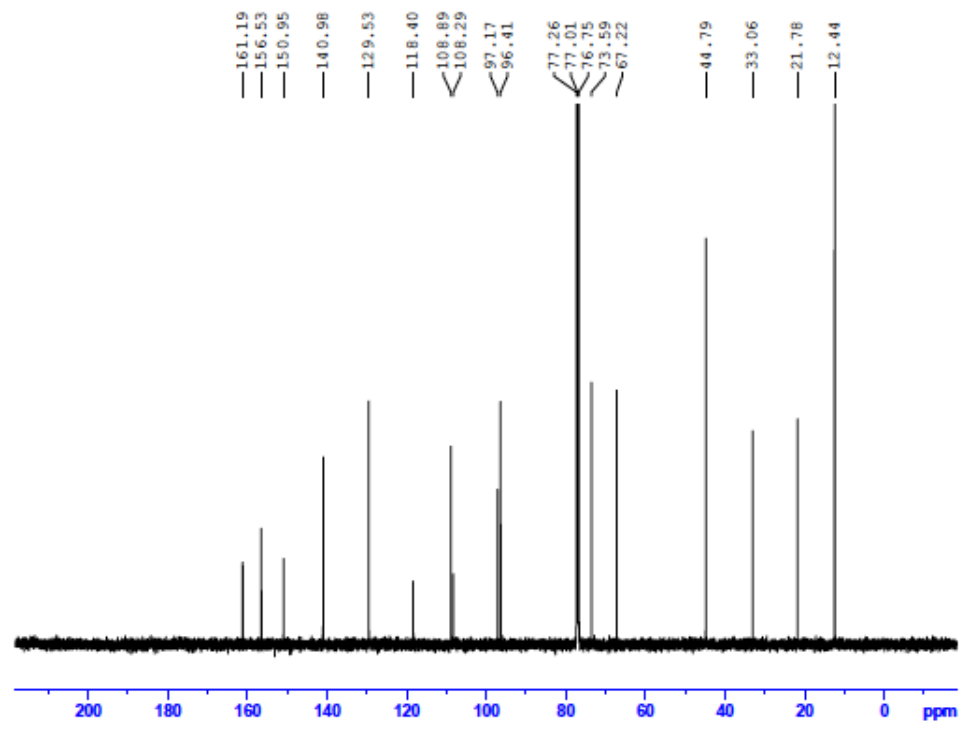
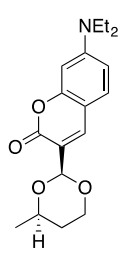
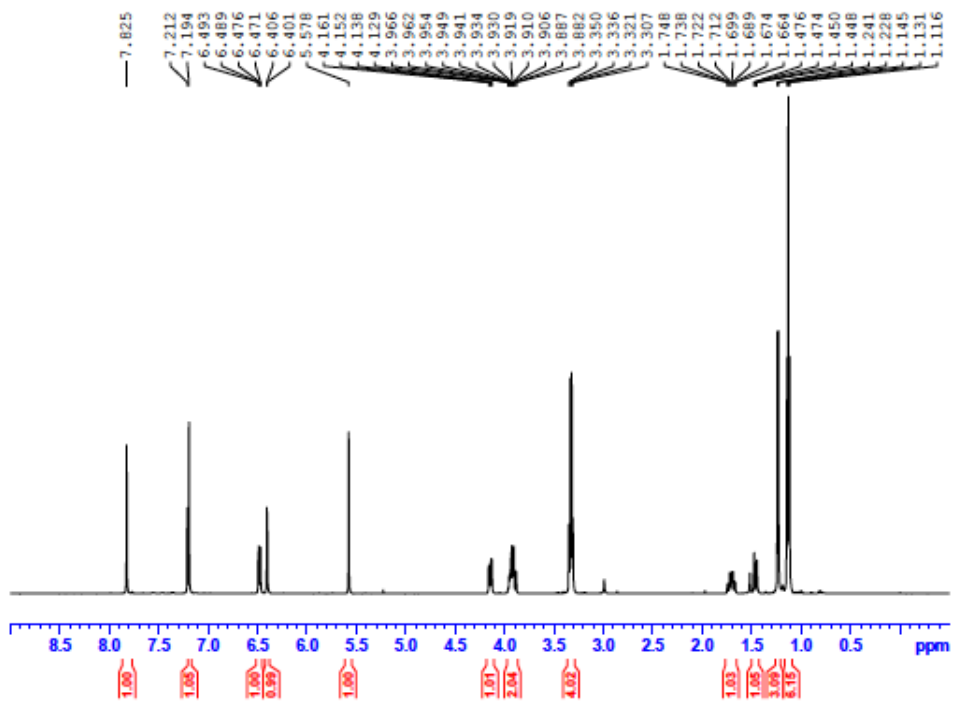
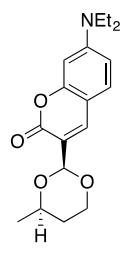


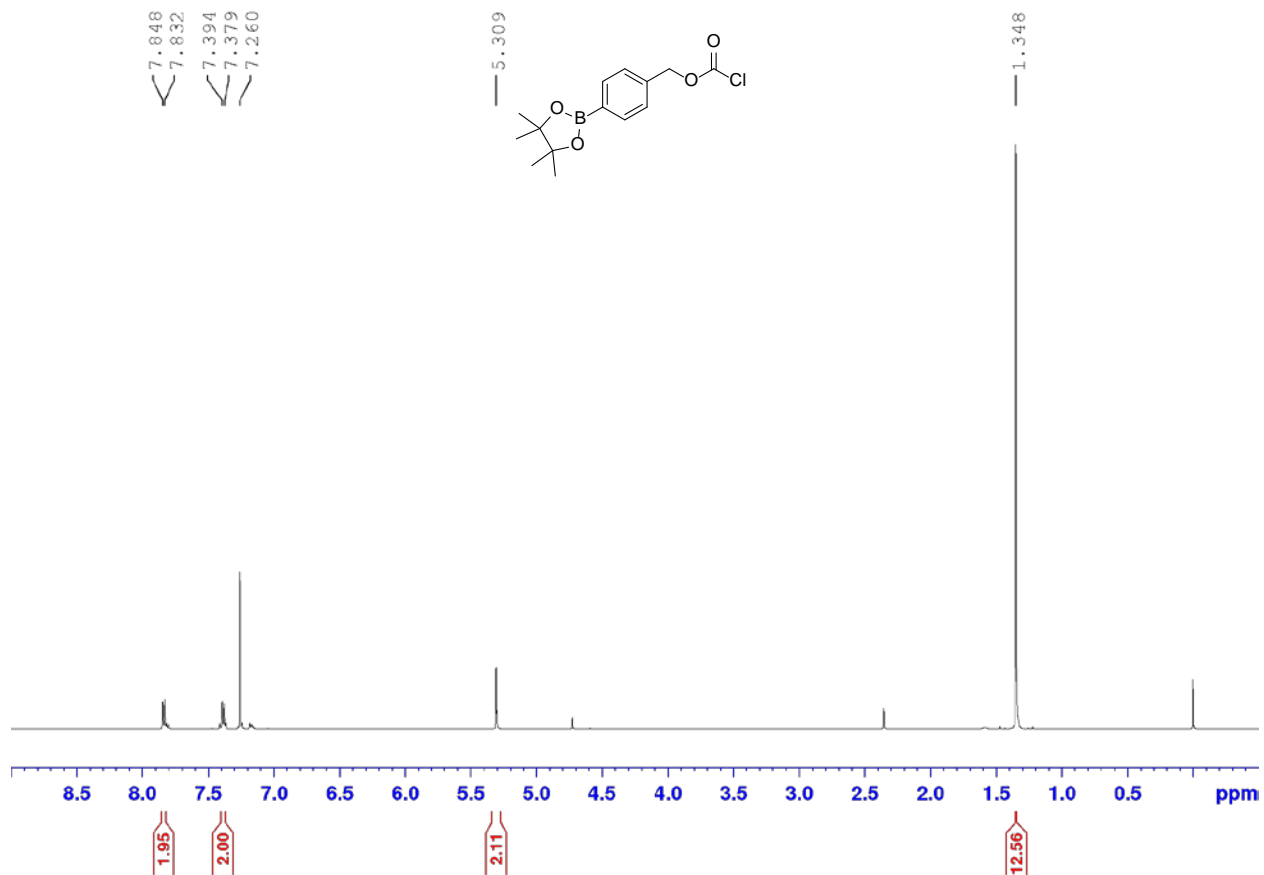


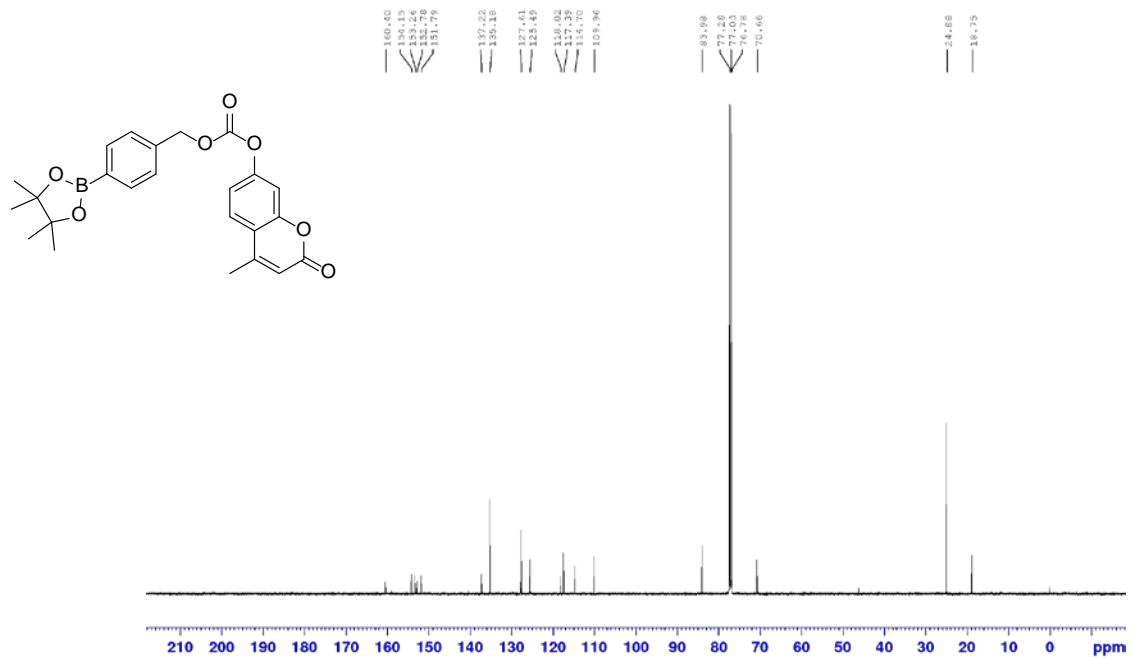
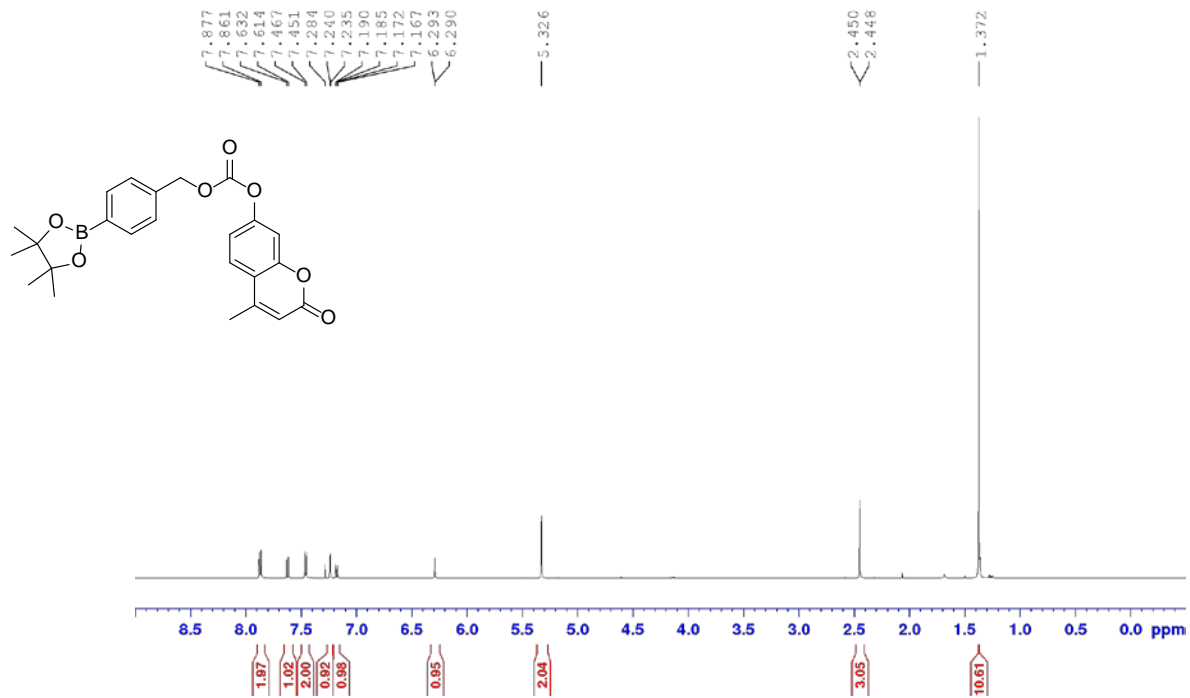


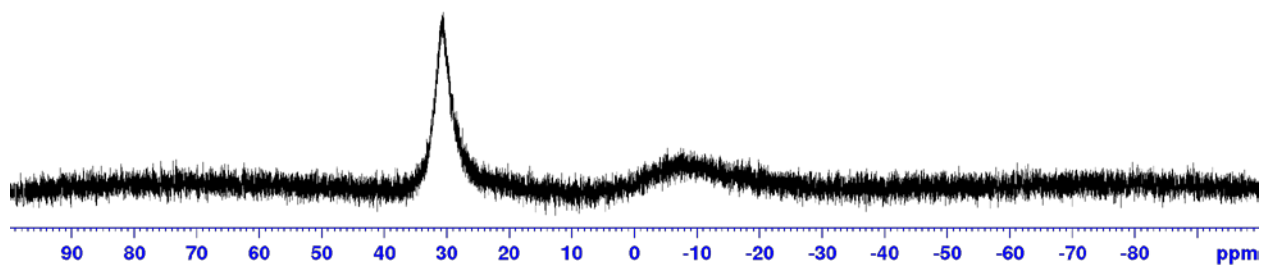
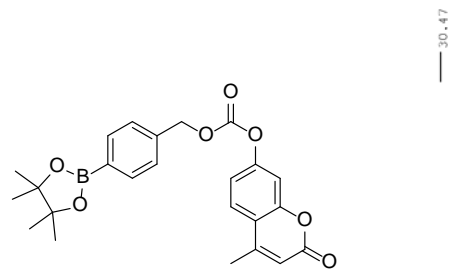






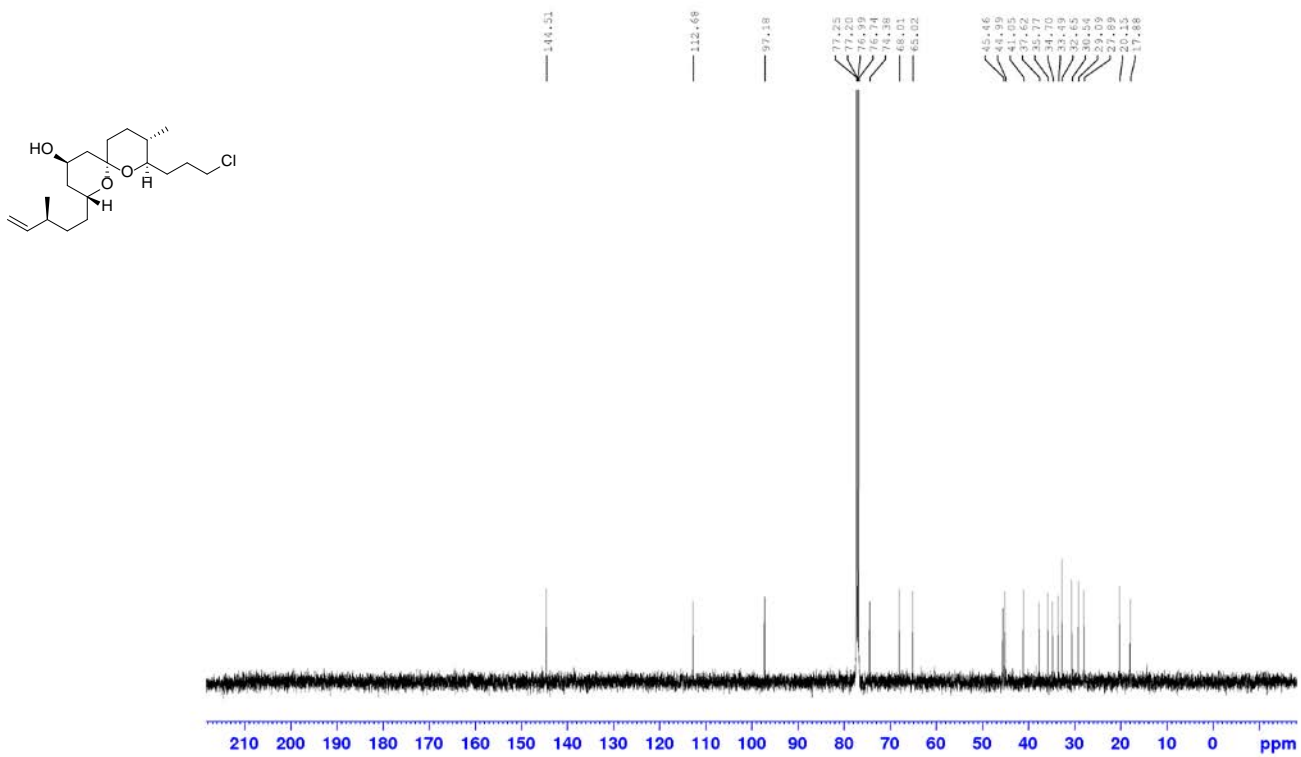
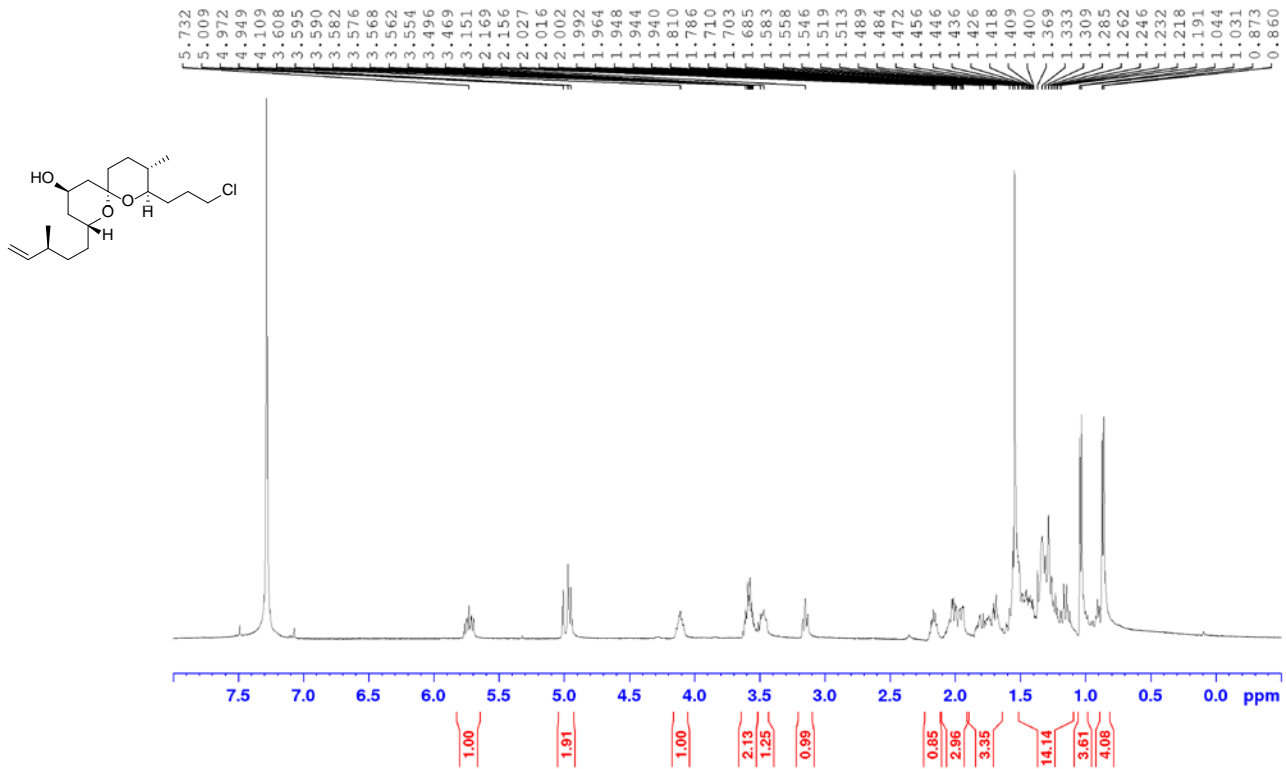


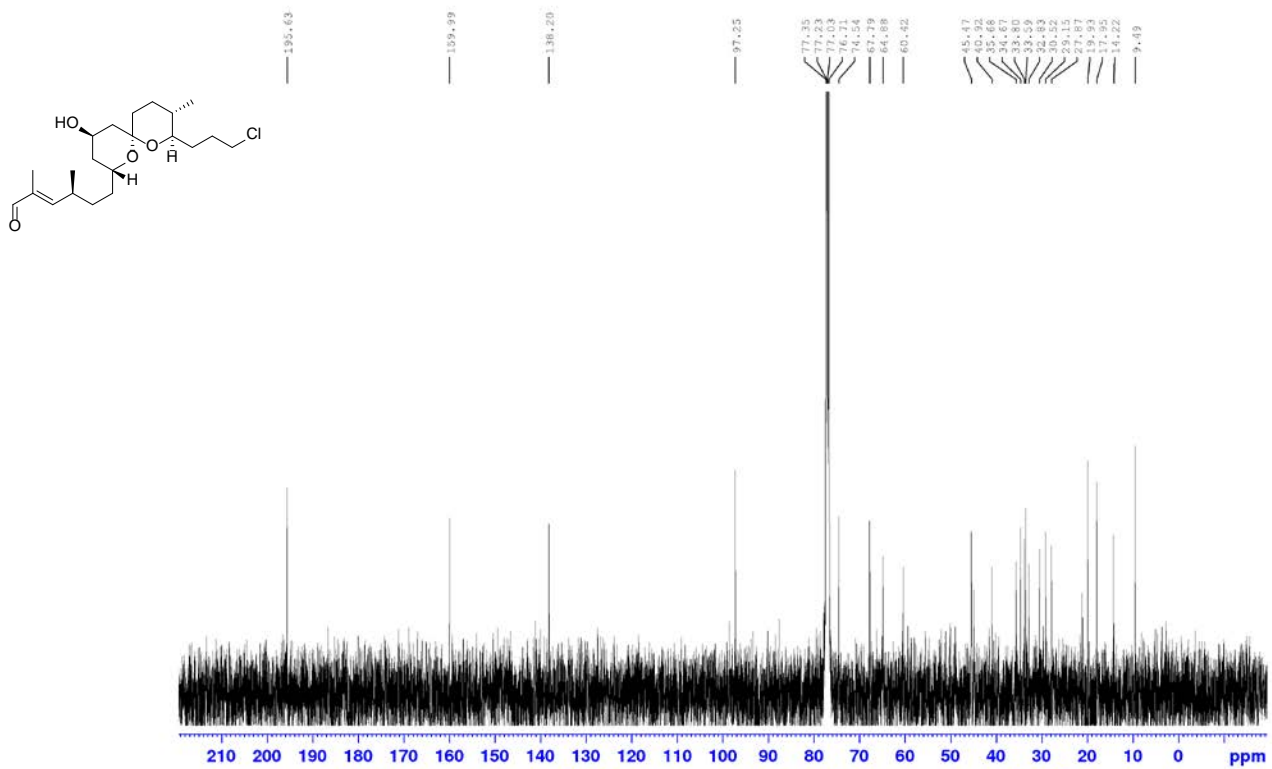
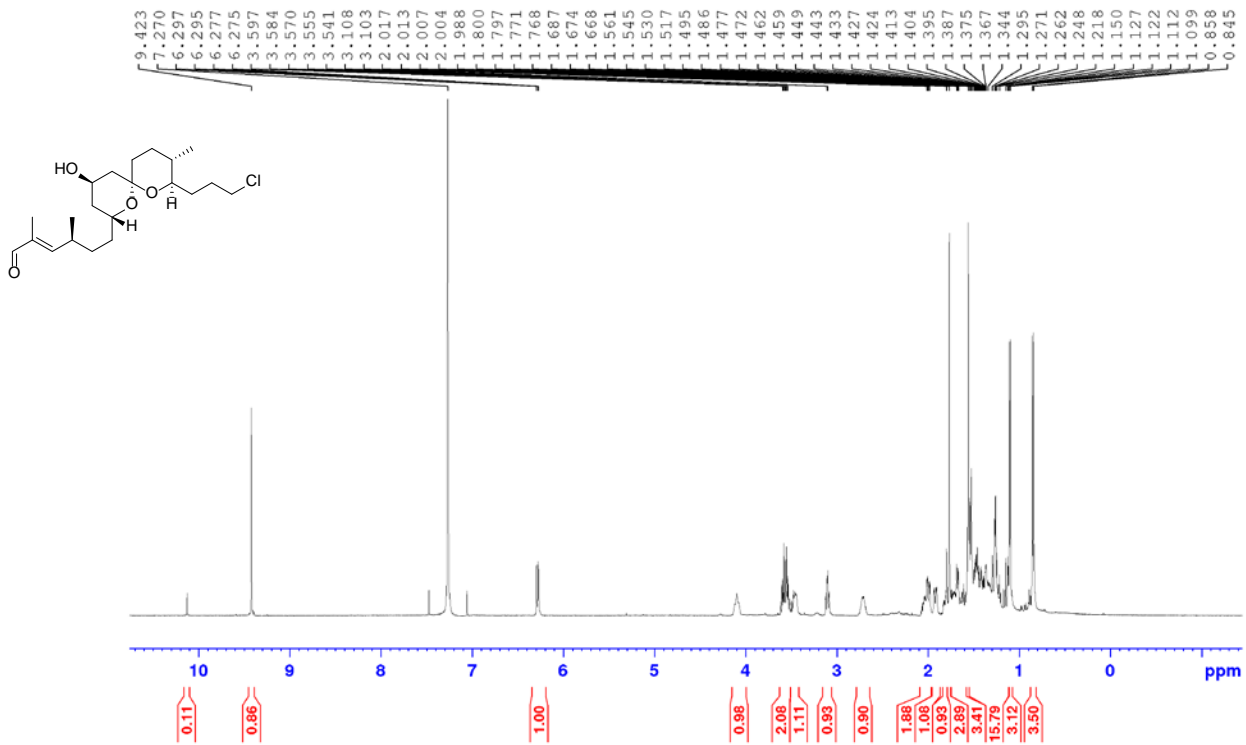


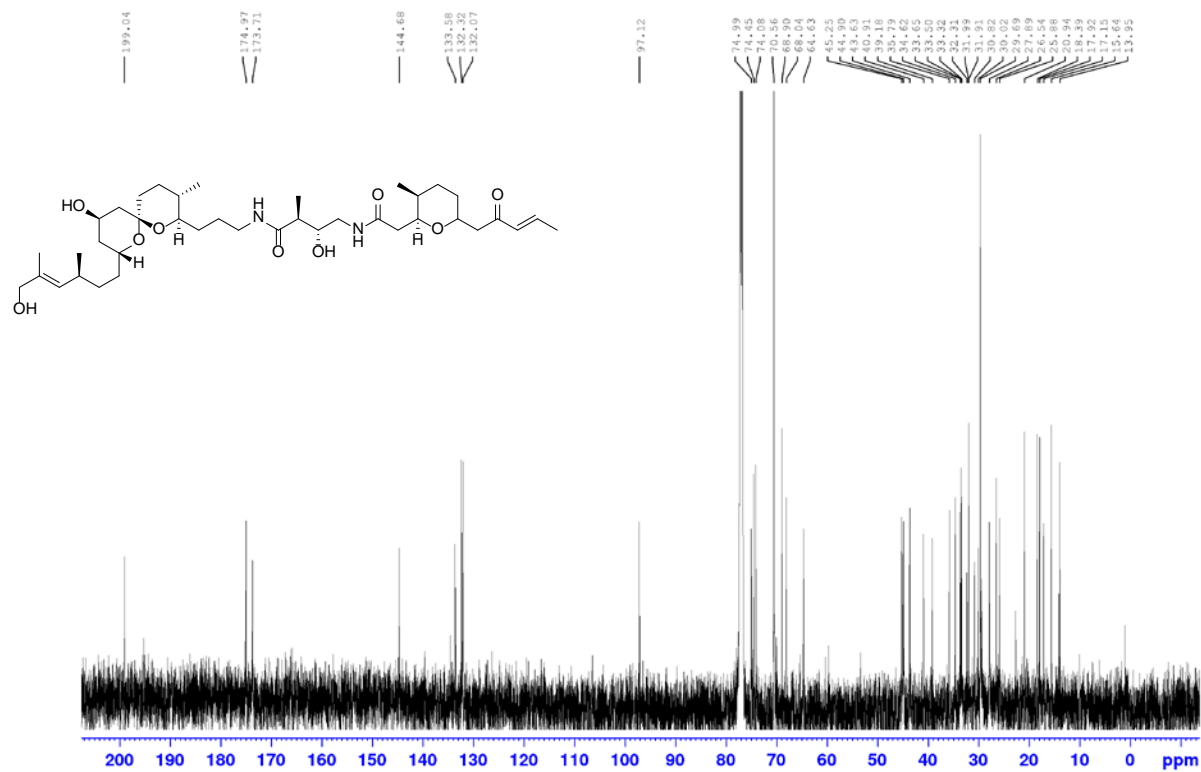
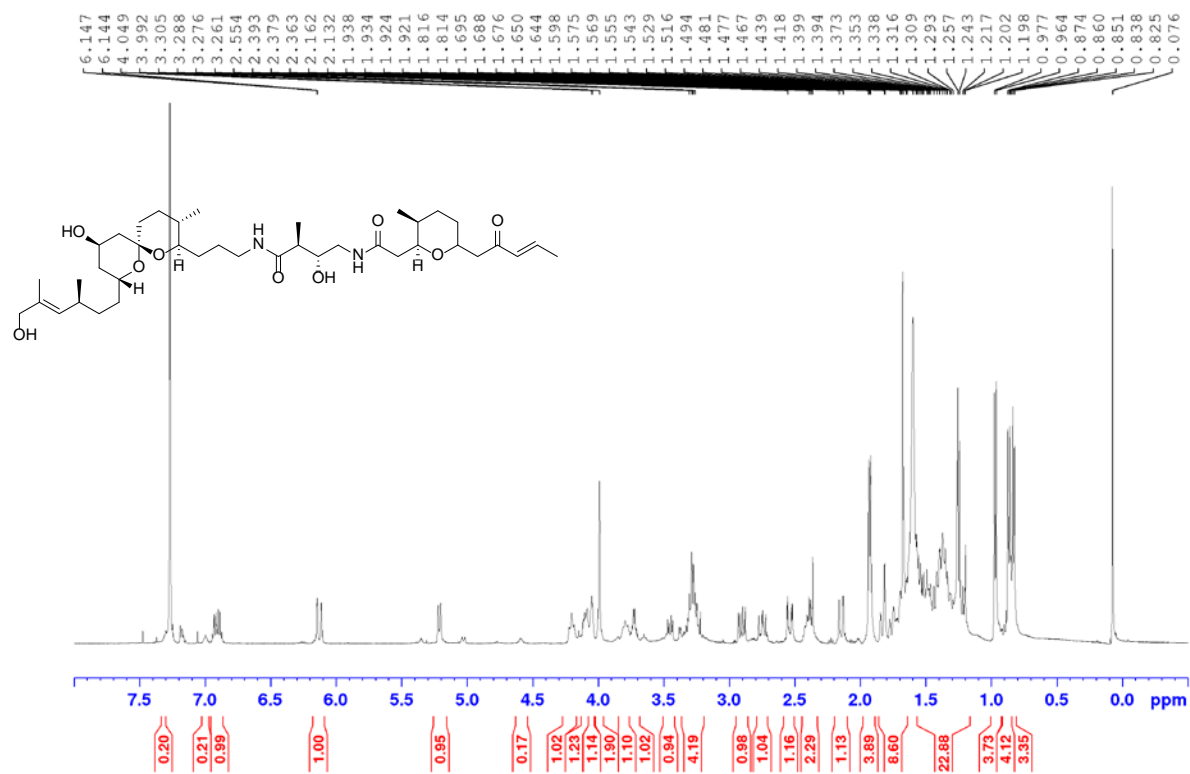


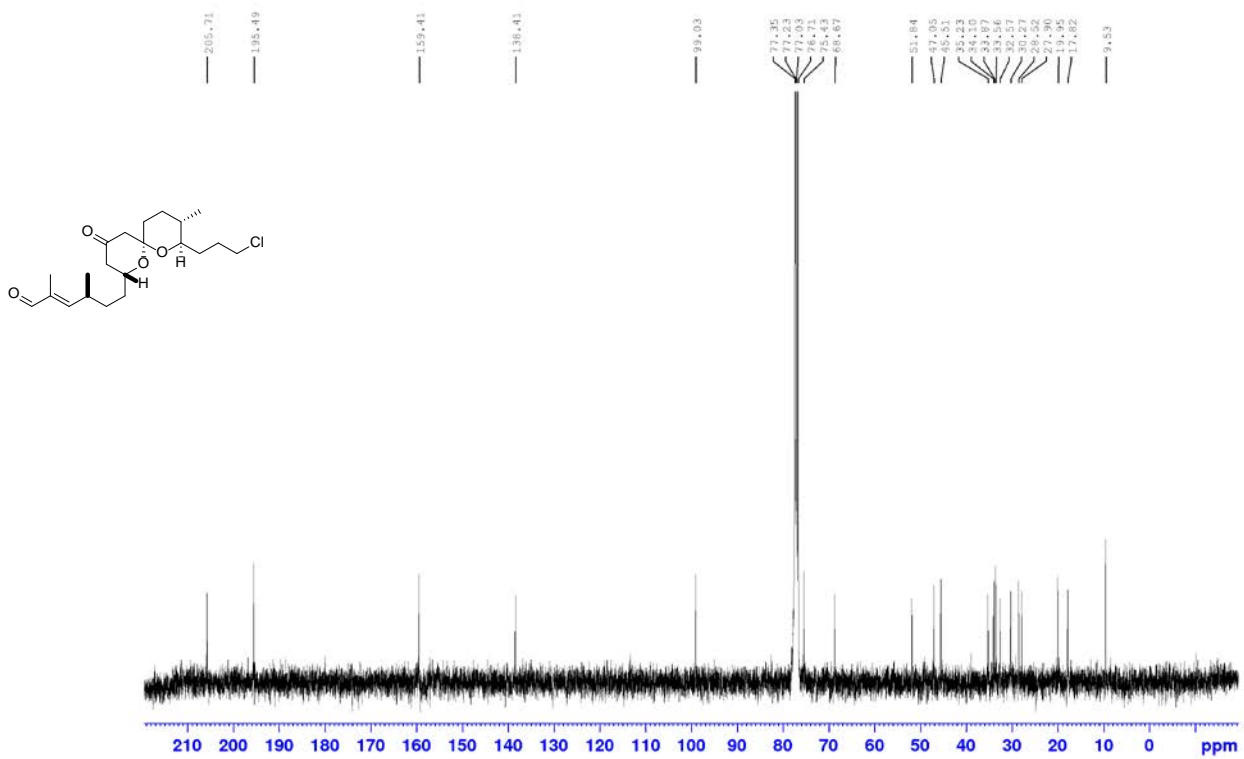
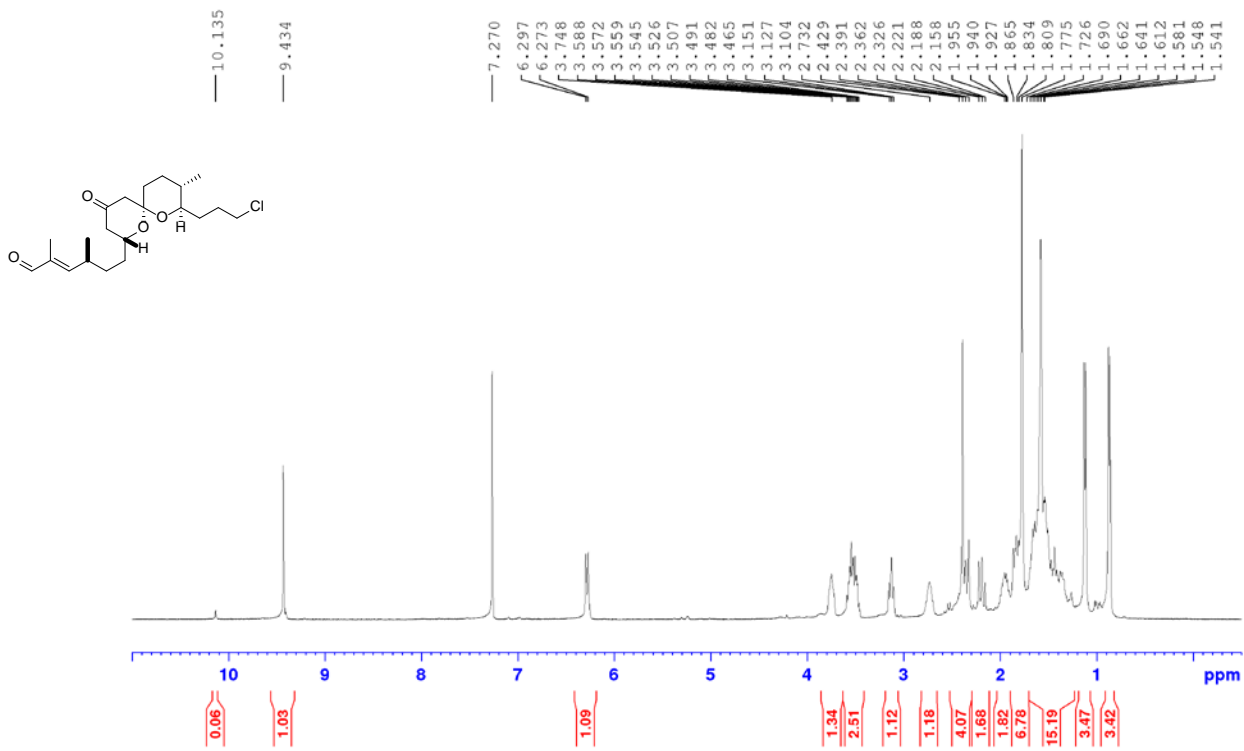
APPENDIX D

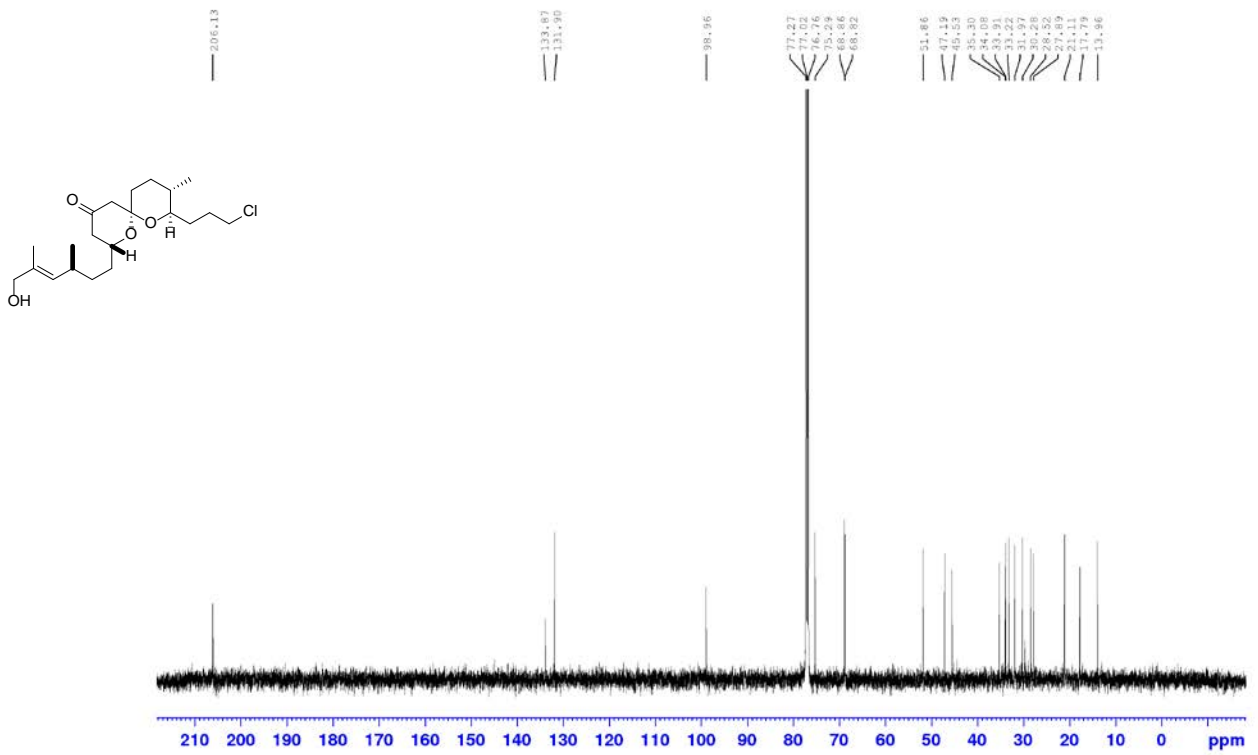
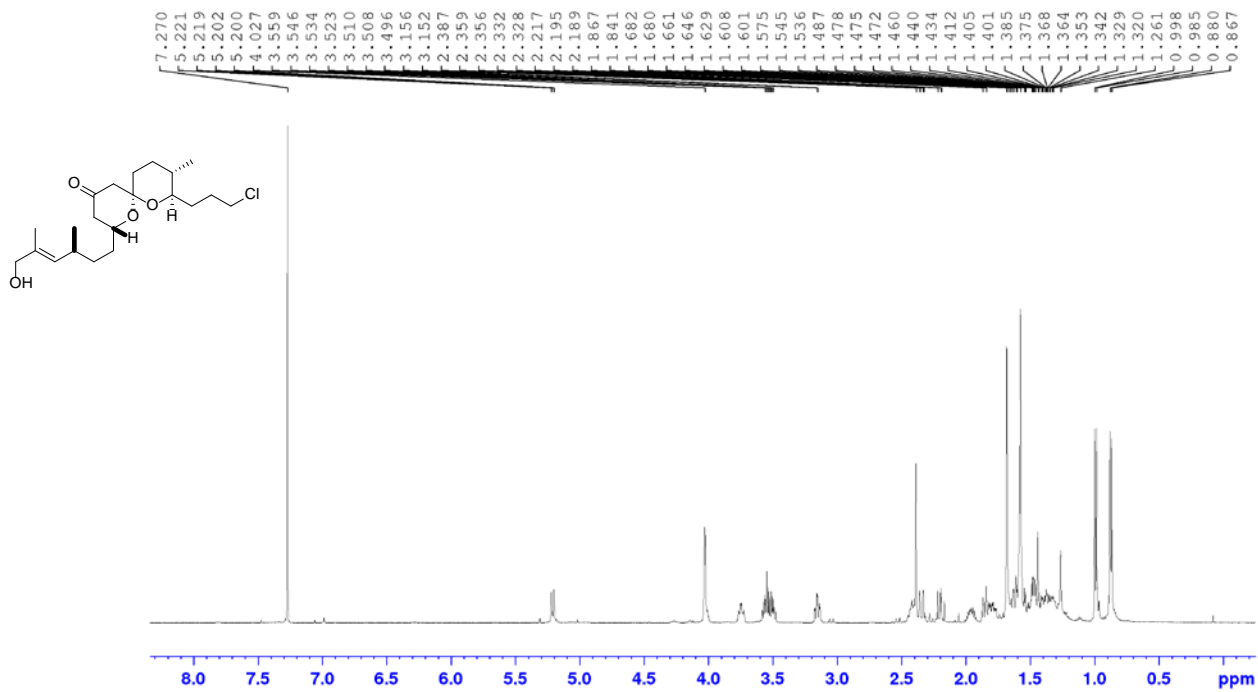
^1H and ^{13}C NMR Spectra for 3.3

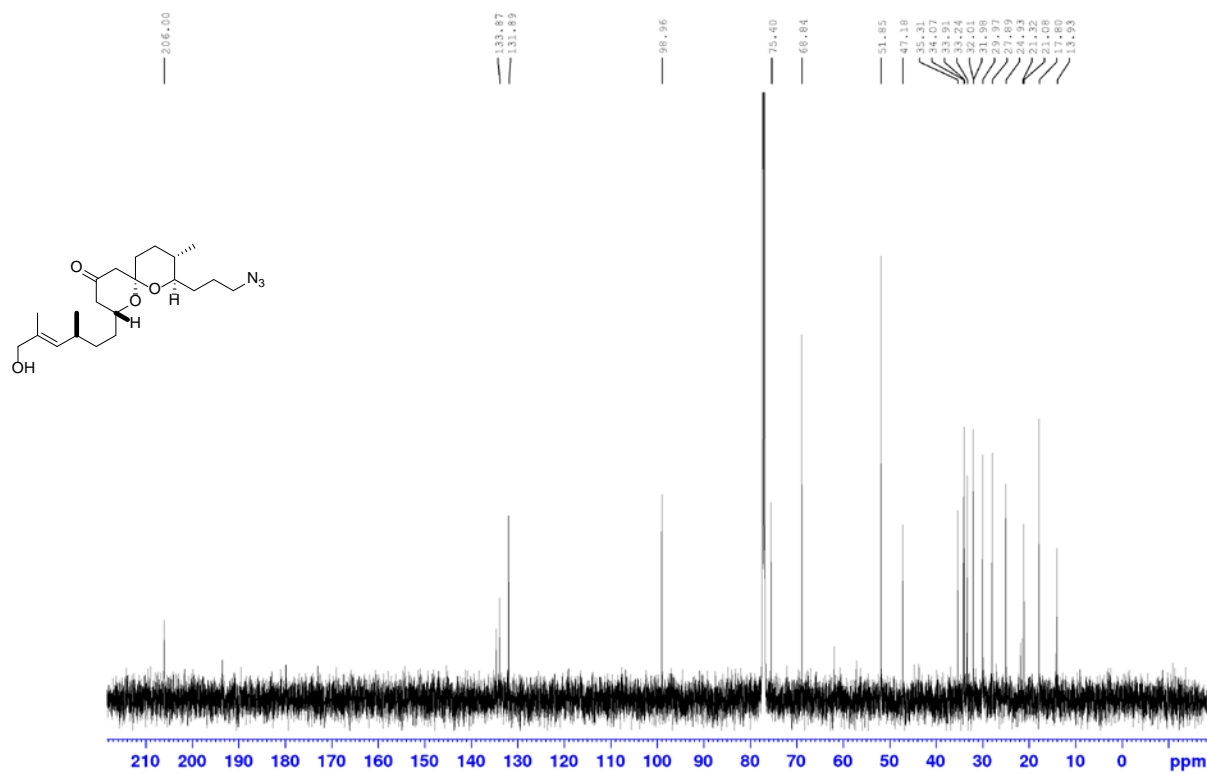
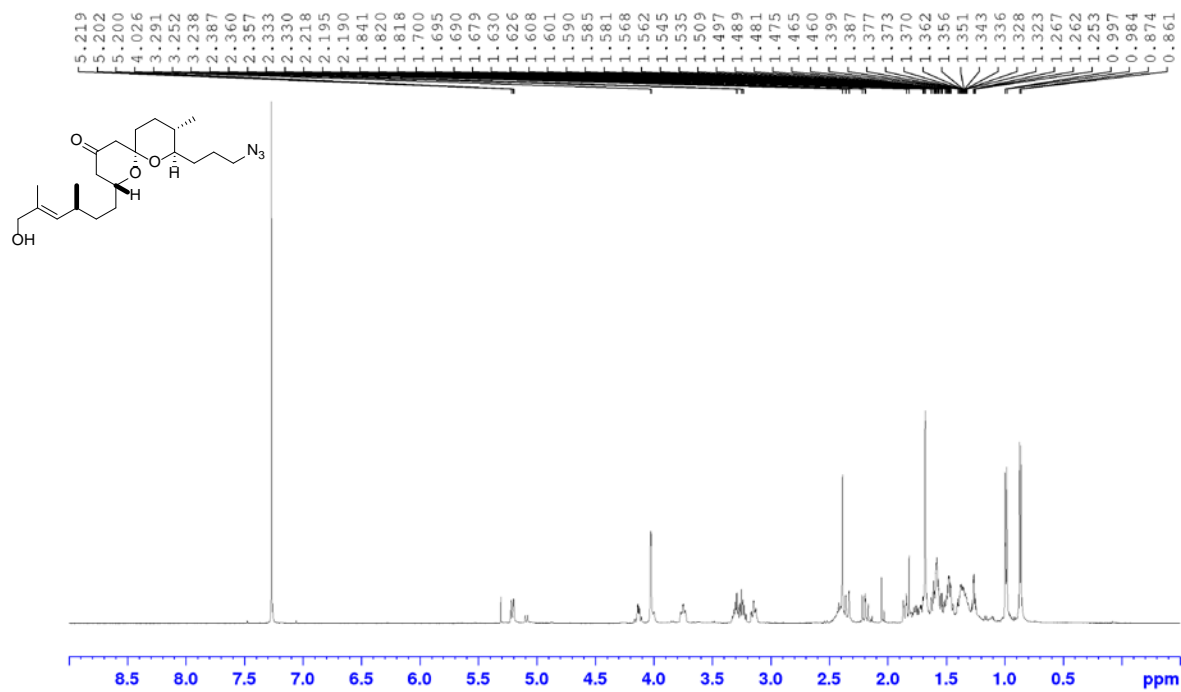


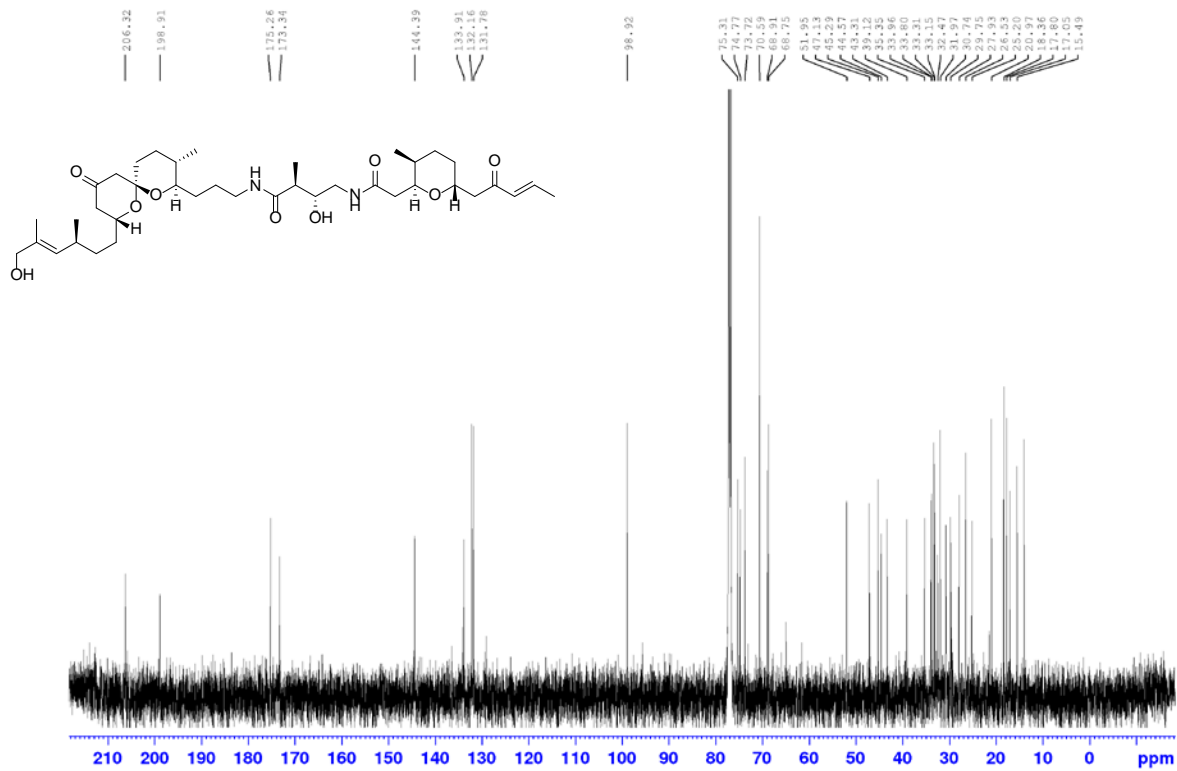
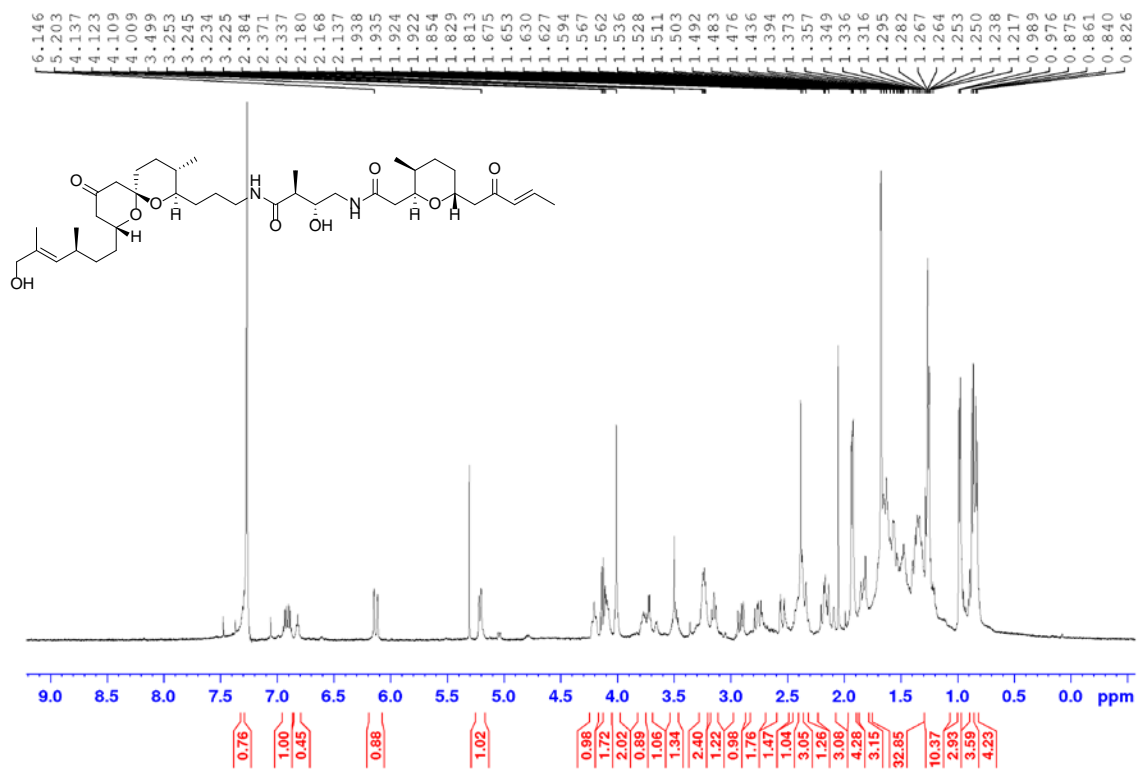


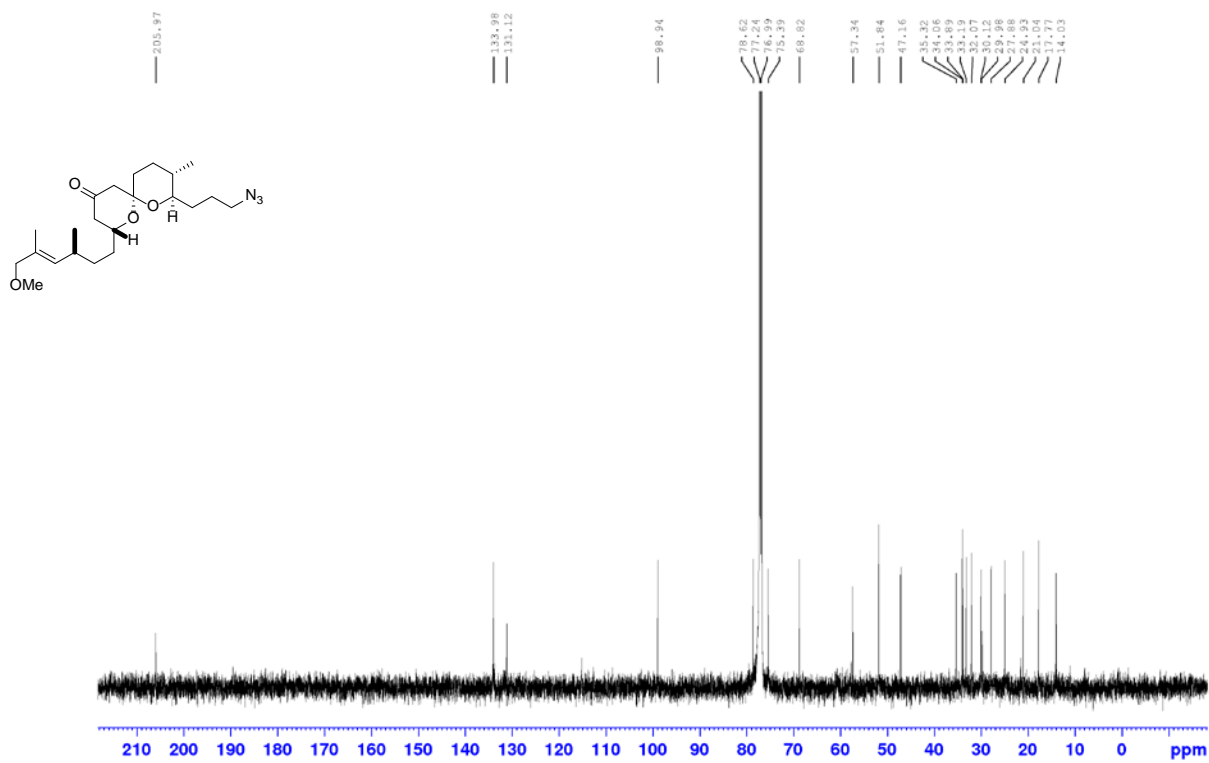
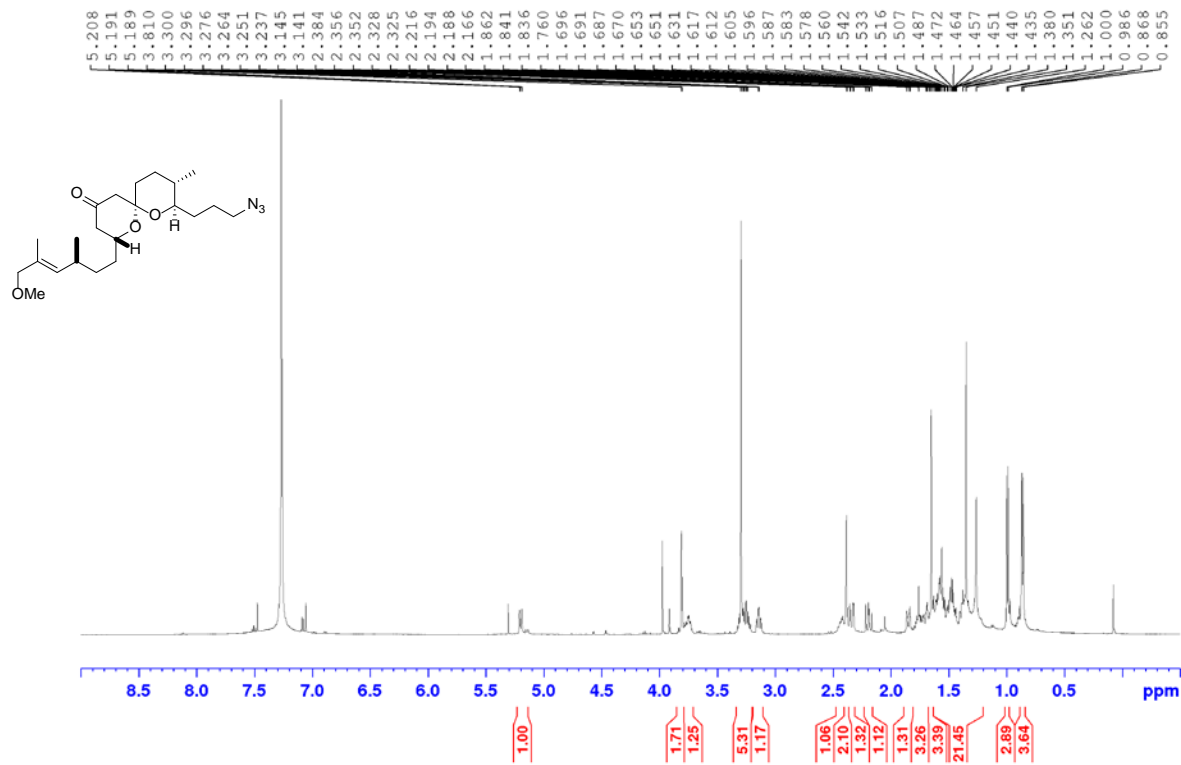


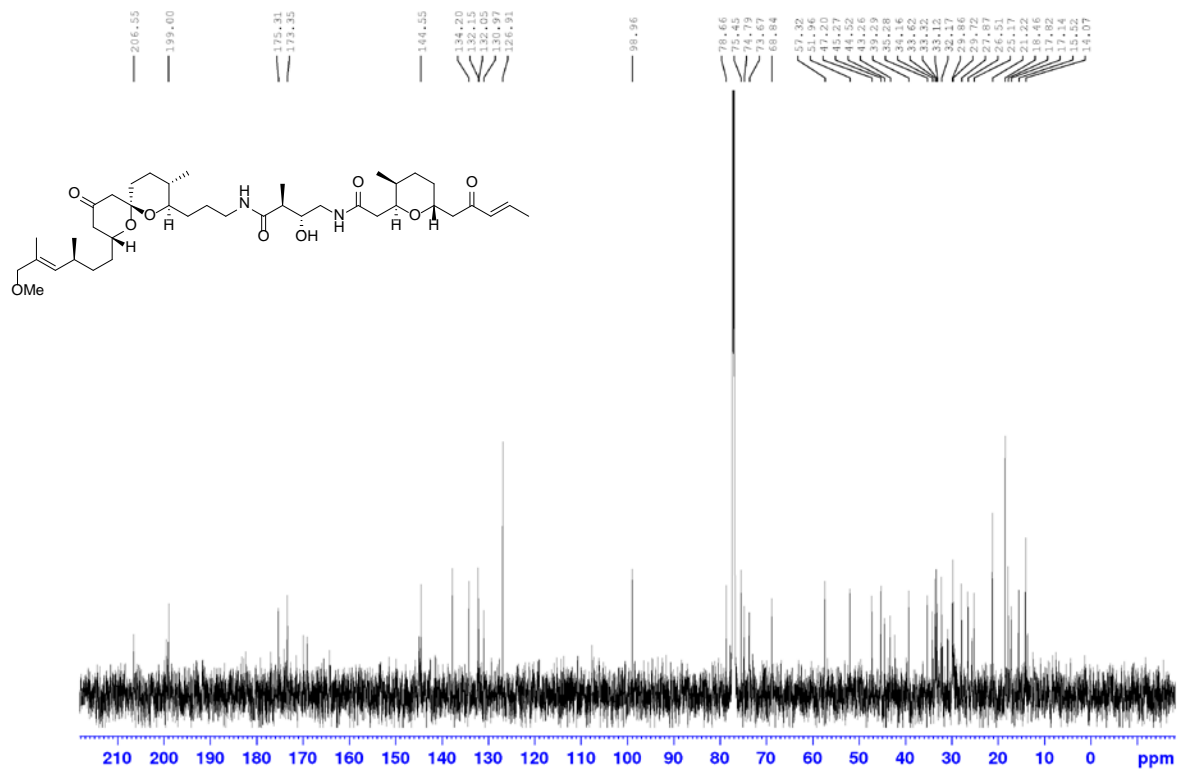
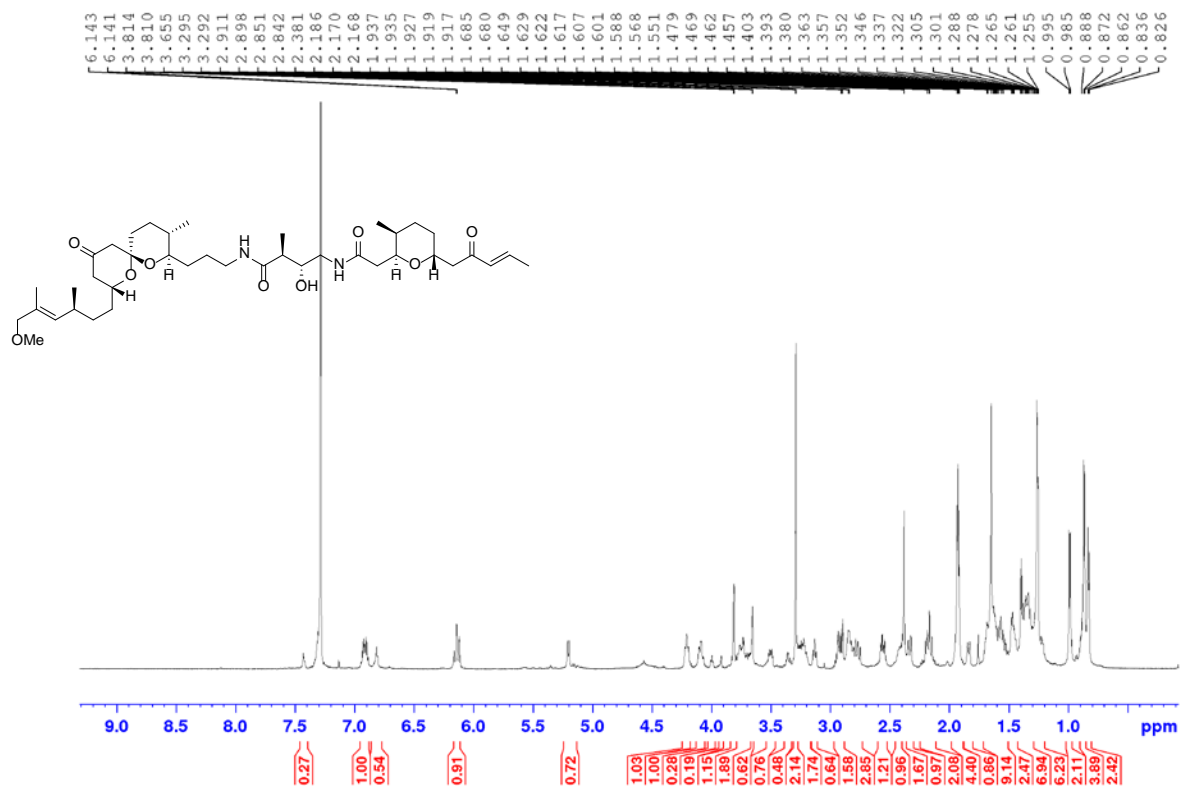


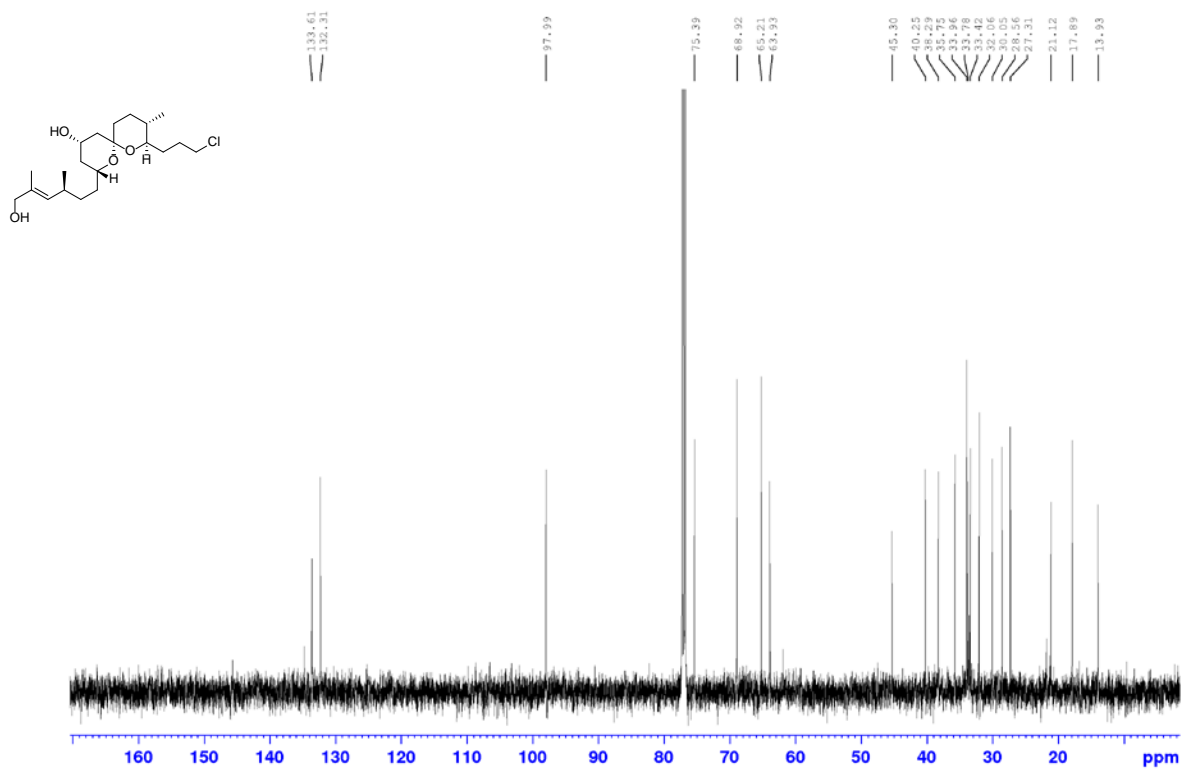
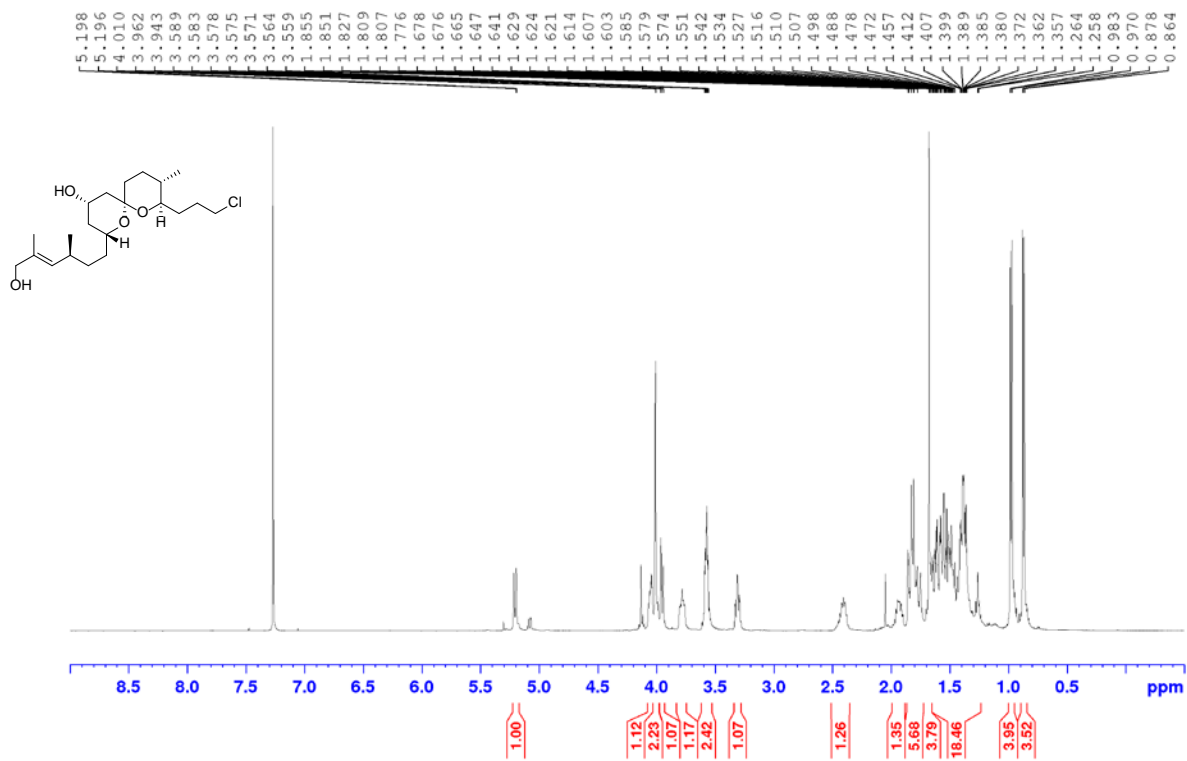


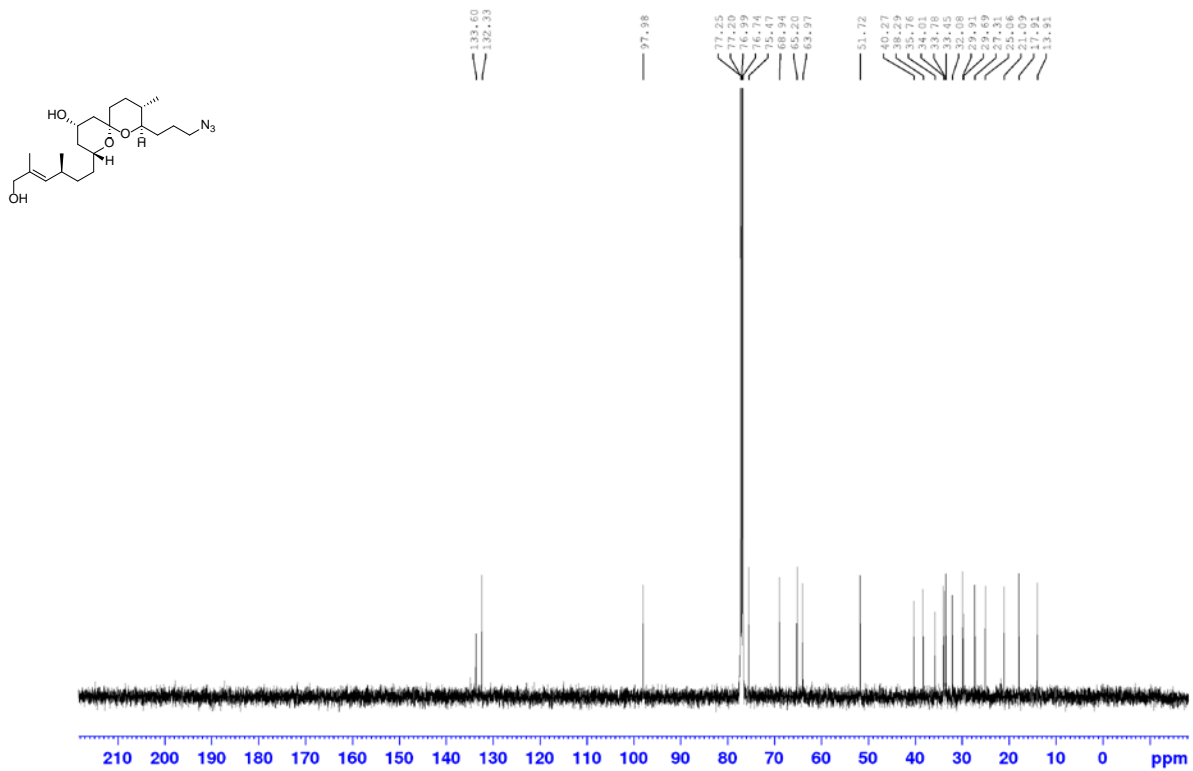
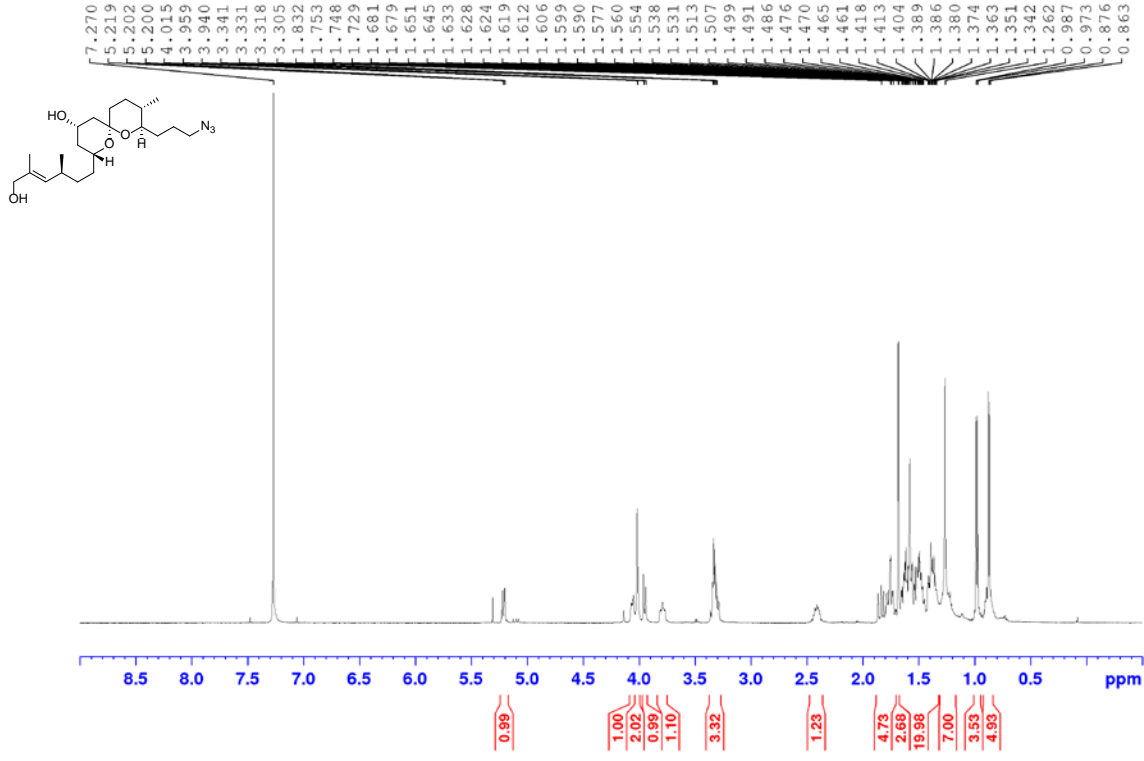


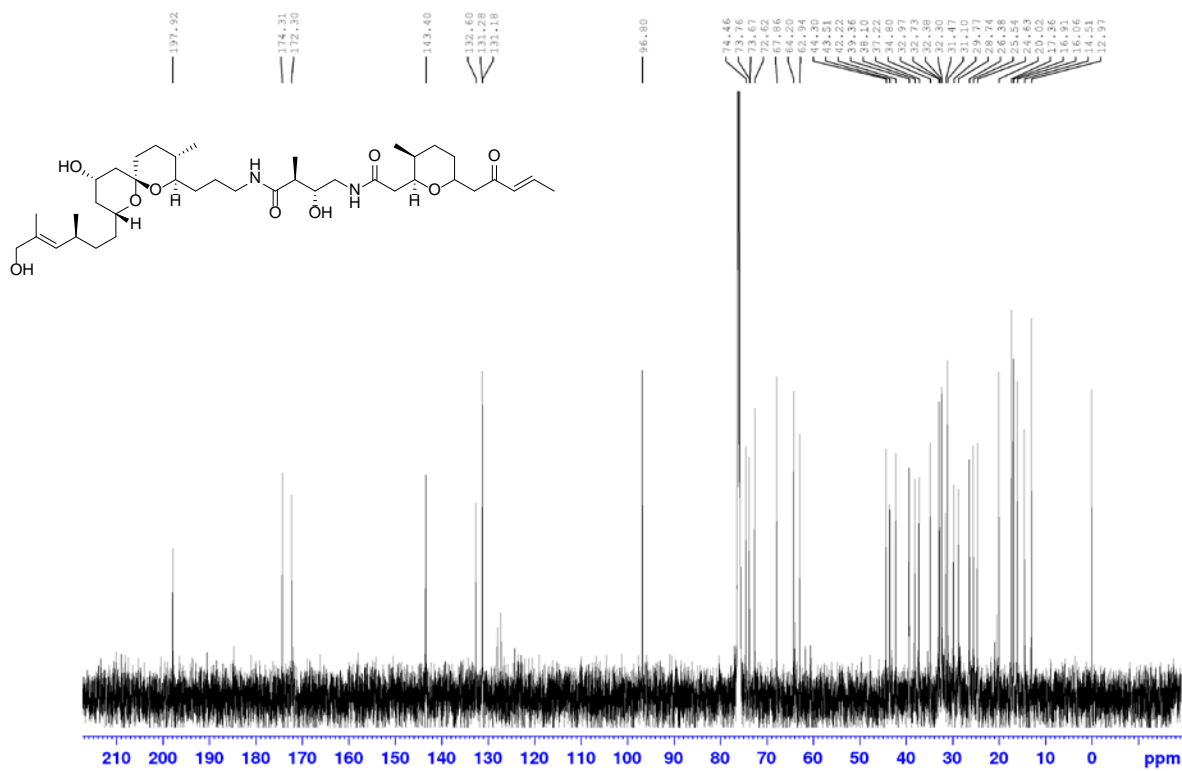
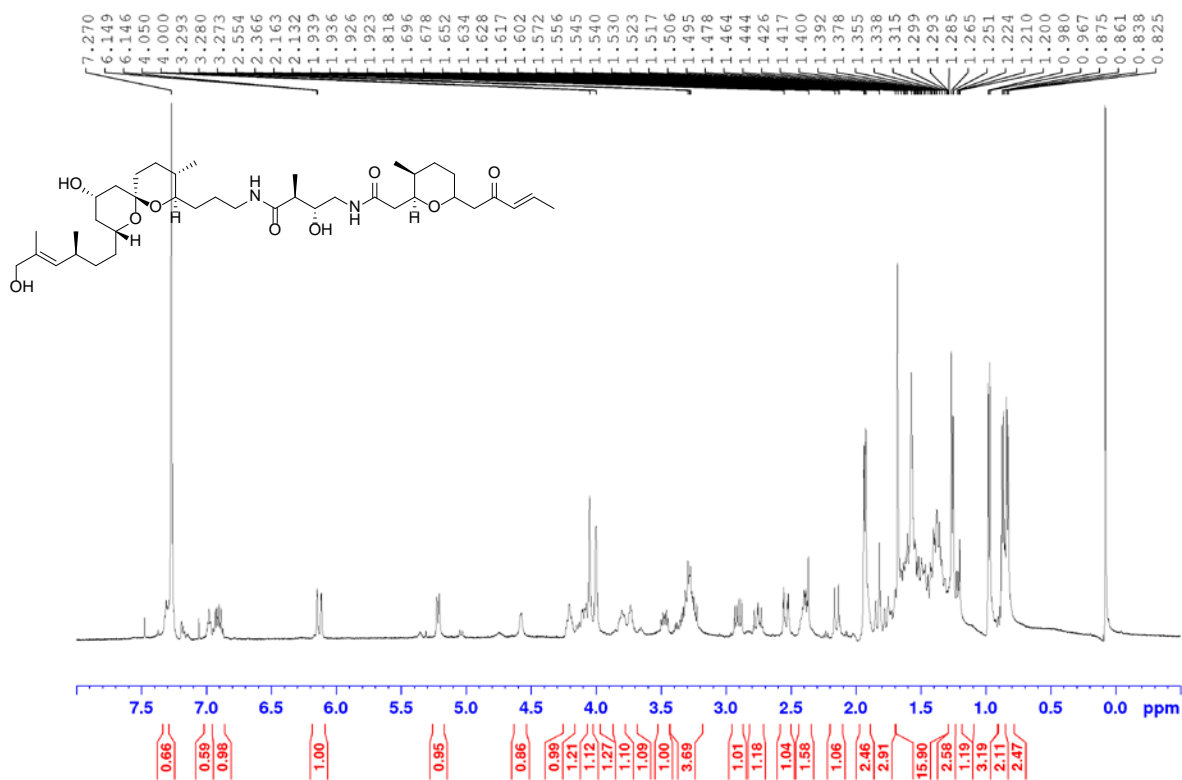


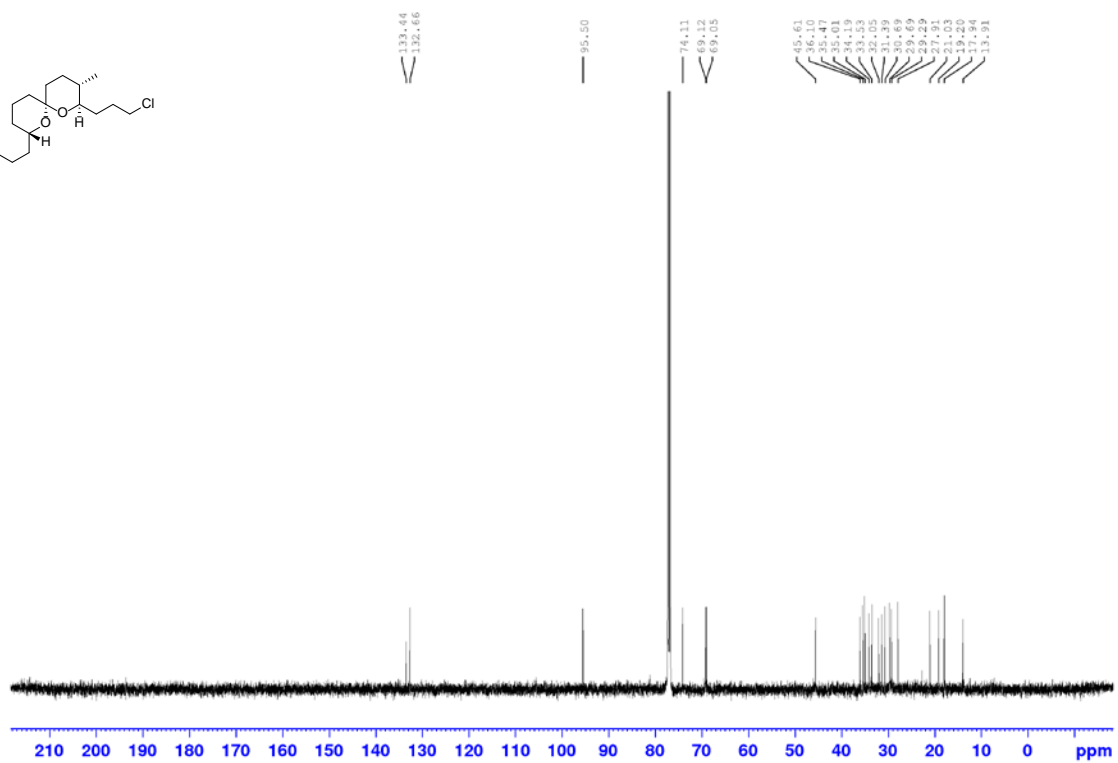
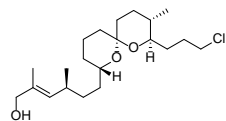
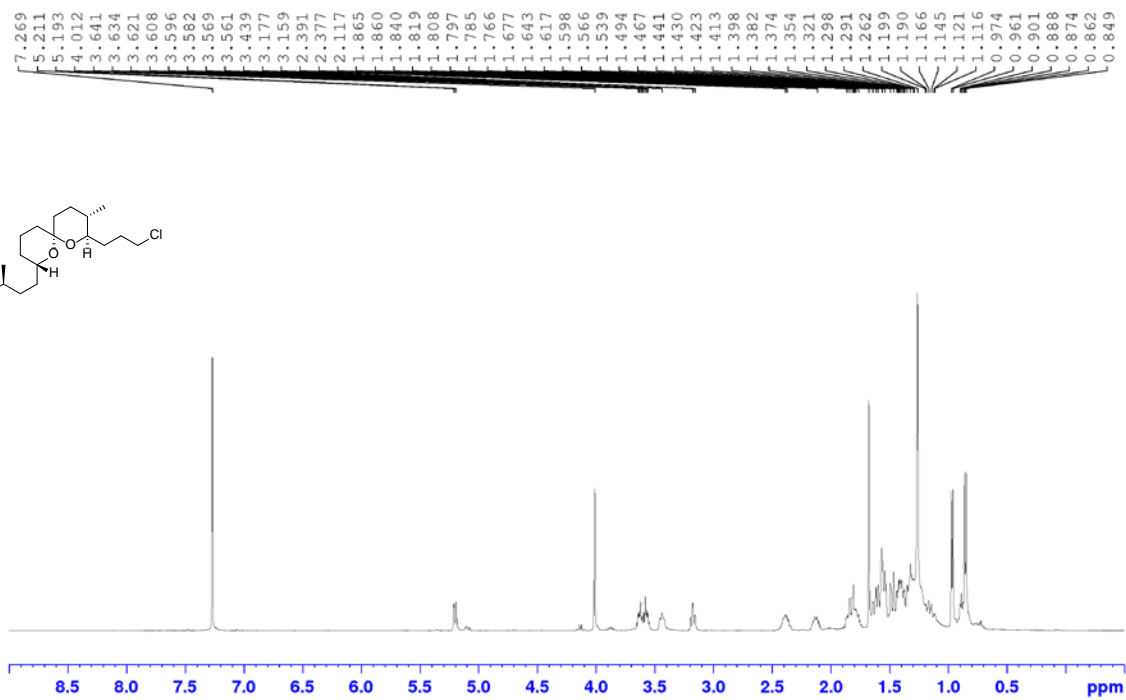
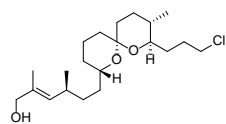


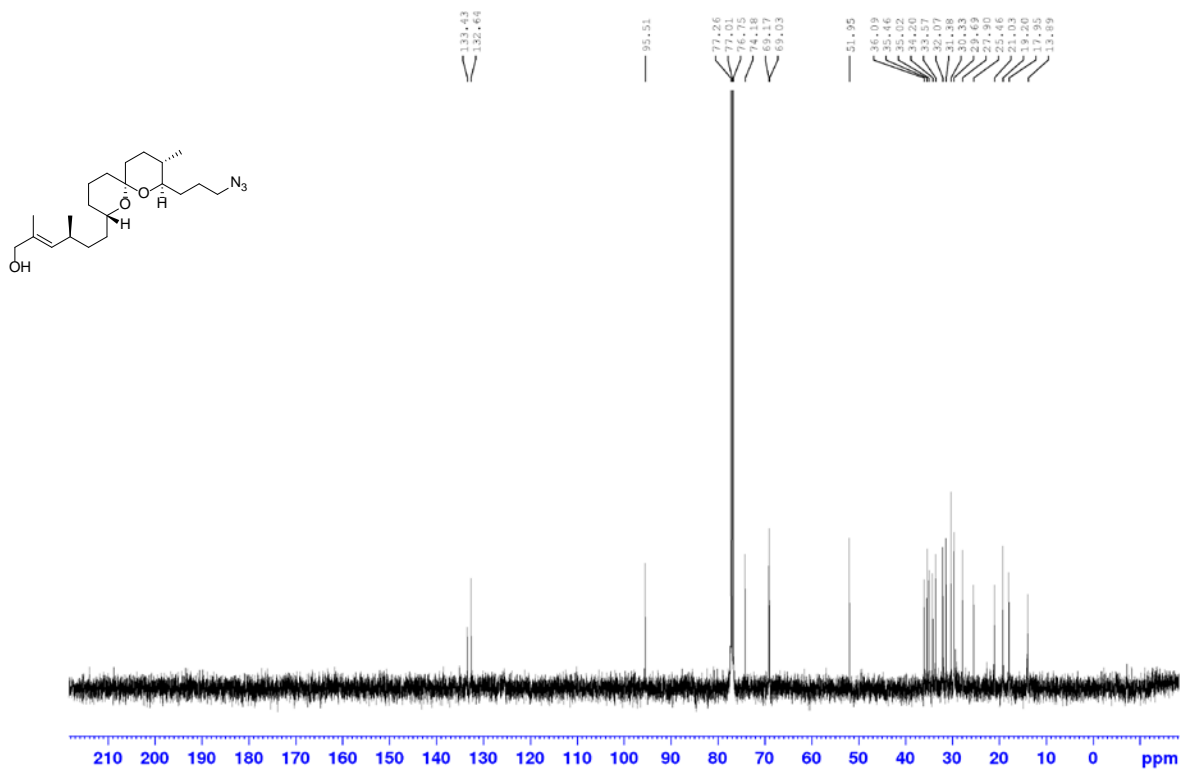
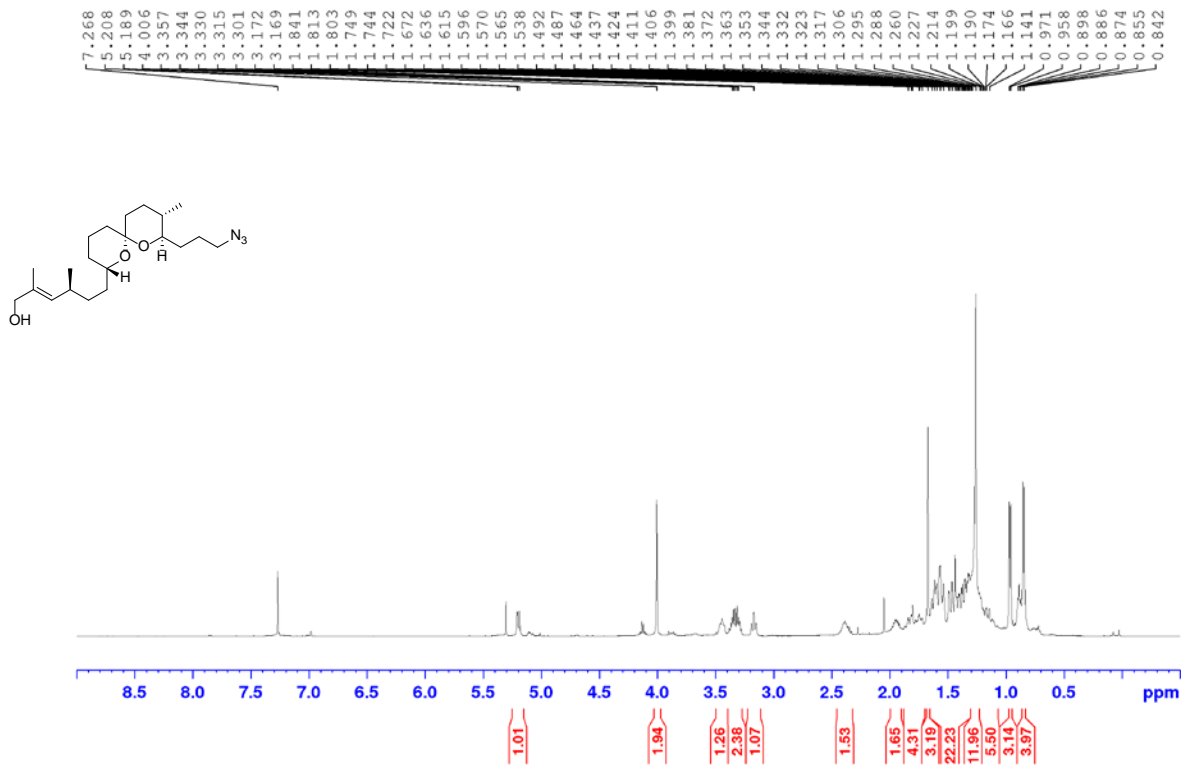


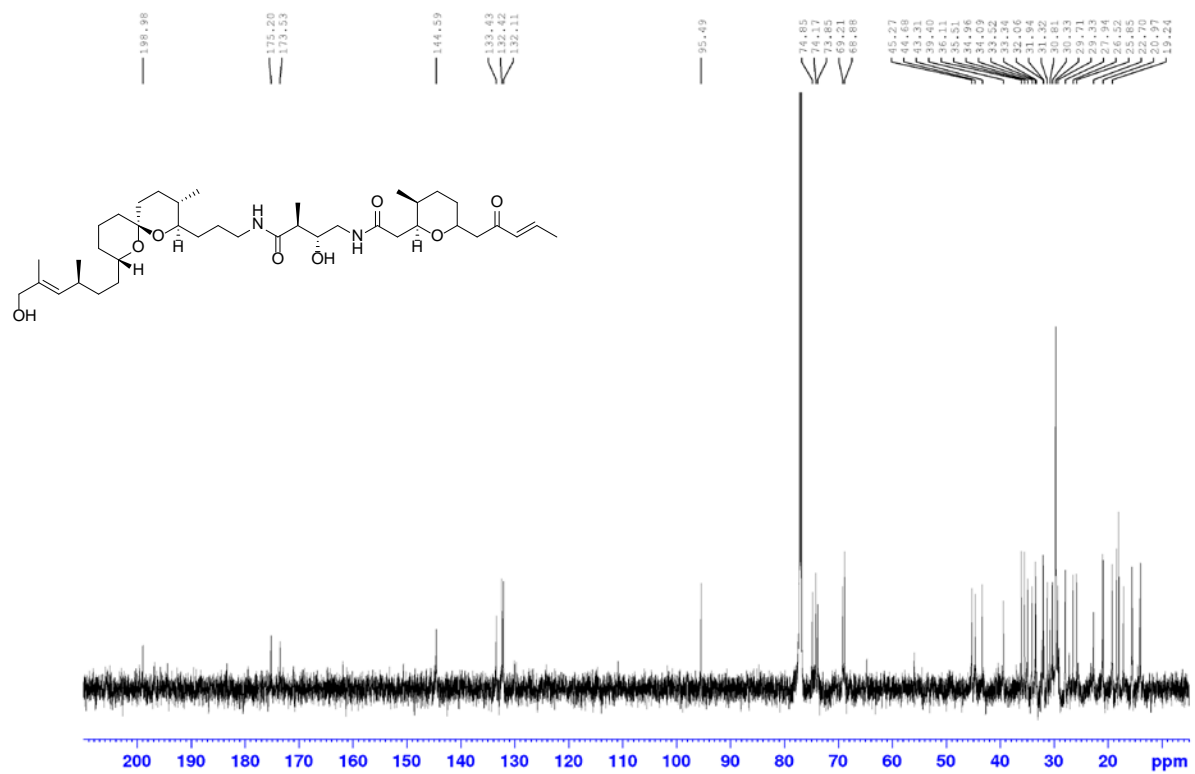
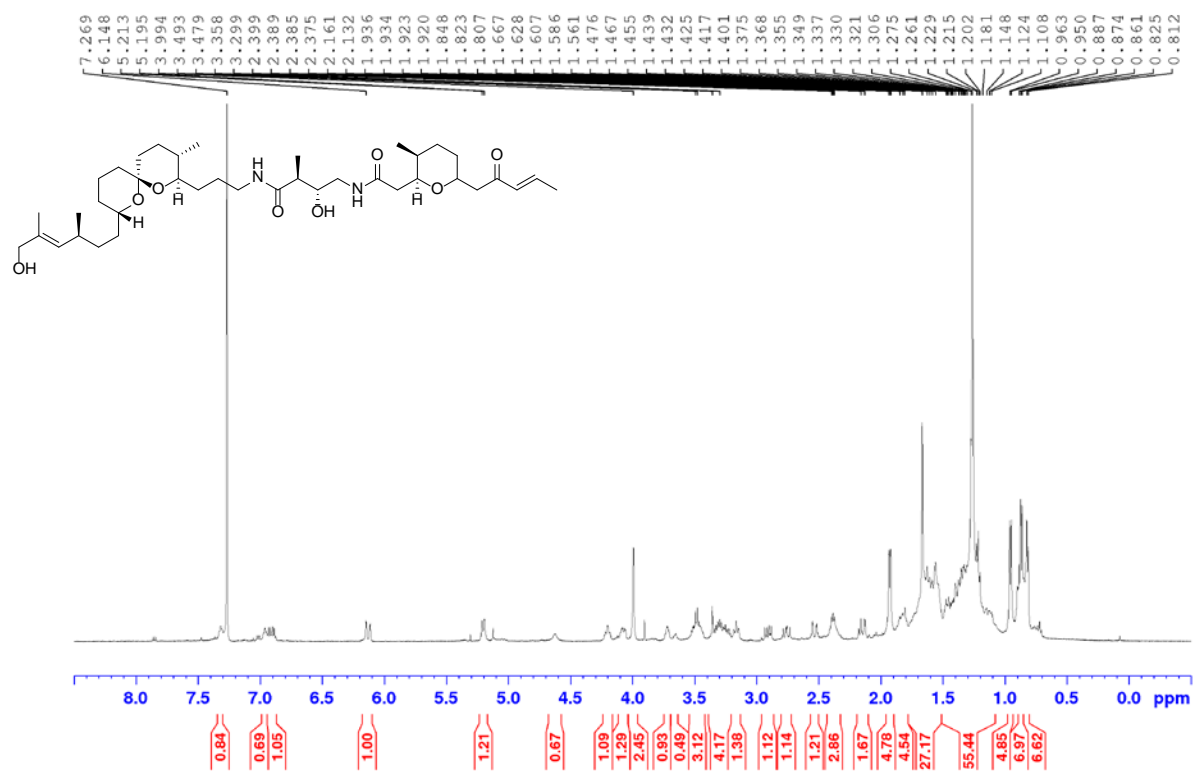


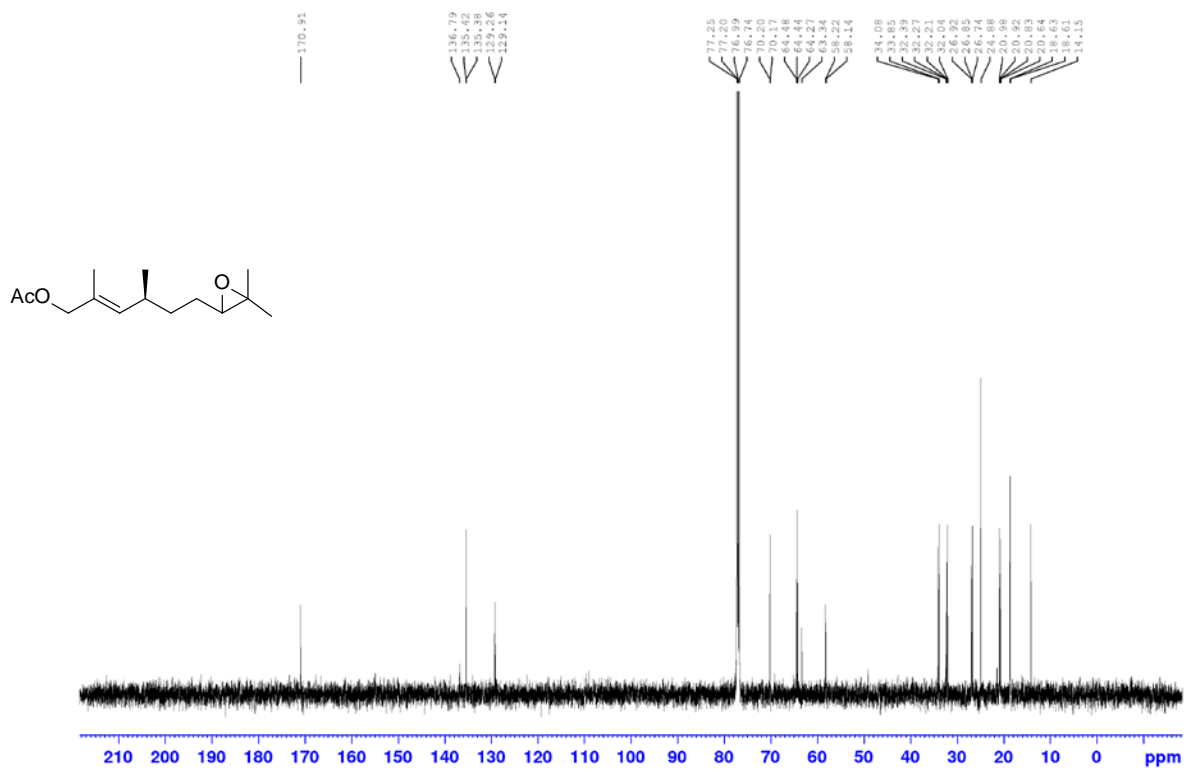
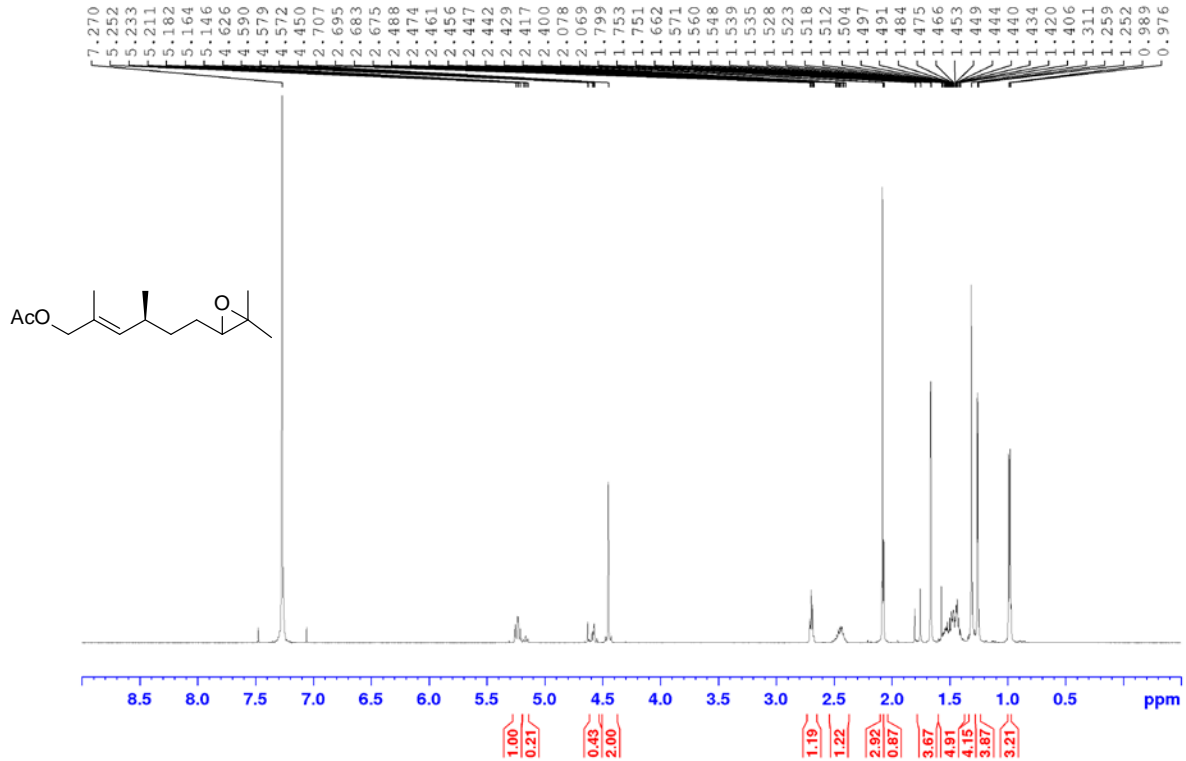


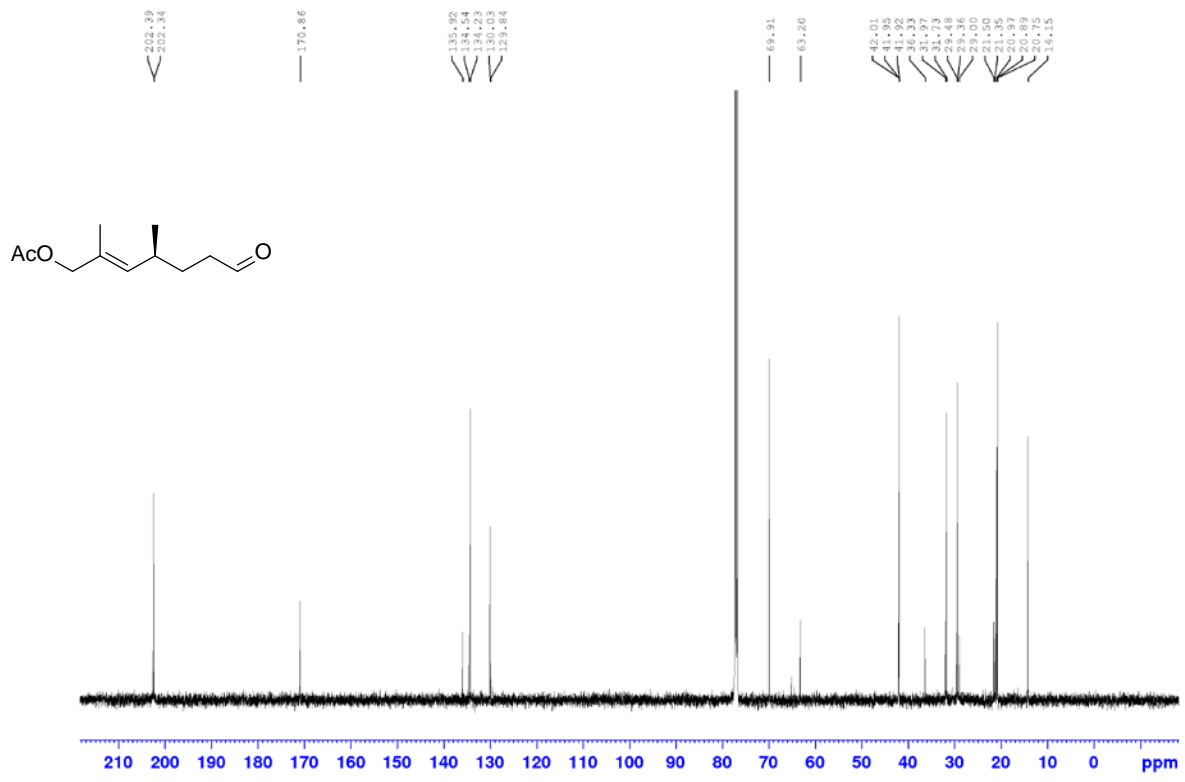
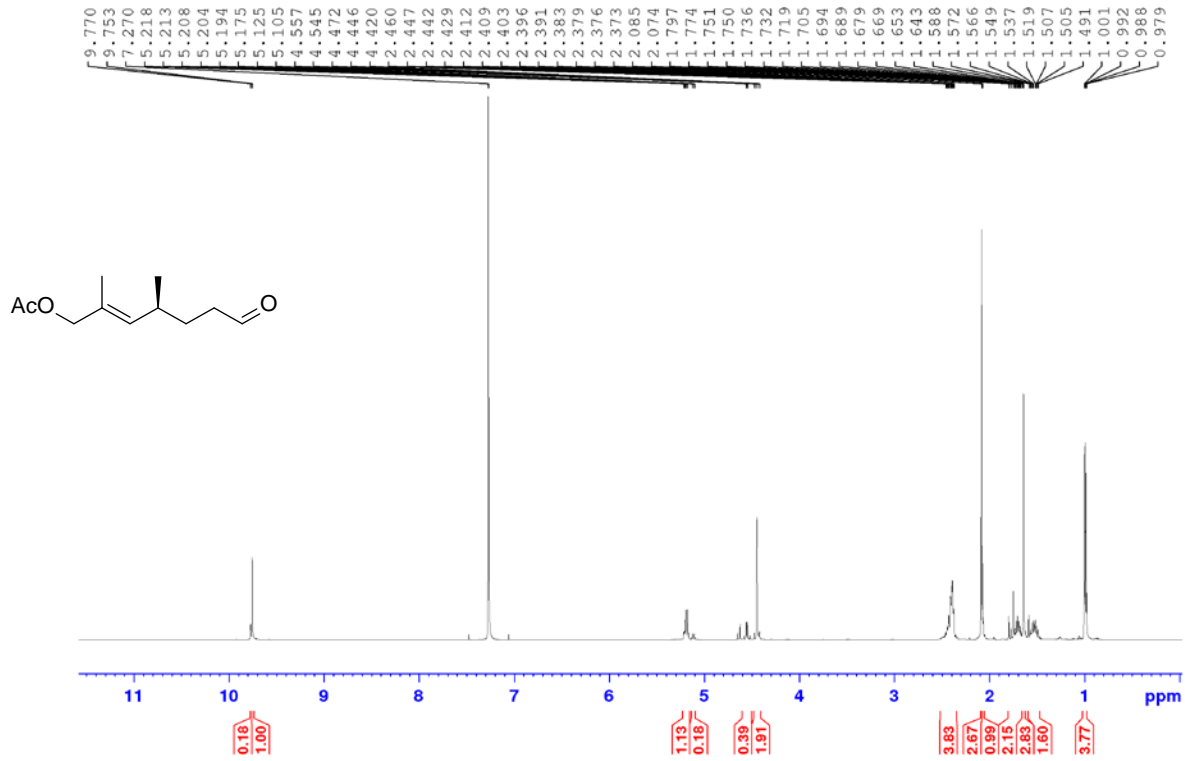


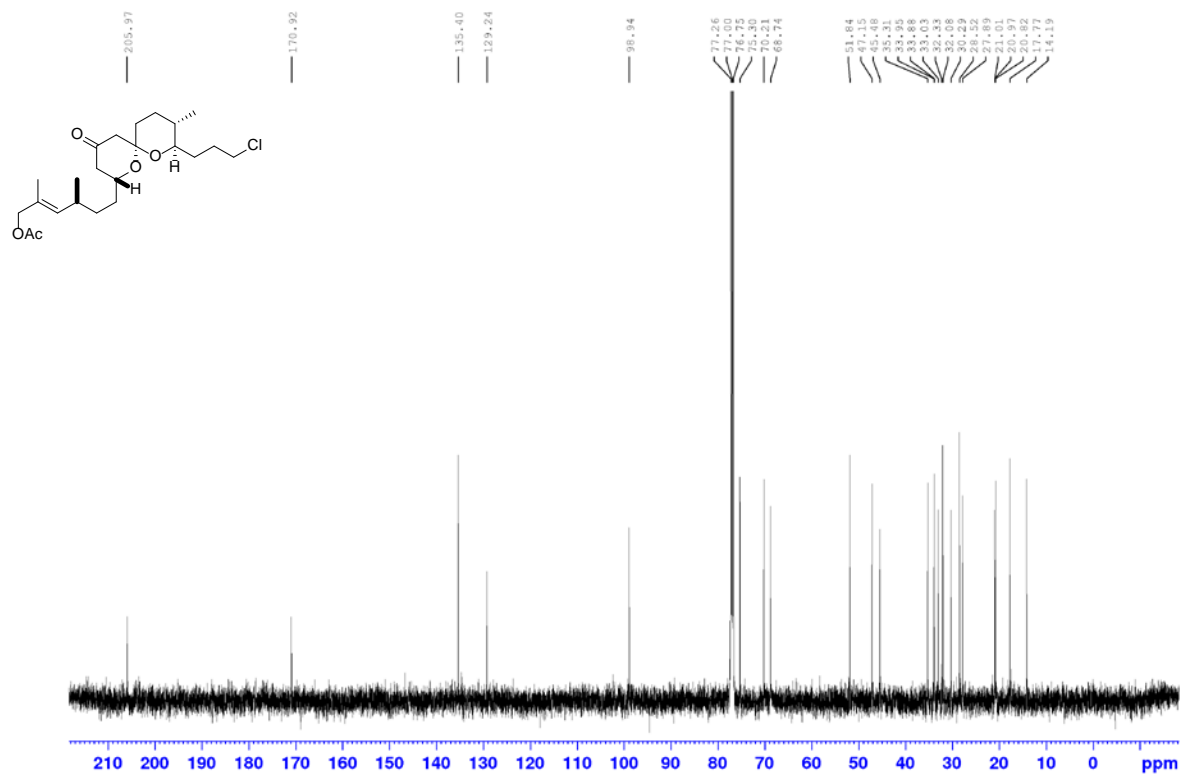
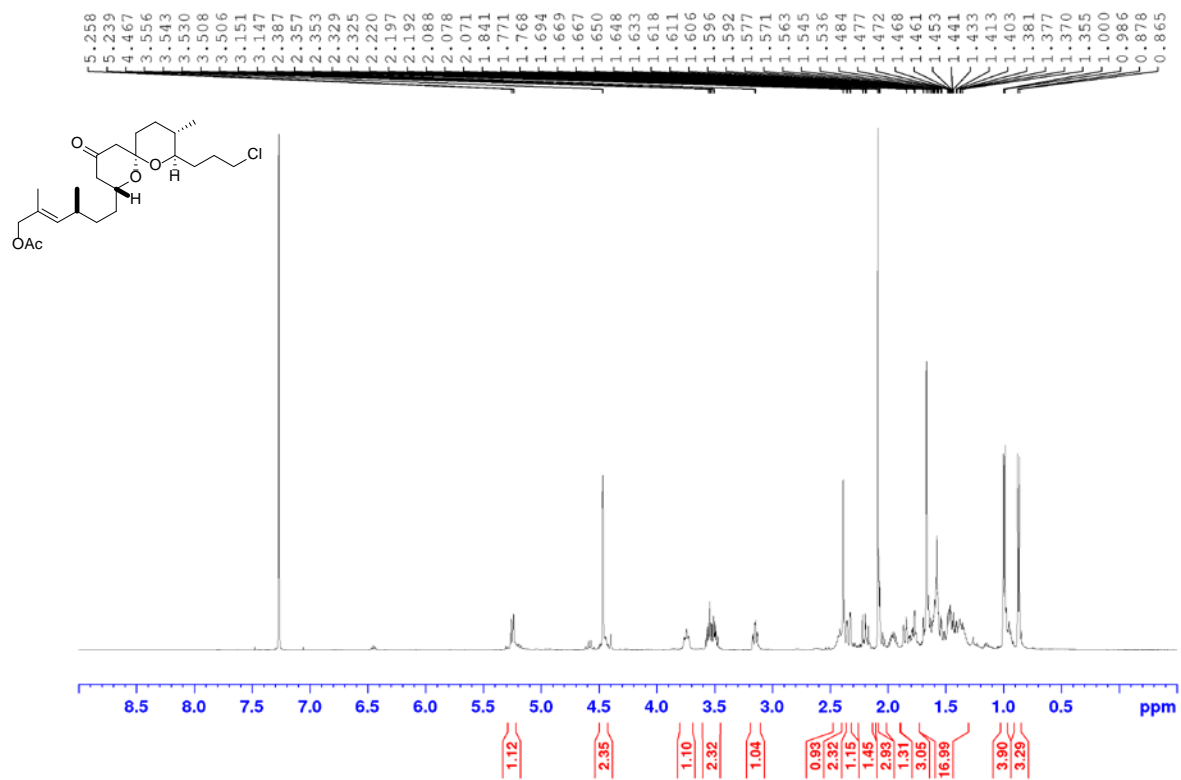












BIBLIOGRAPHY

1. Miyaura, N.; Yamada, K.; Suzuki, A., A new stereospecific cross-coupling by the palladium-catalyzed reaction of 1-alkenylboranes with 1-alkenyl or 1-alkynyl halides. *Tetrahedron Lett.* **1979**, *20* (36), 3437-3440.
2. Lippert, A. R.; Van de Bittner, G. C.; Chang, C. J., Boronate Oxidation as a Bioorthogonal Reaction Approach for Studying the Chemistry of Hydrogen Peroxide in Living Systems. *Acc. Chem. Res.* **2011**, *44* (9), 793-804.
3. Shabat, D.; Amir, R. J.; Gopin, A.; Pessah, N.; Shamis, M., Chemical Adaptor Systems. *Chem. Eur. J.* **2004**, *10* (11), 2626-2634.
4. Levine, M. N.; Raines, R. T., Trimethyl lock: a trigger for molecular release in chemistry, biology, and pharmacology. *Chem. Sci.* **2012**, *3* (8), 2412-2420.
5. Beesley, R. M.; Ingold, C. K.; Thorpe, J. F., CXIX.-The formation and stability of spiro-compounds. Part I. spiro-Compounds from cyclohexane. *J. Chem. Soc. Trans.* **1915**, *107* (0), 1080-1106.
6. Chandran, S. S.; Dickson, K. A.; Raines, R. T., Latent Fluorophore Based on the Trimethyl Lock. *J. Am. Chem. Soc.* **2005**, *127* (6), 1652-1653.
7. Greenwald, R. B.; Choe, Y. H.; Conover, C. D.; Shum, K.; Wu, D.; Royzen, M., Drug Delivery Systems Based on Trimethyl Lock Lactonization: Poly(ethylene glycol) Prodrugs of Amino-Containing Compounds. *J. Med. Chem.* **2000**, *43* (3), 475-487.
8. Dillon, M. P.; Cai, H.; Maag, H., Application of the "trimethyl lock"¹ to Ganciclovir, a pro-prodrug with increased oral bioavailability. *Biorg. Med. Chem. Lett.* **1996**, *6* (14), 1653-1656.

9. Binghe, W.; Huijuan, Z.; Wei, W., Chemical feasibility studies of a potential coumarin-based prodrug system. *Biorg. Med. Chem. Lett.* **1996**, *6* (8), 945-950.
10. Wang, B.; Zhang, H.; Zheng, A.; Wang, W., Coumarin-based prodrugs. Part 3: Structural effects on the release kinetics of esterase-sensitive prodrugs of amines. *Bioorg, Med. Chem.* **1998**, *6* (4), 417-426.
11. Bundgaard, H.; Falch, E.; Larsen, C.; Mosher, G. L.; Mikkelsen, T. J., Pilocarpic acid esters as novel sequentially labile pilocarpine prodrugs for improved ocular delivery. *J. Med. Chem.* **1985**, *28* (8), 979-981.
12. Banaszczyk, M. G., Propofol phosphate, a water-soluble propofol prodrug: in vivo evaluation. *Anesth. Analg.* **2002**, *95*, 1285-1292.
13. Yang, J.; Yin, W.; Liu, J.; Wang, Y.; Zhou, C.; Kang, Y.; Zhang, W.-S., Synthesis and characterization of novel quick-release propofol prodrug via lactonization. *Biorg. Med. Chem. Lett.* **2013**, *23* (6), 1813-1816.
14. Meyer, Y.; Richard, J.-A.; Delest, B.; Noack, P.; Renard, P.-Y.; Romieu, A., A comparative study of the self-immolation of para-aminobenzylalcohol and hemithioaminal-based linkers in the context of protease-sensitive fluorogenic probes. *Org. Bio. Chem.* **2010**, *8* (8), 1777-1780.
15. Rautio, J.; Kumpulainen, H.; Heimbach, T.; Oliyai, R.; Oh, D.; Jarvinen, T.; Savolainen, J., Prodrugs: design and clinical applications. *Nat Rev Drug Discov* **2008**, *7* (3), 255-270.
16. Lee, H. Y.; Jiang, X.; Lee, D., Kinetics of Self-Immolation: Faster Signal Relay over a Longer Linear Distance? *Org. Lett.* **2009**, *11* (10), 2065-2068.
17. Erez, R.; Shabat, D., The azaquinone-methide elimination: comparison study of 1,6- and 1,4-eliminations under physiological conditions. *Org. Bio. Chem.* **2008**, *6* (15), 2669-2672.

18. de Groot, F. M.; Damen, E. W.; Scheeren, H. W., Anticancer prodrugs for application in monotherapy: targeting hypoxia, tumor-associated enzymes, and receptors. *Curr. Med. Chem.* **2001**, *8*, 1093-1122.
19. Percivalle, C.; Doria, F.; Freccero, M., Quinone Methides as DNA Alkylating Agents: An Overview on Efficient Activation Protocols for Enhanced Target Selectivity. *Curr. Org. Chem.* **2014**, *18* (1), 19-43.
20. Kostikov, A. P.; Malashikhina, N.; Popik, V. V., Caging of Carbonyl Compounds as Photolabile (2,5-Dihydroxyphenyl)ethylene Glycol Acetals. *J. Org. Chem.* **2009**, *74* (4), 1802-1804.
21. Wang, P.; Hu, H.; Wang, Y., Novel Photolabile Protecting Group for Carbonyl Compounds. *Org. Lett.* **2007**, *9* (8), 1533-1535.
22. Blanc, A.; Bochet, C. G., Bis(o-nitrophenyl)ethanediol: A Practical Photolabile Protecting Group for Ketones and Aldehydes. *J. Org. Chem.* **2003**, *68* (3), 1138-1141.
23. Lu, M.; Fedoryak, O. D.; Moister, B. R.; Dore, T. M., Bhc-diol as a Photolabile Protecting Group for Aldehydes and Ketones. *Org. Lett.* **2003**, *5* (12), 2119-2122.
24. Kilic, F.; Kashikar, N. D.; Schmidt, R.; Alvarez, L.; Dai, L.; Weyand, I.; Wiesner, B.; Goodwin, N.; Hagen, V.; Kaupp, U. B., Caged Progesterone: A New Tool for Studying Rapid Nongenomic Actions of Progesterone. *J. Am. Chem. Soc.* **2009**, *131* (11), 4027-4030.
25. Ho, O. C.; Soundararajan, R.; Lu, J.; Matteson, D. S.; Wang, Z.; Chen, X.; Wei, M.; Willett, R. D., ((Trityloxy)methyl)boronic Esters. *Organometallics* **1995**, *14* (6), 2855-2860.
26. Yamamoto, Y.; Moritani, I., Carbon-13 nuclear magnetic resonance studies of organoboranes. Relative importance of mesomeric boron-carbon π -bonding forms in alkenyl- and alkynylboranes. *J. Org. Chem.* **1975**, *40* (23), 3434-3437.

27. Yamashita, M.; Yamamoto, Y.; Akiba, K.-y.; Hashizume, D.; Iwasaki, F.; Takagi, N.; Nagase, S., Syntheses and Structures of Hypervalent Pentacoordinate Carbon and Boron Compounds Bearing an Anthracene Skeleton – Elucidation of Hypervalent Interaction Based on X-ray Analysis and DFT Calculation. *J. Am. Chem. Soc.* **2005**, *127* (12), 4354-4371.
28. Matteson, D. S.; Michnick, T. J.; Willett, R. D.; Patterson, C. D., [(1R)-1-acetamido-3-(methylthio)propyl]boronic acid and the x-ray structure of its ethylene glycol ester. *Organometallics* **1989**, *8* (3), 726-729.
29. Roy, C. D.; Brown, H. C., A Comparative Study of the Relative Stability of Representative Chiral and Achiral Boronic Esters Employing Transesterification. *Monatsh. Chem.* **2007**, *138* (9), 879-887.
30. Li, W.; Nelson, D. P.; Jensen, M. S.; Hoerrner, R. S.; Cai, D.; Larsen, R. D.; Reider, P. J., An Improved Protocol for the Preparation of 3-Pyridyl- and Some Arylboronic Acids. *J. Org. Chem.* **2002**, *67* (15), 5394-5397.
31. Trost, B. M.; Editor, *Stereodirected Synthesis with Organoboranes*. Springer: 1995; p 400 pp.(approx.).
32. Docks, E. L., Boric Acid Esters. In *Kirk-Othmer Encyclopedia of Chemical Technology*, John Wiley & Sons, Inc.: 2000.
33. Matteson, D. S., Boronic Esters in Asymmetric Synthesis. *J. Org. Chem.* **2013**, *78* (20), 10009-10023.
34. Dick, G. R.; Knapp, D. M.; Gillis, E. P.; Burke, M. D., General Method for Synthesis of 2-Heterocyclic N-Methyliminodiacetic Acid Boronates. *Org. Lett.* **2010**, *12* (10), 2314-2317.

35. Brown, H. C.; Rao, B. C. S., Hydroboration. II. A Remarkably Fast Addition of Diborane to Olefins—Scope and Stoichiometry of the Reaction. *J. Am. Chem. Soc.* **1959**, *81* (24), 6428-6434.
36. Brown, H. C.; Rao, B. C. S., A NEW TECHNIQUE FOR THE CONVERSION OF OLEFINS INTO ORGANOBORANES AND RELATED ALCOHOLS. *J. Am. Chem. Soc.* **1956**, *78* (21), 5694-5695.
37. Wade, P. L., Boryl Metal Complexes, Boron Complexes, and Catalytic (Hydro)boration. *Angew. Chem. Int. Ed.* **1997**, *36* (22), 2441-2444.
38. Haberberger, M.; Enthaler, S., Straightforward Iron-Catalyzed Synthesis of Vinylboronates by the Hydroboration of Alkynes. *Chem. As. J.* **2013**, *8* (1), 50-54.
39. Brown, H. C.; Liotta, R.; Kramer, G. W., Hydroboration. 51. Hydroboration of representative allenes with 9-borabicyclo[3.3.1]nonane. An exceptional directive effect providing a direct synthesis of B-allyl-9-borabicyclo[3.3.1]nonane derivatives. *J. Am. Chem. Soc.* **1979**, *101* (11), 2966-2970.
40. Wu, J. Y.; Moreau, B.; Ritter, T., Iron-Catalyzed 1,4-Hydroboration of 1,3-Dienes. *J. Am. Chem. Soc.* **2009**, *131* (36), 12915-12917.
41. O'Brien, J. M.; Lee, K.-s.; Hoveyda, A. H., Enantioselective Synthesis of Boron-Substituted Quaternary Carbons by NHC-Cu-Catalyzed Boronate Conjugate Additions to Unsaturated Carboxylic Esters, Ketones, or Thioesters. *J. Am. Chem. Soc.* **2010**, *132* (31), 10630-10633.
42. Fish, R. H., Relative rates of hydroboration of several olefins with 4,4,6-trimethyl-1,3,2-dioxaborinane. *J. Org. Chem.* **1973**, *38* (1), 158-159.

43. Dembitsky, V. M.; Abu Ali, H.; Srebnik, M., Recent developments in bisdiborane chemistry: B-C-B, B-C-C-B, B-C-C-B and B-C-C-B compounds. *Appl. Org. Chem.* **2003**, *17* (6-7), 327-345.
44. Ishiyama, T.; Matsuda, N.; Miyaura, N.; Suzuki, A., Platinum(0)-catalyzed diboration of alkynes. *J. Am. Chem. Soc.* **1993**, *115* (23), 11018-11019.
45. Coombs, J. R.; Haeffner, F.; Kliman, L. T.; Morken, J. P., Scope and Mechanism of the Pt-Catalyzed Enantioselective Diboration of Monosubstituted Alkenes. *J. Am. Chem. Soc.* **2013**, *135* (30), 11222-11231.
46. Yang, F.-Y.; Cheng, C.-H., Unusual Diboration of Allenes Catalyzed by Palladium Complexes and Organic Iodides: A New Efficient Route to Biboronic Compounds. *J. Am. Chem. Soc.* **2001**, *123* (4), 761-762.
47. Lillo, V.; Mata, J.; Ramírez, J.; Peris, E.; Fernandez, E., Catalytic Diboration of Unsaturated Molecules with Platinum(0)-NHC: Selective Synthesis of 1,2-Dihydroxysulfones. *Organometallics* **2006**, *25* (24), 5829-5831.
48. Takaya, J.; Iwasawa, N., Catalytic, Direct Synthesis of Bis(boronate) Compounds. *ACS Cat.* **2012**, *2* (9), 1993-2006.
49. Baker, R. T.; Nguyen, P.; Marder, T. B.; Westcott, S. A., Transition Metal Catalyzed Diboration of Vinylarenes. *Angew. Chem. Int. Ed.* **1995**, *34* (12), 1336-1338.
50. Ely, R. J.; Morken, J. P., Ni(0)-Catalyzed 1,4-Selective Diboration of Conjugated Dienes. *Org. Lett.* **2010**, *12* (19), 4348-4351.
51. Pelz, N. F.; Woodward, A. R.; Burks, H. E.; Sieber, J. D.; Morken, J. P., Palladium-Catalyzed Enantioselective Diboration of Prochiral Allenes. *J. Am. Chem. Soc.* **2004**, *126* (50), 16328-16329.

52. Dang, L.; Zhao, H.; Lin, Z.; Marder, T. B., Understanding the Higher Reactivity of B2cat2 versus B2pin2 in Copper(I)-Catalyzed Alkene Diboration Reactions. *Organometallics* **2008**, *27* (6), 1178-1186.
53. Bonet, A.; Sole, C.; Gulyas, H.; Fernandez, E., Asymmetric organocatalytic diboration of alkenes. *Org. Bio. Chem.* **2012**, *10* (33), 6621-6623.
54. Laitar, D. S.; Tsui, E. Y.; Sadighi, J. P., Catalytic Diboration of Aldehydes via Insertion into the Copper–Boron Bond. *J. Am. Chem. Soc.* **2006**, *128* (34), 11036-11037.
55. Molander, G. A.; Wisniewski, S. R., Stereospecific Cross-Coupling of Secondary Organotrifluoroborates: Potassium 1-(Benzyloxy)alkyltrifluoroborates. *J. Am. Chem. Soc.* **2012**, *134* (40), 16856-16868.
56. Zhao, H.; Dang, L.; Marder, T. B.; Lin, Z., DFT Studies on the Mechanism of the Diboration of Aldehydes Catalyzed by Copper(I) Boryl Complexes. *J. Am. Chem. Soc.* **2008**, *130* (16), 5586-5594.
57. Beenen, M. A.; An, C.; Ellman, J. A., Asymmetric Copper-Catalyzed Synthesis of α -Amino Boronate Esters from N-tert-Butanesulfinyl Aldimines. *J. Am. Chem. Soc.* **2008**, *130* (22), 6910-6911.
58. McIntosh, M. L.; Moore, C. M.; Clark, T. B., Copper-Catalyzed Diboration of Ketones: Facile Synthesis of Tertiary α -Hydroxyboronate Esters. *Org. Lett.* **2010**, *12* (9), 1996-1999.
59. Burgess, K., Stereodirected Synthesis with Organoboranes, by D. S. Matteson. *Synthesis* **1996**, (4), 552.
60. Vedrenne, E.; Wallner, O. A.; Vitale, M.; Schmidt, F.; Aggarwal, V. K., Homologation of Boronic Esters with Lithiated Epoxides for the Stereocontrolled Synthesis of 1,2- and 1,3-Diols and 1,2,4-Triols. *Org. Lett.* **2008**, *11* (1), 165-168.

61. Stymiest, J. L.; Bagutski, V.; French, R. M.; Aggarwal, V. K., Enantiodivergent conversion of chiral secondary alcohols into tertiary alcohols. *Nature* **2008**, *456* (7223), 778-782.
62. Petasis, N. A.; Akritopoulou, I., The boronic acid mannich reaction: A new method for the synthesis of geometrically pure allylamines. *Tetrahedron Lett.* **1993**, *34* (4), 583-586.
63. Chang, M. C. Y.; Pralle, A.; Isacoff, E. Y.; Chang, C. J., A Selective, Cell-Permeable Optical Probe for Hydrogen Peroxide in Living Cells. *J. Am. Chem. Soc.* **2004**, *126* (47), 15392-15393.
64. Sletten, E. M.; Bertozzi, C. R., From Mechanism to Mouse: A Tale of Two Bioorthogonal Reactions. *Acc. Chem. Res.* **2011**, *44* (9), 666-676.
65. Lo, L.-C.; Chu, C.-Y., Development of highly selective and sensitive probes for hydrogen peroxide. *Chem. Comm.* **2003**, (21), 2728-2729.
66. Miller, E. W.; Tulyathan, O.; Isacoff, E. Y.; Chang, C. J., Molecular imaging of hydrogen peroxide produced for cell signaling. *Nat. Chem. Bio.* **2007**, *3*, 263.
67. Albers, A. E.; Okreglak, V. S.; Chang, C. J., A FRET-Based Approach to Ratiometric Fluorescence Detection of Hydrogen Peroxide. *J. Am. Chem. Soc.* **2006**, *128* (30), 9640-9641.
68. Murphy, M. P.; Smith, R. A. J., Targeting antioxidants to mitochondria by conjugation to lipophilic cations. 2007; Vol. 47, pp 629-656.
69. Dickinson, B. C.; Srikun, D.; Chang, C. J., Mitochondrial-targeted fluorescent probes for reactive oxygen species. *Curr. Op. Chem. Bio.* **2010**, *14* (1), 50-56.
70. Van de Bittner, G. C.; Dubikovskaya, E. A.; Bertozzi, C. R.; Chang, C. J., In vivo imaging of hydrogen peroxide production in a murine tumor model with a chemoselective bioluminescent reporter. *Proc. Nat. Aca. Sci.* **2010**, *107* (50), 21316-21321.

71. Szatrowski, T. P.; Nathan, C. F., Production of large amounts of hydrogen peroxide by human tumor cells. *Cancer research* **1991**, *51* (3), 794-8.
72. Trachootham, D.; Alexandre, J.; Huang, P., Targeting cancer cells by ROS-mediated mechanisms: a radical therapeutic approach? *Nat Rev Drug Discov* **2009**, *8* (7), 579-591.
73. Kim, E.-J.; Bhuniya, S.; Lee, H.; Kim, H. M.; Cheong, C.; Maiti, S.; Hong, K. S.; Kim, J. S., An Activatable Prodrug for the Treatment of Metastatic Tumors. *J. Am. Chem. Soc.* **2014**, *136* (39), 13888-13894.
74. Glantzounis, G. K.; Salacinski, H. J.; Yang, W.; Davidson, B. R.; Seifalian, A. M., The contemporary role of antioxidant therapy in attenuating liver ischemia-reperfusion injury: A review. *Liver Transplantation* **2005**, *11* (9), 1031-1047.
75. Halliwell, B., Oxidative stress and cancer: have we moved forward? *Biochemical Journal* **2007**, *401* (1), 1.
76. Lee, D.; Park, S.; Bae, S.; Jeong, D.; Park, M.; Kang, C.; Yoo, W.; Samad, M. A.; Ke, Q.; Khang, G.; Kang, P. M., Hydrogen peroxide-activatable antioxidant prodrug as a targeted therapeutic agent for ischemia-reperfusion injury. *Scientific Reports* **2015**, *5*, 16592.
77. Noh, J.; Kwon, B.; Han, E.; Park, M.; Yang, W.; Cho, W.; Yoo, W.; Khang, G.; Lee, D., Amplification of oxidative stress by a dual stimuli-responsive hybrid drug enhances cancer cell death. *Nature Communications* **2015**, *6*, 6907.
78. Hall, D. G., Structure, Properties, and Preparation of Boronic Acid Derivatives. In *Boronic Acids*, Wiley-VCH Verlag GmbH & Co. KGaA: 2011; pp 1-133.
79. Singh, J.; Petter, R. C.; Baillie, T. A.; Whitty, A., The resurgence of covalent drugs. *Nat Rev Drug Discov* **2011**, *10* (4), 307-317.

80. Diaz, D. B.; Yudin, A. K., The versatility of boron in biological target engagement. *Nature Chemistry* **2017**, *9*, 731.
81. Jiang, Q.; Zhong, Q.; Zhang, Q.; Zheng, S.; Wang, G., Boron-Based 4-Hydroxytamoxifen Bioisosteres for Treatment of de Novo Tamoxifen Resistant Breast Cancer. *ACS Med. Chem. Lett.* **2012**, *3* (5), 392-396.
82. Wang, L.; Xie, S.; Ma, L.; Chen, Y.; Lu, W., 10-Boronic acid substituted camptothecin as prodrug of SN-38. *Eur. J. Med. Chem.* **2016**, *116*, 84-89.
83. Zheng, S.; Guo, S.; Zhong, Q.; Zhang, C.; Liu, J.; Yang, L.; Zhang, Q.; Wang, G., Biocompatible Boron-Containing Prodrugs of Belinostat for the Potential Treatment of Solid Tumors. *ACS Med. Chem. Lett.* **2018**, *9* (2), 149-154.
84. Gorovoy, A. S.; Gozhina, O. V.; Svendsen, J. S.; Domorad, A. A.; Tetz, G. V.; Tetz, V. V.; Lejon, T., Boron-Containing Peptidomimetics – A Novel Class of Selective Anti-tubercular Drugs. *Chemical Biology & Drug Design* **2013**, *81* (3), 408-413.
85. Jacobs, R. T.; Plattner, J. J.; Keenan, M., Boron-based drugs as antiprotozoals. *Current Opinion in Infectious Diseases* **2011**, *24* (6), 586-592 10.1097/QCO.0b013e32834c630e.
86. Hecker, S. J.; Reddy, K. R.; Totrov, M.; Hirst, G. C.; Lomovskaya, O.; Griffith, D. C.; King, P.; Tsivkovski, R.; Sun, D.; Sabet, M.; Tarazi, Z.; Clifton, M. C.; Atkins, K.; Raymond, A.; Potts, K. T.; Abendroth, J.; Boyer, S. H.; Loutit, J. S.; Morgan, E. E.; Durso, S.; Dudley, M. N., Discovery of a Cyclic Boronic Acid β -Lactamase Inhibitor (RPX7009) with Utility vs Class A Serine Carbapenemases. *J. Med. Chem.* **2015**, *58* (9), 3682-3692.
87. Mosey, R. A.; Floreancig, P. E., Versatile approach to [small alpha]-alkoxy carbamate synthesis and stimulus-responsive alcohol release. *Org. Bio. Chem.* **2012**, *10* (39), 7980-7985.

88. Parman, T.; Bunin, D. I.; Ng, H. H.; McDunn, J. E.; Wulff, J. E.; Wang, A.; Swezey, R.; Rasay, L.; Fairchild, D. G.; Kapetanovic, I. M.; Green, C. E., Toxicogenomics and Metabolomics of Pentamethylchromanol (PMCol)-Induced Hepatotoxicity. *Toxicological Sciences* **2011**, *124* (2), 487-501.
89. Hu, N.; Zhao, G.; Zhang, Y.; Liu, X.; Li, G.; Tang, W., Synthesis of Chiral α -Amino Tertiary Boronic Esters by Enantioselective Hydroboration of α -Arylenamides. *J. Am. Chem. Soc.* **2015**, *137* (21), 6746-6749.
90. Kisu, H.; Sakaino, H.; Ito, F.; Yamashita, M.; Nozaki, K., A Qualitative Analysis of a “Bora-Brook Rearrangement”: The Ambident Reactivity of Boryl-Substituted Alkoxide Including the Carbon-to-Oxygen Migration of a Boryl Group. *J. Am. Chem. Soc.* **2016**, *138* (10), 3548-3552.
91. Burk, R. M.; Gac, T. S.; Roof, M. B., A mild procedure for etherification of alcohols with primary alkyl halides in the presence of silver triflate. *Tetrahedron Lett.* **1994**, *35* (44), 8111-8112.
92. Bajwa, J. S.; Jiang, X.; Slade, J.; Prasad, K.; Repič, O.; Blacklock, T. J., In-situ generation of Et₃SiBr from BiBr₃ and Et₃SiH and its use in preparation of dialkyl ethers. *Tetrahedron Lett.* **2002**, *43* (38), 6709-6713.
93. Shi, Y.-J.; Hughes, D. L.; McNamara, J. M., Stereospecific synthesis of chiral tertiary alkyl-aryl ethers via Mitsunobu reaction with complete inversion of configuration. *Tetrahedron Lett.* **2003**, *44* (18), 3609-3611.
94. Shintou, T.; Mukaiyama, T., Efficient Methods for the Preparation of Alkyl–Aryl and Symmetrical or Unsymmetrical Dialkyl Ethers between Alcohols and Phenols or Two Alcohols by Oxidation–Reduction Condensation. *J. Am. Chem. Soc.* **2004**, *126* (23), 7359-7367.

95. Oikaw, Y.; Yoshioka, T.; Yonemitsu, O., Protection of hydroxy groups by intramolecular oxidative formation of methoxybenzylidene acetals with DDQ. *Tetrahedron Lett.* **1982**, *23* (8), 889-892.
96. Kumpulainen, H.; Maehoenen, N.; Laitinen, M.-L.; Jaurakkajaervi, M.; Raunio, H.; Juvonen, R. O.; Vepsaelaeninen, J.; Jaervinen, T.; Rautio, J., Evaluation of Hydroxyimine as Cytochrome P450-Selective Prodrug Structure. *J. Med. Chem.* **2006**, *49* (3), 1207-1211.
97. Tsunoda, T.; Suzuki, M.; Noyori, R., Trialkylsilyl triflates. VI. A facile procedure for acetalization under aprotic conditions. *Tetrahedron Lett.* **1980**, *21* (14), 1357-8.
98. Wu, J.-S.; Liu, W.-M.; Zhuang, X.-Q.; Wang, F.; Wang, P.-F.; Tao, S.-L.; Zhang, X.-H.; Wu, S.-K.; Lee, S.-T., Fluorescence Turn On of Coumarin Derivatives by Metal Cations: A New Signaling Mechanism Based on C=N Isomerization. *Org. Lett.* **2007**, *9* (1), 33-36.
99. Verschoor, M. L.; Wilson, L. A.; Singh, G., Mechanisms associated with mitochondrial-generated reactive oxygen species in cancer This article is one of a selection of papers published in a Special Issue on Oxidative Stress in Health and Disease. *Canadian Journal of Physiology and Pharmacology* **2010**, *88* (3), 204-219.
100. Bellavite, P., The superoxide-forming enzymatic system of phagocytes. *Free Radical Biology and Medicine* **1988**, *4* (4), 225-261.
101. Degnan, B. M.; Hawkins, C. J.; Lavin, M. F.; McCaffrey, E. J.; Parry, D. L.; Watters, D. J., Novel cytotoxic compounds from the ascidian *Lissoclinum bistratum*. *J. Med. Chem.* **1989**, *32* (6), 1354-1359.
102. Biard, J.-F.; Roussakis, C.; Kornprobst, J.-M.; Gouiffes-Barbin, D.; Verbist, J.-F.; Cotellet, P.; Foster, M. P.; Ireland, C. M.; Debitus, C., Bistramides A, B, C, D, and K: A New Class of Bioactive Cyclic Polyethers from *Lissoclinum bistratum*. *J. Nat. Prod.* **1994**, *57* (10), 1336-1345.

103. Statsuk, A. V.; Bai, R.; Baryza, J. L.; Verma, V. A.; Hamel, E.; Wender, P. A.; Kozmin, S. A., Actin is the primary cellular receptor of bistramide A. *Nat. Chem. Bio.* **2005**, *1*, 383.
104. Han, X.; Floreancig, P. E., Spiroacetal Formation through Telescoped Cycloaddition and Carbon–Hydrogen Bond Functionalization: Total Synthesis of Bistramide A. *Angew. Chem. Int. Ed.* **2014**, *53* (41), 11075-11078.
105. Statsuk, A. V.; Liu, D.; Kozmin, S. A., Synthesis of Bistramide A. *J. Am. Chem. Soc.* **2004**, *126* (31), 9546-9547.
106. Brown, H. C.; Bhat, K. S., Enantiomeric Z- and E-crotyldiisopinocampheylboranes. Synthesis in high optical purity of all four possible stereoisomers of β -methylhomoallyl alcohols. *J. Am. Chem. Soc.* **1986**, *108* (2), 293-4.
107. Sen, S. E.; Roach, S. L., A Convenient Two-Step Procedure for the Synthesis of Substituted Allylic Amines from Allylic Alcohols. *Synthesis* **1995**, *1995* (07), 756-758.
108. Binger, P.; Müller, P.; Benn, R.; Mynott, R., Vinylcarbene Complexes of Titanocene. *Angew. Chem. Int. Ed.* **1989**, *28* (5), 610-611.
109. Barma, D. K.; Kundu, A.; Zhang, H.; Mioskowski, C.; Falck, J. R., (Z)- α -Haloacrylates: An Exceptionally Stereoselective Preparation via Cr(II)-Mediated Olefination of Aldehydes with Trihaloacetates. *J. Am. Chem. Soc.* **2003**, *125* (11), 3218-3219.
110. Corey, E. J.; Helal, C. J., Reduction of Carbonyl Compounds with Chiral Oxazaborolidine Catalysts: A New Paradigm for Enantioselective Catalysis and a Powerful New Synthetic Method. *Angew. Chem. Int. Ed.* **1998**, *37* (15), 1986-2012.
111. Crimmins, M. T.; DeBaillie, A. C., Enantioselective Total Synthesis of Bistramide A. *J. Am. Chem. Soc.* **2006**, *128* (15), 4936-4937.

112. Crimmins, M. T.; Emmitte, K. A.; Katz, J. D., Diastereoselective Alkylations of Oxazolidinone Glycolates: A Useful Extension of the Evans Asymmetric Alkylation. *Org. Lett.* **2000**, *2* (14), 2165-2167.
113. Mancuso, A. J.; Huang, S.-L.; Swern, D., Oxidation of long-chain and related alcohols to carbonyls by dimethyl sulfoxide "activated" by oxalyl chloride. *J. Org. Chem.* **1978**, *43* (12), 2480-2482.
114. Blakemore, P. R., The modified Julia olefination: alkene synthesis via the condensation of metallated heteroarylalkylsulfones with carbonyl compounds. *J. Chem. Soc., Perkin Trans. 1* **2002**, (23), 2563-2585.
115. Mitsunobu, O., The use of diethyl azodicarboxylate and triphenylphosphine in synthesis and transformation of natural products. *Synthesis* **1981**, (1), 1-28.
116. Dess, D. B.; Martin, J. C., A useful 12-I-5 triacetoxyperiodinane (the Dess-Martin periodinane) for the selective oxidation of primary or secondary alcohols and a variety of related 12-I-5 species. *J. Am. Chem. Soc.* **1991**, *113* (19), 7277-87.
117. Paterson, I.; Yeung, K. S.; Smaill, J. B., The Horner-Wadsworth-Emmons reaction in natural products synthesis: expedient construction of complex (E)-enones using a barium hydroxide. *Synlett* **1993**, (10), 774-6.
118. Crimmins, M. T.; King, B. W.; Tabet, E. A.; Chaudhary, K., Asymmetric Aldol Additions: Use of Titanium Tetrachloride and (-)-Sparteine for the Soft Enolization of N-Acyl Oxazolidinones, Oxazolidinethiones, and Thiazolidinethiones. *J. Org. Chem.* **2001**, *66* (3), 894-902.
119. Kopecky, D. J.; Rychnovsky, S. D., Improved Procedure for the Reductive Acetylation of Acyclic Esters and a New Synthesis of Ethers. *J. Org. Chem.* **2000**, *65* (1), 191-198.

120. Dossetter, A. G.; Jamison, T. F.; Jacobsen, E. N., Highly enantio- and diastereoselective hetero-Diels-Alder reactions catalyzed by new chiral tridentate chromium (III) catalysts. *Angew. Chem., Int. Ed.* **1999**, *38* (16), 2398-2400.
121. Liu, L.; Floreancig, P. E., Cyclization Reactions through DDQ-Mediated Vinyl Oxazolidinone Oxidation. *Org. Lett.* **2009**, *11* (14), 3152-3155.
122. Donohoe, T. J.; Lipinski, R. M., Interplay of Cascade Oxidative Cyclization and Hydride Shifts in the Synthesis of the ABC Spiroketal Ring System of Pectenotoxin-4. *Angew. Chem., Int. Ed.* **2013**, *52* (9), 2491-2494.
123. Fürstner, A.; Feyen, F.; Prinz, H.; Waldmann, H., Total Synthesis and Reassessment of the Phosphatase-Inhibitory Activity of the Antitumor Agent TMC- 69- 6H. *Angew. Chem. Int. Ed.* **2003**, *42* (43), 5361-5364.
124. Parikh, J. R.; Doering, W. v. E., Sulfur trioxide in the oxidation of alcohols by dimethyl sulfoxide. *J. Am. Chem. Soc.* **1967**, *89* (21), 5505-5507.
125. Miyaura, N.; Ishiyama, T.; Sasaki, H.; Ishikawa, M.; Sato, M.; Suzuki, A., Palladium-catalyzed inter- and intramolecular cross-coupling reactions of B-alkyl-9-borabicyclo[3.3.1]nonane derivatives with 1-halo-1-alkenes or haloarenes. Syntheses of functionalized alkenes, arenes, and cycloalkenes via a hydroboration-coupling sequence. *J. Am. Chem. Soc.* **1989**, *111* (1), 314-21.
126. Nair, V.; Sinhababu, A. K., Selective transformations of sugar tosylhydrazones to deoxy and unsaturated sugars. *J. Org. Chem.* **1978**, *43* (26), 5013-17.
127. Gellrich, U.; Seiche, W.; Keller, M.; Breit, B., Mechanistic insights into a supramolecular self-assembling catalyst system: evidence for hydrogen bonding during rhodium-catalyzed hydroformylation. *Angew. Chem., Int. Ed.* **2012**, *51* (44), 11033-11038.

128. Breit, B.; Seiche, W., Hydrogen Bonding as a Construction Element for Bidentate Donor Ligands in Homogeneous Catalysis: Regioselective Hydroformylation of Terminal Alkenes. *J. Am. Chem. Soc.* **2003**, *125* (22), 6608-6609.
129. Rizvi, S. A.; Tereshko, V.; Kossiakoff, A. A.; Kozmin, S. A., Structure of Bistramide A-Actin Complex at a 1.35 Å Resolution. *J. Am. Chem. Soc.* **2006**, *128* (12), 3882-3883.
130. Rizvi, S. A.; Courson, D. S.; Keller, V. A.; Rock, R. S.; Kozmin, S. A., The dual mode of action of bistramide A entails severing of filamentous actin and covalent protein modification. *Proc. Nat. Aca. Sci.* **2008**, *105* (11), 4088-4092.
131. Otterbein, L. R.; Graceffa, P.; Dominguez, R., The Crystal Structure of Uncomplexed Actin in the ADP State. *Science* **2001**, *293* (5530), 708-711.
132. Rizvi, S. A.; Liu, S.; Chen, Z.; Skau, C.; Pytynia, M.; Kovar, D. R.; Chmura, S. J.; Kozmin, S. A., Rationally Simplified Bistramide Analog Reversibly Targets Actin Polymerization and Inhibits Cancer Progression in Vitro and in Vivo. *J. Am. Chem. Soc.* **2010**, *132* (21), 7288-7290.
133. Lowe, J. T.; Wrona, I. E.; Panek, J. S., Total Synthesis of Bistramide A. *Org. Lett.* **2007**, *9* (2), 327-330.
134. Tomas, L.; Gennäs, G. B. a.; Hiebel, M. A.; Hampson, P.; Gueyrard, D.; Pelotier, B.; Yli-Kauhaluoma, J.; Piva, O.; Lord, J. M.; Goekjian, P. G., Total Synthesis of Bistramide A and Its 36(Z) Isomers: Differential Effect on Cell Division, Differentiation, and Apoptosis. *Chem. Eur. J.* **2012**, *18* (24), 7452-7466.
135. Archer, R. H.; Carpenter, J. R.; Hwang, S.-J.; Burton, A. W.; Chen, C.-Y.; Zones, S. I.; Davis, M. E., Physicochemical Properties and Catalytic Behavior of the Molecular Sieve SSZ-70. *Chem. Mater.* **2010**, *22* (8), 2563-2572.

136. Evans, D. A.; Rieger, D. L.; Jones, T. K.; Kaldor, S. W., Assignment of stereochemistry in the oligomycin/rutamycin/cytovaricin family of antibiotics. Asymmetric synthesis of the rutamycin spiroketal synthon. *J. Org. Chem.* **1990**, *55* (26), 6260-6268.